In future wireless communication systems, full-duplex (FD) and massive multiple-input-multiple-output (mMIMO) are considered as two promising technologies to overcome the capacity crunch and spectrum scarcity. Transmission and reception at the same frequency-time channel in FD and large antenna arrays in mMIMO systems improve the spectral efficiency to a great extent compared to current systems. To make mMIMO systems cost-efficient, inexpensive less-accurate transmit and receive chain components are preferred. This leads to hardware distortions, which in turn become unfavourable for self-interference (SI) cancellation in FD systems.

In this thesis, our main goal is to design distortion-aware FD multi-antenna multi-carrier (MC) systems, from the aspect of resource allocation and the resulting system performance. Particularly the impact of distortions caused by hardware impairments, leading to residual self-interference and inter-carrier leakage as well as the imperfect channel state information is taken into account. Initially, we investigate the linear transceiver design problem for an FD multiple-input-multiple-output (MIMO) MC decode and forward (DF) relaying system. In addition to the traditional per-carrier DF relaying, the case with a joint-carrier DF is also studied, taking advantage of group-wise decoding and encoding.

Furthermore, we focus on the joint sub-carrier and power allocation problem for a DF relay system, where multiple half-duplex (HD) single antenna (SA) MC source-destination pairs communicate with the aid of an FD mMIMO MC relay. Besides maximizing the sum-rate and energy efficiency, we also focus on minimizing the overall delivery time for a given set of communication tasks to the user nodes. We extend the studied framework to a bi-directional MC communication system, where an FD mMIMO base station (BS) serves multiple FD SA user nodes.

Finally, we focus on resource allocation problem for an FD-enabled relaying system, where an mMIMO MC BS simultaneously activates the relay as well as the direct channel for communicating separate data streams to the user terminals. This is implemented by employing successive interference cancellation at the MC SA user terminals. Besides the superior performance under various system conditions, the proposed dual-connectivity enjoys higher robustness when one of the active paths experience an unexpected blockage.

ISBN 978-3-86359-878-5

ELEKTRO- UND INFORMATIONSTECHNIK

ELEKTRO- UND INFORMATIONSTECHNIK

Resource Allocation for Future Wireless Relay Systems

Vimal Radhakrishnan

Vimal Radhakrishnan

Resource Allocation for Future Wireless Relay Systems

Lehrstuhl für Theoretische Informationstechnik
RWTH AACHEN UNIVERSITY

Edition Wissenschaft Apprimus

Resource Allocation for Future Wireless Relay Systems

Von der Fakultät für Elektrotechnik und Informationstechnik
der Rheinisch-Westfälischen Technischen Hochschule Aachen
zur Erlangung des akademischen Grades eines

Doktors der Ingenieurwissenschaften

genehmigte Dissertation

vorgelegt von

Vimal Radhakrishnan, M.Sc

aus Thiruvananthapuram (Trivandrum), Indien

Berichter: Universitätsprofessor Dr. rer. nat. Rudolf Mathar
Universitätsprofessor Dr.-Ing. Peter Knott

Tag der mündlichen Prüfung: 13. Mai 2020

Bibliografische Information der Deutschen Nationalbibliothek
Die Deutsche Nationalbibliothek verzeichnet diese Publikation in der Deutschen Nationalbibliografie; detaillierte bibliografische Daten sind im Internet über https://portal.dnb.de abrufbar.

Vimal Radhakrishnan:

Resource Allocation for Future Wireless Relay Systems

1. Auflage, 2020

Gedruckt auf holz- und säurefreiem Papier, 100% chlorfrei gebleicht.

Apprimus Verlag, Aachen, 2020
Wissenschaftsverlag des Instituts für Industriekommunikation und Fachmedien
an der RWTH Aachen
Steinbachstr. 25, 52074 Aachen
Internet: www.apprimus-verlag.de, E-Mail: info@apprimus-verlag.de

Printed in Germany

ISBN 978-3-86359-878-5

D 82 (Diss. RWTH Aachen University, 2020)

Preface

This dissertation was written during my time as a research assistant at the Institute for Theoretical Information Technology at RWTH Aachen University.

I would like to express my sincere gratitude to my supervisor Univ.-Prof. Dr. rer. nat. Rudolf Mathar for giving me the opportunity to pursue my doctoral degree and to be a part of his research team. I am also grateful for his continuous support and giving me the freedom to conduct my research.

Many thanks to Univ-Prof. Dr.-Ing. Peter Knott for providing constructive comments and taking the effort to act as the second reviewer for my dissertation.

I would like to thank all my current and former colleagues at the Institute for Theoretical Information Technology, for creating a friendly and positive working atmosphere. I am also very thankful to my friend and former colleague, Dr.-Ing. Omid Taghizadeh, who is always available for me, and for his fruitful collaboration, unwavering support and guidance.

I would like to thank my beloved wife Akshaya Muruganandhan for her understanding and relentless support, especially during the last stages of my dissertation.

Finally, I would like to express my deepest gratitude to my parents, Radhakrishnan Kesavareddiar and Selvakumari Radhakrishnan, and my brother, Vivek Radhakrishnan, for their unconditional love and support throughout my life.

Aachen, May 2020 Vimal Radhakrishnan

Contents

1 Introduction

Increasing communication network traffic has always been a challenge in wireless communication. As the number of users or network usage is increased, new technologies are introduced to cope with the demand. In the current fourth-generation (4G) (long time evolution (LTE)) mobile networks, multiple input multiple output (MIMO) as well as multi-carrier modulation (orthogonal frequency division multiplexing (OFDM)) have been introduced, among other promising features, to support the user demand. Subsequently in future wireless systems, for instance in fifth-generation (5G) networks, full-duplex (FD) and massive multiple input multiple output (mMIMO) are considered as two promising technologies to overcome capacity crunch and spectrum scarcity.

In FD systems, simultaneous transmission and reception at the same frequency-time channel improve the spectral efficiency compared to the current half-duplex (HD) wireless systems [1], where the transmission and reception are separated either in time or frequency. The main challenge for such systems is to suppress the strong interference it receives from its own transmitter. A full-duplex node receives a part of its own transmitted signal through the direct path (LOS) or reflections from the scatterers. Recently, efficient self-interference cancellation (SIC) techniques are developed [2–4], which has made feasible to incorporate FD nodes into future communication systems [5–7], and motivated some related studies [8, 9]. Removing the known transmitted signal from the received one is the central idea for SIC. This is significant because the strong self-interference (SI) saturates the front-end components of the receiver, such as analog to digital converter (ADC), low noise amplifiers, to name a few. In order to make the FD operation feasible, SI should be mitigated to avoid saturating the limited dynamic range of the receiver chain. Most SIC techniques work in both analog and digital domains to remove the SI. The major part of the SI is removed at the analog domain, and the remaining signal will be cancelled in the digital domain. This is challenging due to the imperfect transmitter/receiver chain components, ageing of the components, imperfect knowledge of the SI channel.

In an mMIMO communication system, the nodes are equipped with a large number of antennas, which provides a large spatial diversity resulting in improved spectral efficiency. In these systems, less power is required to transmit data as the antennas can operate in conjunction with each other to enhance the gain of transmitted signals at the receiver, which makes it a more energy-efficient system. Moreover, the huge number of antennas makes an mMIMO network far more resistant to interference and intentional jamming than present MIMO systems which only utilize a handful of antennas. On

the other hand, the hardware cost for such a system becomes expensive due to a large number of antenna arrays requirements. In order to reduce the cost, the inexpensive or less accurate transmitter/receiver chain components such as low-resolution ADC, digital to analog converter (DAC) [10], low-cost power amplifiers are preferred. Usage of these less efficient components and their ageing over time will introduce more hardware distortion to the system.

Another benefit of mMIMO is that it can support more users by utilizing spatial multiplexing. In spatial multiplexing, users in different locations will be served by separate narrow beams by employing beamforming techniques that utilize the large-scale antenna array. In the current wireless communication systems, different multiple access techniques are available in different domains such as code (code division multiple access (CDMA)), time (time division multiple access (TDMA)) and frequency (frequency division multiple access (FDMA)).

A wireless multi-carrier (MC) communication system utilizes the frequency domain for multiple access. There are different variant of MC systems currently available such as filter bank multi carrier (FBMC), generalised frequency division multiplexing (GFDM), OFDM, to name a few. In current 4G (LTE) mobile network system, the MC systems used to serve multiple users is OFDM access technique, where orthogonal frequencies are assigned to different users. For the upcoming 5G New Radio (NR) network system, mixed numerology OFDM is considered as the multiple access technique [11, 12]. In an OFDM system, since the frequencies are orthogonal to each other, ideally there should not be any inter-carrier leakage (ICL). However for an MC system, even in an OFDM system, the non-linear hardware distortions at the transmit and receive chains lead to ICL. In case of an FD MC system, due to the ICL, even if one of the sub-carriers is employed with a high-power transmission will introduce a higher residual SI in all of the sub-carrier channels.

Incorporating both mMIMO and FD into an MC system can lead to higher spectral efficiency, enjoying their mutual benefits. High spatial diversity and co-existence of transmission and reception capabilities of mMIMO FD transceiver systems have shown great potential in various paradigms of wireless communications such as relay system, bidirectional communication, cellular networks, physical layer security, radar systems and spectrum sensing. However, in an FD mMIMO MC system, it is essential to have a distortion-aware design which considers the impact of distortions due to the hardware impairments.

1.1 Self Interference Cancellation Techniques

As mentioned earlier, the feasibility of FD communication systems relies on efficient SIC techniques. Since the power of the SI is very high compared to signal-of-interest, the

receiver circuitry (e.g., ADC) becomes saturated while converting the SI and signal-of-interest simultaneously. The conversion can be only done if SI is sufficiently removed in the analog domain to fall within the dynamic range of the ADC. The SIC techniques are mainly classified as passive and active cancellation techniques in radio frequency (RF) domain and digital SI cancellation in the baseband domain.

Passive Cancellation

Passive cancellation is done in the RF domain, where the SI is attenuated (isolated) from propagating the transmit side to the receiver side. This can be attained by implementing cross-polarization, physical separation of transmit and receive antennas, directional isolation and RF absorptive shielding [2, 13]. Furthermore, 3-port RF-circulator can be utilized to attain passive isolation if the antennas are shared for both transmission and reception [14]. The techniques such as directional isolation, RF absorptive shielding and cross-polarization are very effective in suppressing the direct path between the transmit and receive antennas. However, they are not necessarily useful in suppressing reflected SI paths [2]. Hence, for the practical environment, passive cancellation techniques alone are not sufficient, i.e., a combination of passive and active cancellation techniques are necessary.

Active Cancellation

The active cancellation techniques are done in the RF domain by exploiting the knowledge of its own transmit signal to mitigate SI. The main goal in active RF cancellation techniques is to cancel the SI signal in the RF domain by subtracting a copy of the predicted SI signal before reaching the sensitive receiver chain components. Two main approaches in active RF cancellation techniques are antenna cancellation and signal injection.

In the antenna cancellation technique, an additional transmit antenna is utilized to create a null position at the location of the receiver antenna to nullify the signal from the actual transmit antenna [1, 15, 16]. However, this approach is signal bandwidth sensitive and leads to performance degradation in SIC in wide bandwidth scenarios. This problem can be overcome by adopting a pair-wise symmetric antenna placement [17]. Unlike in antenna cancellation techniques where the cancellation is attained by on-air transmissions, the signal injection approach relies on direct injection of reconstructed SI signal. There are different ways to reconstruct the SI signal for SIC. One idea is to tap the up-converted transmit signal at the transmit chain and process it, for example using attenuators and phase shift units, to generate the estimate of the SI signal. In [8, 14], a copy of the tapped transmit signal is fed to the analog cancellation circuit, which consists of fixed lines of varying delays (wires with different lengths) and a tunable attenuator. The main challenge is to choose the fixed delays and to tune the attenuator in order to

maximize the SIC. Furthermore in [18], signal inversion uses a simple design based on a balanced/unbalanced (Balun) transformer and variable attenuators and delay lines are used to cancel the SI. Another idea to reconstruct the estimate of the SI signal is by utilizing an additional transmit chain [19–21]. This reconstructed signal is then subtracted from the received signal right after the reception. However, usage of an auxiliary chain may result in more transmit distortion. After attenuating the SI by applying the passive and active cancellation techniques to a level below the saturation point of receiver chain components, the received signal can be down-converted. The down-converted signal needs to be further processed in the digital domain to remove the residual SI.

Digital Domain Cancellation

Compared to analog domain processing, the main advantage of digital domain cancellation is that even sophisticated processing becomes relatively easy by exploiting advanced digital signal processing techniques. Digital processing is suited to mitigate the SI signal due to the reflective paths (non-line of sight (NLOS) component). Digital SI canceler subtracts the estimated residual SI after the passive and active cancellation from the received down-converted (baseband) signal in the digital domain [14, 22]. At the transmit side, transmit beamforming has been widely used to spatially suppress the SI [5, 23, 24] and to limit the SI power by adding it as a constraint [25]. Furthermore, receive beamforming can also be used for SIC. By adaptively adjusting the receive beamforming weights corresponding to the SI channel condition, the SI can be attenuated. Due to analog-circuit complexity, the receive beamforming is commonly used in digital domain [5,26]. Moreover, the impact of hardware distortion due to non-linearities of the transmit and receive chains can be cancelled out by employing non-linear signal processing at the receiver [14, 27–31].

1.2 Full Duplex Relaying

One of the promising applications of FD capability is on relay systems. A relay node assists communication between a source and a destination by receiving the signal from the source and retransmitting it to the destination. In a relay network, the transmit power required per node can be reduced when compared to direct transmission, thereby making the entire relay communication more energy efficient. In other words, the source node (mostly with limited power) does not need to transmit at high power to communicate with the destination which is located far from the source. However, in traditional relay systems, the reception and retransmission frequencies are kept different in order to avoid SI. Otherwise, the relay has to receive the entire transmit signal first, then retransmits it to the destination in the successive time slot leading to higher latency to the communication. While in an FD relay, simultaneous transmission and reception in

the same frequency-time channel result in SI. The SI signal at the relay is very strong compared to the desired received signal due to the close proximity of transmit and receive front ends. The SI signals saturate the limited dynamic range of the receiver chain components at the relay. The advancement of SIC contributed to consideration of relays that are capable of transmitting and receiving at the same frequency and are referred to as FD relays. In [5], a wide range of SI mitigation schemes, i.e., natural isolation, time-domain cancellation, and spatial suppression such as antenna selection, beam selection and null space projection are analyzed for an FD MIMO relay. The main idea behind spatial suppression schemes are receiving and transmitting in orthogonal subspaces, or joint transmit and receive beam selection to support more spatial streams by choosing the minimum eigenmodes for overlapping subspaces. In [5, 32], various SI mitigation schemes for an FD MIMO relay are discussed in detail. The performance of SIC in mMIMO FD system is analyzed in [33]. The authors show that SI-subtraction outperforms the spatial suppression for SIC in a perfect channel estimation case, and spatial suppression performs relatively better than the SI-subtraction in an imperfect channel estimation case. A combination of different SIC techniques is required to be utilized in order to make FD relaying feasible.

In general, amplify and forward (AF) and decode and forward (DF) are two familiar relaying schemes. In AF relaying, the relay amplifies the received signal and forwards it towards the destination. Thus, AF relaying technique is much simpler and better in terms of less complexity as compared to DF. However, this relaying scheme in the FD system suffers from noise amplification as well as distortion amplification resulting in a distortion loop [34]. This can be avoided in the DF scheme where the relay first decodes the signal received from the source, re-encodes and then retransmits it to the destination. In this thesis, since we consider an FD multi-antenna relay system with hardware impairments, it will be more beneficial to opt DF as the relaying scheme to avoid retransmission of the distortion loop interference, thereby increasing the reliability of the system.

The resource allocation problems are addressed for an FD relaying system by utilizing AF protocols in [34–36] and DF in [37–39]. In [40–42], the application of FD relays is considered for the context of simultaneous wireless information and power transfer (SWIPT) and wireless-powered relay. The works in [43, 44] address the problem of secrecy rate maximization in a relay wire-tap channel by exploiting the FD capability of the relay and show that a significantly higher secrecy rate can be achieved compared to an HD relaying. The resource allocation problem is investigated for the FD relays that assist device-to-device communication underlying cellular networks in [45–48] and cognitive radio networks in [49]. As mentioned earlier, having a large-antenna array provides more spatial diversity to the relay, thereby improving spectral and energy efficiency compared to the MIMO relay. The resource allocation problem to improve the spectral or energy efficiency of FD mMIMO relaying are studied in [38, 50–53]. In this thesis, we discuss different communication scenarios that perform better with the aid of an FD relay such as MIMO source-destination pair, multi-user scenarios and dual connectivity.

1.3 Thesis Outline

The goal of this thesis is to investigate the resource allocation problem for multi-antenna FD MC communication systems by taking into account the impact of the distortions caused by hardware impairments and the impact of imperfect channel state information (CSI). In the following subsections, an outline and main contributions of this thesis are summarized.

Chapter 2: Hardware Impairments-aware Linear Transceiver Design for Multi-carrier FD MIMO DF Relaying

In Chapter 2, we discuss the linear precoding and decoding design problem for an FD MC DF relaying system. We consider the effects of hardware distortions, which contribute to residual SI and ICL. The impact of the imperfect channel estimation is also taken into account. Initially, the problem of linear precoding and decoding design is studied to maximize the system sum-rate, leading to a non-convex optimization problem. Then, the design is extended to power minimization and energy efficiency maximization. In addition to the traditional per-carrier coding strategy, the case with a joint-carrier coding strategies is also studied, taking advantage of the group-wise decoding and encoding. An alternating quadratic convex program (AQCP) is then proposed for sum-rate maximization and power minimization problem, with a monotonic improvement at each iteration, leading to a guaranteed convergence. The proposed AQCP framework is then extended, employing the Dinkelbach algorithm, to solve the energy efficiency maximization problem. We investigate the operation of an FD MIMO MC DF relay system for different system parameters such as hardware inaccuracies, imperfect CSI, to name a few, using numerical simulations. Numerical simulations show a significant gain in performance of the proposed algorithms in terms of the end-to-end system sum-rate and energy efficiency compared to HD counterparts or to the solutions where the impact of impairments are not considered, particularly when the hardware distortions leading to residual SI and ICL become a dominant factor.

Chapter 3: Resource Allocation for Multi-user Multi-carrier FD mMIMO DF Relay System with Hardware Impairments

In Chapter 3, we extend our model to mMIMO scenario, where we investigate the resource allocation problem for an FD mMIMO MC DF relay system which serves multiple MC HD single antenna source-destination pairs. In addition to the prior studies focusing on maximizing the sum-rate and energy efficiency, we also focus on minimizing the overall delivery time for a given set of communication tasks to the user terminals. As our system is an FD MC system, we consider the impact of hardware distortions resulting in residual SI and ICL. We also consider that only limited CSI is available. We analyze the asymptotic rate of our system employed with maximum ratio transmitting (MRT)/maximum ratio combining (MRC) strategy, when the number of antenna

becomes large (goes to ∞). It is noticed that the impact of hardware distortion becomes significant in a large-scale antenna array regime. A joint power and sub-carrier allocation problem to maximize the sum-rate of the system is then formulated. Due to the intractable nature of the underlying problem, an iterative solution is proposed, employing the successive inner approximation (SIA) framework, with guaranteed convergence to the point that satisfies the Karush–Kuhn–Tucker (KKT) conditions. A similar algorithm that follows SIA framework is also proposed to solve the delivery time minimzation problem.

For the energy efficiency maximization problem, a double-loop iterative algorithm which follows the SIA and Dinkelbach algorithm is proposed. The operation of an FD mMIMO MC DF relay system is evaluated for different system parameters using numerical simulations. We also show that the importance of considering delivery time minimization rather than the sum-rate maximization, i.e., maximizing the sum-rate of the system does not necessarily minimize the overall delivery time. Numerical results show the significance of distortion-aware design for such systems and also the significant gain in terms of different objectives such as sum-rate, energy efficiency, and delivery time compared to its HD counterpart.

Chapter 4: Resource Allocation for Multi-carrier FD mMIMO Bidirectional Communication with Hardware Impairments

In the previous chapter, Chapter 3, we investigated an FD mMIMO MC DF relay system where the source and destination nodes are HD nodes. In this chapter, Chapter 4, we consider the resource allocation problem for a bidirectional MC communication system, where an FD mMIMO base station (BS) node communicates with multiple single antenna FD user nodes. Here, the spectral efficiency is measured as the sum of uplink and downlink sum-rate that can be achieved by the FD users. The impact of hardware distortions resulting in residual SI and ICL, and also imperfect CSI are jointly taken into account. We formulate a joint sub-carrier and power allocation problem to maximize the spectral efficiency (sum-rate maximization), and an iterative optimization method is proposed which follows SIA framework to reach the convergence point that satisfies the KKT conditions. Here, a quadratic approximation of our achievable rate function is utilized to transform our non-convex optimization problem into a convex problem. Later, we consider an energy efficiency maximization problem which is solved using a double-loop iterative algorithm that follows the SIA and Dinkelbach algorithm. It is observed that a notable gain can be achieved by such FD-enabled systems compared to the traditional HD systems. It is also noticed that the implementation of hardware distortion-aware design is essential for such bidirectional communication systems, especially in high signal to interference plus noise ratio (SINR) or high transceiver distortion scenario.

Chapter 5: Full-Duplex Relaying: Enabling Dual Connectivity via Impairments-aware Successive Interference Cancellation

In Chapter 5, we address the problem of resource allocation for the downlink of a cellular communication network, where dual connectivity (DuC) at the end-users is enabled with the assistance of an FD relay. In particular, the BS transmits separated data streams through the co-channel direct link as well as the FD relay channel, utilizing the successive interference cancellation (SuIC) capability at the receiver. In addition to the superior performance under various system conditions, the proposed DuC enjoys higher robustness when one of the active paths experience an unexpected blockage.

As an initial setup, we consider a single-user scenario, where the relay is an FD single antenna node. In this regard, we formulate a joint power and sub-carrier allocation problem to maximize the total sum-rate, incorporating the impact of hardware distortions resulting in residual SI and ICL, and also imperfect CSI. An iterative solution is proposed for the non-convex underlying problem, utilizing the SIA framework, with guaranteed convergence to a solution satisfying the KKT optimality conditions. Then we extend our system to a multi-user scenario, where an FD mMIMO relay assists the DuC mode. We also discuss the resource allocation problem for a multi-user HD relay system enabling DuC. Numerical results show performance and roboustness gain of our proposed SuIC scheme in terms of sum-rate compared to previously proposed single-connectivity and HD schemes.

A summary of the main findings and an outlook for the related future research directions are given in Chapter 6.

Parts of this thesis were already published or under consideration for publication in [54–63].

1.4 Mathematical Notations and Conventions

Throughout the thesis, the following mathematical notations and conventions are used. Scalar values are represented using normal italic letters (a). Lower-case and upper-case bold letters are used to denote vectors ($\mathbf{a}$) and matrices ($\mathbf{A}$), respectively. Identity matrix with dimension K is denoted by $\mathbf{I}_K$.

We use $\mathbb{E}\{.\}$, $|.|$, $\mathrm{Tr}(.)$, $(.)^{-1}$, $(.)^*$, $(.)^T$ and $(.)^H$ for mathematical expectation, determinant, trace, inverse, conjugate, transpose and Hermitian transpose, respectively. The Kronecker product is denoted by $\otimes$. The statistical independence is denoted by $\perp$. A complex Gaussian distribution with mean $\mathbf{a}$ and variance $\mathbf{A}$ is denoted as $\mathcal{CN}(\mathbf{a}, \mathbf{A})$. We use diag(.) for the diag operator, which returns a diagonal matrix by setting off-diagonal elements to zero. All-zero matrix of size $m \times n$ is denoted by $\mathbf{0}_{m\times n}$. Euclidean norms and Frobenius norms are respectively denoted as $\|.\|_2$ and $\|.\|_F$. The l-th element (column) of the vector $\mathbf{a}$ (matrix $\mathbf{A}$) is denoted by $\lfloor \mathbf{a} \rfloor_l$ ($\lfloor \mathbf{A} \rfloor_l$). We define delta function δ_{km} such that $\delta_{km} = 1$ when $k = m$, otherwise $\delta_{km} = 0$. We denote the set of real, positive real, and complex numbers as $\mathbb{R}$, $\mathbb{R}^+$ and $\mathbb{C}$, respectively. We use $\overline{\overline{\mathbb{A}}}$ for the cardinality of a set $\mathbb{A}$.

2 Hardware Impairments-aware Linear Transceiver Design for Multi-carrier FD MIMO DF Relaying

2.1 Scope

Full-duplex (FD) relay systems have received recognition as they are one of the cost-effective solutions for throughput enhancement, system reliability, energy savings and coverage extension. By simultaneous reception and transmission on the same frequency channel, FD relaying can compensate for the spectral loss due to conventional half-duplex (HD) relaying, with an expense of self-interference (SI). Utilizing multiple input multiple output (MIMO) in relaying has also attracted research interest as it can increase spectral efficiency by spatial division multiplexing technique. Apart from spectral efficiency enhancement, MIMO relaying provides an opportunity to enable FD operation through spatial SI suppression [5]. However, the impact of hardware inaccuracies/impairments become significant for these FD systems compared to the HD, due to the presence of strong SI. In this chapter we consider FD MIMO multi-carrier (MC) relay system, it is essential to incorporate the impact of the hardware distortions into the transceiver design as the non-linear distortions introduce residual SI as well as inter-carrier leakage (ICL). We also consider the relay utilizes decode and forward (DF) relaying scheme to avoid retransmission of the distortion (distortion-loop interference).

2.2 Related Works

In [37], the authors have proposed a design strategy for a single-carrier multi-user FD DF relaying system to overcome its own loop-back SI, and also provide a solution to the case with erroneous channel state information (CSI) following the worst-case enhancement approach. The simultaneous wireless information and power transfer (SWIPT) for an FD DF relay network is investigated in [64]. The outage probability has been derived for multi-hop FD relaying in [65], for orthogonal frequency division multiplexing (OFDM) FD relaying systems in [66], and for FD DF two-way relay systems in [67]. Furthermore,

[68] shows that by optimally allocating transmit power to an FD MIMO DF relay, a significant spectral efficiency gain can be attained over conventional HD relay, provided that the relay SI is blocked well. In [69], the authors derive the optimal structure of both the source precoding matrix as well as the relay amplifying matrix for the FD MIMO OFDM DF relay networks in order to minimize the overall transmission power from source and relay subject to a given set of quality of service (QoS) constraints. In the works mentioned above, the hardware inaccuracies or hardware distortions are not taken into account.

In [70], the authors have proposed a transmission scheme based on the maximization of the lower bound on the end-to-end achievable rate of DF based FD MIMO relay systems under limited dynamic range. Whereas in [71], a convergent block coordinate ascent algorithm is developed for maximization of end-to-end achievable rate of the same system. The outage analysis of an FD DF relaying with the limited dynamic range of the analog to digital converter (ADC) is studied in [72]. The authors have derived the optimal transmit power of the relay to minimize the outage probability. In the above-mentioned works, the authors consider the impact of hardware distortions for a single carrier system.

2.3 Chapter Outline

In this chapter, we study an FD MC MIMO DF relaying system, where the effect of hardware distortions and imperfect CSI are jointly taken into account. In Section 2.4, we model the operation of the FD MC MIMO DF relaying system. We also formulate the impact of hardware inaccuracy with regard to the intended transmit/received signal as well as the impact of imperfect CSI. In Section 2.5, we devise the linear transceiver design problem for sum-rate maximization, power minimization and energy efficiency maximization. Moreover, we extend the traditional per-carrier (PC) coding into a joint-carrier (JC) coding strategy, where the information decoded in one sub-carrier can be forwarded via another sub-carrier. An alternating quadratic convex program (AQCP) is proposed for sum-rate maximization and power minimization problem. The proposed AQCP framework is then extended, employing the Dinkelbach algorithm, in order to maximize the system energy efficiency. In Section 2.6, we analyse the arithmetic computational complexity of the sum-rate maximization algorithm. In Section 2.7, the performance of the proposed designs is evaluated and compared with the available designs in the literature. The main results of this chapter are summarized in Section 2.8.

2.4 System Model

We consider an FD MC MIMO DF relay which connects an HD MC MIMO source node equipped with N_{s} transmit antenna to an HD MC MIMO destination node equipped

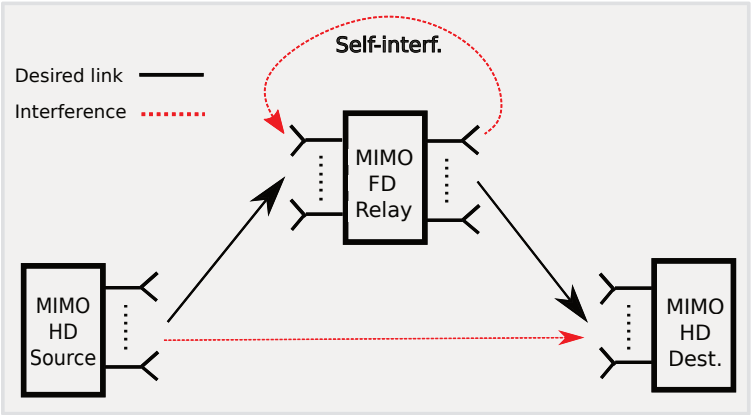

Figure 2.1: Basic system model for FD MIMO relay communication between an HD MIMO source and an HD MIMO destination node.

with M_d receive antennas. A basic model of our system is depicted in Fig 2.1. The number of transmit and receive antennas at the relay can be denoted as N_r and M_r, respectively. Initially, the source transmits the signal to the relay through the channel $\mathbf{H}_{\mathrm{sr}}^{k} \in \mathbb{C}^{M_\mathrm{r} \times N_\mathrm{s}}$ with sub-carrier $k \in \mathbb{K}$, where $\mathbb{K} := \{1, 2, ..., K\}$ and K is the total number of sub-carriers. At the relay, after applying self-interference cancellation (SIC), the received signal is decoded. Then, the relay transmits the decoded signal to the destination through the channel $\mathbf{H}_{\mathrm{rd}}^{k} \in \mathbb{C}^{M_d \times N_\mathrm{r}}$. Due to SI at the relay, a part of the relay transmit signal is received by the relay itself through the SI channel $\mathbf{H}_{\mathrm{rr}}^{k} \in \mathbb{C}^{M_\mathrm{r} \times N_\mathrm{r}}$. Similar to [70, 73], we also consider a weak signal (due to path loss) from the source is received at the destination through the direct channel $\mathbf{H}_{\mathrm{sd}}^{k} \in \mathbb{C}^{M_d \times N_\mathrm{s}}$, which is considered as interference. We assume all channels are constant for each frame, frequency flat in each sub-carrier and only the imperfect CSI is known.

2.4.1 Imperfect Channel State Information

We adapt the channel error model used in [70, 74], where the true channel can be decomposed into the estimated channel plus estimation error, which can be stated as

$$\mathbf{H}_{\mathcal{X}} = \widehat{\mathbf{H}}_{\mathcal{X}} + \widetilde{\mathbf{H}}_{\mathcal{X}}, \quad \widetilde{\mathbf{H}}_{\mathcal{X}} = \mathbf{D}_{\mathcal{X}}^{\frac{1}{2}} \mathbf{\Delta}_{\mathcal{X}}, \tag{2.1}$$

where $\mathcal{X} \in \{\mathrm{sr}, \mathrm{rd}, \mathrm{rr}, \mathrm{sd}\}$, $\widehat{\mathbf{H}}_{\mathcal{X}}$ represents the estimated channel, and the entries of $\mathbf{\Delta}_{\mathcal{X}}$ are independent and identically distributed (i.i.d.) complex Gaussian with zero mean and a variance of one. $\mathbf{D}_{\mathcal{X}}$ shapes the spatial covariance matrix of the CSI estimation error. However, we consider that the receiver performs a minimum mean

square error (MMSE) channel estimation. We also assume that the estimated channel and estimation error becomes uncorrelated, i.e., $\widehat{\mathbf{H}}_{\mathcal{X}} \perp \widetilde{\mathbf{H}}_{\mathcal{X}}$.

2.4.2 Source to Relay

The transmitted signal from the source can be written as

$$\mathbf{x}_{\mathrm{s}}^{k} = \underbrace{\boldsymbol{V}_{\mathrm{s}}^{k}\mathbf{s}_{\mathrm{s}}^{k}}_{=:\widetilde{\mathbf{x}}_{\mathrm{s}}^{k}} + \mathbf{e}_{\mathrm{t,s}}^{k}, \tag{2.2}$$

where $\mathbf{s}_{\mathrm{s}}^{k} \in \mathbb{C}^{d_{\mathrm{s}}}$, $\boldsymbol{V}_{\mathrm{s}}^{k} \in \mathbb{C}^{N_{\mathrm{s}} \times d_{\mathrm{s}}}$, and $\mathbf{e}_{\mathrm{t,s}}^{k} \in \mathbb{C}^{N_{\mathrm{s}}}$ represent the data symbol, the transmit precoding matrix and transmit distortion at the source, respectively. The number of data streams in each sub-carrier from the source is denoted by d_{s} and $\mathbb{E}\{\mathbf{s}_{\mathrm{s}}^{k}\mathbf{s}_{\mathrm{s}}^{k\,H}\} = \mathbf{I}_{d_{\mathrm{s}}}$. Furthermore, $\widetilde{\mathbf{x}}_{\mathrm{s}}^{k}$ represents the desired signal to be transmitted from the source. Accordingly, the received signal at the relay can be written as

$$\mathbf{y}_{\mathrm{r}}^{k} = \underbrace{\mathbf{H}_{\mathrm{sr}}^{k}\mathbf{x}_{\mathrm{s}}^{k} + \mathbf{H}_{\mathrm{rr}}^{k}\mathbf{x}_{\mathrm{r}}^{k} + \mathbf{n}_{\mathrm{r}}^{k}}_{=:\widetilde{\mathbf{y}}_{\mathrm{r}}^{k}} + \mathbf{e}_{\mathrm{r,r}}^{k}, \tag{2.3}$$

where $\mathbf{n}_{\mathrm{r}}^{k} \sim \mathcal{CN}\left(\mathbf{0}_{M_{\mathrm{r}}}, \sigma_{\mathrm{r},k}^{2}\mathbf{I}_{M_{\mathrm{r}}}\right)$ and $\mathbf{e}_{\mathrm{r,r}}^{k}$ are the receiver noise and receive distortion at the relay, respectively. The transmitted signal from the relay is denoted by $\mathbf{x}_{\mathrm{r}}^{k}$. Moreover, $\widetilde{\mathbf{y}}_{\mathrm{r}}^{k}$ represents the intended (distortion-free) signal to be received at the relay. The distortion-free (known) part of the SI can be removed by applying a SIC. The received signal after SIC can be stated as

$$\overline{\mathbf{y}}_{\mathrm{r}}^{k} = \mathbf{y}_{\mathrm{r}}^{k} - \widehat{\mathbf{H}}_{\mathrm{rr}}^{k}\boldsymbol{V}_{\mathrm{r}}^{k}\mathbf{s}_{\mathrm{r}}^{k} = \widehat{\mathbf{H}}_{\mathrm{sr}}^{k}\boldsymbol{V}_{\mathrm{s}}^{k}\mathbf{s}_{\mathrm{s}}^{k} + \boldsymbol{\nu}_{\mathrm{r}}^{k}, \tag{2.4}$$

where $\boldsymbol{V}_{\mathrm{r}}^{k} \in \mathbb{C}^{N_{\mathrm{r}} \times d_{\mathrm{r}}}$ and $\mathbf{s}_{\mathrm{r}}^{k}$ represent the transmit precoding matrix and retransmitted symbol at the relay, respectively. The collective interference-plus-noise at the relay can be represented as

$$\boldsymbol{\nu}_{\mathrm{r}}^{k} = \widetilde{\mathbf{H}}_{\mathrm{sr}}^{k}\boldsymbol{V}_{\mathrm{s}}^{k}\mathbf{s}_{\mathrm{s}}^{k} + \mathbf{H}_{\mathrm{sr}}^{k}\mathbf{e}_{\mathrm{t,s}}^{k} + \widetilde{\mathbf{H}}_{\mathrm{rr}}^{k}\boldsymbol{V}_{\mathrm{r}}^{k}\mathbf{s}_{\mathrm{r}}^{k} + \mathbf{H}_{\mathrm{rr}}^{k}\mathbf{e}_{\mathrm{t,r}}^{k} + \mathbf{n}_{\mathrm{r}}^{k} + \mathbf{e}_{\mathrm{r,r}}^{k}, \tag{2.5}$$

where $\mathbf{e}_{\mathrm{t,r}}^{k} \in \mathbb{C}^{N_{\mathrm{r}}}$ denotes the transmit distortion at the relay. The estimated signal vector at the relay can be obtained as

$$\widetilde{\mathbf{s}}_{\mathrm{s}}^{k} = \left(\boldsymbol{U}_{\mathrm{r}}^{k}\right)^{H}\overline{\mathbf{y}}_{r}^{k}, \tag{2.6}$$

where $\boldsymbol{U}_{\mathrm{r}}^{k} \in \mathbb{C}^{M_{\mathrm{r}} \times d_{\mathrm{s}}}$ represents the linear receive filter at the relay.

2.4.3 Relay to Destination

The transmitted signal from the relay can be written as

$$\mathbf{x}_{\mathrm{r}}^{k} = \underbrace{\boldsymbol{V}_{\mathrm{r}}^{k}\mathbf{s}_{\mathrm{r}}^{k}}_{=:\widetilde{\mathbf{x}}_{\mathrm{r}}^{k}} + \mathbf{e}_{\mathrm{t,r}}^{k}, \tag{2.7}$$

where $\widetilde{\mathbf{x}}_{\mathrm{r}}^{k}$ represents the desired signal to be transmitted from the relay. The number of data streams in each sub-carrier from the relay is denoted by d_{r} and $\mathbb{E}\{\mathbf{s}_{\mathrm{r}}^{k}\mathbf{s}_{\mathrm{r}}^{kH}\} = \mathbf{I}_{d_{\mathrm{r}}}$. Consequently, the signal received at the destination including the interference from the source can be written as

$$\begin{aligned}\mathbf{y}_{\mathrm{d}}^{k} =& \underbrace{\mathbf{H}_{\mathrm{rd}}^{k}\mathbf{x}_{\mathrm{r}}^{k} + \mathbf{H}_{\mathrm{sd}}^{k}\mathbf{x}_{\mathrm{s}}^{k} + \mathbf{n}_{\mathrm{d}}^{k}}_{=:\widetilde{\mathbf{y}}_{\mathrm{d}}^{k}} + \mathbf{e}_{\mathrm{r,d}}^{k} \\ =& \mathbf{H}_{\mathrm{rd}}^{k}\boldsymbol{V}_{\mathrm{r}}^{k}\mathbf{s}_{\mathrm{r}}^{k} + \mathbf{H}_{\mathrm{rd}}^{k}\mathbf{e}_{\mathrm{t,r}}^{k} + \mathbf{H}_{\mathrm{sd}}^{k}\boldsymbol{V}_{\mathrm{s}}^{k}\mathbf{s}_{\mathrm{s}}^{k} + \mathbf{H}_{\mathrm{sd}}^{k}\mathbf{e}_{\mathrm{t,s}}^{k} + \mathbf{n}_{\mathrm{d}}^{k} + \mathbf{e}_{\mathrm{r,d}}^{k},\end{aligned} \tag{2.8}$$

where $\mathbf{n}_{\mathrm{d}}^{k} \sim \mathcal{CN}\left(\mathbf{0}_{M_{\mathrm{d}}}, \sigma_{\mathrm{d},k}^{2}\mathbf{I}_{M_{\mathrm{d}}}\right)$ and $\mathbf{e}_{\mathrm{r,d}}^{k}$ are the receiver noise and receive distortion at the destination, respectively. Furthermore, $\widetilde{\mathbf{y}}_{\mathrm{d}}^{k}$ represents the intended (distortion-free) signal to be received at the destination. The direct link is considered as an interference at the destination as its signal power is very weak (due to path loss). Accordingly, the collective interference-plus-noise at the destination can be stated as

$$\boldsymbol{\nu}_{\mathrm{d}}^{k} = \widetilde{\mathbf{H}}_{\mathrm{rd}}^{k}\boldsymbol{V}_{\mathrm{r}}^{k}\mathbf{s}_{\mathrm{r}}^{k} + \mathbf{H}_{\mathrm{rd}}^{k}\mathbf{e}_{\mathrm{t,r}}^{k} + \mathbf{H}_{\mathrm{sd}}^{k}\boldsymbol{V}_{\mathrm{s}}^{k}\mathbf{s}_{\mathrm{s}}^{k} + \mathbf{H}_{\mathrm{sd}}^{k}\mathbf{e}_{\mathrm{t,s}}^{k} + \mathbf{n}_{\mathrm{d}}^{k} + \mathbf{e}_{\mathrm{r,d}}^{k}. \tag{2.9}$$

The estimated signal vector at the destination can be obtained as

$$\widetilde{\mathbf{s}}_{r}^{k} = \left(\boldsymbol{U}_{\mathrm{d}}^{k}\right)^{H}\mathbf{y}_{\mathrm{d}}^{k}, \tag{2.10}$$

where $\boldsymbol{U}_{\mathrm{d}}^{k} \in \mathbb{C}^{M_{\mathrm{d}} \times d_{\mathrm{r}}}$ is the linear receive filter at the destination.

2.4.4 Limited Dynamic Range

The inaccuracies of hardware components such as ADC and digital to analog converter (DAC) error, noises caused by power amplifiers, automatic gain control (AGC) and oscillator on transmit and receive chains are jointly modelled for FD MIMO transceiver in [70, 74], based on [20, 75–77]. The hardware inaccuracies of the transmit (receive) chain for each antenna is jointly modelled as an additive distortion and can be expressed as

$$\begin{aligned}x_{l}(t) &= \widetilde{x}_{l}(t) + e_{\mathrm{t},l}(t) \\ y_{l}(t) &= \widetilde{y}_{l}(t) + e_{\mathrm{r},l}(t),\end{aligned} \tag{2.11}$$

such that,

$$\begin{aligned}&e_{\mathrm{t},l}(t) \sim \mathcal{CN}\left(0, \kappa_{l}\mathbb{E}\{|\widetilde{x}_{l}(t)|^{2}\}\right),\ e_{\mathrm{t},l}(t) \perp \widetilde{x}_{l}(t),\ e_{\mathrm{t},l}(t) \perp e_{\mathrm{t},l'}(t),\ e_{\mathrm{t},l}(t) \perp e_{\mathrm{t},l}(t'),\ l \neq l',\ t \neq t' \\ &e_{\mathrm{r},l}(t) \sim \mathcal{CN}\left(0, \beta_{l}\mathbb{E}\{|\widetilde{y}_{l}(t)|^{2}\}\right),\ e_{\mathrm{r},l}(t) \perp \widetilde{y}_{l}(t),\ e_{\mathrm{r},l}(t) \perp e_{\mathrm{r},l'}(t),\ e_{\mathrm{r},l}(t) \perp e_{\mathrm{r},l}(t'),\ l \neq l',\ t \neq t',\end{aligned} \tag{2.12}$$

i.e., the distortion terms are proportional to the intensity of the intended signals.

In [59], we discuss the characterization of the impact of these hardware distortions in the frequency domain for an OFDM system. In this thesis, we extend this characterization for a general orthonormal MC strategy, where the sub-carriers k are orthogonal to each other with a linear transformation, for example orthogonal variable spreading factor (OVSF)-MC-code division multiple access (CDMA), OFDM and cyclic prefix (CP)-OFDM. Let $\mathbf{Q}$ be a $N \times K$ transformation matrix with $\mathbf{Q}^H\mathbf{Q} = \mathbf{I}_K$ and $N \geq K$, where the columns of the matrix $\mathbf{Q}$ represent the basis of the generalized sub-carrier waveforms which are orthonormal to each other. The total number of sub-carriers is K. NT_s is the duration of one communication block, where T_s is the sample period.

The linear transformation representation of the sampled time domain signal for each communication block can be written as

$$\begin{aligned} x_l^k &= \sum_{n=0}^{N-1} x_l(nT_\mathrm{s}) q_{n,k}^* = \underbrace{\sum_{n=0}^{N-1} \widetilde{x}_l(nT_\mathrm{s}) q_{n,k}^*}_{=:\widetilde{x}_l^k} + \underbrace{\sum_{n=0}^{N-1} e_{\mathrm{t},l}(nT_\mathrm{s}) q_{n,k}^*}_{=:e_{\mathrm{t},l}^k} \\ y_l^k &= \sum_{n=0}^{N-1} y_l(nT_\mathrm{s}) q_{n,k}^* = \underbrace{\sum_{n=0}^{N-1} \widetilde{y}_l(nT_\mathrm{s}) q_{k,n}^*}_{=:\widetilde{y}_l^k} + \underbrace{\sum_{n=0}^{N-1} e_{\mathrm{r},l}(nT_\mathrm{s}) q_{n,k}^*}_{=:e_{\mathrm{r},l}^k}, \end{aligned} \tag{2.13}$$

where $q_{n,k}^*$ is the element of the transformation matrix $\mathbf{Q}$ at the n-th row and k-th column.

Lemma 2.4.1. *Let us define $\widetilde{x}_l^m$ and $\widetilde{y}_l^m$ as the intended transmit and receive signal via m-th sub-carrier at the l-th transmit/receive chain. The impact of hardware distortions in the linear transformed domain is characterized as*

$$e_{t,l}^k \sim \mathcal{CN}\left(0, \frac{\widetilde{\kappa}_l}{K} \sum_{m=1}^{K} \mathbb{E}\left\{|\widetilde{x}_l^m|^2\right\}\right), \quad e_{t,l}^k \perp \widetilde{x}_l^p, \quad e_{t,l}^k \perp e_{t,l'}^k, \quad \forall p \in \mathbb{K} \tag{2.14}$$

$$e_{r,l}^k \sim \mathcal{CN}\left(0, \frac{\widetilde{\beta}_l}{K} \sum_{m=1}^{K} \mathbb{E}\left\{|\widetilde{y}_l^m|^2\right\}\right), \quad e_{r,l}^k \perp \widetilde{y}_l^p, \quad e_{r,l}^k \perp e_{r,l'}^k, \quad \forall p \in \mathbb{K}, \tag{2.15}$$

transforming the statistical independence, as well as the proportional variance properties from the time domain. Here, K represents the total number of sub-carriers. $\widetilde{\kappa}_l$ and $\widetilde{\beta}_l$ correspond to the transmit and receive distortion coefficient at the l-th transmit/receive chain.

Proof. The time domain statistical independence $e_{\mathrm{t},l}(t) \perp \widetilde{x}_l(t)$ and $e_{\mathrm{t},l}(t) \perp e_{\mathrm{t},l'}(t)$, and the linear nature of the transformation (2.13) are also applicable to the statistical independence properties at the transformed domain. Similarly, the Gaussian and zero-mean properties for $e_{\mathrm{t},l}^k$ becomes a linearly weighted sum of the zero-mean Gaussian values

$e_{\mathrm{t},l}(mT_s)$. The variance of $e^k_{\mathrm{t},l}$ can hence be obtained as

$$\mathbb{E}\left\{\left|e^k_{\mathrm{t},l}\right|^2\right\} = \mathbb{E}\left\{\left(\sum_{m=0}^{N-1} e_{\mathrm{t},l}(mT_{\mathrm{s}})q^*_{m,k}\right) \times \left(\sum_{n=0}^{N-1} e^*_{\mathrm{t},l}(nT_{\mathrm{s}})q_{n,k}\right)\right\} \tag{2.16}$$

$$= \sum_{m=0}^{N-1}\sum_{n=0}^{N-1} \mathbb{E}\left\{e_{\mathrm{t},l}(mT_{\mathrm{s}})e^*_{\mathrm{t},l}(nT_{\mathrm{s}})\right\} q^*_{m,k}q_{n,k} \tag{2.17}$$

$$= \sum_{m=0}^{N-1} \mathbb{E}\left\{e_{\mathrm{t},l}(mT_{\mathrm{s}})e^*_{\mathrm{t},l}(mT_{\mathrm{s}})\right\} q_{m,k}q^*_{m,k} \quad (e_{\mathrm{t},l}(t)\perp e_{\mathrm{t},l}(t')) \tag{2.18}$$

$$= \kappa_l \mathbb{E}\left\{|\widetilde{x}_l(t)|^2\right\} \quad (\text{From 2.12 and } \sum_{m=0}^{N-1} q_{m,k}q^*_{m,k} = 1) \tag{2.19}$$

$$= \frac{\kappa_l}{K}\sum_{m=1}^{K} \mathbb{E}\left\{|\widetilde{x}^m_l|^2\right\} \quad (\text{Parseval's Theorem on the energy conversation}). \tag{2.20}$$

Similarly, the proof to the receiver characterization can be obtained. □

Following the lemma 2.4.1, the statistics of the distortion terms can be written as

$$\mathbf{e}^k_{\mathrm{t,s}} \sim \mathcal{CN}\left(\mathbf{0}_{N_{\mathrm{s}}}, \frac{1}{K}\widetilde{\mathbf{\Theta}}_{\mathrm{tx,s}}\mathbf{P}_{\mathrm{tx,s}}\right), \tag{2.21}$$

$$\mathbf{e}^k_{\mathrm{t,r}} \sim \mathcal{CN}\left(\mathbf{0}_{N_{\mathrm{r}}}, \frac{1}{K}\widetilde{\mathbf{\Theta}}_{\mathrm{tx,r}}\mathbf{P}_{\mathrm{tx,r}}\right), \tag{2.22}$$

$$\mathbf{e}^k_{\mathrm{r,r}} \sim \mathcal{CN}\left(\mathbf{0}_{M_{\mathrm{r}}}, \frac{1}{K}\widetilde{\mathbf{\Theta}}_{\mathrm{rx,r}}\mathbf{P}_{\mathrm{rx,r}}\right), \tag{2.23}$$

$$\mathbf{e}^k_{\mathrm{r,d}} \sim \mathcal{CN}\left(\mathbf{0}_{M_{\mathrm{d}}}, \frac{1}{K}\widetilde{\mathbf{\Theta}}_{\mathrm{rx,d}}\mathbf{P}_{\mathrm{rx,d}}\right), \tag{2.24}$$

where

$$\mathbf{P}_{\mathrm{tx,s}} \coloneqq \sum_{k\in\mathbb{K}} \mathrm{diag}\left(\mathbb{E}\left\{\widetilde{\mathbf{x}}^k_{\mathrm{s}}(\widetilde{\mathbf{x}}^k_{\mathrm{s}})^H\right\}\right), \tag{2.25}$$

$$\mathbf{P}_{\mathrm{tx,r}} \coloneqq \sum_{k\in\mathbb{K}} \mathrm{diag}\left(\mathbb{E}\left\{\widetilde{\mathbf{x}}^k_{\mathrm{r}}(\widetilde{\mathbf{x}}^k_{\mathrm{r}})^H\right\}\right), \tag{2.26}$$

$$\mathbf{P}_{\mathrm{rx,r}} \coloneqq \sum_{k\in\mathbb{K}} \mathrm{diag}\left(\mathbb{E}\left\{\widetilde{\mathbf{y}}^k_{\mathrm{r}}(\widetilde{\mathbf{y}}^k_{\mathrm{r}})^H\right\}\right), \tag{2.27}$$

$$\mathbf{P}_{\mathrm{rx,d}} \coloneqq \sum_{k\in\mathbb{K}} \mathrm{diag}\left(\mathbb{E}\left\{\widetilde{\mathbf{y}}^k_{\mathrm{d}}(\widetilde{\mathbf{y}}^k_{\mathrm{d}})^H\right\}\right). \tag{2.28}$$

The diagonal matrices $\widetilde{\mathbf{\Theta}}_{\mathrm{tx,s}}$ ($\widetilde{\mathbf{\Theta}}_{\mathrm{tx,r}}$) and $\mathbf{P}_{\mathrm{tx,s}}$ ($\mathbf{P}_{\mathrm{tx,r}}$) consisting of transmit distortion coefficients and intended transmit signal power for the corresponding transmit chains at the source (relay), respectively. Similarly, $\widetilde{\mathbf{\Theta}}_{\mathrm{rx,r}}$ ($\widetilde{\mathbf{\Theta}}_{\mathrm{rx,d}}$) and $\mathbf{P}_{\mathrm{rx,r}}$ ($\mathbf{P}_{\mathrm{rx,d}}$) are diagonal matrices consisting of receive distortion coefficients and intended receive signal power at the corresponding receive chains at the relay (destination), respectively. Let us define $\mathbf{\Theta}_{\mathrm{tx,r}} = \frac{1}{K}\widetilde{\mathbf{\Theta}}_{\mathrm{tx,r}}$, $\mathbf{\Theta}_{\mathrm{tx,s}} = \frac{1}{K}\widetilde{\mathbf{\Theta}}_{\mathrm{tx,s}}$, $\mathbf{\Theta}_{\mathrm{rx,r}} = \frac{1}{K}\widetilde{\mathbf{\Theta}}_{\mathrm{rx,r}}$, and $\mathbf{\Theta}_{\mathrm{rx,d}} = \frac{1}{K}\widetilde{\mathbf{\Theta}}_{\mathrm{rx,d}}$ for further calculations.

2.4.5 Mean-Squared Error Matrix

Considering $\boldsymbol{V}_{\mathrm{s}}^{k}$ and $\boldsymbol{U}_{\mathrm{r}}^{k}$ as the linear source transmit precoder and linear relay receive filters, the mean square error (MSE) matrix for the source-relay system can be defined as

$$\begin{aligned}\mathbf{E}_{r}^{k} &= \mathbf{E}\left\{\left(\widetilde{\mathbf{s}}_{\mathrm{s}}^{k}-\mathbf{s}_{\mathrm{s}}^{k}\right)\left(\widetilde{\mathbf{s}}_{\mathrm{s}}^{k}-\mathbf{s}_{\mathrm{s}}^{k}\right)^{H}\right\}\\ &= \left((\boldsymbol{U}_{\mathrm{r}}^{k})^{H}\widehat{\mathbf{H}}_{\mathrm{sr}}^{k}\boldsymbol{V}_{\mathrm{s}}^{k}-\mathbf{I}_{d_{\mathrm{s}}}\right)\left((\boldsymbol{U}_{\mathrm{r}}^{k})^{H}\widehat{\mathbf{H}}_{\mathrm{sr}}^{k}\boldsymbol{V}_{\mathrm{s}}^{k}-\mathbf{I}_{d_{\mathrm{s}}}\right)^{H}+(\boldsymbol{U}_{\mathrm{r}}^{k})^{H}\boldsymbol{\Sigma}_{\mathrm{r}}^{k}\boldsymbol{U}_{\mathrm{r}}^{k},\end{aligned} \tag{2.29}$$

where $\boldsymbol{\Sigma}_{\mathrm{r}}^{k}$ is the covariance of the received collective interference-plus-noise signal at the relay and can be obtained as

$$\begin{aligned}\boldsymbol{\Sigma}_{\mathrm{r}}^{k} &= \mathbb{E}\left\{\boldsymbol{\nu}_{\mathrm{r}}^{k}\boldsymbol{\nu}_{\mathrm{r}}^{k^{H}}\right\}\\ &\approx \underbrace{\widehat{\mathbf{H}}_{\mathrm{sr}}^{k}\boldsymbol{\Theta}_{\mathrm{tx,s}}\mathrm{diag}\left(\sum_{m\in\mathbb{K}}\boldsymbol{V}_{\mathrm{s}}^{m}(\boldsymbol{V}_{\mathrm{s}}^{m})^{H}\right)(\widehat{\mathbf{H}}_{\mathrm{sr}}^{k})^{H}+\mathbf{D}_{\mathrm{sr}}^{k}\mathrm{Tr}\left(\boldsymbol{\Theta}_{\mathrm{tx,s}}\mathrm{diag}\left(\sum_{m\in\mathbb{K}}\boldsymbol{V}_{\mathrm{s}}^{m}(\boldsymbol{V}_{\mathrm{s}}^{m})^{H}\right)\right)}_{\text{Source transmit distortion}}\\ &+ \underbrace{\widehat{\mathbf{H}}_{\mathrm{rr}}^{k}\boldsymbol{\Theta}_{\mathrm{tx,r}}\mathrm{diag}\left(\sum_{m\in\mathbb{K}}\boldsymbol{V}_{\mathrm{r}}^{m}(\boldsymbol{V}_{\mathrm{r}}^{m})^{H}\right)(\widehat{\mathbf{H}}_{\mathrm{rr}}^{k})^{H}+\mathbf{D}_{\mathrm{rr}}^{k}\mathrm{Tr}\left(\boldsymbol{\Theta}_{\mathrm{tx,r}}\mathrm{diag}\left(\sum_{m\in\mathbb{K}}\boldsymbol{V}_{\mathrm{r}}^{m}(\boldsymbol{V}_{\mathrm{r}}^{m})^{H}\right)\right)}_{\text{Relay transmit distortion}}\\ &+ \underbrace{\mathbf{D}_{\mathrm{sr}}^{k}\mathrm{Tr}\left(\boldsymbol{V}_{\mathrm{s}}^{k}(\boldsymbol{V}_{\mathrm{s}}^{k})^{H}\right)+\mathbf{D}_{\mathrm{rr}}^{k}\mathrm{Tr}\left(\boldsymbol{V}_{\mathrm{r}}^{k}(\boldsymbol{V}_{\mathrm{r}}^{k})^{H}\right)}_{\text{CSI error in source-relay and relay SI channel}}\\ &+ \underbrace{\boldsymbol{\Theta}_{\mathrm{rx,r}}\mathrm{diag}\left(\sum_{m\in\mathbb{K}}\left(\widehat{\mathbf{H}}_{\mathrm{sr}}^{m}\boldsymbol{V}_{\mathrm{s}}^{m}(\boldsymbol{V}_{\mathrm{s}}^{m})^{H}(\widehat{\mathbf{H}}_{\mathrm{sr}}^{m})^{H}+\mathbf{D}_{\mathrm{sr}}^{m}\mathrm{Tr}\left(\boldsymbol{V}_{\mathrm{s}}^{m}(\boldsymbol{V}_{\mathrm{s}}^{m})^{H}\right)\right)\right.}_{\text{Relay receive distortion}}\\ &\underbrace{\left.+\sum_{m\in\mathbb{K}}\left(\widehat{\mathbf{H}}_{\mathrm{rr}}^{m}\boldsymbol{V}_{\mathrm{r}}^{m}(\boldsymbol{V}_{\mathrm{r}}^{m})^{H}(\widehat{\mathbf{H}}_{\mathrm{rr}}^{m})^{H}+\mathbf{D}_{\mathrm{rr}}^{m}\mathrm{Tr}\left(\boldsymbol{V}_{\mathrm{r}}^{m}(\boldsymbol{V}_{\mathrm{r}}^{m})^{H}\right)+\sigma_{\mathrm{r},m}^{2}\mathbf{I}_{M_{\mathrm{r}}}\right)\right)}_{\text{Relay receive distortion}}+\underbrace{\sigma_{\mathrm{r},k}^{2}\mathbf{I}_{M_{\mathrm{r}}}}_{\text{Thermal noise}},\quad k\in\mathbb{K}.\end{aligned} \tag{2.30}$$

Here, we ignore the higher-order terms of the transmit and receive distortion since the transmit and receive distortion coefficients of each transmit/receive chains ($\widetilde{\kappa}_l/\widetilde{\beta}_l$) lie within the range of 0 and 1 and mostly have very small values.

Similarly, the MSE matrix for the relay-destination system considering $\boldsymbol{V}_{\mathrm{r}}^{k}$ and $\boldsymbol{U}_{\mathrm{d}}^{k}$ as the linear relay transmit precoder and linear destination receive filters can be obtained as

$$\begin{aligned}\mathbf{E}_{d}^{k} &= \mathbf{E}\left\{\left(\widetilde{\mathbf{s}}_{r}^{k}-\mathbf{s}_{\mathrm{r}}^{k}\right)\left(\widetilde{\mathbf{s}}_{r}^{k}-\mathbf{s}_{\mathrm{r}}^{k}\right)^{H}\right\}\\ &= \left((\boldsymbol{U}_{\mathrm{d}}^{k})^{H}\widehat{\mathbf{H}}_{\mathrm{rd}}^{k}\boldsymbol{V}_{\mathrm{r}}^{k}-\mathbf{I}_{d_{\mathrm{r}}}\right)\left((\boldsymbol{U}_{\mathrm{d}}^{k})^{H}\widehat{\mathbf{H}}_{\mathrm{rd}}^{k}\boldsymbol{V}_{\mathrm{r}}^{k}-\mathbf{I}_{d_{\mathrm{r}}}\right)^{H}+(\boldsymbol{U}_{\mathrm{d}}^{k})^{H}\boldsymbol{\Sigma}_{\mathrm{d}}^{k}\boldsymbol{U}_{\mathrm{d}}^{k}.\end{aligned} \tag{2.31}$$

The covariance of the interference-plus-noise signal at the destination can be written as

$$
\begin{aligned}
&\boldsymbol{\Sigma}_{\mathrm{d}}^{k} = \mathbb{E}\left\{\boldsymbol{\nu}_{\mathrm{d}}^{k}\boldsymbol{\nu}_{\mathrm{d}}^{k^{H}}\right\} \\
&\approx \underbrace{\widehat{\mathbf{H}}_{\mathrm{rd}}^{k}\boldsymbol{\Theta}_{\mathrm{tx,r}}\mathrm{diag}\left(\sum_{m\in\mathbb{K}}\boldsymbol{V}_{\mathrm{r}}^{m}(\boldsymbol{V}_{\mathrm{r}}^{m})^{H}\right)(\widehat{\mathbf{H}}_{\mathrm{rd}}^{k})^{H} + \mathbf{D}_{\mathrm{rd}}^{k}\mathrm{Tr}\left(\boldsymbol{\Theta}_{\mathrm{tx,r}}\mathrm{diag}\left(\sum_{m\in\mathbb{K}}\boldsymbol{V}_{\mathrm{r}}^{m}(\boldsymbol{V}_{\mathrm{r}}^{m})^{H}\right)\right)}_{\text{Relay transmit distortion}} \\
&+ \underbrace{\widehat{\mathbf{H}}_{\mathrm{sd}}^{k}\boldsymbol{\Theta}_{\mathrm{tx,s}}\mathrm{diag}\left(\sum_{m\in\mathbb{K}}\boldsymbol{V}_{\mathrm{s}}^{m}(\boldsymbol{V}_{\mathrm{s}}^{m})^{H}\right)(\widehat{\mathbf{H}}_{\mathrm{sd}}^{k})^{H} + \mathbf{D}_{\mathrm{sd}}^{k}\mathrm{Tr}\left(\boldsymbol{\Theta}_{\mathrm{tx,s}}\mathrm{diag}\left(\sum_{m\in\mathbb{K}}\boldsymbol{V}_{\mathrm{s}}^{m}(\boldsymbol{V}_{\mathrm{s}}^{m})^{H}\right)\right)}_{\text{Source transmit distortion}} \\
&+ \underbrace{\widehat{\mathbf{H}}_{\mathrm{sd}}^{k}\boldsymbol{V}_{\mathrm{s}}^{k}(\boldsymbol{V}_{\mathrm{s}}^{k})^{H}\ (\widehat{\mathbf{H}}_{\mathrm{sd}}^{k})^{H} + \mathbf{D}_{\mathrm{sd}}^{k}\mathrm{Tr}\left(\boldsymbol{V}_{\mathrm{s}}^{k}(\boldsymbol{V}_{\mathrm{s}}^{k})^{H}\right)}_{\text{Interference from Source}} + \underbrace{\mathbf{D}_{\mathrm{rd}}^{k}\mathrm{Tr}\left(\boldsymbol{V}_{\mathrm{r}}^{k}(\boldsymbol{V}_{\mathrm{r}}^{k})^{H}\right)}_{\text{CSI error in relay-destination channel}} \\
&+ \underbrace{\boldsymbol{\Theta}_{\mathrm{rx,d}}\mathrm{diag}\left(\sum_{m\in\mathbb{K}}\left(\widehat{\mathbf{H}}_{\mathrm{rd}}^{m}\boldsymbol{V}_{\mathrm{r}}^{m}(\boldsymbol{V}_{\mathrm{r}}^{m})^{H}(\widehat{\mathbf{H}}_{\mathrm{rd}}^{m})^{H} + \mathbf{D}_{\mathrm{rd}}^{m}\mathrm{Tr}\left(\boldsymbol{V}_{\mathrm{r}}^{m}(\boldsymbol{V}_{\mathrm{r}}^{m})^{H}\right)\right)\right)}_{\text{Destination receive distortion}} \\
&+ \underbrace{\sum_{m\in\mathbb{K}}\left(\widehat{\mathbf{H}}_{\mathrm{sd}}^{m}\boldsymbol{V}_{\mathrm{s}}^{m}(\boldsymbol{V}_{\mathrm{s}}^{m})^{H}(\widehat{\mathbf{H}}_{\mathrm{sd}}^{m})^{H} + \mathbf{D}_{\mathrm{sd}}^{m}\mathrm{Tr}\left(\boldsymbol{V}_{\mathrm{s}}^{m}(\boldsymbol{V}_{\mathrm{s}}^{m})^{H}\right) + \sigma_{\mathrm{d},m}^{2}\mathbf{I}_{M_{\mathrm{d}}}\right)}_{\text{Destination receive distortion}} + \underbrace{\sigma_{\mathrm{d},k}^{2}\mathbf{I}_{M_{\mathrm{d}}}}_{\text{Thermal noise}}\ , k \in \mathbb{K}.
\end{aligned}
\tag{2.32}
$$

2.5 Optimization Problem

In this section, we discuss the linear transceiver design problem of an FD MIMO DF relay system for sum-rate maximization, power minimization and energy efficiency maximization.

2.5.1 Sum-rate Maximization

In recent years, due to the scarcity of spectrum resource, spectral efficiency has become one of the most necessitous factors in wireless communications. Here, we consider spectral efficiency in terms of achievable sum-rate. The total achievable sum-rate for the source-relay link and the relay-destination link are represented by R_{sr} and R_{rd}, respectively. The rate functions can be defined as

$$R_{\mathrm{sr}} = \sum_{k\in\mathbb{K}} R_{\mathrm{sr}}^{k} = \sum_{k\in\mathbb{K}} \log_2|\mathbf{I}_{d_{\mathrm{s}}} + (\boldsymbol{V}_{\mathrm{s}}^{k})^{H}(\widehat{\mathbf{H}}_{\mathrm{sr}}^{k})^{H}(\boldsymbol{\Sigma}_{\mathrm{r}}^{k})^{-1}\widehat{\mathbf{H}}_{\mathrm{sr}}^{k}\boldsymbol{V}_{\mathrm{s}}^{k}|,$$

$$R_{\mathrm{rd}} = \sum_{k\in\mathbb{K}} R_{\mathrm{rd}}^{k} = \sum_{k\in\mathbb{K}} \log_2|\mathbf{I}_{d_{\mathrm{r}}} + (\boldsymbol{V}_{\mathrm{r}}^{k})^{H}(\widehat{\mathbf{H}}_{\mathrm{rd}}^{k})^{H}(\boldsymbol{\Sigma}_{\mathrm{d}}^{k})^{-1}\widehat{\mathbf{H}}_{\mathrm{rd}}^{k}\boldsymbol{V}_{\mathrm{r}}^{k}|,$$

where R_{sr}^k and R_{rd}^k are the achievable sum-rate for the source-relay link and the relay-destination link at sub-carrier k, respectively. The achievable sum-rate of the relay system at sub-carrier k can be written as

$$R^k = \min\{R_{\text{sr}}^k, R_{\text{rd}}^k\}.$$

The sum-rate maximization problem utilizing PC coding strategy can be defined as

$$\begin{aligned} \underset{\mathbb{V}_{\text{s}},\mathbb{V}_{\text{r}}}{\text{maximize}} \quad & \sum_{k\in\mathbb{K}} R^k && \text{(2.33a)} \\ \text{subject to} \quad & \text{Tr}\Big((\mathbf{I}_{N_{\text{s}}} + K\boldsymbol{\Theta}_{\text{tx,s}})\sum_{m\in\mathbb{K}} \boldsymbol{V}_{\text{s}}^m(\boldsymbol{V}_{\text{s}}^m)^H\Big) \le p_{\text{s,max}}, && \text{(2.33b)} \\ & \text{Tr}\Big((\mathbf{I}_{N_{\text{r}}} + K\boldsymbol{\Theta}_{\text{tx,r}})\sum_{m\in\mathbb{K}} \boldsymbol{V}_{\text{r}}^m(\boldsymbol{V}_{\text{r}}^m)^H\Big) \le p_{\text{r,max}}, && \text{(2.33c)} \end{aligned}$$

where $\mathbb{V}_{\text{s}} := \{\boldsymbol{V}_{\text{s}}^k, \forall k \in \mathbb{K}\}$ and $\mathbb{V}_{\text{r}} := \{\boldsymbol{V}_{\text{r}}^k, \forall k \in \mathbb{K}\}$. $p_{\text{s,max}}$ and $p_{\text{r,max}}$ denote the maximum affordable transmit power at the source and the relay, respectively. In PC coding strategy, encoding and decoding are performed separately over all the sub-carriers, i.e., the optimization constraints are considered over the sub-carriers individually. The above optimization problem (2.33) can be written as

$$\begin{aligned} \underset{\mathbb{V}_{\text{s}},\mathbb{V}_{\text{r}},\mathbb{T}}{\text{maximize}} \quad & \sum_{k\in\mathbb{K}} t_k \\ \text{subject to} \quad & R_{\text{sr}}^k \ge t_k,\ R_{\text{rd}}^k \ge t_k, \\ & \text{(2.33b), (2.33c)}, \end{aligned} \qquad (2.34)$$

where $\mathbb{T} := \{t_k, \forall k \in \mathbb{K}\}$[1]. It can be observed that the problem (2.34) is a non-convex optimization problem. In the following, we apply the known weighted minimum mean square error (WMMSE) method [78] to facilitate a convergent alternating optimization.

We can write the optimal MMSE receive filter at the relay as,

$$\boldsymbol{U}_{\text{r,mmse}}^k = \Big(\boldsymbol{\Sigma}_{\text{r}}^k + \widehat{\mathbf{H}}_{\text{sr}}^k \boldsymbol{V}_{\text{s}}^k (\boldsymbol{V}_{\text{s}}^k)^H (\widehat{\mathbf{H}}_{\text{sr}}^k)^H\Big)^{-1} \widehat{\mathbf{H}}_{\text{sr}}^k \boldsymbol{V}_{\text{s}}^k \qquad (2.35)$$

and at the destination as

$$\boldsymbol{U}_{\text{d,mmse}}^k = \Big(\boldsymbol{\Sigma}_{\text{d}}^k + \widehat{\mathbf{H}}_{\text{rd}}^k \boldsymbol{V}_{\text{r}}^k (\boldsymbol{V}_{\text{r}}^k)^H (\widehat{\mathbf{H}}_{\text{rd}}^k)^H\Big)^{-1} \widehat{\mathbf{H}}_{\text{rd}}^k \boldsymbol{V}_{\text{r}}^k. \qquad (2.36)$$

By applying (2.35) and (2.36) in (2.29) and (2.31), we get,

$$\mathbf{E}_{\text{r,mmse}}^k = \Big(\mathbf{I}_{d_s} + (\boldsymbol{V}_{\text{s}}^k)^H (\widehat{\mathbf{H}}_{\text{sr}}^k)^H (\boldsymbol{\Sigma}_{\text{r}}^k)^{-1} \widehat{\mathbf{H}}_{\text{sr}}^k \boldsymbol{V}_{\text{s}}^k\Big)^{-1}, \qquad (2.37)$$

$$\mathbf{E}_{\text{d,mmse}}^k = \Big(\mathbf{I}_{d_r} + (\boldsymbol{V}_{\text{r}}^k)^H (\widehat{\mathbf{H}}_{\text{rd}}^k)^H (\boldsymbol{\Sigma}_{\text{d}}^k)^{-1} \widehat{\mathbf{H}}_{\text{rd}}^k \boldsymbol{V}_{\text{r}}^k\Big)^{-1}. \qquad (2.38)$$

Using (2.37) and (2.38), the rate functions can be written as

$$R_{\text{sr}}^k = -\log_2|\mathbf{E}_{\text{r,mmse}}^k|, \qquad (2.39)$$

$$R_{\text{rd}}^k = -\log_2|\mathbf{E}_{\text{d,mmse}}^k|. \qquad (2.40)$$

[1] t_k is an auxiliary variable.

Lemma 2.5.1. *[59, lemma III.1.] [79, lemma 2] Let* $\mathbf{E} \in \mathbb{C}^{d\times d}$ *be a positive definite matrix. The maximization of the term* $-\log|\mathbf{E}|$ *is equivalent to the maximization*

$$\underset{\mathbf{E},\mathbf{S}}{\text{maximize}} \; -\text{Tr}(\mathbf{SE}) + \log|\mathbf{S}| + d \tag{2.41}$$

where $\mathbf{S} \in \mathbb{C}^{d\times d}$ *is a positive definite matrix, and we have*

$$\mathbf{S} = \mathbf{E}^{-1}, \tag{2.42}$$

for the optimal solution.

By using the Lemma 2.5.1, the optimization problem (2.34) can be written as

$$\begin{aligned}
\underset{\mathbb{V}_\text{s},\mathbb{V}_\text{r},\mathbb{U}_\text{r},\mathbb{U}_\text{d},\mathbb{S}_\text{r},\mathbb{S}_\text{d},\mathbb{T}}{\text{maximize}} \quad & \sum_{k\in\mathbb{K}} t_k && \text{(2.43a)}\\
\text{subject to} \quad & -\text{Tr}(\mathbf{S}_\text{r}^k\mathbf{E}_\text{r}^k) + \log|\mathbf{S}_\text{r}^k| + d_\text{s} \geq t_k, && \text{(2.43b)}\\
& -\text{Tr}(\mathbf{S}_\text{d}^k\mathbf{E}_\text{d}^k) + \log|\mathbf{S}_\text{d}^k| + d_\text{r} \geq t_k, && \text{(2.43c)}\\
& (2.33\text{b}), (2.33\text{c}),
\end{aligned}$$

where $\mathbb{U}_\text{r} := \{\boldsymbol{U}_\text{r}^k, \forall k \in \mathbb{K}\}$, $\mathbb{U}_\text{d} := \{\boldsymbol{U}_\text{d}^k, \forall k \in \mathbb{K}\}$, $\mathbb{S}_\text{r} := \{\mathbf{S}_\text{r}^k \succ 0, \forall k \in \mathbb{K}\}$ and $\mathbb{S}_\text{d} := \{\mathbf{S}_\text{d}^k \succ 0, \forall k \in \mathbb{K}\}$. Please note that the obtained problem is not a jointly convex problem. However, it is a quadratic convex program over $\mathbb{V}_\text{s}$, $\mathbb{V}_\text{r}$ and $\mathbb{T}$, when other variables are fixed. Moreover, the optimization over $\mathbb{U}_\text{r}$ and $\mathbb{U}_\text{d}$ can be obtained from (2.35) and (2.36), respectively. Whereas, the optimization over $\mathbb{S}_\text{r}$ and $\mathbb{S}_\text{d}$ can be acquired using (2.37) and (2.38), as $\mathbf{S}_\text{r}^k = \mathbf{E}_\text{r}^{k^{-1}}$ and $\mathbf{S}_\text{d}^k = \mathbf{E}_\text{d}^{k^{-1}}$. This facilitates an alternating optimization, where in each step the corresponding problem is solved to optimality. Due to the monotonic increase of the objective in each step and the fact that the system sum-rate is bounded from above, the alternating optimization steps lead to convergence. Algorithm 1 defines the detailed algorithm.

Algorithm 1 AQCP-WMMSE design for PC sum-rate maximization

1: $a \leftarrow 0$ (set iteration number to zero)
2: $\mathbb{V}_\text{s}, \mathbb{V}_\text{r} \leftarrow$ right singular matrix initialization [80, Appendix A]
3: **repeat**
4: $\quad a \leftarrow a + 1$
5: $\quad \mathbb{U}_\text{r}, \mathbb{U}_\text{d} \leftarrow$ solve (2.35) and (2.36), respectively
6: $\quad \mathbb{S}_\text{r}, \mathbb{S}_\text{d} \leftarrow \mathbf{S}_\text{r}^k = \mathbf{E}_\text{r}^{k^{-1}}$ and $\mathbf{S}_\text{d}^k = \mathbf{E}_\text{d}^{k^{-1}}$, respectively
7: $\quad \mathbb{V}_\text{s}, \mathbb{V}_\text{r}, \mathbb{T} \leftarrow$ solve (2.43), with fixed $\mathbb{U}_\text{r}, \mathbb{U}_\text{d}, \mathbb{S}_\text{r}$and $\mathbb{S}_\text{d}$
8: **until** a stable point, or maximum number of a reached
9: **return** $\{\mathbb{V}_\text{s}, \mathbb{V}_\text{r}\}$

Joint-carrier Decoding and Remapping

In this section, we consider that the system employs JC coding strategy, i.e., encoding and decoding are performed jointly over all sub-carriers. In other words, the optimization constraints are considered over all the sub-carriers jointly. This way, we can take advantage of the MC system, by allowing the relay to decode the signal from one sub-carrier and forward it to the destination through another sub-carrier, thereby improving the system in terms of total sum-rate. Accordingly, the sum-rate maximization problem with JC decoding and remapping can be defined as

$$\underset{\mathbb{V}_{\rm s},\mathbb{V}_{\rm r}}{\text{maximize}} \quad \min\{R_{\rm sr}, R_{\rm rd}\} \tag{2.44}$$

$$\text{subject to} \quad (2.33\text{b}),\ (2.33\text{c}). \tag{2.45}$$

The optimization problem can be written as

$$\begin{aligned} \underset{\mathbb{V}_{\rm s},\mathbb{V}_{\rm r},t}{\text{maximize}} \quad & t \\ \text{subject to} \quad & \sum_{k\in\mathbb{K}} R_{\rm sr}^k \geq t, \quad \sum_{k\in\mathbb{K}} R_{\rm rd}^k \geq t, \\ & (2.33\text{b}),\ (2.33\text{c}). \end{aligned} \tag{2.46}$$

where t is an auxiliary variable. Using the similar steps (WMMSE method) as in PC coding strategy, the optimization problem can be written as

$$\begin{aligned} \underset{\mathbb{V}_{\rm s},\mathbb{V}_{\rm r},\mathbb{U}_{\rm r},\mathbb{U}_{\rm d},\mathbb{S}_{\rm r},\mathbb{S}_{\rm d},t}{\text{maximize}} \quad & t \\ \text{subject to} \quad & \sum_{k\in\mathbb{K}} (-\text{Tr}(\mathbf{S}_{\rm r}^k\mathbf{E}_{\rm r}^k) + \log|\mathbf{S}_{\rm r}^k| + d_{\rm s}) \geq t, \\ & \sum_{k\in\mathbb{K}} (-\text{Tr}(\mathbf{S}_{\rm d}^k\mathbf{E}_{\rm d}^k) + \log|\mathbf{S}_{\rm d}^k| + d_{\rm r}) \geq t, \\ & (2.33\text{b}), (2.33\text{c}). \end{aligned} \tag{2.47}$$

Alternating quadratic convex program steps that are applied to (2.43) can be used to solve the above optimization problem (2.47). Algorithm 2 defines the detailed algorithm.

Algorithm 2 AQCP-WMMSE design for JC sum-rate maximization

1: Algorithm 1, Steps 1-2 (initialization)
2: **repeat**
3: Algorithm 1, Steps 4-6
4: $\mathbb{V}_{\rm s}, \mathbb{V}_{\rm r}, t \leftarrow$ solve (2.47), with fixed $\mathbb{U}_{\rm r}, \mathbb{U}_{\rm d}, \mathbb{S}_{\rm r}$and $\mathbb{S}_{\rm d}$
5: **until** a stable point, or maximum number of a reached
6: **return** $\{\mathbb{V}_{\rm s}, \mathbb{V}_{\rm r}\}$

2.5.2 Power Minimization

In this section, our goal is to attain a design that minimizes the total power consumption for a guaranteed pre-defined rate requirement γ. The total power consumption P_{tot} can be defined as

$$P_{\text{tot}} = P_{\text{s}} + P_{\text{r}}, \tag{2.48}$$

where $P_{\text{s}} = \frac{1}{\mu_{\text{s}}} \sum_{k\in\mathbb{K}} \mathbb{E}\{\|\boldsymbol{x}_s^k\|^2\} + P_{\text{s}_{\text{zero}}}$ and $P_{\text{r}} = \frac{1}{\mu_r} \sum_{k\in\mathbb{K}} \mathbb{E}\{\|\boldsymbol{x}_{\text{r}}^k\|^2\} + P_{\text{r}_{\text{zero}}} + P_{\text{FD}}$. μ_{s} and μ_r are the efficiencies of the power amplifier at the source and relay, respectively. $P_{\text{s}_{\text{zero}}}$ and $P_{\text{r}_{\text{zero}}}$ are the power dissipated by other circuit blocks at the transmitter chain of source and relay, respectively. P_{FD} is the power required for SIC. By using the above definition, the total power minimization problem for JC coding strategy can be expressed as

$$\begin{aligned}
\underset{\mathbb{V}_{\text{s}},\mathbb{V}_{\text{r}}}{\text{minimize}} \quad & P_{\text{tot}} && \text{(2.49a)}\\
\text{subject to} \quad & P_{\text{s}} \le P_{\text{s,max}},\ P_{\text{r}} \le P_{\text{r,max}}, && \text{(2.49b)}\\
& \min\{R_{\text{sr}}, R_{\text{rd}}\} \ge \gamma, && \text{(2.49c)}
\end{aligned}$$

where $P_{\text{s,max}}$ and $P_{\text{r,max}}$ denote the maximum available power for consumption at the source and the relay, respectively. The above optimization problem can be solved by using WMMSE method and AQCP steps similar to (2.47). However, the initialization of the variables $\mathbb{V}_{\text{s}}$ and $\mathbb{V}_{\text{r}}$ must belong to the feasible set of the problem. In order to find a feasible initialization point, we need to solve the following optimization problem,

$$\begin{aligned}
\underset{\mathbb{V}_{\text{s}},\mathbb{V}_{\text{r}},\varepsilon}{\text{minimize}} \quad & \varepsilon && \text{(2.50a)}\\
\text{subject to} \quad & P_{\text{s}} \le P_{\text{s,max}},\ P_{\text{r}} \le P_{\text{r,max}}, && \text{(2.50b)}\\
& R_{\text{sr}} + \varepsilon \ge \gamma,\ R_{\text{rd}} + \varepsilon \ge \gamma,\ \ \varepsilon \ge 0. && \text{(2.50c)}
\end{aligned}$$

Here, the solution to the above problem is obtained by an alternating one similar to (2.47), and can be used as the initialization point for (2.49). Algorithm 3 defines the detailed algorithm.

Algorithm 3 AQCP-WMMSE design for power minimization

1: $a \leftarrow 0$ (set iteration number to zero)
2: $\mathbb{V}_{\text{s}}, \mathbb{V}_{\text{r}} \leftarrow$ solve (2.50)
3: **repeat**
4: $\quad a \leftarrow a + 1$
5: $\quad \mathbb{U}_{\text{r}}, \mathbb{U}_{\text{d}} \leftarrow$ solve (2.35) and (2.36), respectively
6: $\quad \mathbb{S}_{\text{r}}, \mathbb{S}_{\text{d}} \leftarrow \mathbf{S}_{\text{r}}^k = \mathbf{E}_{\text{r}}^{k^{-1}}$ and $\mathbf{S}_{\text{d}}^k = \mathbf{E}_{\text{d}}^{k^{-1}}$, respectively
7: $\quad \mathbb{V}_{\text{s}}, \mathbb{V}_{\text{r}} \leftarrow$ solve (2.49), with fixed $\mathbb{U}_{\text{r}}, \mathbb{U}_{\text{d}}, \mathbb{S}_{\text{r}}$and $\mathbb{S}_{\text{d}}$
8: **until** a stable point, or maximum number of a reached
9: **return** $\{\mathbb{V}_{\text{s}}, \mathbb{V}_{\text{r}}\}$

2.5.3 Energy Efficiency Maximization

The main idea behind energy efficiency is to perform the same amount of tasks utilizing less energy. Eliminating energy waste also provides economic benefits and ecological sustainability. Therefore, energy-efficient or green technologies have gained more attention in designing a future wireless system. In this section, the energy efficiency is defined as the ratio of the system sum-rate to the total power consumption of both the source and the relay. The energy efficiency maximization problem for JC coding strategy can be expressed as

$$\underset{\mathbb{V}_{\mathrm{s}},\mathbb{V}_{\mathrm{r}},t}{\text{maximize}} \quad t/P_{\mathrm{tot}} \tag{2.51a}$$

$$\text{subject to} \quad P_{\mathrm{s}} \leq P_{\mathrm{s,max}}, \;\; P_{\mathrm{r}} \leq P_{\mathrm{r,max}}, \tag{2.51b}$$

$$\min\{R_{\mathrm{sr}}, R_{\mathrm{rd}}\} \geq t. \tag{2.51c}$$

Using the similar approach of sum-rate maximization problem, the above optimization (2.51) can also be written as

$$\underset{\mathbb{V}_{\mathrm{s}},\mathbb{V}_{\mathrm{r}},\mathbb{U}_{\mathrm{r}},\mathbb{U}_{\mathrm{d}},\mathbb{S}_{\mathrm{r}},\mathbb{S}_{\mathrm{d}},t}{\text{maximize}} \quad t/P_{\mathrm{tot}} \tag{2.52a}$$

$$\text{subject to} \quad P_{\mathrm{s}} \leq P_{\mathrm{s,max}}, \; P_{\mathrm{r}} \leq P_{\mathrm{r,max}}, \tag{2.52b}$$

$$\sum_{k\in\mathbb{K}} (-\mathrm{Tr}(\mathbf{S}_{\mathrm{r}}^{k}\mathbf{E}_{\mathrm{r}}^{k}) + \log|\mathbf{S}_{\mathrm{r}}^{k}| + d_{\mathrm{s}}) \geq t, \tag{2.52c}$$

$$\sum_{k\in\mathbb{K}} (-\mathrm{Tr}(\mathbf{S}_{\mathrm{d}}^{k}\mathbf{E}_{\mathrm{d}}^{k}) + \log|\mathbf{S}_{\mathrm{d}}^{k}| + d_{\mathrm{r}}) \geq t. \tag{2.52d}$$

We utilize Dinkelbach's algorithm [81] to tackle the above fractional optimization problem. The optimization problem can be reformulated as

$$\underset{\mathbb{V}_{\mathrm{s}},\mathbb{V}_{\mathrm{r}},\mathbb{U}_{\mathrm{r}},\mathbb{U}_{\mathrm{d}},\mathbb{S}_{\mathrm{r}},\mathbb{S}_{\mathrm{d}},t,\lambda}{\text{maximize}} \quad t - \lambda P_{\mathrm{tot}} \tag{2.53a}$$

$$\text{subject to} \quad P_{\mathrm{s}} \leq P_{\mathrm{s,max}}, \; P_{\mathrm{r}} \leq P_{\mathrm{r,max}}, \tag{2.53b}$$

$$\sum_{k\in\mathbb{K}} (-\mathrm{Tr}(\mathbf{S}_{\mathrm{r}}^{k}\mathbf{E}_{\mathrm{r}}^{k}) + \log|\mathbf{S}_{\mathrm{r}}^{k}| + d_{\mathrm{s}}) \geq t, \tag{2.53c}$$

$$\sum_{k\in\mathbb{K}} (-\mathrm{Tr}(\mathbf{S}_{\mathrm{d}}^{k}\mathbf{E}_{\mathrm{d}}^{k}) + \log|\mathbf{S}_{\mathrm{d}}^{k}| + d_{\mathrm{r}}) \geq t. \tag{2.53d}$$

For fixed $\mathbb{V}_{\mathrm{s}}$, $\mathbb{V}_{\mathrm{r}}$ and t, the MMSE filters and the MMSE error matrix can be calculated from (2.35), (2.36), and (2.37), (2.38) respectively. The λ can be determined from

$$t - \lambda P_{\mathrm{tot}} = 0. \tag{2.54}$$

The variables $\mathbb{V}_{\mathrm{s}}, \mathbb{V}_{\mathrm{r}}$ and t are updated by solving (2.53) with fixed $\mathbb{U}_{\mathrm{r}}, \mathbb{U}_{\mathrm{d}}, \mathbb{S}_{\mathrm{r}}, \mathbb{S}_{\mathrm{d}}$ and λ. The optimization problem is solved iteratively until a stable point is reached. Algorithm 4 defines the detailed algorithm procedure.

Algorithm 4 AQCP-WMMSE design for energy efficiency maximization

$a \leftarrow 0$ (set iteration number to zero)
$\mathbb{V}_{\mathrm{s}}, \mathbb{V}_{\mathrm{r}} \leftarrow$ right singular matrix initialization [80, Appendix A]
$\lambda = 0 \leftarrow$ Lambda initialization
repeat
  $a \leftarrow a + 1$
  $\mathbb{U}_{\mathrm{r}}, \mathbb{U}_{\mathrm{d}} \leftarrow$ solve (2.35) and (2.36), respectively
  $\mathbb{S}_{\mathrm{r}}, \mathbb{S}_{\mathrm{d}} \leftarrow \mathbf{S}_{\mathrm{r}}^{k} = \mathbf{E}_{r}^{k^{-1}}$ and $\mathbf{S}_{\mathrm{d}}^{k} = \mathbf{E}_{\mathrm{d}}^{k^{-1}}$, respectively
  $\mathbb{V}_{\mathrm{s}}, \mathbb{V}_{\mathrm{r}}, t \leftarrow$ solve (2.53), with fixed $\mathbb{U}_{\mathrm{r}}, \mathbb{U}_{\mathrm{d}}, \mathbb{S}_{\mathrm{r}}, \mathbb{S}_{\mathrm{d}}$and λ
  $\lambda \leftarrow$ solve (2.54)
until a stable point, or maximum number of a reached
return $\{\mathbb{V}_{\mathrm{s}}, \mathbb{V}_{\mathrm{r}}\}$

2.6 Computational Complexity

In this section, we evaluate the arithmetic computational complexity corresponding to Algorithm 1. In this algorithm, the consideration of the impact of hardware distortions and CSI error escalates the problem dimension and also adds complexity to the optimization problem structure.

In the algorithm, the optimization variables $\mathbb{U}_{\mathrm{r}}, \mathbb{U}_{\mathrm{d}}$, $\mathbb{S}_{\mathrm{r}}$, and $\mathbb{S}_{\mathrm{d}}$ are obtained using their closed-form solution. Therefore, the computational complexity is dominated by the calculation of the variables $\mathbb{V}_{\mathrm{s}}, \mathbb{V}_{\mathrm{r}}$, and $\mathbb{T}$. The optimization problem over $\mathbb{V}_{\mathrm{s}}, \mathbb{V}_{\mathrm{r}}$, and $\mathbb{T}$ can be cast as a conic quadratic program (CQP). The general CQP can be stated as

$$\underset{\mathbf{x}}{\text{minimize}}\{\mathbf{c}^T\mathbf{x} : \|\mathbf{A}_i\mathbf{x} + \mathbf{b}_i\|_2 \leq \mathbf{c}_i^T\mathbf{x} + \mathbf{d}_i, i = 1, 2, ...m; \|\mathbf{x}\| \leq R\} \quad \mathbf{x} \in \mathbb{R}^n; \mathbf{b}_i \in \mathbb{R}^{k_i}.$$

For the definition of problem structure; please refer to [82, Section 4.6.2]. The arithmetic complexity for attaining an ε-solution to the above problem is upper bounded by

$$\mathcal{O}(1)(m+1)^{\frac{1}{2}} n\Big(n^2 + m + \sum_{i=0}^{m}(k_i)^2\Big)\mathrm{digit}(\varepsilon),$$

where $\mathcal{O}(1)$ is a positive constant, and digit(ε) corresponds to the required solution precision [82, Section 4.6.2]. The computation necessary for each step depends on the size of the variable space (n), the number of constraints (m) and their corresponding block size (k_i). For our problem, the size of the variable space is given as $n = K(2(N_{\mathrm{s}} + N_{\mathrm{r}}) + 1)$. The block size for each constraint, $k_i = 2(d_{\mathrm{s}}^2(1 + 2KN_{\mathrm{s}}) + 2KN_{\mathrm{r}}d_{\mathrm{s}}d_{\mathrm{r}} + KN_{\mathrm{s}}d_{\mathrm{s}} + KN_{\mathrm{r}}d_{\mathrm{r}} + 2K + 2)$ corresponding to constraint (2.43b), as $k_i = 2(d_{\mathrm{r}}^2(1 + 2KN_{\mathrm{r}}) + (2KN_{\mathrm{s}} + 1)d_{\mathrm{s}}d_{\mathrm{r}} + KN_{\mathrm{s}}d_{\mathrm{s}} + KN_{\mathrm{r}}d_{\mathrm{r}} + 2K + 2)$ corresponding to constraint (2.43c), furthermore $k_i = 2KN_{\mathrm{s}}d_{\mathrm{s}}$ belongs to power constraint (2.33b) and $k_i = 2KN_{\mathrm{r}}d_{\mathrm{r}}$ belongs to constraint (2.33c). The total number of constraints can be concluded to be $m = 2K + 2$.

For the JC decoding and mapping scenario, the size of the variable space changes to $n = 2K(N_{\mathrm{s}} + N_{\mathrm{r}}) + 1$. The number of constraints will be reduced to $m = 4$, where the

block size for each constraint increases by K fold. As a remark, the actual computation load may differ from the above mentioned, as it depends on the utilized numerical solver and other structure simplification methods.

2.7 Numerical Evaluations

In this section, we evaluate the performance of the proposed transceiver design for both JC and PC introduced in Section 2.5 in terms of sum-rate and energy efficiency for an FD MIMO OFDM DF relay system under various system conditions. All communication channels follow an uncorrelated Rayleigh flat fading model. The SI channel follows the characterization reported in [20]:

$$\mathbf{H}_{rr} \sim \mathcal{CN}\left(\sqrt{\frac{\rho_{si}K_R}{1+K_R}}\mathbf{H}_0, \frac{\rho_{si}}{1+K_R}\mathbf{I}_{M_r} \otimes \mathbf{I}_{N_r}\right),$$

where ρ_{si} is the SI channel strength, $\mathbf{H}_0$ is a deterministic matrix of all-1 elements, and K_R is the Rician coefficient. The spatial covariance matrix of the estimated error is assumed to be the identity matrix. The overall system performance is averaged over 100 channel realizations. For numerical analysis, the default parameter values are chosen as in Table 2.1.

K	4
$N = N_{\mathrm{s}} = M_{\mathrm{r}} = N_{\mathrm{r}} = M_{\mathrm{d}}$	2
$\rho = \rho_{\mathrm{sr}} = \rho_{\mathrm{rd}}$	-20dB
ρ_{sd}, ρ_{si}, K_R	-30 dB, 0 dB, 1
$\sigma^2_{\mathrm{n}} = \sigma^2_{\mathrm{r},k} = \sigma^2_{\mathrm{d},k}$	-30 dB
$P_{\max} = P_{\mathrm{s,max}} = P_{\mathrm{r,max}}$	1
$\mu_{\mathrm{s}} = \mu_{\mathrm{r}}$	0.9
$P_{\mathrm{s_{zero}}} = P_{\mathrm{r_{zero}}} = P_{\mathrm{FD}}$	0.01
$d = d_{\mathrm{s}} = d_{\mathrm{r}}$	2
$\kappa = \beta, \mathbf{\Theta}_{\mathrm{tx,s}} = \mathbf{\Theta}_{\mathrm{tx,r}} = \kappa\mathbf{I}_N$ and $\mathbf{\Theta}_{\mathrm{rx,r}} = \mathbf{\Theta}_{\mathrm{rx,d}} = \beta\mathbf{I}_N$	-40dB

Table 2.1: Default setup

Comparison Benchmarks

For comparison using numerical simulations, the following benchmarks are considered:

- JC: It represents the proposed algorithms for joint-carrier (JC) design, with consideration of the impact of imperfect CSI as well as the hardware distortions.
- PC: It represents the proposed algorithms for per-carrier (PC) design, with consideration of the impact of imperfect CSI as well as the hardware distortions.

- LD (less-distortion): It indicates the algorithms that do not consider the impact of hardware distortions at the source and the destination in the design , i.e., only hardware inaccuracy at the relay is considered since hardware impairments are more significant for FD nodes.
- ND (non-distortion) : It indicates the algorithms that do not consider the impact of hardware distortions in the design , i.e., hardware inaccuracy is not taken into account. It only considers the impact of imperfect CSI.
- WoCSI (without-CSI) : It indicates the algorithms that assumes a perfect CSI is attained.
- HD: It indicates the scenarios when an HD MIMO relay is employed. We consider the HD relay utilizes TDD, hence SI is not present.

Visualization

In Fig. 2.2a, the average convergence behaviour is plotted for different values of hardware inaccuracy κ dB. We apply right-singular matrix (RSM) initialization proposed in [80, Appendix A]. It is observed that the algorithm converges within 10-25 iterations. As expected, it can be seen that the objective has a higher value for smaller hardware inaccuracy. Even though the global optimality of the final solution can not be verified due to the possibility of the local solutions; the numerical simulations exhibit that the algorithm shows good convergence behaviour when the RSM initialization is applied.

In Fig. 2.2b, the performance of the design, in terms of system sum-rate, is evaluated for different values of transceiver inaccuracy. As we can observe, the sum-rate decreases as the transceiver inaccuracy increases, i.e., the higher the κ, the smaller the sum-rate. It is clear that the proposed design JC outperforms all the other benchmarks. As the value of κ increases, JC and PC algorithms show better performance compared to their ND counterparts. This indicates that a design with consideration of hardware impairments is essential as transceiver inaccuracy κ increases.

In Fig. 2.2c, the impact of the receiver noise is depicted. The sum-rate of the system decreases as the receiver noise increases. As it can be seen that, for lower values of receiver noise, the JC design performs better compared to all other benchmarks. It can also be noticed that at smaller noise values, the JC (PC) design shows better performance than the ND-JC (ND-PC) design as the hardware distortions become dominant. This implies the importance of considering a hardware-distortion aware design, especially at high signal to noise ratio (SNR) values.

In Fig. 2.2d, the system performance in terms of sum-rate for JC coding strategy is evaluated with respect to the channel estimation error. It can be clearly observed, as the channel estimation error increases the sum-rate of the system decreases. For small values for channel estimation error, the JC algorithm and Wo-CSI algorithm show almost similar performance. However, both the algorithms outperform the ND

design. This is due to the fact that the hardware distortions become dominant for small values of channel estimation error (similar to the receiver noise case). As the channel estimation error value increases, the performance of the design degrades compared to the JC and ND designs.

In Fig. 2.2e, the total sum-rate of the system is plotted against the number of antennas ($M_{\mathrm{r}} = N_{\mathrm{r}}$) at the relay. As expected, the system sum-rate increases as the number of antennas at the relay increases. An interesting observation is that as the number of antennas at the relay increases, the performance of ND algorithms degrades compared to the corresponding JC/PC algorithm performance. This implies that as the number of antennas increases, hardware-distortion aware design becomes more relevant.

Fig. 2.2f, illustrates the dependency of our algorithms on the number of sub-carriers, in terms of sum-rate. The performance of all the algorithms improves as the number of sub-carriers increases. It can be observed that as the number of sub-carriers increases, the more gain in terms of sum-rate can be achieved by the JC algorithm over the PC algorithm and other ND algorithms. This is because the JC algorithm is more flexible with respect to the allocation of resources. It will allocate more resources to the better sub-carriers in both the source-relay link and the relay-destination link. Whereas in the PC algorithm, more resources can be allocated to the sub-carriers which are better only in the source-relay link. Sometimes, the relay to destination link is worst compared to the source to relay link for some sub-carriers. This results in an overall reduced sum-rate.

In Fig. 2.3a, the impact of the transceiver inaccuracy on the energy efficiency of the systen is depicted. The general trend is similar to that in the case of the sum-rate. The energy efficiency of the system decreases as the transceiver inaccuracy (κ) increases. It is observed that the ND designs becomes less efficient compared to the corresponding JC/PC design, as the value of (κ) increases. This implies the importance of considering a hardware-distortion aware design. It is interesting to observe that the less distortion (LD) design performs similar to the JC design except for the higher values of κ, which is very unusual in the practical case.

In Fig. 2.3b, the performance of all the algorithms in terms of energy efficiency, with respect to the channel estimation error is plotted. It can be clearly observed that as the channel estimation error increases the energy efficiency of the system decreases. Similar to the sum-rate case, the Wo-CSI design performs worst compared to the JC and ND design, particularly for higher values of channel estimation error.

Fig. 2.3c shows the impact of power consumed for channel estimation on the energy efficiency of the system. Initially, as the power consumed for channel estimation increases, which in turn reduces the channel estimation error, improves the energy efficiency of the system. However after a certain point, the energy efficiency starts to degrade. This is because the energy required for the transmission becomes less as more power is allocated to the channel estimation. Hence, it is better to restrict the power consumption for channel estimation with some budget constraint to gain better energy efficiency.

In Fig. 2.3d, the impact of the receiver noise is depicted. Similar to the sum-rate case, it can be observed that the energy efficiency of the system decreases as the receiver noise increases. It is observed that at smaller noise values, the JC/PC design outperforms their ND counterparts as the hardware distortions become dominant at high SNR scenario. It can be also noticed the JC is more energy-efficient compared to the other benchmarks.

Computational Time

In Table.2.2, the computational complexity of the algorithms in terms of the required computational time (CT) is depicted for different values of transceiver accuracy [2]. It can be seen that the JC design requires a high CT compared to other algorithms. This is due to the consideration of distortion of all the nodes as well as joint sub-carrier optimization. It is interesting to observe that LD design performs similar to the JC design with less CT. It also outperforms the PC design even though both designs require almost similar CT. Hence for complex systems, one can use LD design without significant degradation.

κdB	JC	PC	LD	LD-PC	ND
-40	80.32	46.41	53.45	30.59	27.14
-20	63.18	46.15	53.45	30.59	27.18
-5	69.23	50.15	43.93	33.60	27.18

Table 2.2: Comparison of computational complexity in terms of CT (in seconds)

2.8 Conclusions

FD MC systems are usually limited by the residual SI, which spreads over multiple subcarriers (ICL) due to the non-linear hardware distortion. We proposed a linear transceiver design for an FD MC MIMO DF relaying system by taking into account the impact of hardware distortions leading to ICL as well as the impact of CSI error. We investigated the linear precoding and decoding design problem for different system objectives such as system sum-rate maximization, power minimization and energy efficiency maximization. From our numerical simulations, it is observed that a significant gain can be obtained via the application of the proposed distortion-aware designs, when transceiver inaccuracy increases, and ICL becomes a dominant factor. This indicates that the consideration of hardware distortion is essential for an FD MIMO MC relay system. Furthermore, it is observed that the JC approach performs better compared to the PC and the HD benchmarks. It can also be noticed that the LD approach, which is computationally less complex, performs similar to the proposed design. So for more complex systems such as multi-user setup, LD design can be used without significant performance degradation.

[2]The reported CT is obtained using an Intel Core i7-4790S processor with a clock rate of 3.2 GHz and 16 GB RAM. We use MATLAB 2016b on a 64-bit operating system.

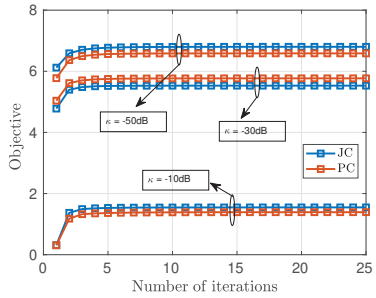

(a) Average convergence behaviour of JC and PC algorithms

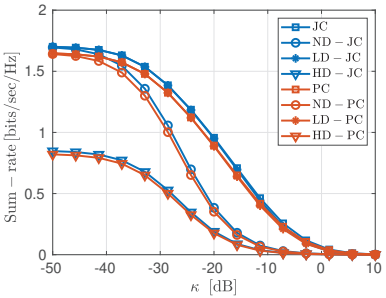

(b) Sum-rate vs. Hardware inaccuracy

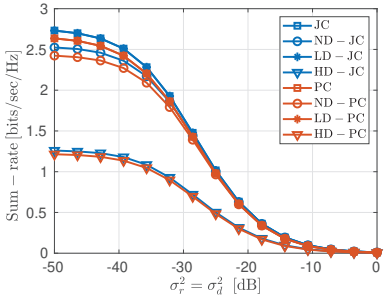

(c) Sum-rate vs. Receiver noise

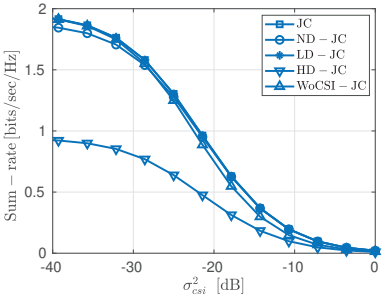

(d) Sum-rate vs. Channel estimation error

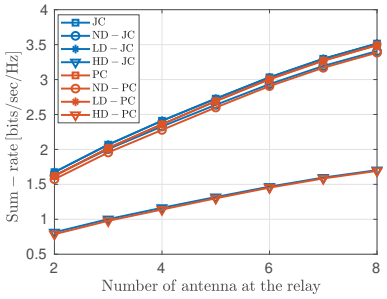

(e) Sum-rate vs. Number of relay antennas

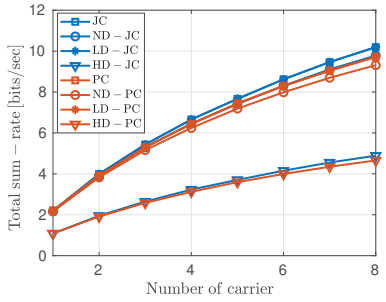

(f) Sum-rate vs. Number of sub-carriers

Figure 2.2: Sum-rate vs. Different system parameters.

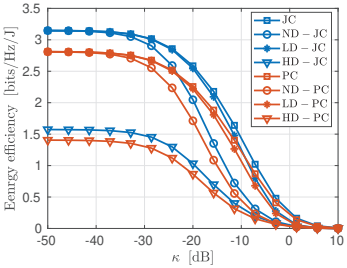

(a) Energy efficiency vs. Hardware inaccuracy

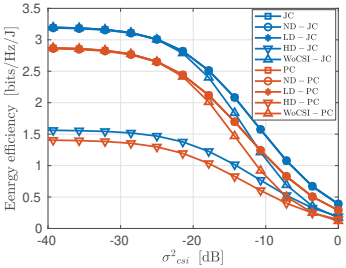

(b) Energy efficiency vs. Channel estimation error

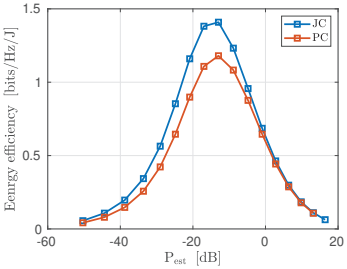

(c) Energy efficiency vs. Power consumed for channel estimation

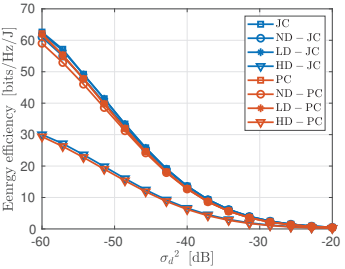

(d) Energy efficiency vs. Receiver noise

Figure 2.3: Energy efficiency vs. Different system parameters.

3 Resource Allocation for Multi-user Multi-carrier FD mMIMO DF Relay System with Hardware Impairments

3.1 Scope

Multiple input multiple output (MIMO) relay has been widely studied as a practical approach to extend coverage as well as to improve spectral efficiency, especially at the cell edges. Nevertheless, these systems require complex power allocation and precoder/decoder design. On the contrary, massive multiple input multiple output (mMIMO) relaying has received a substantial recognition over the past years, due to its ability to mitigate noise, inter-user interference and fast fading using simple linear processing. Increasing the number of antennas reap all the benefits of MIMO systems in terms of power and multiplexing gains. Moreover, large scale antennas provide more spatial degree of freedom that helps in better self-interference cancellation (SIC). Therefore, a relaying system with a large scale antenna array at the relay station appears to be a viable candidate to address the above-mentioned transceiver design challenges as well as to enable full-duplex (FD) operation.

3.2 Related Works

The spectral/energy efficiency of FD mMIMO relaying has been investigated in [38, 50–53, 83, 84]. In [51], a power allocation scheme is proposed for FD mMIMO decode and forward (DF) to maximize the energy efficiency for a given quality of service (sum spectral efficiency) under transmit power constraints. It is also shown that by increasing the number of transmit/receive antenna at the relay station, the transmit power at the source as well as the relay can be reduced. In [53], the authors demonstrate that, for an FD mMIMO DF relay system over Rician fading channels, the self-interference (SI) can be significantly cancelled by zero-forcing (ZF) processing at the relay station when the number of receive and transmit antennas tend to infinity. However, the impact of hardware distortions is not taken into account in the above-mentioned works.

In [38, 84], the authors consider the FD mMIMO DF relaying system, where the FD relay is equipped with a large-scale antenna array simultaneously serve multiple source-destination pairs by taking into account the hardware impairments. In [84], an end-to-end achievable rate of the system is derived for the large-antenna regime by assuming maximum ratio transmitting (MRT)/maximum ratio combining (MRC) at the relay for single antenna source-destination users. A power control scheme is also proposed to optimize the energy efficiency of the system. Furthermore, in [38], a hardware impairment aware transceiver scheme is proposed to cancel out the distortion noise for a more general model, where the source and destination are allowed to equipped with multiple antennas. An asymptotic end-to-end achievable rate of the system with the proposed transceiver scheme is derived. A joint degree of freedom and power allocation is also presented to enhance the spectral efficiency of the proposed system. However, the aforementioned works [38,84] consider the hardware impairments in an FD mMIMO relay for a single carrier system.

3.3 Chapter Outline

In this chapter, we consider the resource allocation problem for an FD mMIMO multi-carrier (MC) DF relay system, which serves L number of source-destination pairs. In Section 3.4, the system model and the operation of the relay system by taking into account the hardware distortions leading to residual SI and inter-carrier leakage (ICL) as well as the imperfect channel state information (CSI) are discussed. We also devise the asymptotic rate analysis of our system employed with MRT/MRC strategy, when the number of antennas become large (goes to ∞) in Section 3.4.4. In Section 3.5, joint sub-carrier and power allocation problem are discussed for three different optimization objectives such as sum-rate maximization (Section 3.5.1), energy efficiency maximization (Section 3.5.2), and delivery time minimization (Section 3.5.3). The performance of the proposed algorithms is evaluated in Section 3.6, and our main results are summarized in Section 3.7.

3.4 System Model

We consider an MC DF relay setup, where L number of single antenna half-duplex (HD) source-destination pairs communicate through an FD mMIMO relay. The FD mMIMO relay consists of N antennas for both transmission and reception. Fig 3.1 presents a basic model for our system. We denote the index sets of all the source-destination pairs and sub-carriers by $\mathbb{L}$ and $\mathbb{K}$ respectively, where $\overline{\mathbb{L}} = L$ and $\overline{\mathbb{K}} = K$. Initially, the source nodes transmit signals to the relay through the source-relay channel. The desired source-relay channel from i-th source to the relay using sub-carrier k can be represented as $\mathbf{h}_{\mathrm{sr}}^{i,k} \in \mathbb{C}^{N\times 1}$. The signals received by the relay are decoded at the relay

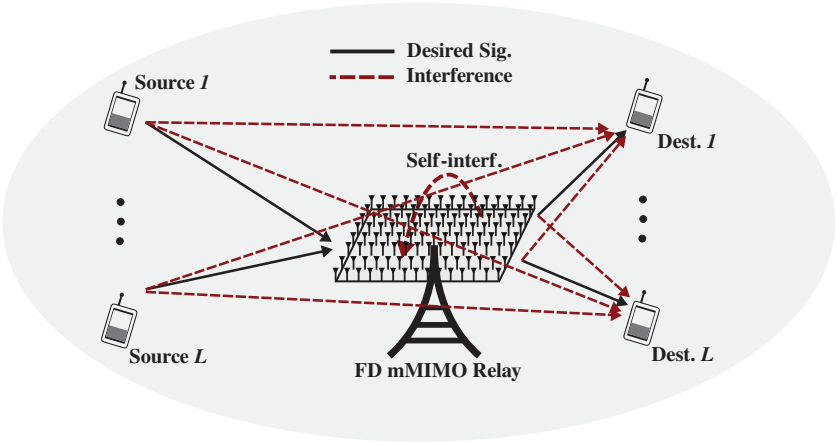

Figure 3.1: Basic system model for FD mMIMO relay communication between the L single antenna source-destination pairs

after employing SIC techniques. Then, the decoded signals are retransmitted to the destination nodes through the relay-destination channel. The $\mathbf{h}_{\mathrm{rd}}^{i,k} \in \mathbb{C}^{1\times N}$ represents desired relay-destination channel between the relay and i-th destination node using k-th sub-carrier. The SI channel at the relay can be denoted by $\mathbf{H}_{\mathrm{rr}}^{k} \in \mathbb{C}^{N\times N}$. We consider weak signals, due to path loss, that are received at the destination nodes directly from source nodes to be an interference [70, 73]. The direct channel between the source j and destination i through k-th sub-carrier can be represented as $h_{\mathrm{sd}}^{i,j,k} \in \mathbb{C}^{1}$. We assume all channels are constant for each frame and frequency flat in each carrier.

We consider a limited availability of CSI, i.e., only imperfect CSI of the channels are available. As in [85], the true channel, decomposed into the estimated channel and estimation error, can be represented as

$$\begin{aligned}
\mathbf{h}_{\mathrm{sr}}^{i,k} &= \widehat{\mathbf{h}}_{\mathrm{sr}}^{i,k} + \widetilde{\mathbf{h}}_{\mathrm{sr}}^{i,k}, \;\; \widehat{\mathbf{h}}_{\mathrm{sr}}^{i,k} \perp \widetilde{\mathbf{h}}_{\mathrm{sr}}^{i,k} \\
h_{\mathrm{sd}}^{i,j,k} &= \widehat{h}_{\mathrm{sd}}^{i,j,k} + \widetilde{h}_{\mathrm{sd}}^{i,j,k}, \;\; \widehat{h}_{\mathrm{sd}}^{i,j,k} \perp \widetilde{h}_{\mathrm{sd}}^{i,j,k} \\
\mathbf{h}_{\mathrm{rd}}^{i,k} &= \widehat{\mathbf{h}}_{\mathrm{rd}}^{i,k} + \widetilde{\mathbf{h}}_{\mathrm{rd}}^{i,k}, \;\; \widehat{\mathbf{h}}_{\mathrm{rd}}^{i,k} \perp \widetilde{\mathbf{h}}_{\mathrm{rd}}^{i,k} \\
\mathbf{H}_{\mathrm{rr}}^{k} &= \widehat{\mathbf{H}}_{\mathrm{rr}}^{k} + \widetilde{\mathbf{H}}_{\mathrm{rr}}^{k}, \;\; \widehat{\mathbf{H}}_{\mathrm{rr}}^{k} \perp \widetilde{\mathbf{H}}_{\mathrm{rr}}^{k}, \;\; \forall i,j \in \mathbb{L}, \forall k \in \mathbb{K},
\end{aligned} \tag{3.1}$$

where the estimated channels of source-relay, source-destination, relay-destination, and SI channel are represented by $\widehat{\mathbf{h}}_{\mathrm{sr}}^{i,k}, \widehat{h}_{\mathrm{sd}}^{i,j,k}, \widehat{\mathbf{h}}_{\mathrm{rd}}^{i,k}$ and $\widehat{\mathbf{H}}_{\mathrm{rr}}^{k}$, respectively. The entries of channel estimation error $\widetilde{\mathbf{h}}_{\mathrm{sr}}^{i,k}, \widetilde{h}_{\mathrm{sd}}^{i,j,k}, \widetilde{\mathbf{h}}_{\mathrm{rd}}^{i,k}$ and $\widetilde{\mathbf{H}}_{\mathrm{rr}}^{k}$ are assumed to be independent and identically distributed (i.i.d.) complex Gaussian with zero mean and variance $(\sigma_{e,\mathrm{sr}}^{i,k})^2$, $(\sigma_{e,\mathrm{sd}}^{i,j,k})^2$, $(\sigma_{e,\mathrm{rd}}^{i,k})^2$ and $(\sigma_{e,\mathrm{rr}}^{k})^2$, respectively. The estimated channel and the estimation error are as-

sumed to be statistically uncorrelated. We consider the receiver employs the minimum mean square error (MMSE) channel estimation strategy.

3.4.1 Source to Relay

As mentioned earlier, initially, all the source nodes transmit their desired signal to the relay. The transmit signal from the i-th source node to the relay using the sub-carrier k can be written as

$$x_{\mathrm{s}}^{i,k} = \underbrace{\sqrt{p_{\mathrm{s}}^{i,k}} s_{\mathrm{s}}^{i,k}}_{:=\widetilde{x}_{\mathrm{s}}^{i,k}} + e_{\mathrm{t,s}}^{i,k}\ ,\ i \in \mathbb{L}, \forall k \in \mathbb{K}, \tag{3.2}$$

where $s_{\mathrm{s}}^{i,k} \in \mathbb{C}^1$ and $e_{\mathrm{t,s}}^{i,k}$ represent the source symbol from the source i to the relay and transmit distortion at the i-th source node, respectively. We assume the source symbols are i.i.d. with unit power, i.e., $\mathbb{E}\{s_{\mathrm{s}}^{i,k}(s_{\mathrm{s}}^{i,k})^*\} = 1$. The intended transmit signal and transmit power at the i-th source node are denoted by $\widetilde{x}_{\mathrm{s}}^{i,k}$ and $p_{\mathrm{s}}^{i,k}$.

Subsequently, the received signal at the relay from all the source nodes using k-th sub-carrier can be stated as

$$\mathbf{y}_{\mathrm{r}}^{k} = \underbrace{\sum_{i\in\mathbb{L}} \mathbf{h}_{\mathrm{sr}}^{i,k} x_{\mathrm{s}}^{i,k} + \mathbf{H}_{\mathrm{rr}}^{k}\mathbf{x}_{\mathrm{r}}^{k} + \mathbf{n}_{\mathrm{r}}^{k}}_{:=\widetilde{\mathbf{y}}_{\mathrm{r}}^{k}} + \mathbf{e}_{\mathrm{r,r}}^{k},\ \ \forall k \in \mathbb{K}, \tag{3.3}$$

where $\mathbf{n}_{\mathrm{r}}^{k} \sim \mathcal{CN}(\mathbf{0}_N, (\sigma_{\mathrm{n,r}}^{k})^2\mathbf{I}_N)$ and $\mathbf{e}_{\mathrm{r,r}}^{k}$ represent the receiver noise and receive distortion at the relay, respectively. The intended receive signal at the relay is defined as $\widetilde{\mathbf{y}}_{\mathrm{r}}^{k}$. The second term in equation (3.3), i.e.,$(\widehat{\mathbf{H}}_{\mathrm{rr}}^{k} + \widetilde{\mathbf{H}}_{\mathrm{rr}}^{k})\mathbf{x}_{\mathrm{r}}^{k}$ refers to the SI at the relay, where $\mathbf{x}_{\mathrm{r}}^{k}$ is the transmitted signal at the relay. The known part of the transmit signal can be mitigated from the SI by utilizing SIC techniques. Hence, the received signal after applying SIC can be obtained as

$$\overline{\mathbf{y}}_{\mathrm{r}}^{k} = \mathbf{y}_{\mathrm{r}}^{k} - \widehat{\mathbf{H}}_{\mathrm{rr}}^{k}\widetilde{\mathbf{x}}_{\mathrm{r}}^{k}\ ,\ \forall k \in \mathbb{K}, \tag{3.4}$$

where $\widetilde{\mathbf{x}}_{\mathrm{r}}^{k}$ denotes the intended transmit signal at the relay. Correspondingly, the received signal from the i-th source at the relay after SIC can be written as

$$\overline{\mathbf{y}}_{\mathrm{r}}^{i,k} = \widehat{\mathbf{h}}_{\mathrm{sr}}^{i,k}\widetilde{x}_{\mathrm{s}}^{i,k} + \boldsymbol{\nu}_{\mathrm{r}}^{i,k}\ ,\ \forall k \in \mathbb{K}, \tag{3.5}$$

where the collective interference plus noise at the relay corresponding to the i-th source and k-th sub-carrier can be defined as

$$\boldsymbol{\nu}_{\mathrm{r}}^{i,k} := \widehat{\mathbf{h}}_{\mathrm{sr}}^{i,k} e_{\mathrm{t,s}}^{i,k} + \widetilde{\mathbf{h}}_{\mathrm{sr}}^{i,k} x_{\mathrm{s}}^{i,k} + \sum_{\substack{j\in\mathbb{L}\\ j\neq i}} \mathbf{h}_{\mathrm{sr}}^{j,k} x_{\mathrm{s}}^{j,k} + \widehat{\mathbf{H}}_{\mathrm{rr}}^{k}\mathbf{e}_{\mathrm{t,r}}^{k} + \widetilde{\mathbf{H}}_{\mathrm{rr}}^{k}\mathbf{x}_{\mathrm{r}}^{k} + \mathbf{n}_{\mathrm{r}}^{k} + \mathbf{e}_{\mathrm{r,r}}^{k}\ ,\ \forall k \in \mathbb{K}, \tag{3.6}$$

where $\mathbf{e}_{\mathrm{t,r}}^{k}$ represents the transmit distortion at the relay. The estimated received source symbol at the relay corresponding to the source i and sub-carrier k can be obtained as

$$\widetilde{s}_{\mathrm{s}}^{i,k} = (\mathbf{u}_{\mathrm{r}}^{i,k})^H \overline{\mathbf{y}}_{\mathrm{r}}^{i,k},\ \ \forall k \in \mathbb{K}, \tag{3.7}$$

where $\mathbf{u}_{\mathrm{r}}^{i,k} \in \mathbb{C}^{N\times 1}$ is the normalized linear receive filter at the relay for the source i and sub-carrier k.

3.4.2 Relay to Destination

The transmit signal from the relay to the destination nodes using sub-carrier k can be expressed as

$$\mathbf{x}_{\mathrm{r}}^{k} = \underbrace{\sum_{i\in\mathbb{L}} \mathbf{v}_{\mathrm{r}}^{i,k}\sqrt{p_{\mathrm{r}}^{i,k}}s_{\mathrm{r}}^{i,k}}_{:=\widetilde{\mathbf{x}}_{\mathrm{r}}^{k}} + \mathbf{e}_{\mathrm{t,r}}^{k}\ ,\ \forall k \in \mathbb{K}, \tag{3.8}$$

where $s_{\mathrm{r}}^{i,k} \in \mathbb{C}^1$, $p_{\mathrm{r}}^{i,k}$ and $\mathbf{v}_{\mathrm{r}}^{i,k} \in \mathbb{C}^{N\times 1}$ are the retransmitting source symbol, transmit power and normalized transmit precoder at the relay for the destination i utilizing sub-carrier k. We consider the source symbols to be i.i.d. with unit power ($\mathbb{E}\{s_{\mathrm{r}}^{i,k}(s_{\mathrm{r}}^{i,k})^*\} = 1$). Subsequently, the signal received at the destination i, including the interference from the source nodes, can be expressed as

$$y_{\mathrm{d}}^{i,k} = \underbrace{\mathbf{h}_{\mathrm{rd}}^{i,k}\mathbf{x}_{\mathrm{r}}^{k} + \sum_{j\in\mathbb{L}} h_{\mathrm{sd}}^{i,j,k}x_{\mathrm{s}}^{j,k} + n_{\mathrm{d}}^{i,k}}_{:=\widetilde{y}_{\mathrm{d}}^{i,k}} + e_{\mathrm{r,d}}^{i,k}\ ,\ i \in \mathbb{L}, \forall k \in \mathbb{K}, \tag{3.9}$$

where the receive distortion and receiver noise at the i-th desination node are denoted by $e_{\mathrm{r,d}}^{i,k}$ and $n_{\mathrm{d}}^{i,k} \sim \mathcal{CN}(0, (\sigma_{\mathrm{n,d}}^{i,k})^2)$, respectively. The intended receive signal at the destination i using sub-carrier k is defined as $\widetilde{y}_{\mathrm{d}}^{i,k}$. The above equation (3.9) can be rewritten as

$$y_{\mathrm{d}}^{i,k} = \widehat{\mathbf{h}}_{\mathrm{rd}}^{i,k}\mathbf{v}_{\mathrm{r}}^{i,k}\sqrt{p_{\mathrm{r}}^{i,k}}s_{\mathrm{r}}^{i,k} + \nu_{\mathrm{d}}^{i,k},\quad i \in \mathbb{L}, \forall k \in \mathbb{K}, \tag{3.10}$$

where the collective interference plus noise at the destination i can be defined as

$$\begin{aligned}\nu_{\mathrm{d}}^{i,k} :=& \widetilde{\mathbf{h}}_{\mathrm{rd}}^{i,k}\mathbf{v}_{\mathrm{r}}^{i,k}\sqrt{p_{\mathrm{r}}^{i,k}}s_{\mathrm{r}}^{i,k} + \sum_{\substack{j\in\mathbb{L}\\ j\neq i}}\mathbf{h}_{\mathrm{rd}}^{i,k}\mathbf{v}_{\mathrm{r}}^{j,k}\sqrt{p_{\mathrm{r}}^{j,k}}s_{\mathrm{r}}^{j,k} + \mathbf{h}_{\mathrm{rd}}^{i,k}\mathbf{e}_{\mathrm{t,r}}^{k} \\ &+ \sum_{j\in\mathbb{L}} h_{\mathrm{sd}}^{i,j,k}x_{\mathrm{s}}^{j,k} + n_{\mathrm{d}}^{i,k} + e_{\mathrm{r,d}}^{i,k},\quad i \in \mathbb{L}, \forall k \in \mathbb{K}.\end{aligned} \tag{3.11}$$

Similar to the previous chapter, the distortion terms are considered to be proportional to the intensity of the intended signals. Following the Lemma 2.4.1, the statistics of the distortion terms can be obtained as

$$e_{\mathrm{t,s}}^{i,k} \sim \mathcal{CN}\left(0, \frac{\widetilde{\kappa}_{\mathrm{s}}^{i}}{K}\sum_{k\in\mathbb{K}}\left(\mathbb{E}\{\widetilde{x}_{\mathrm{s}}^{i,k}(\widetilde{x}_{\mathrm{s}}^{i,k})^H\}\right)\right), \tag{3.12}$$

$$\mathbf{e}_{\mathrm{t,r}}^{k} \sim \mathcal{CN}\left(\mathbf{0}_N, \frac{1}{K}\widetilde{\mathbf{\Theta}}_{\mathrm{t,r}}\sum_{k\in\mathbb{K}}\mathrm{diag}\left(\mathbb{E}\{\widetilde{\mathbf{x}}_{\mathrm{r}}^{k}(\widetilde{\mathbf{x}}_{\mathrm{r}}^{k})^H\}\right)\right), \tag{3.13}$$

$$\mathbf{e}_{\mathrm{r,r}}^{k} \sim \mathcal{CN}\left(\mathbf{0}_N, \frac{1}{K}\widetilde{\mathbf{\Theta}}_{\mathrm{r,r}}\sum_{k\in\mathbb{K}}\mathrm{diag}\left(\mathbb{E}\{\widetilde{\mathbf{y}}_{\mathrm{r}}^{k}(\widetilde{\mathbf{y}}_{\mathrm{r}}^{k})^H\}\right)\right), \tag{3.14}$$

$$e_{\mathrm{r,d}}^{i,k} \sim \mathcal{CN}\left(0, \frac{\widetilde{\beta}_{\mathrm{d}}^{i}}{K}\sum_{k\in\mathbb{K}}\left(\mathbb{E}\{\widetilde{y}_{\mathrm{d}}^{i,k}(\widetilde{y}_{\mathrm{d}}^{i,k})^{H}\}\right)\right), \tag{3.15}$$

where the transmit distortion coefficient of the i-th source node can be denoted as $\widetilde{\kappa}_{\mathrm{s}}^{i}$ and the receive distortion coefficient for destination i can be represented using $\widetilde{\beta}_{\mathrm{d}}^{i}$. The diagonal matrices $\widetilde{\mathbf{\Theta}}_{\mathrm{t,r}}$ and $\widetilde{\mathbf{\Theta}}_{\mathrm{r,r}}$ consist of transmit and receive distortion coefficients for the corresponding chains at the mMIMO relay, respectively. For further calculations, we define $\kappa_{\mathrm{s}}^{i} = \frac{\widetilde{\kappa}_{\mathrm{s}}^{i}}{K}$, $\beta_{\mathrm{d}}^{i} = \frac{\widetilde{\beta}_{\mathrm{d}}^{i}}{K}$, $\mathbf{\Theta}_{\mathrm{t,r}} = \frac{1}{K}\widetilde{\mathbf{\Theta}}_{\mathrm{t,r}}$, and $\mathbf{\Theta}_{\mathrm{r,r}} = \frac{1}{K}\widetilde{\mathbf{\Theta}}_{\mathrm{r,r}}$.

3.4.3 Collective Interference plus Noise Signal Covariance

By employing Lemma 2.4.1, and equations (3.12), (3.13), and (3.14) on (3.6), the covariance of received collective interference-plus-noise signal at the relay corresponding to the i-th source node and sub-carrier k can be expressed as

$$\begin{aligned}
\mathbf{\Sigma}_{\mathrm{r}}^{i,k} \approx{}& \underbrace{\sum_{\substack{j\in\mathbb{L}\\ j\neq i}}\widehat{\mathbf{h}}_{\mathrm{sr}}^{j,k}p_{\mathrm{s}}^{j,k}(\widehat{\mathbf{h}}_{\mathrm{sr}}^{j,k})^{H} + \sum_{j\in\mathbb{L}}(\sigma_{e,\mathrm{sr}}^{j,k})^{2}p_{\mathrm{s}}^{j,k}\mathbf{I}_{N}}_{\text{Co-channel interference}}\\
&+ \underbrace{\sum_{j\in\mathbb{L}}\widehat{\mathbf{h}}_{\mathrm{sr}}^{j,k}\kappa_{\mathrm{s}}^{j}\sum_{m\in\mathbb{K}}p_{\mathrm{s}}^{j,m}(\widehat{\mathbf{h}}_{\mathrm{sr}}^{j,k})^{H} + \sum_{j\in\mathbb{L}}(\sigma_{e,\mathrm{sr}}^{j,k})^{2}\kappa_{\mathrm{s}}^{j}\sum_{m\in\mathbb{K}}p_{\mathrm{s}}^{j,m}\mathbf{I}_{N}}_{\text{Source transmit distortion}}\\
&+ \underbrace{(\sigma_{e,\mathrm{rr}}^{k})^{2}\mathrm{Tr}\left(\sum_{j\in\mathbb{L}}\mathbf{v}_{\mathrm{r}}^{j,k}p_{\mathrm{r}}^{j,k}(\mathbf{v}_{\mathrm{r}}^{j,k})^{H}\right)\mathbf{I}_{N}}_{\text{SI channel esimation error}} + \underbrace{\widehat{\mathbf{H}}_{\mathrm{rr}}^{k}\mathbf{\Theta}_{\mathrm{t,r}}\mathrm{diag}\left(\sum_{j\in\mathbb{L}}\sum_{m\in\mathbb{K}}\mathbf{v}_{\mathrm{r}}^{j,m}p_{\mathrm{r}}^{j,m}(\mathbf{v}_{\mathrm{r}}^{j,m})^{H}\right)(\widehat{\mathbf{H}}_{\mathrm{rr}}^{k})^{H}}_{\text{Relay transmit distortion}}\\
&+ \underbrace{(\sigma_{e,\mathrm{rr}}^{k})^{2}\mathrm{Tr}\left(\mathbf{\Theta}_{\mathrm{t,r}}\mathrm{diag}\left(\sum_{j\in\mathbb{L}}\sum_{m\in\mathbb{K}}\mathbf{v}_{\mathrm{r}}^{j,m}p_{\mathrm{r}}^{j,m}(\mathbf{v}_{\mathrm{r}}^{j,m})^{H}\right)\right)\mathbf{I}_{N}}_{\text{Relay transmit distortion}}\\
&+ \underbrace{\mathbf{\Theta}_{\mathrm{r,r}}\sum_{m\in\mathbb{K}}\mathrm{diag}\left(\sum_{j\in\mathbb{L}}\widehat{\mathbf{h}}_{\mathrm{sr}}^{j,m}p_{\mathrm{s}}^{j,m}(\widehat{\mathbf{h}}_{\mathrm{sr}}^{j,m})^{H} + \sum_{j\in\mathbb{L}}(\sigma_{e,\mathrm{sr}}^{j,m})^{2}p_{\mathrm{s}}^{j,m}\mathbf{I}_{N} + \widehat{\mathbf{H}}_{\mathrm{rr}}^{m}\sum_{j\in\mathbb{L}}\mathbf{v}_{\mathrm{r}}^{j,m}p_{\mathrm{r}}^{j,m}(\mathbf{v}_{\mathrm{r}}^{j,m})^{H}(\widehat{\mathbf{H}}_{\mathrm{rr}}^{m})^{H}\right)}_{\text{Relay receive distortion}}\\
&+ \underbrace{(\sigma_{e,\mathrm{rr}}^{m})^{2}\mathrm{Tr}\left(\sum_{j\in\mathbb{L}}\mathbf{v}_{\mathrm{r}}^{j,m}p_{\mathrm{r}}^{j,m}(\mathbf{v}_{\mathrm{r}}^{j,m})^{H}\right)\mathbf{I}_{N} + (\sigma_{\mathrm{n,r}}^{m})^{2}\mathbf{I}_{N}}_{\text{Relay receive distortion}} + \underbrace{(\sigma_{\mathrm{n,r}}^{k})^{2}\mathbf{I}_{N}}_{\text{Thermal noise}}.
\end{aligned} \tag{3.16}$$

Since the transmit and receive distortion coefficients lie within the range of 0 and 1 and mostly have very small values, the higher-order terms of the transmit and receive distortion are ignored.

Similarly, the covariance of the received collective interference-plus-noise signal for sub-carrier k at the i-th destination node can be calculated as

$$\begin{aligned}\Sigma_{\mathrm{d}}^{i,k} \approx & \underbrace{\widehat{\mathbf{h}}_{\mathrm{rd}}^{i,k}\sum_{\substack{j\in\mathbb{L}\\ j\neq i}}\mathbf{v}_{\mathrm{r}}^{j,k}p_{\mathrm{r}}^{j,k}(\mathbf{v}_{\mathrm{r}}^{j,k})^H(\widehat{\mathbf{h}}_{\mathrm{rd}}^{i,k})^H + (\sigma_{e,\mathrm{rd}}^{i,k})^2\mathrm{Tr}\left(\sum_{j\in\mathbb{L}}\mathbf{v}_{\mathrm{r}}^{j,k}p_{\mathrm{r}}^{j,k}(\mathbf{v}_{\mathrm{r}}^{j,k})^H\right)}_{\text{Co-channel interference}}\\
& + \underbrace{\widehat{\mathbf{h}}_{\mathrm{rd}}^{i,k}\boldsymbol{\Theta}_{\mathrm{t,r}}\mathrm{diag}\left(\sum_{j\in\mathbb{L}}\sum_{m\in\mathbb{K}}\mathbf{v}_{\mathrm{r}}^{j,m}p_{\mathrm{r}}^{j,m}(\mathbf{v}_{\mathrm{r}}^{j,m})^H\right)(\widehat{\mathbf{h}}_{\mathrm{rd}}^{i,k})^H}_{\text{Relay transmit distortion}}\\
& + \underbrace{(\sigma_{e,\mathrm{rd}}^{i,k})^2\mathrm{Tr}\left(\boldsymbol{\Theta}_{\mathrm{t,r}}\mathrm{diag}\left(\sum_{j\in\mathbb{L}}\sum_{m\in\mathbb{K}}\mathbf{v}_{\mathrm{r}}^{j,m}p_{\mathrm{r}}^{j,m}(\mathbf{v}_{\mathrm{r}}^{j,m})^H\right)\right)}_{\text{Relay transmit distortion}}\\
& + \underbrace{\sum_{j\in\mathbb{L}}\widehat{h}_{\mathrm{sd}}^{i,j,k}p_{\mathrm{s}}^{j,k}(\widehat{h}_{\mathrm{sd}}^{i,j,k})^* + \sum_{j\in\mathbb{L}}(\sigma_{e,\mathrm{sd}}^{i,j,k})^2p_{\mathrm{s}}^{j,k}}_{\text{Direct channel interference}}\\
& + \underbrace{\sum_{j\in\mathbb{L}}\widehat{h}_{\mathrm{sd}}^{i,j,k}\kappa_{\mathrm{s}}^{j}\sum_{m\in\mathbb{K}}p_{\mathrm{s}}^{j,m}(\widehat{h}_{\mathrm{sd}}^{i,j,k})^* + \sum_{j\in\mathbb{L}}(\sigma_{e,\mathrm{sd}}^{i,j,k})^2\kappa_{\mathrm{s}}^{j}\sum_{m\in\mathbb{K}}p_{\mathrm{s}}^{j,m}}_{\text{Source transmit distortion}}\\
& + \underbrace{\beta_{\mathrm{d}}^{i}\sum_{j\in\mathbb{L}}\sum_{m\in\mathbb{K}}\left(\widehat{\mathbf{h}}_{\mathrm{rd}}^{i,m}\mathbf{v}_{\mathrm{r}}^{j,m}p_{\mathrm{r}}^{j,m}(\mathbf{v}_{\mathrm{r}}^{j,m})^H(\widehat{\mathbf{h}}_{\mathrm{rd}}^{i,m})^H + (\sigma_{e,\mathrm{rd}}^{i,m})^2\mathrm{Tr}\left(\mathbf{v}_{\mathrm{r}}^{j,m}p_{\mathrm{r}}^{j,m}(\mathbf{v}_{\mathrm{r}}^{j,m})^H\right)\right)}_{\text{Destination receive distortion}}\\
& + \underbrace{\beta_{\mathrm{d}}^{i}\sum_{m\in\mathbb{K}}\left(\sum_{j\in\mathbb{L}}\widehat{h}_{\mathrm{sd}}^{i,j,m}p_{\mathrm{s}}^{j,m}(\widehat{h}_{\mathrm{sd}}^{i,j,m})^* + \sum_{j\in\mathbb{L}}(\sigma_{e,\mathrm{sd}}^{i,j,m})^2p_{\mathrm{s}}^{j,m} + (\sigma_{\mathrm{n,d}}^{i,m})^2\right)}_{\text{Destination receive distortion}} + \underbrace{(\sigma_{\mathrm{n,d}}^{i,k})^2}_{\text{Thermal noise}}.
\end{aligned} \tag{3.17}$$

3.4.4 Achievable Information Rate

In this section, we analyze the achievable information rate of our system under hardware impairments. The achievable information rate between the relay and the i-th source node using k-th sub-carrier can be obtained as

$$R_{\mathrm{sr}}^{i,k} = \gamma_0\log_2\left(1 + \frac{\mu_{\mathrm{s}}^{i,k}p_{\mathrm{s}}^{i,k}}{\alpha_{\mathrm{n,r}}^{i,k} + \sum_{m\in\mathbb{K}}\sum_{j\in\mathbb{L}}(\gamma_{\mathrm{s}}^{i,j,k,m}p_{\mathrm{s}}^{j,m} + \gamma_{\mathrm{r}}^{i,j,k,m}p_{\mathrm{r}}^{j,m})}\right), \tag{3.18}$$

where

$$\mu_{\mathrm{s}}^{i,k} = |(\mathbf{u}_{\mathrm{r}}^{i,k})^H\widehat{\mathbf{h}}_{\mathrm{sr}}^{i,k}|^2, \tag{3.19}$$

$$\begin{aligned}\gamma_{\mathrm{s}}^{i,j,k,m} =&\delta_{km}(1-\delta_{ij})(\mathbf{u}_{\mathrm{r}}^{i,k})^H\widehat{\mathbf{h}}_{\mathrm{sr}}^{j,k}(\widehat{\mathbf{h}}_{\mathrm{sr}}^{j,k})^H\mathbf{u}_{\mathrm{r}}^{i,k}+\delta_{km}(\mathbf{u}_{\mathrm{r}}^{i,k})^H(\sigma_{e,\mathrm{sr}}^{j,k})^2\mathbf{I}_N\mathbf{u}_{\mathrm{r}}^{i,k}\\&+(\mathbf{u}_{\mathrm{r}}^{i,k})^H\widehat{\mathbf{h}}_{\mathrm{sr}}^{j,k}\kappa_{\mathrm{s}}^{j}(\widehat{\mathbf{h}}_{\mathrm{sr}}^{j,k})^H\mathbf{u}_{\mathrm{r}}^{i,k}+(\mathbf{u}_{\mathrm{r}}^{i,k})^H(\sigma_{e,\mathrm{sr}}^{j,k})^2\kappa_{\mathrm{s}}^{j}\mathbf{I}_N\mathbf{u}_{\mathrm{r}}^{i,k}\\&+(\mathbf{u}_{\mathrm{r}}^{i,k})^H\boldsymbol{\Theta}_{\mathrm{r,r}}\mathrm{diag}\left(\widehat{\mathbf{h}}_{\mathrm{sr}}^{j,m}(\widehat{\mathbf{h}}_{\mathrm{sr}}^{j,m})^H\right)\mathbf{u}_{\mathrm{r}}^{i,k}+(\mathbf{u}_{\mathrm{r}}^{i,k})^H\boldsymbol{\Theta}_{\mathrm{r,r}}(\sigma_{e,\mathrm{sr}}^{j,m})^2\mathbf{u}_{\mathrm{r}}^{i,k},\end{aligned}\tag{3.20}$$

$$\begin{aligned}\gamma_{\mathrm{r}}^{i,j,k,m} =&\delta_{km}(\mathbf{u}_{\mathrm{r}}^{i,k})^H(\sigma_{e,\mathrm{rr}}^{k})^2\mathbf{u}_{\mathrm{r}}^{i,k}+(\mathbf{u}_{\mathrm{r}}^{i,k})^H\widehat{\mathbf{H}}_{\mathrm{rr}}^{k}\boldsymbol{\Theta}_{\mathrm{t,r}}\mathrm{diag}\left(\mathbf{v}_{\mathrm{r}}^{j,m}(\mathbf{v}_{\mathrm{r}}^{j,m})^H\right)(\widehat{\mathbf{H}}_{\mathrm{rr}}^{k})^H\mathbf{u}_{\mathrm{r}}^{i,k}\\&+(\mathbf{u}_{\mathrm{r}}^{i,k})^H(\sigma_{e,\mathrm{rr}}^{k})^2\mathrm{Tr}\left(\boldsymbol{\Theta}_{\mathrm{t,r}}\mathrm{diag}\left(\mathbf{v}_{\mathrm{r}}^{j,m}(\mathbf{v}_{\mathrm{r}}^{j,m})^H\right)\right)\mathbf{I}_N\mathbf{u}_{\mathrm{r}}^{i,k}\\&+(\mathbf{u}_{\mathrm{r}}^{i,k})^H\boldsymbol{\Theta}_{\mathrm{r,r}}\mathrm{diag}\left(\widehat{\mathbf{H}}_{\mathrm{rr}}^{m}\mathbf{v}_{\mathrm{r}}^{j,m}(\mathbf{v}_{\mathrm{r}}^{j,m})^H(\widehat{\mathbf{H}}_{\mathrm{rr}}^{m})^H\right)\mathbf{u}_{\mathrm{r}}^{i,k}+(\mathbf{u}_{\mathrm{r}}^{i,k})^H\boldsymbol{\Theta}_{\mathrm{r,r}}(\sigma_{e,\mathrm{rr}}^{m})^2\mathbf{u}_{\mathrm{r}}^{i,k},\end{aligned}\tag{3.21}$$

$$\alpha_{\mathrm{n,r}}^{i,k}=(\mathbf{u}_{\mathrm{r}}^{i,k})^H\left(\boldsymbol{\Theta}_{\mathrm{r,r}}\sum_{m\in\mathbb{K}}(\sigma_{\mathrm{n,r}}^{m})^2\mathbf{I}_N+(\sigma_{\mathrm{n,r}}^{k})^2\mathbf{I}_N\right)\mathbf{u}_{\mathrm{r}}^{i,k}\tag{3.22}$$

and $0<\gamma_0<1$ indicates the portion of the frame duration dedicated to data communication.

Subsequently, the achievable information rate between the relay and the i-th destination node using k-th sub-carrier can be obtained as

$$R_{\mathrm{rd}}^{i,k}=\gamma_0\log_2\left(1+\frac{\mu_{\mathrm{r}}^{i,k}p_{\mathrm{r}}^{i,k}}{\alpha_{\mathrm{n,d}}^{i,k}+\sum\limits_{m\in\mathbb{K}}\sum\limits_{j\in\mathbb{L}}(\overline{\gamma}_{\mathrm{s}}^{i,j,k,m}p_{\mathrm{s}}^{j,m}+\overline{\gamma}_{\mathrm{r}}^{i,j,k,m}p_{\mathrm{r}}^{j,m})}\right),\tag{3.23}$$

where

$$\mu_{\mathrm{r}}^{i,k}=|\widehat{\mathbf{h}}_{\mathrm{rd}}^{i,k}\mathbf{v}_{\mathrm{r}}^{i,k}|^2,\tag{3.24}$$

$$\begin{aligned}\overline{\gamma}_{\mathrm{s}}^{i,j,k,m} =&\delta_{km}\widehat{h}_{\mathrm{sd}}^{i,j,k}(\widehat{h}_{\mathrm{sd}}^{i,j,k})^*+\delta_{km}(\sigma_{e,\mathrm{sd}}^{i,j,k})^2+\widehat{h}_{\mathrm{sd}}^{i,j,k}\kappa_{\mathrm{s}}^{j}(\widehat{h}_{\mathrm{sd}}^{i,j,k})^*+(\sigma_{e,\mathrm{sd}}^{i,j,k})^2\kappa_{\mathrm{s}}^{j}\\&+\beta_{\mathrm{d}}^{i}\left(\widehat{h}_{\mathrm{sd}}^{i,j,m}(\widehat{h}_{\mathrm{sd}}^{i,j,m})^H+(\sigma_{e,\mathrm{sd}}^{i,j,m})^2\right),\end{aligned}\tag{3.25}$$

$$\begin{aligned}\overline{\gamma}_{\mathrm{r}}^{i,j,k,m} =&\delta_{km}(1-\delta_{ij})\widehat{\mathbf{h}}_{\mathrm{rd}}^{i,k}\mathbf{v}_{\mathrm{r}}^{j,k}(\mathbf{v}_{\mathrm{r}}^{j,k})^H(\widehat{\mathbf{h}}_{\mathrm{rd}}^{i,k})^H+\delta_{km}(\sigma_{e,\mathrm{rd}}^{i,k})^2\\&+\widehat{\mathbf{h}}_{\mathrm{rd}}^{i,k}\boldsymbol{\Theta}_{\mathrm{t,r}}\mathrm{diag}\left(\mathbf{v}_{\mathrm{r}}^{j,m}(\mathbf{v}_{\mathrm{r}}^{j,m})^H\right)(\widehat{\mathbf{h}}_{\mathrm{rd}}^{i,k})^H+(\sigma_{e,\mathrm{rd}}^{i,k})^2\mathrm{Tr}\left(\boldsymbol{\Theta}_{\mathrm{t,r}}\mathrm{diag}\left(\mathbf{v}_{\mathrm{r}}^{j,m}(\mathbf{v}_{\mathrm{r}}^{j,m})^H\right)\right)\\&+\beta_{\mathrm{d}}^{i}\left(\widehat{\mathbf{h}}_{\mathrm{rd}}^{i,m}\mathbf{v}_{\mathrm{r}}^{j,m}(\mathbf{v}_{\mathrm{r}}^{j,m})^H(\widehat{\mathbf{h}}_{\mathrm{rd}}^{i,m})^H+(\sigma_{e,\mathrm{rd}}^{i,m})^2\right)\end{aligned}\tag{3.26}$$

and

$$\alpha_{\mathrm{n,d}}^{i,k}=\beta_{\mathrm{d}}^{i}\sum_{m\in\mathbb{K}}(\sigma_{\mathrm{n,d}}^{i,m})^2+(\sigma_{\mathrm{n,d}}^{i,k})^2.\tag{3.27}$$

Since the relay is equipped with a large antenna array, well-studied linear beamforming and precoding techniques such as MRT/MRC, ZF, MMSE can be considered for the precoder-decoder strategies at the relay.

The achievable information rate for the i-th source-destination pair using k-th sub-carrier can be written as

$$R^{i,k}=\min\{R_{\mathrm{sr}}^{i,k},R_{\mathrm{rd}}^{i,k}\}.\tag{3.28}$$

3.4.5 Asymptotic Rate Analysis for MRC/MRT Strategy

In Section 3.4.4, the calculation of the γ variables will become a computationally expensive task, especially when N becomes large. In this section, we discuss how to reduce the complexity with some assumptions on the channel model and channel estimation.

First, we consider a similar channel model used in [84, 86, 87]. The channel vectors between the relay and i-th source node, and between the relay and i-th destination node can be written as

$$\begin{aligned} \mathbf{h}_{\mathrm{sr}}^{i,k} &= \sqrt{\psi_{\mathrm{sr}}^{i,k}}\,\mathbf{g}_{\mathrm{sr}}^{i,k} \in \mathbb{C}^{N\times 1}, \\ \mathbf{h}_{\mathrm{rd}}^{i,k} &= \sqrt{\psi_{\mathrm{rd}}^{i,k}}\,\mathbf{g}_{\mathrm{rd}}^{i,k} \in \mathbb{C}^{1\times N}. \end{aligned} \tag{3.29}$$

The variables $\psi_{\mathrm{sr}}^{i,k}$ and $\psi_{\mathrm{rd}}^{i,k}$ correspond to the large-scale fading of the source i to relay and relay to i-th destination channel, respectively. Moreover, the vectors $\mathbf{g}_{\mathrm{sr}}^{i,k} \in \mathbb{C}^{N\times 1}$ and $\mathbf{g}_{\mathrm{rd}}^{i,k} \in \mathbb{C}^{1\times N}$, whose entries are i.i.d. with distribution $\mathcal{CN}(0,1)$, characterize the small-scale fading of the channel between the relay and i-th source node, and the channel between the relay and i-th destination node, respectively. The channel $h_{\mathrm{sd}}^{i,j,k}$ and entries of SI channel $\mathbf{H}_{\mathrm{rr}}^{k}$ are assumed to be i.i.d. with distribution $\mathcal{CN}(0,\psi_{\mathrm{sd}}^{i,j,k})$ and $\mathcal{CN}(0,\psi_{\mathrm{rr}}^{k})$, respectively.

We assume that a good estimation of the channel (for our channel error model (3.1)) can be achieved such that

$$\mathbf{H}_{\mathcal{X}} = \widehat{\mathbf{H}}_{\mathcal{X}} + \widetilde{\mathbf{H}}_{\mathcal{X}}, \quad \mathcal{X} \in \{\mathrm{sr}, \mathrm{rr}, \mathrm{rd}, \mathrm{sd}\}, \tag{3.30}$$

where the entries of $\widehat{\mathbf{h}}_{\mathrm{sr}}^{i,k}$, $\widehat{\mathbf{h}}_{\mathrm{rd}}^{i,k}$, $\widehat{h}_{\mathrm{sd}}^{i,j,k}$ and $\widehat{\mathbf{H}}_{\mathrm{rr}}^{k}$ are i.i.d. with distribution $\mathcal{CN}(0,\widehat{\psi}_{\mathrm{sr}}^{i,k})$, $\mathcal{CN}(0,\widehat{\psi}_{\mathrm{rd}}^{i,k})$, $\mathcal{CN}(0,\widehat{\psi}_{\mathrm{sd}}^{i,j,k})$ and $\mathcal{CN}(0,\widehat{\psi}_{\mathrm{rr}}^{k})$, respectively. Subsequently, the covariance matrix of the estimated desired channels $\widehat{\mathbf{h}}_{\mathrm{sr}}^{i,k}$ and $\widehat{\mathbf{h}}_{\mathrm{rd}}^{i,k}$ can be obtained as $\mathbb{E}\{\widehat{\mathbf{h}}_{\mathrm{sr}}^{i,k}(\widehat{\mathbf{h}}_{\mathrm{sr}}^{i,k})^H\} = \widehat{\psi}_{\mathrm{sr}}^{i,k}\mathbf{I}_N$, $\mathbb{E}\{(\widehat{\mathbf{h}}_{\mathrm{rd}}^{i,k})^H\widehat{\mathbf{h}}_{\mathrm{rd}}^{i,k}\} = \widehat{\psi}_{\mathrm{rd}}^{i,k}\mathbf{I}_N$, respectively. We also assume that the estimated channels of each user at each sub-carrier are mutually independent.

We consider MRT/MRC as transmit precoding/receive filter strategy at the relay. The normalized receive filter coefficients and normalized transmit precoders can be formulated as $\mathbf{u}_{\mathrm{r}}^{i,k} = \widehat{\mathbf{h}}_{\mathrm{sr}}^{i,k}/||\widehat{\mathbf{h}}_{\mathrm{sr}}^{i,k}|| \in \mathbb{C}^{N\times 1}$ and $\mathbf{v}_{\mathrm{r}}^{i,k} = (\widehat{\mathbf{h}}_{\mathrm{rd}}^{i,k})^H/||\widehat{\mathbf{h}}_{\mathrm{rd}}^{i,k}|| \in \mathbb{C}^{N\times 1}$, respectively. Then we know that $(\mathbf{u}_{\mathrm{r}}^{i,k})^H(\mathbf{u}_{\mathrm{r}}^{i,k}) = \mathrm{Tr}\big(\mathbf{u}_{\mathrm{r}}^{i,k}(\mathbf{u}_{\mathrm{r}}^{i,k})^H\big) = 1$, and $(\mathbf{v}_{\mathrm{r}}^{i,k})^H\mathbf{v}_{\mathrm{r}}^{i,k} = \mathrm{Tr}\big(\mathbf{v}_{\mathrm{r}}^{i,k}(\mathbf{v}_{\mathrm{r}}^{i,k})^H\big) = 1$. We assume the transmit and receive distortion coefficient are same for all the transmit and receive chains of the relay, i.e., $\mathbf{\Theta}_{\mathrm{t,r}} = \kappa_{\mathrm{r}}\mathbf{I}_N = \frac{\widetilde{\kappa}_{\mathrm{r}}}{K}\mathbf{I}_N$ and $\mathbf{\Theta}_{\mathrm{r,r}} = \beta_{\mathrm{r}}\mathbf{I}_N = \frac{\widetilde{\beta}_{\mathrm{r}}}{K}\mathbf{I}_N$.

We introduce Lemma 3.4.1 and Lemma 3.4.2, which will be used for further calculations.

Lemma 3.4.1. *[88, Lemma 1] Assuming* $\mathbf{p} = [p_1....p_N]^T$ *and* $\mathbf{q} = [q_1....q_N]^T$ *to be mutually independent* $N \times 1$ *vectors whose elements are i.i.d. zero-mean complex-Gaussian random variables with variances of* $\mathbb{E}|p_i|^2 = \sigma_p^2$ *and* $\mathbb{E}|q_i|^2 = \sigma_q^2$*, respectively,* $i = 1, ..., N$.

According to the law of large numbers [89], we have

$$\begin{aligned} \frac{1}{N}\mathbf{p}^H\mathbf{p} &\underset{N\to\infty}{\overset{a.s.}{\longrightarrow}} \sigma_p^2, \\ \frac{1}{N}\mathbf{p}^H\mathbf{q} &\underset{N\to\infty}{\overset{a.s.}{\longrightarrow}} 0, \end{aligned} \tag{3.31}$$

where $\underset{N\to\infty}{\overset{a.s.}{\longrightarrow}}$ *represents the almost sure convergence when the length of vector* N *approaches to infinity.*

According to the Lindeberg-Levy central limit theorem [89], we have

$$\frac{1}{\sqrt{N}}\mathbf{p}^H\mathbf{q} \underset{N\to\infty}{\overset{d}{\longrightarrow}} \mathcal{CN}(0, \sigma_p^2\sigma_q^2), \tag{3.32}$$

where $\underset{N\to\infty}{\overset{d}{\longrightarrow}}$ *denotes the convergence in distribution, when the length of vector* N *approaches to infinity.*

Remark 1: From Lemma 3.4.1, we can deduce that

$$\mathbf{p}^H\mathbf{p} \underset{N\to\infty}{\overset{a.s.}{\longrightarrow}} \mathbb{E}\{\mathbf{p}^H\mathbf{p}\} = \mathbb{E}\left\{\sum_{i=1}^{N}|p_i|^2\right\} = N\sigma_p^2. \tag{3.33}$$

On the same context, we assume that as $N \to \infty$, $\sum_{i=1}^{N}|p_i|^4$ also converges to its expectation. The expected value $\mathbb{E}\{\sum_{i=1}^{N}|p_i|^4\}$ can be obtained as $2N\sigma_p^4$ [89]. It is calculated by assuming that the real and the imaginary parts of the complex Gaussian variable p_i to be mutually independent and has equal variance $(\sigma_p^2/2)$. In other words, for large N regime, the deterministic equivalent of $\sum_{i=1}^{N}|p_i|^4$ becomes its expected value.

Lemma 3.4.2. *[87, Lemma 1] Let* $\mathbf{A}$ *be a deterministic* $N \times N$ *complex matrix with uniformly bounded spectral radius for all* N*. Let* $\mathbf{p} = \frac{1}{\sqrt{N}}[p_1, ..., p_N]^T$ *and* $\mathbf{q} = \frac{1}{\sqrt{N}}[q_1, ..., q_N]^T$ *denote two mutually independent* $N \times 1$ *complex random vectors, whose elements are i.i.d. zero-mean random complex variables with unit variance and finite eighth moment. Then*

$$\mathbf{p}^H\mathbf{A}\mathbf{p} \to \frac{1}{N}\mathrm{Tr}(\mathbf{A}) \tag{3.34}$$

$$\mathbf{p}^H\mathbf{A}\mathbf{q} \to 0, \tag{3.35}$$

almost surely as $N \to \infty$*.*

Further calculations are done by considering large N regime ($N \to \infty$). We use a similar approach as in [87] to perform asymptotic rate analysis, i.e., to calculate the deterministic equivalent rate in large N regime. With this model, the achievable rate

between the relay and i-th source node using k-th sub-carrier (3.18) can be rewritten as

$$R_{\mathrm{sr}}^{i,k} = \gamma_0 \log_2 \left(1 + \frac{\frac{1}{N}\mu_{\mathrm{s}}^{i,k} p_{\mathrm{s}}^{i,k}}{\frac{1}{N}\Big(\alpha_{\mathrm{n,r}}^{i,k} + \sum\limits_{m\in\mathbb{K}}\sum\limits_{j\in\mathbb{L}} (\gamma_{\mathrm{s}}^{i,j,k,m} p_{\mathrm{s}}^{j,m} + \gamma_{\mathrm{r}}^{i,j,k,m} p_{\mathrm{r}}^{j,m})\Big)} \right) \tag{3.36}$$

with

$$\begin{aligned} \frac{1}{N}\mu_{\mathrm{s}}^{i,k} &= \frac{1}{N}\frac{(\widehat{\mathbf{h}}_{\mathrm{sr}}^{i,k})^H}{||\widehat{\mathbf{h}}_{\mathrm{sr}}^{i,k}||}\widehat{\mathbf{h}}_{\mathrm{sr}}^{i,k}(\widehat{\mathbf{h}}_{\mathrm{sr}}^{i,k})^H\frac{\widehat{\mathbf{h}}_{\mathrm{sr}}^{i,k}}{||\widehat{\mathbf{h}}_{\mathrm{sr}}^{i,k}||} \\ &= \frac{1}{N}(\widehat{\mathbf{h}}_{\mathrm{sr}}^{i,k})^H\widehat{\mathbf{h}}_{\mathrm{sr}}^{i,k} \underset{N\to\infty}{\overset{a.s.}{\longrightarrow}} \widehat{\psi}_{\mathrm{sr}}^{i,k}. [\text{from } \textit{Lemma } 3.4.1] \end{aligned} \tag{3.37}$$

Now, $\frac{1}{N}\gamma_{\mathrm{s}}^{i,j,k,m}$ can be reformulated as

$$\begin{aligned} \frac{1}{N}\gamma_{\mathrm{s}}^{i,j,k,m} = &\underbrace{\frac{1}{N}\delta_{km}(1-\delta_{ij})\frac{(\widehat{\mathbf{h}}_{\mathrm{sr}}^{i,k})^H}{||\widehat{\mathbf{h}}_{\mathrm{sr}}^{i,k}||}\widehat{\mathbf{h}}_{\mathrm{sr}}^{j,k}(\widehat{\mathbf{h}}_{\mathrm{sr}}^{j,k})^H\frac{\widehat{\mathbf{h}}_{\mathrm{sr}}^{i,k}}{||\widehat{\mathbf{h}}_{\mathrm{sr}}^{i,k}||}}_{\gamma_{\mathrm{s},1}^{i,j,k,m}} + \underbrace{\frac{1}{N}\delta_{km}(\sigma_{e,\mathrm{sr}}^{j,k})^2}_{\gamma_{\mathrm{s},2}^{i,j,k,m}} \\ &+ \underbrace{\frac{1}{N}\frac{(\widehat{\mathbf{h}}_{\mathrm{sr}}^{i,k})^H}{||\widehat{\mathbf{h}}_{\mathrm{sr}}^{i,k}||}\widehat{\mathbf{h}}_{\mathrm{sr}}^{j,k}\kappa_{\mathrm{s}}^{j}(\widehat{\mathbf{h}}_{\mathrm{sr}}^{j,k})^H\frac{\widehat{\mathbf{h}}_{\mathrm{sr}}^{i,k}}{||\widehat{\mathbf{h}}_{\mathrm{sr}}^{i,k}||}}_{\gamma_{\mathrm{s},3}^{i,j,k,m}} + \underbrace{\frac{1}{N}(\sigma_{e,\mathrm{sr}}^{j,k})^2\kappa_{\mathrm{s}}^{j}}_{\gamma_{\mathrm{s},4}^{i,j,k,m}} \\ &+ \underbrace{\frac{1}{N}\frac{(\widehat{\mathbf{h}}_{\mathrm{sr}}^{i,k})^H}{||\widehat{\mathbf{h}}_{\mathrm{sr}}^{i,k}||}\beta_{\mathrm{r}}\mathrm{diag}\left(\widehat{\mathbf{h}}_{\mathrm{sr}}^{j,m}(\widehat{\mathbf{h}}_{\mathrm{sr}}^{j,m})^H\right)\frac{\widehat{\mathbf{h}}_{\mathrm{sr}}^{i,k}}{||\widehat{\mathbf{h}}_{\mathrm{sr}}^{i,k}||}}_{\gamma_{\mathrm{s},5}^{i,j,k,m}} + \underbrace{\frac{1}{N}\beta_{\mathrm{r}}(\sigma_{e,\mathrm{sr}}^{j,m})^2}_{\gamma_{\mathrm{s},6}^{i,j,k,m}} \end{aligned} \tag{3.38}$$

We compute deterministic equivalent in large N regime for each term in (3.38),

$$\begin{aligned} \gamma_{\mathrm{s},1}^{i,j} &:= \frac{1}{N}\left(\frac{(\widehat{\mathbf{h}}_{\mathrm{sr}}^{i,k})^H}{||\widehat{\mathbf{h}}_{\mathrm{sr}}^{i,k}||}\widehat{\mathbf{h}}_{\mathrm{sr}}^{j,k}(\widehat{\mathbf{h}}_{\mathrm{sr}}^{j,k})^H\frac{\widehat{\mathbf{h}}_{\mathrm{sr}}^{i,k}}{||\widehat{\mathbf{h}}_{\mathrm{sr}}^{i,k}||}\right) \\ &= \frac{||\widehat{\mathbf{h}}_{\mathrm{sr}}^{j,k}||^2}{N||\widehat{\mathbf{h}}_{\mathrm{sr}}^{i,k}||^2}\left((\widehat{\mathbf{h}}_{\mathrm{sr}}^{i,k})^H\overline{\mathbf{h}}_{\mathrm{sr}}^{j,k}(\overline{\mathbf{h}}_{\mathrm{sr}}^{j,k})^H\widehat{\mathbf{h}}_{\mathrm{sr}}^{i,k}\right) \quad \left[\text{where } \overline{\mathbf{h}}_{\mathrm{sr}}^{j,k} = \frac{(\widehat{\mathbf{h}}_{\mathrm{sr}}^{j,k})^H}{||\widehat{\mathbf{h}}_{\mathrm{sr}}^{j,k}||}\right] \\ &= \widehat{\psi}_{\mathrm{sr}}^{i,k}\frac{||\widehat{\mathbf{h}}_{\mathrm{sr}}^{j,k}||^2}{||\widehat{\mathbf{h}}_{\mathrm{sr}}^{i,k}||^2}\left(\frac{(\widehat{\mathbf{h}}_{\mathrm{sr}}^{i,k})^H}{\sqrt{N\widehat{\psi}_{\mathrm{sr}}^{i,k}}}\overline{\mathbf{h}}_{\mathrm{sr}}^{j,k}(\overline{\mathbf{h}}_{\mathrm{sr}}^{j,k})^H\frac{(\widehat{\mathbf{h}}_{\mathrm{sr}}^{i,k})}{\sqrt{N\widehat{\psi}_{\mathrm{sr}}^{i,k}}}\right). \end{aligned} \tag{3.39}$$

Employing (3.34) from Lemma 3.4.2 and by knowing $\mathrm{Tr}\Big(\overline{\mathbf{h}}_{\mathrm{sr}}^{j,k}(\overline{\mathbf{h}}_{\mathrm{sr}}^{j,k})^H\Big) = 1$, we obtain

$$\frac{(\widehat{\mathbf{h}}_{\mathrm{sr}}^{i,k})^H}{\sqrt{N\widehat{\psi}_{\mathrm{sr}}^{i,k}}}\overline{\mathbf{h}}_{\mathrm{sr}}^{j,k}(\overline{\mathbf{h}}_{\mathrm{sr}}^{j,k})^H\frac{(\widehat{\mathbf{h}}_{\mathrm{sr}}^{i,k})^H}{\sqrt{N\widehat{\psi}_{\mathrm{sr}}^{i,k}}} \underset{N\to\infty}{\overset{a.s.}{\longrightarrow}} \frac{1}{N}, \tag{3.40}$$

For $i \neq j$

$$\gamma_{\mathrm{s},1}^{i,j} = \frac{1}{N}\frac{(\widehat{\mathbf{h}}_{\mathrm{sr}}^{i,k})^H}{||\widehat{\mathbf{h}}_{\mathrm{sr}}^{i,k}||}\widehat{\mathbf{h}}_{\mathrm{sr}}^{j,k}(\widehat{\mathbf{h}}_{\mathrm{sr}}^{j,k})^H\frac{\widehat{\mathbf{h}}_{\mathrm{sr}}^{i,k}}{||\widehat{\mathbf{h}}_{\mathrm{sr}}^{i,k}||} \underset{N\to\infty}{\overset{a.s.}{\longrightarrow}} \frac{1}{N}\widehat{\psi}_{\mathrm{sr}}^{j,k} \tag{3.41}$$

For $i = j$,

$$\begin{aligned}\gamma_{\mathrm{s},1}^{i,i} &= \frac{1}{N}\frac{(\widehat{\mathbf{h}}_{\mathrm{sr}}^{i,k})^H}{||\widehat{\mathbf{h}}_{\mathrm{sr}}^{i,k}||}\widehat{\mathbf{h}}_{\mathrm{sr}}^{j,k}(\widehat{\mathbf{h}}_{\mathrm{sr}}^{j,k})^H\frac{\widehat{\mathbf{h}}_{\mathrm{sr}}^{i,k}}{||\widehat{\mathbf{h}}_{\mathrm{sr}}^{i,k}||} = \frac{1}{N}\mu_{\mathrm{s}}^{i,k} = \frac{1}{N}\frac{(\widehat{\mathbf{h}}_{\mathrm{sr}}^{i,k})^H}{||\widehat{\mathbf{h}}_{\mathrm{sr}}^{i,k}||}\widehat{\mathbf{h}}_{\mathrm{sr}}^{i,k}(\widehat{\mathbf{h}}_{\mathrm{sr}}^{i,k})^H\frac{\widehat{\mathbf{h}}_{\mathrm{sr}}^{i,k}}{||\widehat{\mathbf{h}}_{\mathrm{sr}}^{i,k}||} \\ &= \frac{1}{N}(\widehat{\mathbf{h}}_{\mathrm{sr}}^{i,k})^H\widehat{\mathbf{h}}_{\mathrm{sr}}^{i,k} \underset{N\to\infty}{\overset{a.s.}{\longrightarrow}} \widehat{\psi}_{\mathrm{sr}}^{i,k}\big[\text{from (3.37)}\big].\end{aligned} \tag{3.42}$$

Using (3.44), the term $\gamma_{\mathrm{s},1}^{i,j,k,m}$ in large N regime can be obtained as

$$\gamma_{\mathrm{s},1}^{i,j,k,m} \underset{N\to\infty}{\overset{a.s.}{\longrightarrow}} \frac{1}{N}\delta_{km}\widehat{\psi}_{\mathrm{sr}}^{j,k}. \tag{3.43}$$

Similarly, by employing (3.42), $\gamma_{\mathrm{s},3}^{i,j,k,m}$ in large N regime can be calculated as

$$\gamma_{\mathrm{s},3}^{i,j,k,m} \underset{N\to\infty}{\overset{a.s.}{\longrightarrow}} \delta_{ij}\kappa_{\mathrm{s}}^{j}\widehat{\psi}_{\mathrm{sr}}^{i,k}. \tag{3.44}$$

Let us consider the term $\gamma_{\mathrm{s},5}^{i,j,k,m}$, for $i \neq j$ and $i = j; k \neq m$

$$\begin{aligned}\gamma_{\mathrm{s},5}^{i,j,k,m} &= \frac{1}{N}\frac{(\widehat{\mathbf{h}}_{\mathrm{sr}}^{i,k})^H}{||\widehat{\mathbf{h}}_{\mathrm{sr}}^{i,k}||}\beta_{\mathrm{r}}\mathrm{diag}\left(\widehat{\mathbf{h}}_{\mathrm{sr}}^{j,m}(\widehat{\mathbf{h}}_{\mathrm{sr}}^{j,m})^H\right)\frac{\widehat{\mathbf{h}}_{\mathrm{sr}}^{i,k}}{||\widehat{\mathbf{h}}_{\mathrm{sr}}^{i,k}||} \\ &= \frac{\beta_{\mathrm{r}}\widehat{\psi}_{\mathrm{sr}}^{i,k}||\widehat{\mathbf{h}}_{\mathrm{sr}}^{j,m}||^2}{||\widehat{\mathbf{h}}_{\mathrm{sr}}^{i,k}||^2}\frac{(\widehat{\mathbf{h}}_{\mathrm{sr}}^{i,k})^H}{\sqrt{N\widehat{\psi}_{\mathrm{sr}}^{i,k}}}\mathrm{diag}\left(\overline{\mathbf{h}}_{\mathrm{sr}}^{j,m}(\overline{\mathbf{h}}_{\mathrm{sr}}^{j,m})^H\right)\frac{(\widehat{\mathbf{h}}_{\mathrm{sr}}^{i,k})}{\sqrt{N\widehat{\psi}_{\mathrm{sr}}^{i,k}}} \quad \left[\text{where } \overline{\mathbf{h}}_{\mathrm{sr}}^{j,m} = \frac{(\widehat{\mathbf{h}}_{\mathrm{sr}}^{j,m})^H}{||\widehat{\mathbf{h}}_{\mathrm{sr}}^{j,m}||}\right],\end{aligned} \tag{3.45}$$

and we know $\mathrm{Tr}\left(\overline{\mathbf{h}}_{\mathrm{sr}}^{j,m}(\overline{\mathbf{h}}_{\mathrm{sr}}^{j,m})^H\right) = 1$ and similar to (3.40) using Lemma 3.4.2, we obtain

$$\gamma_{\mathrm{s},5}^{i,j,k,m} \underset{N\to\infty}{\overset{a.s.}{\longrightarrow}} \frac{1}{N}\beta_{\mathrm{r}}\widehat{\psi}_{\mathrm{sr}}^{j,m} \text{ for } i \neq j \text{ and } i = j; k \neq m. \tag{3.46}$$

For $i = j; k = m$

$$\gamma_{\mathrm{s},5}^{i,i,k,k} = \beta_{\mathrm{r}}\frac{1}{N}\frac{(\widehat{\mathbf{h}}_{\mathrm{sr}}^{i,k})^H}{||\widehat{\mathbf{h}}_{\mathrm{sr}}^{i,k}||}\mathrm{diag}\left(\widehat{\mathbf{h}}_{\mathrm{sr}}^{i,k}(\widehat{\mathbf{h}}_{\mathrm{sr}}^{i,k})^H\right)\frac{\widehat{\mathbf{h}}_{\mathrm{sr}}^{i,k}}{||\widehat{\mathbf{h}}_{\mathrm{sr}}^{i,k}||} = \frac{\beta_{\mathrm{r}}\sum_{l=1}^{N}|\lfloor\widehat{h}_{\mathrm{sr}}^{i,k}\rfloor_l|^4}{N||\widehat{\mathbf{h}}_{\mathrm{sr}}^{i,k}||^2}. \tag{3.47}$$

Using Remark 1, for large N regime the deterministic equivalent of term $\sum_{l=1}^{N}|\lfloor\widehat{h}_{\mathrm{sr}}^{i,k}\rfloor_l|^4$ can be calculated as $\mathbb{E}\{\sum_{l=1}^{N}|\lfloor\widehat{h}_{\mathrm{sr}}^{i,k}\rfloor_l|^4\} = 2N(\widehat{\psi}_{\mathrm{sr}}^{i,k})^2$, where $\lfloor\widehat{h}_{\mathrm{sr}}^{i,k}\rfloor_l$ denotes the l-th element of the vector $\widehat{\mathbf{h}}_{\mathrm{sr}}^{i,k}$. Hence the term $\gamma_{\mathrm{s},5}^{i,i,k,k}$ in large N regime can be obtained as

$$\gamma_{\mathrm{s},5}^{i,i,k,k} \underset{N\to\infty}{\overset{a.s.}{\longrightarrow}} \frac{2\beta_{\mathrm{r}}}{N}\widehat{\psi}_{\mathrm{sr}}^{i,k}. \tag{3.48}$$

Finally, $\frac{1}{N}\gamma_{\mathrm{s}}^{i,j,k,m}$ in large N regime can the obtained as

$$\frac{1}{N}\gamma_{\mathrm{s}}^{i,j,k,m} \underset{N\to\infty}{\overset{a.s.}{\longrightarrow}} \delta_{ij}\kappa_{\mathrm{s}}^{j}\widehat{\psi}_{\mathrm{sr}}^{i,k}, \tag{3.49}$$

and the rest of terms goes to zero as N goes to infinity.

Similarly, $\frac{1}{N}\gamma_{\mathrm{r}}^{i,j,k,m}$ can be reformulated as

$$\begin{aligned}\frac{1}{N}\gamma_{\mathrm{r}}^{i,j,k,m} =& \underbrace{\frac{1}{N}\delta_{km}(\sigma_{e,\mathrm{rr}}^{k})^2}_{\gamma_{\mathrm{r},1}^{i,j,k,m}} + \underbrace{\frac{1}{N}\frac{(\widehat{\mathbf{h}}_{\mathrm{sr}}^{i,k})^H}{||\widehat{\mathbf{h}}_{\mathrm{sr}}^{i,k}||}\widehat{\mathbf{H}}_{\mathrm{rr}}^{k}\kappa_{\mathrm{r}}\mathrm{diag}\left(\frac{(\widehat{\mathbf{h}}_{\mathrm{rd}}^{j,m})^H}{||\widehat{\mathbf{h}}_{\mathrm{rd}}^{j,m}||}\frac{\widehat{\mathbf{h}}_{\mathrm{rd}}^{j,m}}{||\widehat{\mathbf{h}}_{\mathrm{rd}}^{j,m}||}\right)(\widehat{\mathbf{H}}_{\mathrm{rr}}^{k})^H\frac{\widehat{\mathbf{h}}_{\mathrm{sr}}^{i,k}}{||\widehat{\mathbf{h}}_{\mathrm{sr}}^{i,k}||}}_{\gamma_{\mathrm{r},2}^{i,j,k,m}} \\ &+ \underbrace{\frac{1}{N}(\sigma_{e,\mathrm{rr}}^{k})^2\mathrm{Tr}\left(\kappa_{\mathrm{r}}\mathrm{diag}\left(\frac{(\widehat{\mathbf{h}}_{\mathrm{rd}}^{j,m})^H}{||\widehat{\mathbf{h}}_{\mathrm{rd}}^{j,m}||}\frac{\widehat{\mathbf{h}}_{\mathrm{rd}}^{j,m}}{||\widehat{\mathbf{h}}_{\mathrm{rd}}^{j,m}||}\right)\right)}_{\gamma_{\mathrm{r},3}^{i,j,k,m}} \\ &+ \underbrace{\frac{1}{N}\frac{(\widehat{\mathbf{h}}_{\mathrm{sr}}^{i,k})^H}{||\widehat{\mathbf{h}}_{\mathrm{sr}}^{i,k}||}\beta_{\mathrm{r}}\mathrm{diag}\left(\widehat{\mathbf{H}}_{\mathrm{rr}}^{m}\frac{(\widehat{\mathbf{h}}_{\mathrm{rd}}^{j,m})^H}{||\widehat{\mathbf{h}}_{\mathrm{rd}}^{j,m}||}\frac{\widehat{\mathbf{h}}_{\mathrm{rd}}^{j,m}}{||\widehat{\mathbf{h}}_{\mathrm{rd}}^{j,m}||}(\widehat{\mathbf{H}}_{\mathrm{rr}}^{m})^H\right)\frac{\widehat{\mathbf{h}}_{\mathrm{sr}}^{i,k}}{||\widehat{\mathbf{h}}_{\mathrm{sr}}^{i,k}||}}_{\gamma_{\mathrm{r},4}^{i,j,k,m}} + \underbrace{\frac{1}{N}\beta_{\mathrm{r}}(\sigma_{e,\mathrm{rr}}^{m})^2}_{\gamma_{\mathrm{r},5}^{i,j,k,m}}.\end{aligned} \tag{3.50}$$

The term $\gamma_{\mathrm{r},4}^{i,j,k,m}$ of the above equation (3.50) can be rewritten as

$$\begin{aligned}\gamma_{\mathrm{r},4}^{i,j,k,m} =& \frac{1}{N}\frac{(\widehat{\mathbf{h}}_{\mathrm{sr}}^{i,k})^H}{||\widehat{\mathbf{h}}_{\mathrm{sr}}^{i,k}||}\beta_{\mathrm{r}}\mathrm{diag}\left(\widehat{\mathbf{H}}_{\mathrm{rr}}^{m}\frac{(\widehat{\mathbf{h}}_{\mathrm{rd}}^{j,m})^H}{||\widehat{\mathbf{h}}_{\mathrm{rd}}^{j,m}||}\frac{\widehat{\mathbf{h}}_{\mathrm{rd}}^{j,m}}{||\widehat{\mathbf{h}}_{\mathrm{rd}}^{j,m}||}(\widehat{\mathbf{H}}_{\mathrm{rr}}^{m})^H\right)\frac{\widehat{\mathbf{h}}_{\mathrm{sr}}^{i,k}}{||\widehat{\mathbf{h}}_{\mathrm{sr}}^{i,k}||} \\ =& \frac{\beta_{\mathrm{r}}}{N||\widehat{\mathbf{h}}_{\mathrm{rd}}^{j,m}||^2||\widehat{\mathbf{h}}_{\mathrm{sr}}^{i,k}||^2}(\widehat{\mathbf{h}}_{\mathrm{sr}}^{i,k})^H\mathrm{diag}\left(\widehat{\mathbf{H}}_{\mathrm{rr}}^{m}(\widehat{\mathbf{h}}_{\mathrm{rd}}^{j,m})^H\widehat{\mathbf{h}}_{\mathrm{rd}}^{j,m}(\widehat{\mathbf{H}}_{\mathrm{rr}}^{m})^H\right)\widehat{\mathbf{h}}_{\mathrm{sr}}^{i,k} \\ =& \frac{\beta_{\mathrm{r}}\widehat{\psi}_{\mathrm{sr}}^{i,k}}{||\widehat{\mathbf{h}}_{\mathrm{rd}}^{j,m}||^2||\widehat{\mathbf{h}}_{\mathrm{sr}}^{i,k}||^2}\frac{(\widehat{\mathbf{h}}_{\mathrm{sr}}^{i,k})^H}{\sqrt{N\widehat{\psi}_{\mathrm{sr}}^{i,k}}}\mathrm{diag}\left(\widehat{\mathbf{H}}_{\mathrm{rr}}^{m}(\widehat{\mathbf{h}}_{\mathrm{rd}}^{j,m})^H\widehat{\mathbf{h}}_{\mathrm{rd}}^{j,m}(\widehat{\mathbf{H}}_{\mathrm{rr}}^{m})^H\right)\frac{\widehat{\mathbf{h}}_{\mathrm{sr}}^{i,k}}{\sqrt{N\widehat{\psi}_{\mathrm{sr}}^{i,k}}}.\end{aligned} \tag{3.51}$$

Using Lemma 3.4.2, we can write

$$\gamma_{\mathrm{r},4}^{i,j,k,m} \underset{N\to\infty}{\overset{a.s.}{\longrightarrow}} \frac{\beta_{\mathrm{r}}}{N^2\widehat{\psi}_{\mathrm{rd}}^{j,m}}\frac{1}{N}\mathrm{Tr}\left(\widehat{\mathbf{H}}_{\mathrm{rr}}^{m}(\widehat{\mathbf{h}}_{\mathrm{rd}}^{j,m})^H\widehat{\mathbf{h}}_{\mathrm{rd}}^{j,m}(\widehat{\mathbf{H}}_{\mathrm{rr}}^{m})^H\right), \tag{3.52}$$

where

$$\begin{aligned}&\mathrm{Tr}\left(\widehat{\mathbf{H}}_{\mathrm{rr}}^{m}(\widehat{\mathbf{h}}_{\mathrm{rd}}^{j,m})^H\widehat{\mathbf{h}}_{\mathrm{rd}}^{j,m}(\widehat{\mathbf{H}}_{\mathrm{rr}}^{m})^H\right) = \widehat{\mathbf{h}}_{\mathrm{rd}}^{j,m}(\widehat{\mathbf{H}}_{\mathrm{rr}}^{m})^H\widehat{\mathbf{H}}_{\mathrm{rr}}^{m}(\widehat{\mathbf{h}}_{\mathrm{rd}}^{j,m})^H \\ &=N\widehat{\psi}_{\mathrm{rd}}^{j,m}\frac{\widehat{\mathbf{h}}_{\mathrm{rd}}^{j,m}}{\sqrt{N\widehat{\psi}_{\mathrm{rd}}^{j,m}}}(\widehat{\mathbf{H}}_{\mathrm{rr}}^{m})^H\widehat{\mathbf{H}}_{\mathrm{rr}}^{m}\frac{(\widehat{\mathbf{h}}_{\mathrm{rd}}^{j,m})^H}{\sqrt{N\widehat{\psi}_{\mathrm{rd}}^{j,m}}} \\ &\underset{N\to\infty}{\overset{a.s.}{\longrightarrow}} N\widehat{\psi}_{\mathrm{rd}}^{j,m}\frac{1}{N}\mathrm{Tr}\left((\widehat{\mathbf{H}}_{\mathrm{rr}}^{m})^H\widehat{\mathbf{H}}_{\mathrm{rr}}^{m}\right) \underset{N\to\infty}{\overset{a.s.}{\longrightarrow}} N\widehat{\psi}_{\mathrm{rd}}^{j,m}\frac{1}{N}\sum_{l=1}^{N}|\lfloor\widehat{\mathbf{H}}_{\mathrm{rr}}^{m}\rfloor_l|^2 \underset{N\to\infty}{\overset{a.s.}{\longrightarrow}} N^2\widehat{\psi}_{\mathrm{rd}}^{j,m}\widehat{\psi}_{\mathrm{rr}}^{m}.\end{aligned} \tag{3.53}$$

Hence

$$\begin{aligned}\gamma_{\mathrm{r},4}^{i,j,k,m} &\underset{N\to\infty}{\overset{a.s.}{\longrightarrow}} \frac{\beta_{\mathrm{r}}}{N^2\widehat{\psi}_{\mathrm{rd}}^{j,m}}\frac{1}{N}\mathrm{Tr}\left(\widehat{\mathbf{H}}_{\mathrm{rr}}^{m}(\widehat{\mathbf{h}}_{\mathrm{rd}}^{j,m})^H\widehat{\mathbf{h}}_{\mathrm{rd}}^{j,m}(\widehat{\mathbf{H}}_{\mathrm{rr}}^{m})^H\right) \\ &\underset{N\to\infty}{\overset{a.s.}{\longrightarrow}} \frac{\beta_{\mathrm{r}}}{N^2\widehat{\psi}_{\mathrm{rd}}^{j,m}}\frac{1}{N}N^2\widehat{\psi}_{\mathrm{rd}}^{j,m}\widehat{\psi}_{\mathrm{rr}}^{m} \underset{N\to\infty}{\overset{a.s.}{\longrightarrow}} \frac{1}{N}\beta_{\mathrm{r}}\widehat{\psi}_{\mathrm{rr}}^{m}.\end{aligned} \tag{3.54}$$

For the calculation of $\gamma_{\mathrm{r},2}^{i,j,k,m}$, we approximate the term $\widehat{\mathbf{H}}_{\mathrm{rr}}^{k}\mathrm{diag}\left((\widehat{\mathbf{h}}_{\mathrm{rd}}^{j,m})^{H}\widehat{\mathbf{h}}_{\mathrm{rd}}^{j,m}\right)(\widehat{\mathbf{H}}_{\mathrm{rr}}^{k})^{H}$ to $\mathrm{diag}\left(\widehat{\mathbf{H}}_{\mathrm{rr}}^{k}(\widehat{\mathbf{h}}_{\mathrm{rd}}^{j,m})^{H}\widehat{\mathbf{h}}_{\mathrm{rd}}^{j,m}(\widehat{\mathbf{H}}_{\mathrm{rr}}^{k})^{H}\right)$ as in [38]. The term $\gamma_{\mathrm{r},2}^{i,j,k,m}$ can be written as

$$\gamma_{\mathrm{r},2}^{i,j,k,m} \approx \frac{1}{N}\frac{(\widehat{\mathbf{h}}_{\mathrm{sr}}^{i,k})^{H}}{||\widehat{\mathbf{h}}_{\mathrm{sr}}^{i,k}||}\kappa_{\mathrm{r}}\mathrm{diag}\left(\widehat{\mathbf{H}}_{\mathrm{rr}}^{k}\frac{(\widehat{\mathbf{h}}_{\mathrm{rd}}^{j,m})^{H}}{||\widehat{\mathbf{h}}_{\mathrm{rd}}^{j,m}||}\frac{\widehat{\mathbf{h}}_{\mathrm{rd}}^{j,m}}{||\widehat{\mathbf{h}}_{\mathrm{rd}}^{j,m}||}(\widehat{\mathbf{H}}_{\mathrm{rr}}^{k})^{H}\right)\frac{\widehat{\mathbf{h}}_{\mathrm{sr}}^{i,k}}{||\widehat{\mathbf{h}}_{\mathrm{sr}}^{i,k}||} \tag{3.55}$$

By using the similar steps to calculate $\gamma_{\mathrm{r},4}^{i,j,k,m}$, we get

$$\gamma_{\mathrm{r},2}^{i,j,k,m} \underset{N\to\infty}{\overset{a.s.}{\longrightarrow}} \frac{1}{N}\kappa_{\mathrm{r}}\widehat{\psi}_{\mathrm{rr}}^{k}. \tag{3.56}$$

The term $\gamma_{\mathrm{r},3}^{i,j,k,m}$ can be rewritten as

$$\begin{aligned}&\frac{1}{N}(\sigma_{e,\mathrm{rr}}^{k})^{2}\mathrm{Tr}\left(\kappa_{\mathrm{r}}\mathrm{diag}\left(\frac{(\widehat{\mathbf{h}}_{\mathrm{rd}}^{j,m})^{H}}{||\widehat{\mathbf{h}}_{\mathrm{rd}}^{j,m}||}\frac{\widehat{\mathbf{h}}_{\mathrm{rd}}^{j,m}}{||\widehat{\mathbf{h}}_{\mathrm{rd}}^{j,m}||}\right)\right)\\ &\quad=\frac{1}{N}(\sigma_{e,\mathrm{rr}}^{k})^{2}\kappa_{\mathrm{r}}\mathrm{Tr}\left(\mathrm{diag}\left(\frac{(\widehat{\mathbf{h}}_{\mathrm{rd}}^{j,m})^{H}}{||\widehat{\mathbf{h}}_{\mathrm{rd}}^{j,m}||}\frac{\widehat{\mathbf{h}}_{\mathrm{rd}}^{j,m}}{||\widehat{\mathbf{h}}_{\mathrm{rd}}^{j,m}||}\right)\right)=\frac{1}{N}(\sigma_{e,\mathrm{rr}}^{k})^{2}\kappa_{\mathrm{r}}\end{aligned} \tag{3.57}$$

It can be noticed that, since all the terms in $\frac{1}{N}\gamma_{\mathrm{r}}^{i,j,k,m}$ contain N in its denominator, as N goes to infinity all the terms goes to zero. Similarly, terms in $\frac{1}{N}\alpha_{\mathrm{n,r}}^{i,k}$ also vanish in large N regime.

Now, using a similar approach for achievable information rate between the relay and i-th destination node using k-th sub-carrier can be obtained as

$$R_{\mathrm{rd}}^{i,k} = \gamma_{0}\log_{2}\left(1+\frac{\frac{1}{N}\mu_{\mathrm{r}}^{i,k}p_{\mathrm{r}}^{i,k}}{\frac{1}{N}\left(\alpha_{\mathrm{n,d}}^{i,k}+\sum_{m\in\mathbb{K}}\sum_{j\in\mathbb{L}}(\overline{\gamma}_{\mathrm{s}}^{i,j,k,m}p_{\mathrm{s}}^{j,m}+\overline{\gamma}_{\mathrm{r}}^{i,j,k,m}p_{\mathrm{r}}^{j,m})\right)}\right) \tag{3.58}$$

with

$$\begin{aligned}\frac{1}{N}\mu_{\mathrm{r}}^{i,k} &= \frac{1}{N}\widehat{\mathbf{h}}_{\mathrm{rd}}^{i,k}\frac{(\widehat{\mathbf{h}}_{\mathrm{rd}}^{i,k})^{H}}{||\widehat{\mathbf{h}}_{\mathrm{rd}}^{i,k}||}\frac{\widehat{\mathbf{h}}_{\mathrm{rd}}^{i,k}}{||\widehat{\mathbf{h}}_{\mathrm{rd}}^{i,k}||}(\widehat{\mathbf{h}}_{\mathrm{rd}}^{i,k})^{H}\ \ [\widehat{\mathbf{h}}_{\mathrm{rd}}^{i,k}\in\mathbb{C}^{1\times N}]\\ &= \frac{1}{N}\widehat{\mathbf{h}}_{\mathrm{rd}}^{i,k}(\widehat{\mathbf{h}}_{\mathrm{rd}}^{i,k})^{H}\underset{N\to\infty}{\overset{a.s.}{\longrightarrow}}\widehat{\psi}_{\mathrm{rd}}^{i,k}\ [\text{from (3.37)}],\end{aligned} \tag{3.59}$$

$$\begin{aligned}\frac{1}{N}\overline{\gamma}_{\mathrm{s}}^{i,j,k,m} =& \frac{1}{N}\delta_{km}\widehat{h}_{\mathrm{sd}}^{i,j,k}(\widehat{h}_{\mathrm{sd}}^{i,j,k})^{*}+\frac{1}{N}\delta_{km}(\sigma_{e,\mathrm{sd}}^{i,j,k})^{2}+\frac{1}{N}\widehat{h}_{\mathrm{sd}}^{i,j,k}\kappa_{\mathrm{s}}^{j}(\widehat{h}_{\mathrm{sd}}^{i,j,k})^{*}+\frac{1}{N}(\sigma_{e,\mathrm{sd}}^{i,j,k})^{2}\kappa_{\mathrm{s}}^{j}\\ &+\frac{1}{N}\beta_{\mathrm{d}}^{i}\left(\widehat{h}_{\mathrm{sd}}^{i,j,m}(\widehat{h}_{\mathrm{sd}}^{i,j,m})^{*}+(\sigma_{e,\mathrm{sd}}^{i,j,m})^{2}\right)\end{aligned} \tag{3.60}$$

It can be easily observed, when N goes to infinity all the terms in $\frac{1}{N}\overline{\gamma}_{\mathrm{s}}^{i,j,k,m}$ goes to zero. The term $\frac{1}{N}\overline{\gamma}_{\mathrm{r}}^{i,j,k,m}$ can be written as

$$\begin{aligned}\frac{1}{N}\overline{\gamma}_{\mathrm{r}}^{i,j,k,m} =&\delta_{km}(1-\delta_{ij})\frac{1}{N}\widehat{\mathbf{h}}_{\mathrm{rd}}^{i,k}\frac{(\widehat{\mathbf{h}}_{\mathrm{rd}}^{j,k})^H}{||\widehat{\mathbf{h}}_{\mathrm{rd}}^{j,k}||}\frac{\widehat{\mathbf{h}}_{\mathrm{rd}}^{j,k}}{||\widehat{\mathbf{h}}_{\mathrm{rd}}^{j,k}||}(\widehat{\mathbf{h}}_{\mathrm{rd}}^{i,k})^H+\frac{1}{N}\delta_{km}(\sigma_{e,\mathrm{rd}}^{i,k})^2\\
&+\frac{1}{N}\widehat{\mathbf{h}}_{\mathrm{rd}}^{i,k}\kappa_r\mathbf{I}_N\mathrm{diag}\left(\frac{(\widehat{\mathbf{h}}_{\mathrm{rd}}^{j,m})^H}{||\widehat{\mathbf{h}}_{\mathrm{rd}}^{j,m}||}\frac{\widehat{\mathbf{h}}_{\mathrm{rd}}^{j,m}}{||\widehat{\mathbf{h}}_{\mathrm{rd}}^{j,m}||}\right)(\widehat{\mathbf{h}}_{\mathrm{rd}}^{i,k})^H\\
&+\frac{1}{N}(\sigma_{e,\mathrm{rd}}^{i,k})^2\mathrm{Tr}\left(\kappa_r\mathbf{I}_N\mathrm{diag}\left(\frac{(\widehat{\mathbf{h}}_{\mathrm{rd}}^{j,m})^H}{||\widehat{\mathbf{h}}_{\mathrm{rd}}^{j,m}||}\frac{\widehat{\mathbf{h}}_{\mathrm{rd}}^{j,m}}{||\widehat{\mathbf{h}}_{\mathrm{rd}}^{j,m}||}\right)\right)\\
&+\frac{1}{N}\beta_{\mathrm{d}}^{i}\left(\widehat{\mathbf{h}}_{\mathrm{rd}}^{i,m}\frac{(\widehat{\mathbf{h}}_{\mathrm{rd}}^{j,m})^H}{||\widehat{\mathbf{h}}_{\mathrm{rd}}^{j,m}||}\frac{\widehat{\mathbf{h}}_{\mathrm{rd}}^{j,m}}{||\widehat{\mathbf{h}}_{\mathrm{rd}}^{j,m}||}(\widehat{\mathbf{h}}_{\mathrm{rd}}^{i,m})^H+\frac{1}{N}(\sigma_{e,\mathrm{rd}}^{i,m})^2\right)\end{aligned}\tag{3.61}$$

By utilizing a similar approach as for source-relay case, we obtain,

$$\frac{1}{N}\overline{\gamma}_{\mathrm{r}}^{i,j,k,m}\underset{N\to\infty}{\overset{a.s.}{\longrightarrow}}\delta_{ij}\beta_{\mathrm{d}}^{i}\widehat{\psi}_{\mathrm{rd}}^{i,m},\tag{3.62}$$

and rest of terms vanish as N goes to infinity. Similar to the source-relay case, the terms in $\frac{1}{N}\alpha_{\mathrm{n,d}}^{k}$ will also vanish in large N regime.

Finally, the upper bound on the achievable information rate for the i-th source-destination pair using k-th sub-carrier can be obtained as

$$\begin{aligned}R^{i,k}&=\min\{R_{\mathrm{sr}}^{i,k},R_{\mathrm{rd}}^{i,k}\}\\
&=\gamma_0\log_2\left(1+\min\left\{\frac{K}{\widetilde{\kappa}_{\mathrm{s}}^{i}\sum\limits_{m\in\mathbb{K}}\frac{p_{\mathrm{s}}^{i,m}}{p_{\mathrm{s}}^{i,k}}},\frac{K}{\widetilde{\beta}_{\mathrm{d}}^{i}\sum\limits_{m\in\mathbb{K}}\frac{p_{\mathrm{r}}^{i,m}\widehat{\psi}_{\mathrm{rd}}^{i,m}}{p_{\mathrm{r}}^{i,k}\widehat{\psi}_{\mathrm{rd}}^{i,k}}}\right\}\right).\end{aligned}\tag{3.63}$$

A similar achievable rate expression is obtained for the case of the single carrier system in [38, Remark 1]. It can be noticed that the effect of multi-user interference and receiver noise vanish in large N regime ($N\to\infty$). Another interesting observation is that the achievable rate for an FD MC DF system, where the relay equipped with a large number of antennas ($N\to\infty$), is restricted by the hardware distortions at the single antenna source and destination nodes.

Special Case: Perfect CSI

In the case of the perfect CSI, $\psi_{\mathcal{X}}^{j,m}$ are known, where $\mathcal{X}\in\{\mathrm{sr},\mathrm{rd},\mathrm{rr},\mathrm{sd}\}$, j represents the destination as well as the relay, and m represents the sub-carrier. Moreover, the $(\sigma_{e,\mathcal{X}}^{j,m})^2$ in the gamma equations vanish. We can use the same approach as in the above section

and the upper bound on the achievable information rate for the i-th source-destination pair using k-th sub-carrier for perfect CSI can be obtained as

$$\begin{aligned} R^{i,k} &= \min\{R_{\mathrm{sr}}^{i,k}, R_{\mathrm{rd}}^{i,k}\} \\ &= \gamma_0 \log_2 \left(1 + \min \left\{ \frac{K}{\widetilde{\kappa}_{\mathrm{s}}^{i} \sum\limits_{m \in \mathbb{K}} \frac{p_{\mathrm{s}}^{i,m}}{p_{\mathrm{s}}^{i,k}}}, \frac{K}{\widetilde{\beta}_{\mathrm{d}}^{i} \sum\limits_{m \in \mathbb{K}} \frac{p_{\mathrm{r}}^{i,m} \psi_{\mathrm{rd}}^{i,m}}{p_{\mathrm{r}}^{i,k} \psi_{\mathrm{rd}}^{i,k}}} \right\} \right). \end{aligned} \tag{3.64}$$

This signifies the importance of considering the hardware distortion in the resource allocation problem for an FD mMIMO MC DF relay system, even when the number of relay antennas goes to infinity and a perfect CSI can be achieved.

3.5 Optimization

In this section, we formulate the joint sub-carrier and power allocation optimization problem for FD mMIMO DF relay system. We incorporate the sub-carrier allocation into the power allocation problem such that if the power allocated to a particular sub-carrier associated with the source/destination node is zero, then the node is not transmitting or receiving in that sub-carrier. We consider the joint-carrier (JC) coding strategy introduced in Section 2.5.1 for each source-destination pair. Three optimization problems namely weighted sum-rate maximization, energy efficiency maximization, and delivery time minimization, are considered in the following.

3.5.1 Weighted Sum-rate Maximization

In this section, we present the joint sub-carrier and power allocation optimization problem to maximize spectral efficiency in terms of the total sum-rate under transmit power constraints. The sum-rate maximization problem for an FD mMIMO DF relay system can be formulated as

$$\begin{aligned} \underset{p_{\mathrm{s}}^{i,k} \geq 0, p_{\mathrm{r}}^{i,k} \geq 0}{\text{maximize}} \quad & \sum_{i \in \mathbb{L}} w_i \sum_{k \in \mathbb{K}} R^{i,k} \\ \text{subject to} \quad & \sum_{i \in \mathbb{L}} \sum_{k \in \mathbb{K}} p_{\mathrm{r}}^{i,k} \leq p_{\mathrm{r}}, \ \sum_{k \in \mathbb{K}} p_{\mathrm{s}}^{i,k} \leq p_{\mathrm{s}}^{i}, i \in \mathbb{L}, \end{aligned} \tag{3.65}$$

where p_{s}^{i} and p_{r} are the maximum available transmit power at the i-th source node and the relay, respectively. The weight corresponding to the i-th source-destionation pair is

denoted by w_i. The optimization problem can be rewritten as

$$\begin{aligned} \underset{p_{\rm s}^{i,k}\geq 0, p_{\rm r}^{i,k}\geq 0, t_i}{\text{maximize}} \quad & \sum_{i\in\mathbb{L}} w_i t_i \\ \text{subject to} \quad & \sum_{k\in\mathbb{K}} R_{\rm sr}^{i,k} \geq t_i,\ \sum_{k\in\mathbb{K}} R_{\rm rd}^{i,k} \geq t_i, \\ & \sum_{i\in\mathbb{L}}\sum_{k\in\mathbb{K}} p_{\rm r}^{i,k} \leq p_{\rm r},\ \sum_{k\in\mathbb{K}} p_{\rm s}^{i,k} \leq p_{\rm s}^{i}, i\in\mathbb{L}. \end{aligned} \tag{3.66}$$

It can be clearly seen that the above optimization problem belongs to the class of smooth difference-of-convex (DC) optimization problems. We propose an iterative algorithm that utilizes the successive inner approximation (SIA) framework [90], which reaches a converging point that satisfies the Karush–Kuhn–Tucker (KKT) optimality conditions. Let us first select $p_{\rm s,o}^{i,k}$ and $p_{\rm r,o}^{i,k}$ as a feasible transmit power value at the i-th source and relay node, respectively. Next, we use Taylor's approximation on the concave terms of $R_{\rm sr}^{i,k}$, and a lower-bound of $R_{\rm sr}^{i,k}$ can be obtained as

$$\begin{aligned} R_{\rm sr}^{i,k} \geq\ & \gamma_0 \log_2\left(\alpha_{\rm n,r}^{i,k} + \sum_{m\in\mathbb{K}}\sum_{j\in\mathbb{L}} (\gamma_{\rm s}^{i,j,k,m} p_{\rm s}^{j,m} + \gamma_{\rm r}^{i,j,k,m} p_{\rm r}^{j,m}) + |(\mathbf{u}_{\rm r}^{i,k})^H \widehat{\mathbf{h}}_{\rm sr}^{i,k}|^2 p_{\rm s}^{i,k}\right) \\ & - \gamma_0 \log_2\left(\alpha_{\rm n,r}^{i,k} + \sum_{m\in\mathbb{K}}\sum_{j\in\mathbb{L}} (\gamma_{\rm s}^{i,j,k,m} p_{\rm s,o}^{j,m} + \gamma_{\rm r}^{i,j,k,m} p_{\rm r,o}^{j,m})\right) \\ & - \frac{\gamma_0 \sum_{m\in\mathbb{K}}\sum_{j\in\mathbb{L}} \left(\gamma_{\rm s}^{i,j,k,m}(p_{\rm s}^{j,m} - p_{\rm s,o}^{j,m}) + \gamma_{\rm r}^{i,j,k,m}(p_{\rm r}^{j,m} - p_{\rm r,o}^{j,m})\right)}{\log(2)\left(\alpha_{\rm n,r}^{i,k} + \sum_{m\in\mathbb{K}}\sum_{j\in\mathbb{L}} (\gamma_{\rm s}^{i,j,k,m} p_{\rm s,o}^{j,m} + \gamma_{\rm r}^{i,j,k,m} p_{\rm r,o}^{j,m})\right)} =: \overline{R}_{\rm sr}^{i,k}. \end{aligned} \tag{3.67}$$

Similarly, the lower bound $\overline{R}_{\rm rd}^{i,k}$ of $R_{\rm rd}^{i,k}$, after applying Taylor's approximation, can be written as

$$\begin{aligned} R_{\rm rd}^{i,k} \geq\ & \gamma_0 \log_2\left(\alpha_{\rm n,d}^{i,k} + \sum_{m\in\mathbb{K}}\sum_{j\in\mathbb{L}} (\overline{\gamma}_{\rm s}^{i,j,k,m} p_{\rm s}^{j,m} + \overline{\gamma}_{\rm r}^{i,j,k,m} p_{\rm r}^{j,m}) + |\widehat{\mathbf{h}}_{\rm rd}^{i,k} \mathbf{v}_{\rm r}^{i,k}|^2 p_{\rm r}^{i,k}\right) \\ & - \gamma_0 \log_2\left(\alpha_{\rm n,d}^{i,k} + \sum_{m\in\mathbb{K}}\sum_{j\in\mathbb{L}} (\overline{\gamma}_{\rm s}^{i,j,k,m} p_{\rm s,o}^{j,m} + \overline{\gamma}_{\rm r}^{i,j,k,m} p_{\rm r,o}^{j,m})\right) \\ & - \frac{\gamma_0 \sum_{m\in\mathbb{K}}\sum_{j\in\mathbb{L}} \left(\overline{\gamma}_{\rm s}^{i,j,k,m}(p_{\rm s}^{j,m} - p_{\rm s,o}^{j,m}) + \overline{\gamma}_{\rm r}^{i,j,k,m}(p_{\rm r}^{j,m} - p_{\rm r,o}^{j,m})\right)}{\log(2)\left(\alpha_{\rm n,d}^{i,k} + \sum_{m\in\mathbb{K}}\sum_{j\in\mathbb{L}} (\overline{\gamma}_{\rm s}^{i,j,k,m} p_{\rm s,o}^{j,m} + \overline{\gamma}_{\rm r}^{i,j,k,m} p_{\rm r,o}^{j,m})\right)} =: \overline{R}_{\rm rd}^{i,k}. \end{aligned} \tag{3.68}$$

By replacing the actual rate functions with the obtained lower bounds, the objective of the above optimization problem (3.66) becomes a jointly concave function over $p_{\rm s}^{i,k}$ and $p_{\rm r}^{i,k}$. We propose an iterative algorithm, where for each iterative update, we now solve

the convex problem:

$$\begin{aligned} \underset{p_{\mathrm{s}}^{i,k}\geq 0, p_{\mathrm{r}}^{i,k}\geq 0, t_i}{\text{maximize}} \quad & \sum_{i\in\mathbb{L}} w_i t_i \\ \text{subject to} \quad & \sum_{k\in\mathbb{K}} \overline{R}_{\mathrm{sr}}^{i,k} \geq t_i,\ \sum_{k\in\mathbb{K}} \overline{R}_{\mathrm{rd}}^{i,k} \geq t_i \\ & \sum_{i\in\mathbb{L}}\sum_{k\in\mathbb{K}} p_{\mathrm{r}}^{i,k} \leq p_{\mathrm{r}},\ \sum_{k\in\mathbb{K}} p_{\mathrm{s}}^{i,k} \leq p_{\mathrm{s}}^{i},\ i\in\mathbb{L}, \end{aligned} \tag{3.69}$$

to obtain the optimality. At each iteration, the approximated rate functions are updated with the solution of (3.69) from the previous iteration as their initial points. The iterative update is continued until a stable point is reached. Since we use a first-order Taylor approximation on a smooth concave terms, we can conclude that $\overline{R}_{\mathrm{sr}}^{i,k}$ represents a global and tight lower bound to $R_{\mathrm{sr}}^{i,k}$, with a shared slope at the point of approximation [91] [1] . The proposed iterative update also fulfils the requirements set in [90, Theorem 1], so that the solution can achieve a convergence point that satisfies KKT optimality conditions. Algorithm 5 defines the detailed algorithm.

Algorithm 5 For sum-rate maximization

1: $a \leftarrow 0$ (set iteration number to zero)
2: $p_{\mathrm{s,o}}^{i,k}, p_{\mathrm{r,o}}^{i,k} \leftarrow$ feasible power value initialization
3: **repeat**
4: $\quad a \leftarrow a+1$
5: $\quad p_{\mathrm{s}}^{i,k}, p_{\mathrm{r}}^{i,k}, t_i \leftarrow$ solve (3.69)
6: $\quad p_{\mathrm{s,o}}^{i,k}, p_{\mathrm{r,o}}^{i,k} \leftarrow p_{\mathrm{s,o}}^{i,k} = p_{\mathrm{s}}^{i,k}$ and $p_{\mathrm{r,o}}^{i,k} = p_{\mathrm{r}}^{i,k}$, respectively
7: **until** a stable point, or maximum number of a reached
8: **return** $\{p_{\mathrm{s}}^{i,k}, p_{\mathrm{r}}^{i,k}\}$

3.5.2 Energy Efficiency Maximization

Energy efficiency has become an essential measure for designing a future wireless system. In this section, the energy efficiency is defined as the ratio of the sum-rate to the total power consumption of all the user nodes and the relay. The total power consumption P_{tot} can be expressed as

$$P_{\mathrm{tot}} = \sum_{i\in\mathbb{L}} P_{\mathrm{s}}^{i} + P_{\mathrm{r}}, \tag{3.70}$$

where

$$\begin{aligned} P_{\mathrm{s}}^{i} &:= \frac{1}{\mu_{\mathrm{s}}^{i}} \sum_{k\in\mathbb{K}} \mathbb{E}\{\|x_{\mathrm{s}}^{i,k}\|^2\} + P_{\mathrm{s,zero}}^{i}, \\ P_{\mathrm{r}} &:= \frac{1}{\mu_{\mathrm{r}}} \sum_{k\in\mathbb{K}} \mathbb{E}\{\|\mathbf{x}_{\mathrm{r}}^{k}\|^2\} + P_{\mathrm{r,zero}} + P_{\mathrm{r,FD}}. \end{aligned}$$

[1] Similarly for the approximation $\overline{R}_{\mathrm{rd}}^{i,k}$ in relation to $R_{\mathrm{rd}}^{i,k}$

The efficiency of the power amplifier and power dissipated by other circuit blocks at the transmitter chain of the i-th source node (relay) are respectively denoted by μ_{s}^{i} (μ_{r}) and $P_{\mathrm{s,zero}}^{i}$ ($P_{\mathrm{r,zero}}$) . $P_{\mathrm{r,FD}}$ is the power required for SIC at the relay. By using the above definition, the energy efficiency maximization problem can be expressed as

$$\begin{aligned} \underset{p_{\mathrm{s}}^{i,k}\geq 0, p_{\mathrm{r}}^{i,k}\geq 0}{\text{maximize}} \quad & \sum_{i\in\mathbb{L}} w_i \sum_{k\in\mathbb{K}} \frac{R^{i,k}}{P_{\mathrm{tot}}} \\ \text{subject to} \quad & P_{\mathrm{r}} \leq P_{\mathrm{r,max}}, P_{\mathrm{s}}^{i} \leq P_{\mathrm{s,max}}^{i}, i \in \mathbb{L}, \end{aligned} \tag{3.71}$$

where $P_{\mathrm{s,max}}^{i}$ and $P_{\mathrm{r,max}}$ are the maximum total available power for consumption at the i-th source node and the relay, respectively. The optimization problem can be reformulated as

$$\begin{aligned} \underset{p_{\mathrm{s}}^{i,k}\geq 0, p_{\mathrm{r}}^{i,k}\geq 0, t_i}{\text{maximize}} \quad & \sum_{i\in\mathbb{L}} \frac{w_i t_i}{P_{\mathrm{tot}}} \\ \text{subject to} \quad & \sum_{k\in\mathbb{K}} R_{\mathrm{sr}}^{i,k} \geq t_i, \ \sum_{k\in\mathbb{K}} R_{\mathrm{rd}}^{i,k} \geq t_i, \\ & P_{\mathrm{r}} \leq P_{\mathrm{r,max}}, \ P_{\mathrm{s}}^{i} \leq P_{\mathrm{s,max}}^{i}, i \in \mathbb{L}. \end{aligned} \tag{3.72}$$

To solve the above fractional non-convex problem, we propose a double-loop iterative algorithm (Algorithm 6) using SIA framework and Dinkelbach algorithm. Let us first select $p_{\mathrm{s,o}}^{i,k}$ and $p_{\mathrm{r,o}}^{i,k}$ as a feasible transmit power value at the i-th source node and relay, respectively. In the outer loop, we calculate the rate approximations $\overline{R}_{\mathrm{sr}}^{i,k}$ and $\overline{R}_{\mathrm{rd}}^{i,k}$ using (3.67) and (3.68) for the point of approximation $p_{\mathrm{s,o}}^{i,k}$ and $p_{\mathrm{r,o}}^{i,k}$. We fix these values for the inner loop. In the inner loop, we use Dinkelbach algorithm [81], using which we can rewrite the optimization problem as

$$\begin{aligned} \underset{p_{\mathrm{s}}^{i,k}\geq 0, p_{\mathrm{r}}^{i,k}\geq 0, t_i}{\text{maximize}} \quad & \sum_{i\in\mathbb{L}} w_i t_i - \lambda P_{\mathrm{tot}} \\ \text{subject to} \quad & \sum_{k\in\mathbb{K}} \overline{R}_{\mathrm{sr}}^{i,k} \geq t_i, \ \sum_{k\in\mathbb{K}} \overline{R}_{\mathrm{rd}}^{i,k} \geq t, \\ & P_{\mathrm{r}} \leq P_{\mathrm{r,max}}, \ P_{\mathrm{s}}^{i} \leq P_{\mathrm{s,max}}^{i}, i \in \mathbb{L}. \end{aligned} \tag{3.73}$$

For fixed $p_{\mathrm{s,o}}^{i,k}$ and $p_{\mathrm{r,o}}^{i,k}$, we iteratively solve for $p_{\mathrm{s}}^{i,k}$, $p_{\mathrm{r}}^{i,k}$ and t_i, and λ. The value of λ can be determined from

$$\sum_{i\in\mathbb{L}} w_i t_i - \lambda P_{\mathrm{tot}} = 0. \tag{3.74}$$

Since Dinkelbach algorithm is applied to the concave-affine fractional problem, we can conclude that a global optimal can be achieved [92, Section 3.2]. Then in the outer loop, we update $p_{\mathrm{s,o}}^{i,k}$ and $p_{\mathrm{r,o}}^{i,k}$ in order to calculate the new rate approximations and solve the optimization problem until a stable point is reached. Algorithm 6 defines the detailed algorithm.

Algorithm 6 For energy efficiency maximization

$p_{\mathrm{s,o}}^{i,k}, p_{\mathrm{r,o}}^{i,k} \leftarrow$ feasible power value initialization
$\lambda = 0 \leftarrow$ Lambda initialization
$a \leftarrow 0$ (set iteration number to zero for outer loop)
repeat
  $a \leftarrow a + 1$
  repeat
    $p_{\mathrm{s}}^{i,k}, p_{\mathrm{r}}^{i,k}, t_i \leftarrow$ solve (3.73)
    $\lambda \leftarrow$ solve (3.74)
  until a stable point is reached
  $p_{\mathrm{s,o}}^{i,k} \leftarrow p_{\mathrm{s}}^{i,k}$ and $p_{\mathrm{r,o}}^{i,k} \leftarrow p_{\mathrm{r}}^{i,k}$
until a stable point, or maximum number of a reached
return $\{p_{\mathrm{s}}^{i,k}, p_{\mathrm{r}}^{i,k}\}$

3.5.3 Delivery Time Minimization

In this section, we address the joint sub-carrier and power allocation optimization problem to minimize the overall delivery time of an FD mMIMO relay system. Let us consider delivery time as the amount of time required to transmit D_i number of bits (size of a file) from i-th source to the i-th destination. It can be defined as the ratio of the size of the file (amount of information D_i) required to be communicated between i-th source-destination pairs to the achievable information rate. In this work, as the source-destination pair communicate using an FD mMIMO relay, the achievable information rate will be the minimum of the achievable information rate between i-th source and the relay, and the achievable information rate between the relay and i-th destination as mentioned in Section 3.4.4. Here, we formulate the optimization problem to minimize the overall delivery time for all the source-destination pairs.

The overall delivery time minimization problem can be defined as

$$\begin{aligned} \underset{p_{\mathrm{s}}^{i,k}\geq 0, p_{\mathrm{r}}^{i,k}\geq 0}{\text{minimize}} \quad & \sum_{i\in\mathbb{L}} \frac{D_i}{\sum\limits_{k\in\mathbb{K}} R_{i,k}} \\ \text{subject to} \quad & \sum_{i\in\mathbb{L}}\sum_{k\in\mathbb{K}} p_{\mathrm{r}}^{i,k} \leq p_{\mathrm{r}},\ \sum_{k\in\mathbb{K}} p_{\mathrm{s}}^{i,k} \leq p_{\mathrm{s}}^{i}, i \in \mathbb{L}. \end{aligned} \tag{3.75}$$

The above optimization can be rewritten as

$$\begin{aligned} \underset{p_{\mathrm{s}}^{i,k}\geq 0, p_{\mathrm{r}}^{i,k}\geq 0, t_i}{\text{minimize}} \quad & \sum_{i\in\mathbb{L}} \frac{D_i}{t_i} \\ \text{subject to} \quad & \sum_{k\in\mathbb{K}} R_{\mathrm{sr}}^{i,k} \geq t_i,\ \sum_{k\in\mathbb{K}} R_{\mathrm{rd}}^{i,k} \geq t_i, \\ & \sum_{i\in\mathbb{L}}\sum_{k\in\mathbb{K}} p_{\mathrm{r}}^{i,k} \leq p_{\mathrm{r}},\ \sum_{k\in\mathbb{K}} p_{\mathrm{s}}^{i,k} \leq p_{\mathrm{s}}^{i}, i \in \mathbb{L}. \end{aligned} \tag{3.76}$$

This optimization belongs to the class of smooth DC optimization problems similar to (3.65). After applying Taylor's approximation (3.67) and (3.68) for the point of approximation $p_{\mathrm{s,o}}^{i,k}$ and $p_{\mathrm{r,o}}^{i,k}$, the convex optimization can be reformulated as

$$\begin{aligned} \underset{p_{\mathrm{s}}^{i,k}\geq 0, p_{\mathrm{r}}^{i,k}\geq 0, t_i}{\text{minimize}} \quad & \sum_{i\in\mathbb{L}} \frac{D_i}{t_i} \\ \text{subject to} \quad & \sum_{k\in\mathbb{K}} \overline{R}_{\mathrm{sr}}^{i,k} \geq t_i, \ \sum_{k\in\mathbb{K}} \overline{R}_{\mathrm{rd}}^{i,k} \geq t_i, \\ & \sum_{i\in\mathbb{L}}\sum_{k\in\mathbb{K}} p_{\mathrm{r}}^{i,k} \leq p_{\mathrm{r}}, \ \sum_{k\in\mathbb{K}} p_{\mathrm{s}}^{i,k} \leq p_{\mathrm{s}}^{i}, i \in \mathbb{L}. \end{aligned} \tag{3.77}$$

Here, the optimization problem is solved using an iterative algorithm similar to Algorithm 5 that follows SIA framework, which reaches a converging point that satisfies the KKT optimality conditions. Algorithm 7 defines the detailed algorithm.

Algorithm 7 For delivery time minimization

1: $a \leftarrow 0$ (set iteration number to zero)
2: $p_{\mathrm{s,o}}^{i,k}, p_{\mathrm{r,o}}^{i,k} \leftarrow$ feasible power value initialization
3: **repeat**
4: $\quad a \leftarrow a + 1$
5: $\quad p_{\mathrm{s}}^{i,k}, p_{\mathrm{r}}^{i,k}, t_i \leftarrow$ solve (3.77)
6: $\quad p_{\mathrm{s,o}}^{i,k}, p_{\mathrm{r,o}}^{i,k} \leftarrow p_{\mathrm{s,o}}^{i,k} = p_{\mathrm{s}}^{i,k}$ and $p_{\mathrm{r,o}}^{i,k} = p_{\mathrm{r}}^{i,k}$, respectively
7: **until** a stable point, or maximum number of a reached
8: **return** $\{p_{\mathrm{s}}^{i,k}, p_{\mathrm{r}}^{i,k}\}$

3.6 Simulation Results

In this section, using numerical simulations, we evaluate the performance of the proposed algorithms introduced in Section 3.5 for an FD mMIMO MC DF relay system. We evaluate the performance in terms of different optimization strategies such as sum-rate maximization, delivery time minimization, and energy efficiency maximization for different system parameters.

We consider a relay communication setup where the distance between the sources/ destinations to the FD mMIMO relay varying from 200m to 400m. The minimum distance between a source and a destination node is 400m. We adopt simulation system parameters from [93, 94], which are chosen as in Table 3.1. We consider our path loss model as a simplified path loss model in [95]. We consider the relay system employs orthogonal frequency division multiplexing (OFDM) as MC strategy. The weight corresponding to the i-th source-destination pair is chosen as $w_i = 1, \forall i \in \mathbb{L}$. To provide fairness in resource allocation, the transmit power budget is restricted to support the number of

active sub-carriers ($\overline{\overline{\mathbb{K}}}$) , i.e., the transmit power budgets are factorized by k_t, where $k_t = \overline{\overline{\mathbb{K}}}/\overline{\overline{\mathbb{K}}}_{\text{sys}}$. The total number of sub-carriers available in the system are denoted by $\overline{\overline{\mathbb{K}}}_{\text{sys}}$. For energy efficiency maximization problem, the power dissipated by circuit components other than power amplifier and power for SIC is also considered. The power dissipated by circuit blocks other than power amplifier at the transmitter chain of the i-th source node $P^i_{\text{s,zero}}$ and relay including SIC ($P_{\text{r,zero}} + P_{\text{r,FD}}$) are chosen as 10dBm and 14dBm, respectively. For the delivery time minimization case, the file size (amount of information D_i) for each source-destination pair is chosen between 0 and 100 bits. All communication channels follow an uncorrelated Rayleigh flat fading model. The SI channel follows the Rician distribution as characterization reported in [20] with Rician coefficient K_{r} and the SI channel strength after SIC ρ_{si}. We assume the covariance for the SI channel to be low rank as in [5]. Here, the rank of the covariance matrix of SI channel is chosen as 5. The overall system performance is then averaged over 100 channel realizations.

Carrier center frequency and system bandwidth	2.5 GHz and 5MHz
Number of sub-carriers ($\overline{\overline{\mathbb{K}}}_{\text{sys}}$), and sub-carrier bandwidth	64 and 78kHz
Number of active sub-carriers ($\overline{\overline{\mathbb{K}}}$)	10
Number of source-destination pairs ($\overline{\overline{\mathbb{L}}}$)	3
Reference distance and path loss exponent	15m and 3.6
Efficiency of power amplifier at relay (μ_r) and source (μ^i_s)	0.39
Noise power at destination i and relay (σ^2_n)	-125dBm and -125dBm
Max. tx. power at the source and relay	22dBm and 37dBm
Number of antennas at the relay N	32
Hardware distortion coefficient $\kappa = \beta$	-90dB
Covariance of the CSI estimation error $(\sigma^k_{e,\text{sr}})^2 = (\sigma^k_{e,\text{rd}})^2 = (\sigma^k_{e,\text{sd}})^2 = (\sigma^k_{e,\text{rr}})^2 \forall k \in \mathbb{K}$,	-150dB
SI channel strength ρ_{si} after SIC and Rician coeffient K_{r}	-50 dB and 10

Table 3.1: Default System parameters used for numerical simulations

Benchmarks

For comparison, we consider different transmit/receive strategies at the relay for different system designs. The benchmarks considered for the numerical simulations are as follows.

- MRT/MRC: It represents the proposed algorithms Algorithms 5 to 7 employing MRT/MRC as its transmit/receive strategy at the relay for the sum-rate maximization, energy efficiency maximization and delivery time minimization, respectively.

- MRT/MRC-SI-ZF: In addition to considering MRT/MRC as its transmit/receive strategy at the relay, spatial suppression scheme (null-space projection [5]) for ZF the SI is employed at the transmit side of the relay. This algorithm allows to eliminate the receive distortion caused by the SI channel, as the transmit beams are projected to the null-space of the SI channel.
- ZF: The proposed algorithms Algorithms 5 to 7 employ ZF as its transmit/receive strategy at the relay for the sum-rate maximization, energy efficiency maximization and delivery time minimization, respectively.
- ZF-SI-ZF: In addition to considering ZF as its transmit/receive strategy at the relay, spatial suppression scheme (null-space projection [5]) is also employed at the transmit side of the relay.

For the above-mentioned transmit strategies, we consider joint decoding and remapping strategy at the relay, see Section 2.5.1. It allows the relay system to decode the signal from one sub-carrier and forward it to the destination through another sub-carrier, thereby improving the performance of the system. We compare it to the per-carrier (PC) design, where the optimization constraints are considered for each sub-carrier individually, please refer Section 2.5.1. Moreover, the JC and PC designs for above-mentioned transmit strategies are further classified as:

- OPT: It represents the proposed algorithms employing different transmit-receive strategies for both joint-carrier and per-carrier design, with consideration of the impact of imperfect CSI as well as the hardware distortions.
- ND (non-distortion): It indicates the algorithms that do not consider the impact of hardware distortions in the design , i.e., hardware inaccuracy is not taken into account. It only considers the impact of imperfect CSI.
- HD: It indicates the scenarios when an HD mMIMO relay is employed. We consider the HD relay utilizes time division duplex (TDD) to seperate the source-relay and relay-destination links, hence SI is not present.

Visualization

Figs. 3.2a to 3.2f illustrate the performance of the system for the sum-rate maximization algorithm with respect to different system parameters. In general, it can be observed that the algorithms employing ZF perform better compared the algorithms employed with MRT/MRC. However, the ZF strategy is more complex (computationally expensive) compared to MRT/MRC as it involves inversion of matrices with large dimensions. Even there is a gain in performance of algorithms using ZF compared to MRT/MRC, the algorithms (OPT, ND, HD) show almost similar behaviour for the different system parameters irrespective of the transmit strategies used.

The performance of the algorithm in terms of sum-rate with respect to the hardware inaccuracies (κ) is shown in Fig. 3.2a. As it can be clearly seen, the sum-rate decreases as hardware inaccuracies increases. The JC algorithms show a similar or better performance than the PC algorithms for different values of κ. It can be observed that a performance gain can be achieved by utilizing spatial suppression scheme (null-space projection) in addition to the transmit strategies. By transmitting along the null-space of the SI channel, the impact of receive distortion leading to residual SI (caused by the SI channel) can be eliminated at the receive side of the relay. Furthermore, the non-distortion (ND) algorithms performance similar to the proposed OPT algorithm for small values of κ. A gain in performance of JC strategy can also be noticed compared to the PC strategy algorithm employing MRT/MRC. However, as the value of κ increases, the performance of the ND algorithms degrades drastically compared to the OPT. As it can be observed, the achievable sum-rate of FD algorithms become less than that of the HD algorithms for higher values of κ. This implies that the impact of hardware distortion is more in FD systems compared to HD systems due to the presence of SI.

The system performance with respect to κ for different SI channel strength ($\rho_{si} = -30dB, -50dB$ and $-70dB$) is depicted in Fig. 3.2b. It can be noticed that as the strength of the SI channel decreases (or better SIC techniques), the performance of the FD systems also improves compared to the HD counterpart. For smaller values of SI channel strength, the FD systems also become more robust to the hardware distortion (hardware inaccuracies) indicating the impact of hardware distortions leading to residual SI. In other words, HD mMIMO MC DF relay system shows better performance compared to the FD mMIMO MC DF relay system if sufficient SIC can not be achieved. For higher values of κ, the HD-ND algorithm performance degrades compared to the HD. This shows that even for HD mMIMO systems, consideration of hardware distortions into the design improves the system robustness and performance, especially in high hardware inaccuracies scenario.

In Fig. 3.2c, the performance of the algorithm for different values of receiver noise at the relay and the destination nodes is plotted. As expected, the sum-rate decreases as the receiver noise increases. The OPT algorithm (ZF-SI-ZF) employing JC and ZF with SI suppression scheme performs better compared to other benchmarks. A similar trend can be observed in Fig. 3.2d concerning channel estimation error. For both the parameters, it is interesting to notice that, for small values of receiver noise or channel estimation error, the OPT algorithm in both JC and PC strategies attains a better gain compared to its ND counterpart. Employing spatial suppression scheme also provides an additional gain, especially when the receiver noise or channel estimation error is small. This is due to the fact that, for small values of receiver noise or channel estimation error, the impact of hardware distortion becomes dominant compared to receiver noise or channel estimation error resulting in degradation of algorithm performance that does not consider the hardware distortion.

In Figs. 3.2e and 3.2f, the performance of the algorithm in terms of sum-rate for different

values of transmit power at the relay and source nodes is depicted, respectively. It can be noticed that when the maximum transmit power at the source/relay increases the overall sum-rate also increases. It is interesting to observe that for high transmit power the ND algorithm performs worse compared to its OPT counterpart. This is because as the power increases, the distortion part becomes dominant and therefore not considering hardware distortion will lead to performance degradation at high transmit power scenario. The performance of the system in terms of sum-rate can be improved by considering hardware distortion and spatial suppression scheme, especially in high transmit power, low receiver noise or less channel estimation error scenarios.

In Figs. 3.3a to 3.3d, the performance of the energy efficiency algorithm for different system parameters is evaluated. In Fig. 3.3a, the energy efficiency of the system degrades as the hardware inaccuracies increases, even for HD design. The proposed algorithm shows similar behaviour as in the case of sum-rate maximization. Moreover, as the hardware inaccuracies increase, the HD algorithm performs better compared to the ND algorithm indicating that consideration of hardware distortion provides better gain for higher values of κ. Furthermore, Fig. 3.3b shows that, the energy efficiency of the system degrades when the receiver noise at the relay and destination nodes increases. When the receiver noise is small, the OPT algorithms perform better compared to ND counterparts as the hardware distortion becomes dominant. In Fig. 3.3c the performance of the system in terms of energy efficiency is depicted with respect to the transmit power of the source node. As it can be observed, when the transmit power of the source node increases, the energy efficiency of the system also increases. However, for high transmit power values, the performance of the OPT algorithm utilizing JC spatial suppression scheme attained better gain in terms of energy efficiency compared to algorithm ND algorithm as the hardware distortion becomes dominant. Another interesting observation is that the energy efficiency of the system becomes saturated at high transmit power budget. After a certain point, the optimum energy-efficient design does not consume more power if it degrades the energy efficiency of the system, i.e., if more power is required for a small improvement in sum-rate. Furthermore, Figure 3.3d reveals that as the CSI estimation error in the system increases the energy efficiency of the system decreases. It can also be observed that employing spatial suppression scheme helps to make the system more energy efficient. For the above-mentioned system parameters except κ, it can be noticed that the algorithm utilizing JC and ZF with spatial suppression scheme is more energy efficient compared to all the other benchmarks.

Figs. 3.4a to 3.4d illustrate the performance of the proposed delivery time minimization algorithm for different system parameters. Similarly as in sum-rate and energy efficiency maximization case, it is observed that the ZF algorithms outperform the algorithms utilizing MRT/MRC. In Fig. 3.4a, the performance of our proposed algorithm in terms of delivery time is evaluated for different values of transceiver inaccuracy. It can be observed that the delivery time increases as the transceiver inaccuracy increases, i.e., higher the κ higher the delivery time. The OPT algorithms show better performance gain, i.e., less overall delivery time, compared to ND algorithms as the value of transceiver inaccuracies increases. This signifies the importance of consideration of

the impact of hardware inaccuracies in an FD mMIMO MC relay system. However, for high transceiver inaccuracy, the FD algorithm performs worst compared to the HD algorithms. Due to strong SI, the impact of hardware distortions is more in the FD system compared to HD resulting in higher residual SI. Fig. 3.4b is plotted in terms of delivery time with respect to different values of receiver noise at the relay and the destination. Furthermore, we can observe that the proposed OPT algorithms outperform their respective benchmarks. As the receiver noise increases, the overall delivery time also increases. It is interesting to observe that for small values of receiver noise variance, the ND algorithm performance degrades compared to OPT algorithm. It is because, in high signal to noise (SNR) scenarios, the hardware distortions become dominant, thereby affecting the performance of ND algorithms which does not consider these hardware distortions. As the receiver noise variance increases, hardware distortions becomes less significant compared to the receiver noise results in better performance of ND algorithms compared to HD algorithms. A similar behaviour of the algorithm is observed in Fig. 3.4c for channel estimation error. As channel estimation error increases, the overall delivery time also increases. It can also be observed that when the channel estimation error is small, the ND algorithms require more delivery time compared to its OPT algorithm counterpart. Similar as in the case of receiver noise, the hardware distortion becomes dominant when channel estimation error has small values.

In Fig. 3.4d the performance of the proposed algorithm in terms of the delivery time for different values of transmit power at the relay is depicted. It can be noticed, as the maximum transmit power at the relay increases the overall delivery time decreases for all the algorithms except ND. For low transmit power values, the algorithms employing JC require less delivery time compared to PC counterparts. This is because JC strategy has the flexibility to select the better channel on both the link, i.e., source-relay and relay-destination for each source-destination pair, which becomes significant in low transmit power scenarios. As the transmit power increases, the overall delivery time for all the algorithms decreases. However after a certain point, the performance of the ND algorithms degrade compared to its OPT counterparts. It can also be observed that for a high transmit power scenario, the ND algorithm requires higher delivery time compared to OPT algorithm. This is due to the fact that as transmit power increases the impact of hardware distortions also increases (because of the presence of SI), resulting in performance degradation of ND algorithms. This signifies the importance of consideration of the impact of hardware inaccuracies leading to residual SI and ICL in an FD mMIMO MC relay system, especially for high transmit power and low noise scenarios (high signal to interference plus noise ratio (SINR) scenarios). In case of delivery time minimization also, it is observed that the proposed algorithm (ZF-SI-ZF) with JC outperforms all the other benchmarks. Moreover, the proposed algorithm (MRT/MRC-SI-ZF) with JC outperforms all the algorithms utilizing MRT/MRC. This shows the benefit of considering hardware distortions, imperfect CSI, and utilizing JC and spatial suppression scheme in designing an FD mMIMO MC DF relay system for both the transmit strategies (MRT/MRC and ZF).

In Fig. 3.4e, the performance of our proposed delivery time minimization algorithm

is compared with the sum-rate maximization algorithm in terms of the delivery time for different values of transceiver accuracy. Here, the maximum file size (amount of information D_i) is chosen to be 10 Mbits. As it can be noticed, the delivery time algorithm performs better compared to the sum-rate algorithm, which implies that maximizing the throughput/sum-rate of the system does not necessarily minimize the overall delivery time. Fig. 3.4f shows the performance gain of delivery time algorithm compared to sum-rate algorithm for different maximum allowed file size (D_i). Here, the hardware distortion coefficients are chosen as $\kappa = \beta = -60$dB. It can be noticed that as the amount of information (D_i) to be communicated increases, the overall delievery time also increases. Furthermore, when the file size (D_i) is large, a significant gain in terms delivery time can be achieved (the overall delivery time can be reduced) by utilizing the delivery time minimization algorithm in comparison with the sum-rate maximization algorithm.

3.7 Conclusions

In this chapter, we addressed a joint sub-carrier and power allocation problem for an FD mMIMO MC DF relay system, which relays the communication between multiple single antenna HD source-destination pairs. We modelled the operation of the system by jointly considering the impact of hardware distortion leading to residual SI and ICL, and imperfect CSI. Asymptotic rate for the system employing MRT/MRC is analyzed. It is noticed that the consideration of the hardware distortion is crucial in the resource allocation problem for an FD mMIMO MC relay system, even when the number of antennas at the relay goes to infinity and a perfect CSI can be achieved. An iterative algorithm that follows the SIA framework is proposed for both the sum-rate maximization and delivery time minimization problems, which converge to the point that satisfies the KKT conditions. We extend it to energy efficiency maximization problem, which is solved by utilizing the SIA framework and Dinkelbach algorithm. The performance of the proposed algorithms are evaluated using numerical simulations. It can be noticed that the algorithm utilizing JC and ZF with spatial suppression scheme performs better compared to all the other benchmarks. It is also observed that a performance gain can be achieved by utilizing spatial suppression scheme (null-space projection) in addition to the transmit strategies. A notable gain in terms of delivery time is achieved when compared with the sum-rate maximization algorithm, shows the benefit of considering delivery time as an objective. Significance of distortion-aware design for FD mMIMO MC DF relay system is observed, especially for high SINR scenarios.

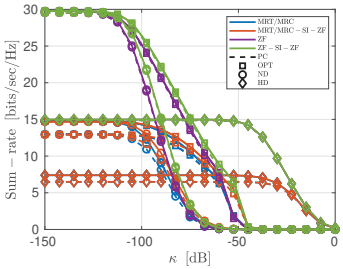

(a) Sum-rate vs. Hardware inaccuracy

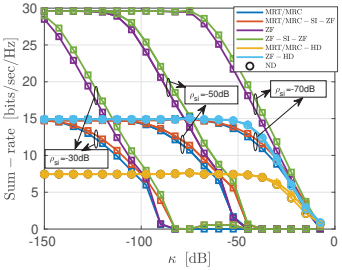

(b) Sum-rate vs. Hardware inaccuracy, for different SI channel strength (ρ_{si})

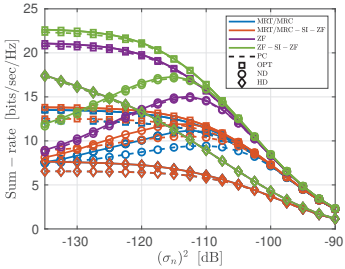

(c) Sum-rate vs. Receiver noise

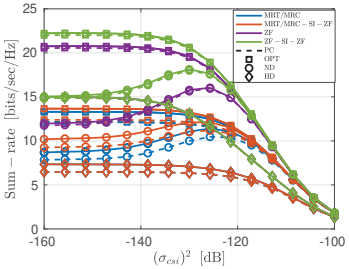

(d) Sum-rate vs. Channel estimation error

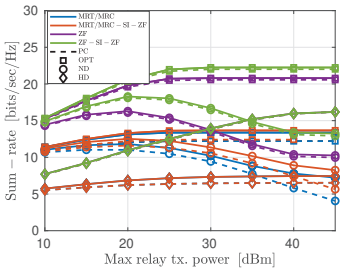

(e) Sum-rate vs. Maximum relay transmit power

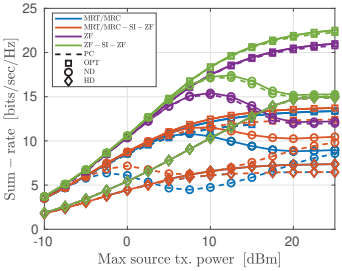

(f) Sum-rate vs. Maximum source transmit power

Figure 3.2: Sum-rate vs. Different system parameters.

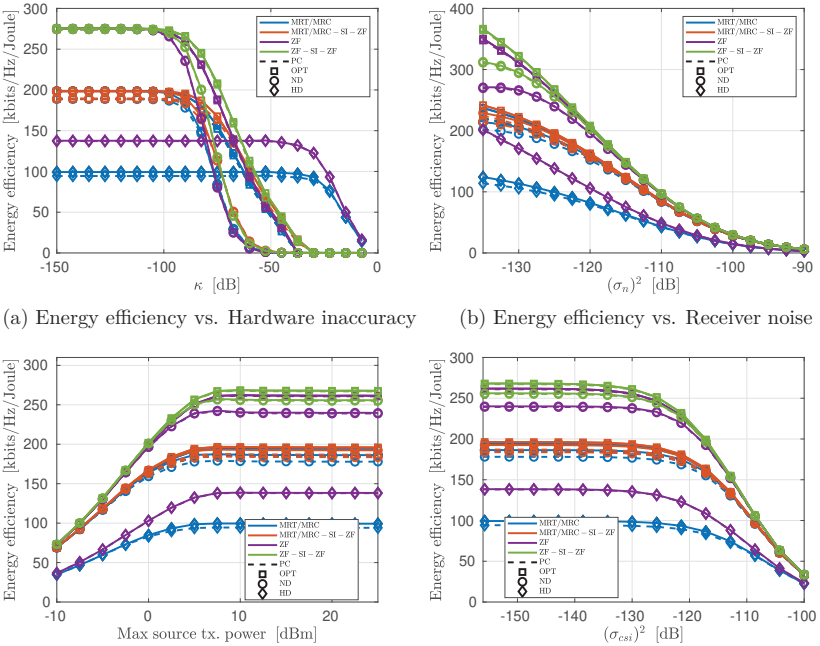

(a) Energy efficiency vs. Hardware inaccuracy

(b) Energy efficiency vs. Receiver noise

(c) Energy efficiency vs. Maximum source transmit power

(d) Energy efficiency vs. Channel estimation error

Figure 3.3: Energy efficiency vs. Different system parameters.

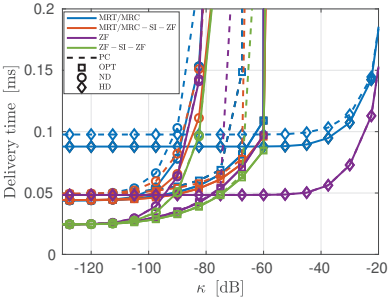

(a) Delivery time vs. Hardware inaccuracy

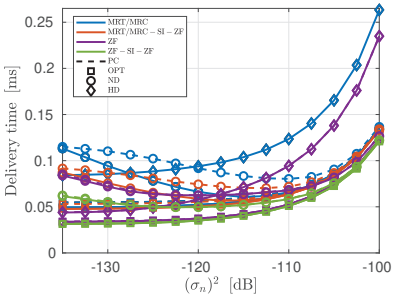

(b) Delivery time vs. Receiver noise

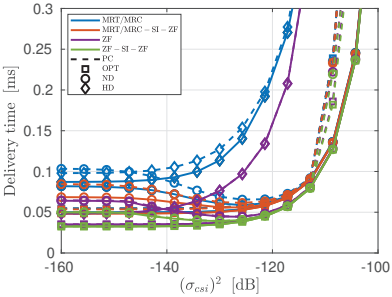

(c) Delivery time vs. Channel estimation error

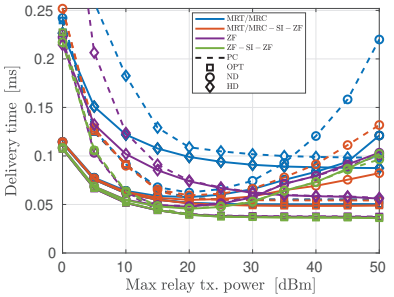

(d) Delivery time vs. Maximum relay transmit power ($P_{t,r,max}$)

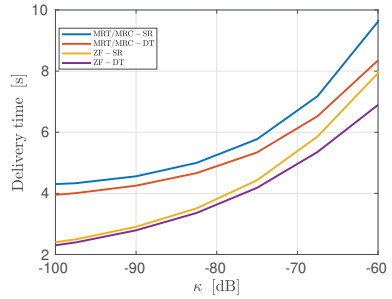

(e) Comparison between delivery time algorithm and sum-rate algorithm for different values of hardware inaccuracy

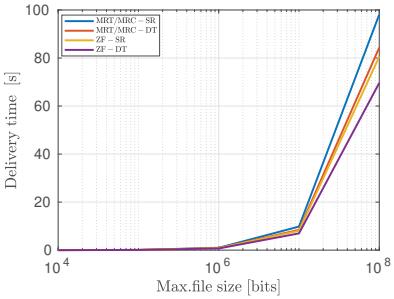

(f) Comparison between delivery time algorithm and sum-rate algorithm for different maximum allowed file size

Figure 3.4: Delivery time vs. Different system parameters.

4 Resource Allocation for Multi-carrier FD mMIMO Bidirectional Communication with Hardware Impairments

4.1 Scope

Utilizing massive antenna array at the base station (BS) improves the spectral and energy efficiency of the system and reduces the inter-user interference even by employing simple linear processing such as maximum ratio transmitting (MRT)/maximum ratio combining (MRC) and zero-forcing transmitting (ZFT)/zero-forcing receiving (ZFR) precoding scheme [96]. By using these linear transmit/receive strategies, the overall power requirement of the system can be reduced, i.e., the transmit power of the BS as well as the user equipment (UE) can also be reduced through coherent combining and an increased antenna aperture. In cooperating the full-duplex (FD) capability into the large-scale antenna cellular system exploits the entire spectral resources that are limited to the half-duplex (HD) systems. However, the performance of these systems is restricted due to the hardware distortions and self-interference (SI).

4.2 Related Works

In [97–99], the resource allocation is addressed for an FD multi-carrier (MC) system while considering the single antenna transceivers. In recent years, some studies were done in the context of FD massive multiple input multiple output (mMIMO) cellular networks [87, 100–102]. In [101], for an FD multi-cell multi-user mMIMO system, an SI aware fractional power control mechanism is proposed where the user nodes adjust their transmit power based on the distance-dependent path-loss, SI, and maximum available transmit power. In [87], for a multi-user multiple input multiple output (MIMO) system with an FD mMIMO BS and multiple FD users equipped with two antennas, the authors derived the asymptotic expressions of signal to interference plus noise ratio (SINR) of uplink and downlink by adopting MRC/MRT at the BS when the number of antennas of the BS tends to infinity. It is also shown through the theoretical derivation that

the detrimental impact of the loop interference, multi-user interference and inter-user interference can be eliminated by the very large number of antennas at the BS utilizing the power scaling scheme. However, in [87, 101], the impact of hardware distortions are not considered for the single carrier multi-user mMIMO FD BS system.

4.3 Chapter Outline

In this chapter, we investigate an MC bidirectional communication between an FD mMIMO transceiver BS and multiple FD user nodes equipped with a single antenna. In Section 4.4, we model the operation of a bidirectional MC communication system by taking into account the impact of imperfect channel state information (CSI) as well as the impact of hardware distortions. In Section 4.5.1, we frame an optimization problem to maximize the system sum-rate, which falls into the class of smooth difference-of-convex (DC) optimization problems. We propose a successive inner approximation (SIA) iterative optimization solution, which converges to the point that satisfies Karush–Kuhn–Tucker (KKT) conditions. We also extend it to an energy efficiency maximization problem in Section 4.5.2 and solve it using SIA and Dinkelbach algorithm [81]. In Section 4.6, we evaluate the performance of our proposed algorithms for both the energy efficiency and sum-rate maximization problem using numerical simulations. In Section 4.7, we summarize our main results.

4.4 System Model

We consider an MC bidirectional communication setup, where an FD mMIMO BS serves L FD single antenna user nodes. The number of transmit and receive antennas at the BS node is represented as N_{BS} and M_{BS}, respectively. Fig 4.1 illustrates the bidirectional communication between the mMIMO FD BS and L FD single antenna user nodes. We denote the index set of all user nodes and sub-carriers by $\mathbb{L}$ and $\mathbb{K}$, respectively. Let us define a set of nodes including the BS as $\widetilde{\mathbb{L}} = \{\mathbb{L} \cup 0\}$, where 0 is the index of the BS. Furthermore, $\mathbf{h}_{0i}^{k} \in \mathbb{C}^{M_{\mathrm{BS}} \times 1}$ and $\mathbf{h}_{i0}^{k} \in \mathbb{C}^{1 \times N_{\mathrm{BS}}}$ represent the k-th sub-carrier uplink and downlink channel, respectively. $h_{ii} \in \mathbb{C}^{1}$ is the SI of the user node $i \in \mathbb{L}$. The SI channel of the BS is denoted by $\mathbf{H}_{00}^{k} \in \mathbb{C}^{M_{\mathrm{BS}} \times N_{\mathrm{BS}}}$. $h_{ij}^{k} \in \mathbb{C}^{1}$ represents the co-channel interference channel from the j-th node to i-th user node when $i \neq j$.

In this chapter, we assume all the channels are constant for each frame, frequency-flat in each sub-carrier, and only the imperfect CSI is known. Similarly, as in the previous chapter, we adapt the channel error model used in [85], where the actual channel can

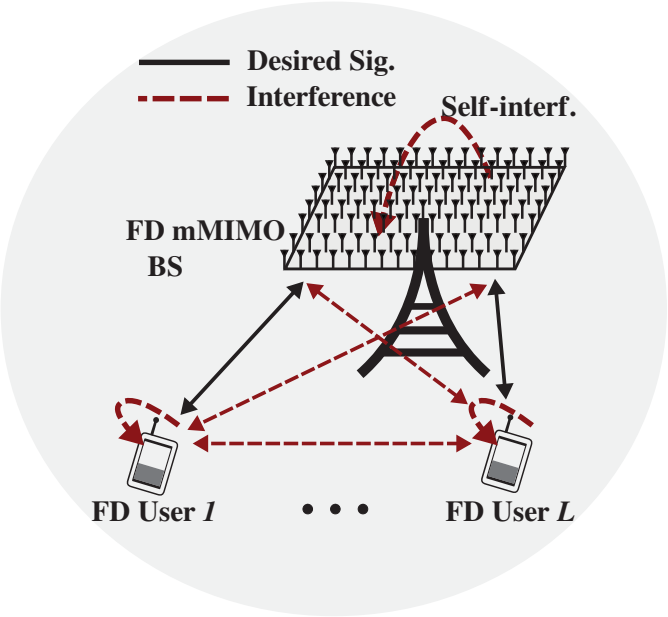

Figure 4.1: Basic system Model for Bidirectional communication between FD mMIMO BS and single antenna FD users

be decomposed into the estimated channel plus estimation error, can be stated as

$$\begin{aligned}
\mathbf{h}_{i0}^{k} &= \widehat{\mathbf{h}}_{i0}^{k} + \widetilde{\mathbf{h}}_{i0}^{k}, \;\; \widehat{\mathbf{h}}_{i0}^{k} \perp \widetilde{\mathbf{h}}_{i0}^{k}, \\
\mathbf{h}_{0i}^{k} &= \widehat{\mathbf{h}}_{0i}^{k} + \widetilde{\mathbf{h}}_{0i}^{k}, \;\; \widehat{\mathbf{h}}_{i0}^{k} \perp \widetilde{\mathbf{h}}_{i0}^{k}, \\
h_{ij}^{k} &= \widehat{h}_{ij}^{k} + \widetilde{h}_{ij}^{k}, \;\; \widehat{h}_{ij}^{k} \perp \widetilde{h}_{ij}^{k}, \\
\mathbf{H}_{00}^{k} &= \widehat{\mathbf{H}}_{00}^{k} + \widetilde{\mathbf{H}}_{00}^{k}, \;\; \widehat{\mathbf{H}}_{00}^{k} \perp \widetilde{\mathbf{H}}_{00}^{k}, \;\; \forall i, j \in \mathbb{L}, \forall k \in \mathbb{K},
\end{aligned} \tag{4.1}$$

where $\widehat{\mathbf{h}}_{i0}^{k}, \widehat{\mathbf{h}}_{0i}^{k}, \widehat{h}_{ij}^{k}$ and $\widehat{\mathbf{H}}_{00}^{k}$ represent the estimated channels. The entries of channel estimation error $\widetilde{\mathbf{h}}_{i0}^{k}, \widetilde{\mathbf{h}}_{0i}^{k}, \widetilde{h}_{ij}^{k}$ and $\widetilde{\mathbf{H}}_{00}^{k}$ are independent and identically distributed (i.i.d.) complex Gaussian with zero mean and variance $(\sigma_{e,i0}^{k})^2, (\sigma_{e,0i}^{k})^2, (\sigma_{e,ij}^{k})^2$ and $(\sigma_{e,00}^{k})^2$, respectively. We assume that the estimated channel and the estimation error become statistically uncorrelated. We consider the receiver performs the minimum mean square error (MMSE) channel estimation strategy.

The source symbol to BS from the i-th user node using the k-th sub-carrier can be represented as $s_{i,k}^{\mathrm{UL}} \in \mathbb{C}^1$. $s_{i,k}^{\mathrm{DL}} \in \mathbb{C}^1$ denotes the source symbol from the BS to the i-th user node. We assume the symbols are i.i.d. with unit power, i.e. $\mathbb{E}\{s_{i,k}^{\mathrm{UL}}(s_{i,k}^{\mathrm{UL}})^*\} = 1$

and $\mathbb{E}\{s_{i,k}^{\mathrm{DL}}(s_{i,k}^{\mathrm{DL}})^*\} = 1$. Let $\mathbf{v}_i^k$ and $\mathbf{u}_i^k$ represent the normalized transmit precoders and receive decoders (linear filters) at the BS for the i-th user node utilizing sub-carrier k, respectively. The transmit power of i-th user node for sub-carrier k is denoted by $p_{i,k}^{\mathrm{UL}}$, where $i \in \mathbb{L}$. The transmit power dedicated to the i-th user node and sub-carrier k for downlink at the BS is $p_{i,k}^{\mathrm{DL}}$. The transmit signal of the i-th user node and the BS at sub-carrier k can be written as

$$\begin{aligned} x_i^k &= \underbrace{\sqrt{p_{i,k}^{\mathrm{UL}}}s_{i,k}^{\mathrm{UL}}}_{:=\widetilde{x}_i^k} + e_{\mathrm{t},i}^k, \quad i \in \mathbb{L}, \forall k \in \mathbb{K}, \\ \mathbf{x}_0^k &= \underbrace{\sum_{i\in\mathbb{L}} \mathbf{v}_i^k \sqrt{p_{i,k}^{\mathrm{DL}}}s_{i,k}^{\mathrm{DL}}}_{:\widetilde{\mathbf{x}}_0^k} + \mathbf{e}_{\mathrm{t},0}^k, \quad \forall k \in \mathbb{K}, \end{aligned} \tag{4.2}$$

where $e_{\mathrm{t},i}^k$ ($\widetilde{x}_i^k$) and $\mathbf{e}_{\mathrm{t},0}^k$ ($\widetilde{\mathbf{x}}_0^k$) are the transmit distortion (intended transmit signal) at the i-th user node and the BS, respectively.

Correspondingly, the received signal at the i-th user node and the BS for sub-carrier k can be obtained as

$$\begin{aligned} y_i^k &= \underbrace{\mathbf{h}_{i0}^k\mathbf{x}_0^k + \sum_{j\in\mathbb{L}} h_{ij}^k x_j^k + n_i^k}_{:=\widetilde{y}_i^k} + e_{\mathrm{r},i}^k, \quad i \in \mathbb{L}, \forall k \in \mathbb{K}, \\ \mathbf{y}_0^k &= \underbrace{\sum_{i\in\mathbb{L}} \mathbf{h}_{0i}^k x_i^k + \mathbf{H}_{00}^k\mathbf{x}_0^k + \mathbf{n}_0^k}_{:=\widetilde{\mathbf{y}}_0^k} + \mathbf{e}_{\mathrm{r},0}^k, \quad \forall k \in \mathbb{K}, \end{aligned} \tag{4.3}$$

where the receiver noise at the i-th user node and the BS are represented using $n_i^k \sim \mathcal{CN}\left(0, (\sigma_{n_i}^k)^2\right)$ and $\mathbf{n}_0^k \sim \mathcal{CN}\left(\mathbf{0}_{M_{\mathrm{BS}}}, (\sigma_{n_0}^k)^2\mathbf{I}_{M_{\mathrm{BS}}}\right)$. The receive distortion (intended received signal) at the i-th user node and BS are denoted by $e_{\mathrm{r},i}^k$ ($\widetilde{y}_i^k$) and $\mathbf{e}_{\mathrm{r},0}^k$ ($\widetilde{\mathbf{y}}_0^k$), respectively. The self-interference cancellation (SIC) is applied to the received signal, i.e., only the known part of the transmit signal can be mitigated. The received signal after SIC can be expressed as

$$\begin{aligned} \overline{y}_i^k &= y_i^k - \widehat{h}_{ii}^k\sqrt{p_{i,k}^{\mathrm{UL}}}s_{i,k}^{\mathrm{UL}}, \quad i \in \mathbb{L}, \forall k \in \mathbb{K}, \\ \overline{\mathbf{y}}_0^k &= \mathbf{y}_0^k - \sum_{i\in\mathbb{L}} \widehat{\mathbf{H}}_{00}^k\mathbf{v}_i^k\sqrt{p_{i,k}^{\mathrm{DL}}}s_{i,k}^{\mathrm{DL}}, \quad \forall k \in \mathbb{K}. \end{aligned} \tag{4.4}$$

Similarly as in the previous chapter, the inaccuracies of hardware components such as analog to digital converter (ADC) and digital to analog converter (DAC) error, noises caused by power amplifiers, automatic gain control (AGC) and oscillator on transmit and receive chain are considered. The distortion terms are proportional to the intensity of the intended signals. Following the Lemma 2.4.1, the statistics of the distortion terms can be formulated as

$$\mathbf{e}_{\mathrm{t},i}^k \sim \mathcal{CN}\left(0, \frac{\widetilde{\kappa}_i}{K}\sum_{k\in\mathbb{K}}\left(\mathbb{E}\{\widetilde{x}_i^k(\widetilde{x}_i^k)^H\}\right)\right), \tag{4.5}$$

$$\mathbf{e}_{\mathrm{t},0}^{k} \sim \mathcal{CN}\left(\mathbf{0}_{N_{\mathrm{BS}}}, \frac{1}{K}\widetilde{\mathbf{\Theta}}_{\mathrm{t},0}\sum_{k\in\mathbb{K}}\mathrm{diag}\left(\mathbb{E}\{\tilde{\mathbf{x}}_{0}^{k}(\tilde{\mathbf{x}}_{0}^{k})^{H}\}\right)\right), \tag{4.6}$$

$$\mathbf{e}_{\mathrm{r},i}^{k} \sim \mathcal{CN}\left(0, \frac{\widetilde{\beta}_{i}}{K}\sum_{k\in\mathbb{K}}\left(\mathbb{E}\{\widetilde{y}_{i}^{k}(\widetilde{y}_{i}^{k})^{H}\}\right)\right), \tag{4.7}$$

$$\mathbf{e}_{\mathrm{r},0}^{k} \sim \mathcal{CN}\left(\mathbf{0}_{M_{\mathrm{BS}}}, \frac{1}{K}\widetilde{\mathbf{\Theta}}_{\mathrm{r},0}\sum_{k\in\mathbb{K}}\mathrm{diag}\left(\mathbb{E}\{\widetilde{\mathbf{y}}_{0}^{k}(\widetilde{\mathbf{y}}_{0}^{k})^{H}\}\right)\right), \tag{4.8}$$

where the transmit and receive distortion coefficient of the i-th user node are given by $\widetilde{\kappa}_i$ and $\widetilde{\beta}_i$, respectively. The diagonal matrix $\widetilde{\mathbf{\Theta}}_{\mathrm{t},0}$ ($\widetilde{\mathbf{\Theta}}_{\mathrm{r},0}$) consists of transmit (receive) distortion coefficients for the corresponding chains at the BS. For the detailed definition of the used distortion model, please refer to Section 2.4.4. The equations (4.5), (4.6), (4.7), and (4.8) explicitly indicate the impact of the inter-carrier leakage (ICL), i.e., the distortion signal variance at each sub-carrier is related to the total distortion-free signal power over all the sub-carriers at the corresponding chain.

Let us define $\kappa_i = \frac{\widetilde{\kappa}_i}{K}$, $\beta_i = \frac{\widetilde{\beta}_i}{K}$, $\mathbf{\Theta}_{\mathrm{t},0} = \frac{1}{K}\widetilde{\mathbf{\Theta}}_{\mathrm{t},0}$, and $\mathbf{\Theta}_{\mathrm{r},0} = \frac{1}{K}\widetilde{\mathbf{\Theta}}_{\mathrm{r},0}$ for further calculations. By employing Lemma 2.4.1, and equations (4.5), (4.6), (4.7), and (4.8) on (4.4), the covariance of the received collective interference-plus-noise signal at the i-th user node for sub-carrier k can be calculated as

$$\begin{aligned}
\Sigma_{i}^{k} \approx\ & \underbrace{\sum_{\substack{j\in\mathbb{L}\\ j\neq i}}\widehat{h}_{ij}^{k}p_{j,k}^{\mathrm{UL}}(\widehat{h}_{ij}^{k})^{*} + \sum_{j\in\mathbb{L}}(\sigma_{e,ij}^{k})^{2}p_{j,k}^{\mathrm{UL}} + \sum_{\substack{j\in\mathbb{L}\\ j\neq i}}\widehat{\mathbf{h}}_{i0}^{k}\mathbf{v}_{j}^{k}p_{j,k}^{\mathrm{DL}}(\mathbf{v}_{j}^{k})^{H}(\widehat{\mathbf{h}}_{i0}^{k})^{H} + \sum_{j\in\mathbb{L}}(\sigma_{e,i0}^{k})^{2}p_{j,k}^{\mathrm{DL}}}_{\text{Co-channel interference}} \\
& + \underbrace{\sum_{j\in\mathbb{L}}\kappa_{j}\sum_{m\in\mathbb{K}}\widehat{h}_{ij}^{k}p_{j,m}^{\mathrm{UL}}(\widehat{h}_{ij}^{k})^{*} + \sum_{j\in\mathbb{L}}(\sigma_{e,ij}^{k})^{2}\kappa_{j}\sum_{m\in\mathbb{K}}p_{j,m}^{\mathrm{UL}}}_{\text{User transmit distortion}} + \underbrace{(\sigma_{n_i}^{k})^{2}}_{\text{Thermal noise}} \\
& + \underbrace{\sum_{j\in\mathbb{L}}\widehat{\mathbf{h}}_{i0}^{k}\mathbf{\Theta}_{\mathrm{t},0}\mathrm{diag}\left(\sum_{m\in\mathbb{K}}\mathbf{v}_{j}^{m}p_{j,m}^{\mathrm{DL}}(\mathbf{v}_{j}^{m})^{H}\right)(\widehat{\mathbf{h}}_{i0}^{k})^{H} + \sum_{j\in\mathbb{L}}(\sigma_{e,i0}^{k})^{2}\mathrm{Tr}\left(\mathbf{\Theta}_{\mathrm{t},0}\mathrm{diag}\left(\sum_{m\in\mathbb{K}}\mathbf{v}_{j}^{m}p_{j,m}^{\mathrm{DL}}(\mathbf{v}_{j}^{m})^{H}\right)\right)}_{\text{BS transmit distortion}} \\
& + \underbrace{\beta_{i}\sum_{m\in\mathbb{K}}\left(\sum_{j\in\mathbb{L}}\left(\widehat{h}_{ij}^{m}p_{j,m}^{\mathrm{UL}}(\widehat{h}_{ij}^{m})^{H} + (\sigma_{e,ij}^{m})^{2}p_{j,m}^{\mathrm{UL}} + \widehat{\mathbf{h}}_{i0}^{m}\mathbf{v}_{j}^{m}p_{j,m}^{\mathrm{DL}}(\mathbf{v}_{j}^{m})^{H}(\widehat{\mathbf{h}}_{i0}^{m})^{H} + (\sigma_{e,i0}^{m})^{2}p_{j,m}^{\mathrm{DL}}\right) + (\sigma_{n_i}^{m})^{2}\right)}_{\text{User receive distortion}}.
\end{aligned} \tag{4.9}$$

Here, we ignore the higher-order terms of the transmit and receive distortion since the transmit and receive distortion coefficients lie within the range of 0 and 1 and mostly have minimal values. Similarly, the covariance of the received collective interference-

plus-noise signal at the BS for user node i and sub-carrier k can be expressed as

$$\begin{aligned}\mathbf{\Sigma}_{0,i}^{k} \approx & \underbrace{\sum_{\substack{j\in\mathbb{L}\\ j\neq i}}(\widehat{\mathbf{h}}_{0j}^{k}p_{j,k}^{\mathrm{UL}}(\widehat{\mathbf{h}}_{0j}^{k})^{H}) + \sum_{j\in\mathbb{L}}(\sigma_{e,0j}^{k})^{2}p_{j,k}^{\mathrm{UL}}\mathbf{I}_{M_{\mathrm{BS}}}}_{\text{Co-channel interference}} \\ & + \underbrace{\sum_{j\in\mathbb{L}}\kappa_{j}\sum_{m\in\mathbb{K}}\widehat{\mathbf{h}}_{0j}^{k}p_{j,m}^{\mathrm{UL}}(\widehat{\mathbf{h}}_{0j}^{k})^{H} + \sum_{j\in\mathbb{L}}\kappa_{j}\sum_{m\in\mathbb{K}}(\sigma_{e,0j}^{k})^{2}p_{j,m}^{\mathrm{UL}}\mathbf{I}_{M_{\mathrm{BS}}}}_{\text{User transmit distortion}} + \underbrace{\sum_{j\in\mathbb{L}}(\sigma_{e,00}^{k})^{2}p_{j,k}^{\mathrm{DL}}\mathbf{I}_{M_{\mathrm{BS}}}}_{\text{SI channel estimation error}} \\ & + \underbrace{\sum_{j\in\mathbb{L}}\widehat{\mathbf{H}}_{00}^{k}\mathbf{\Theta}_{\mathrm{t},0}\mathrm{diag}\left(\sum_{m\in\mathbb{K}}\mathbf{v}_{j}^{m}p_{j,m}^{\mathrm{DL}}(\mathbf{v}_{j}^{m})^{H}\right)(\widehat{\mathbf{H}}_{00}^{k})^{H}}_{\text{BS transmit distortion}} \\ & + \underbrace{\sum_{j\in\mathbb{L}}(\sigma_{e,00}^{k})^{2}\mathrm{Tr}\left(\mathbf{\Theta}_{\mathrm{t},0}\mathrm{diag}\left(\sum_{m\in\mathbb{K}}\mathbf{v}_{j}^{m}p_{j,m}^{\mathrm{DL}}(\mathbf{v}_{j}^{m})^{H}\right)\right)\mathbf{I}_{M_{\mathrm{BS}}}}_{\text{BS transmit distortion}} \\ & + \underbrace{\mathbf{\Theta}_{\mathrm{r},0}\sum_{j\in\mathbb{L}}\mathrm{diag}\left(\sum_{m\in\mathbb{K}}\widehat{\mathbf{h}}_{0j}^{m}p_{j,m}^{\mathrm{UL}}(\widehat{\mathbf{h}}_{0j}^{m})^{H}\right) + \mathbf{\Theta}_{\mathrm{r},0}\sum_{j\in\mathbb{L}}\sum_{m\in\mathbb{K}}\left((\sigma_{e,00}^{m})^{2}p_{j,m}^{\mathrm{DL}} + (\sigma_{e,0j}^{m})^{2}p_{j,m}^{\mathrm{UL}}\right)}_{\text{BS receive distortion}} \\ & + \underbrace{\mathbf{\Theta}_{\mathrm{r},0}\sum_{j\in\mathbb{L}}\mathrm{diag}\left(\sum_{m\in\mathbb{K}}\widehat{\mathbf{H}}_{00}^{m}\mathbf{v}_{j}^{m}p_{j,m}^{\mathrm{DL}}(\mathbf{v}_{j}^{m})^{H}(\widehat{\mathbf{H}}_{00}^{m})^{H}\right) + \mathbf{\Theta}_{\mathrm{r},0}\sum_{m\in\mathbb{K}}(\sigma_{n_0}^{m})^{2}}_{\text{BS receive distortion}} + \underbrace{(\sigma_{n_0}^{k})^{2}\mathbf{I}_{M_{\mathrm{BS}}}}_{\text{Thermal noise}}.\end{aligned} \tag{4.10}$$

4.4.1 Achievable Information Rate

The achievable information rate for the uplink of the i-th user node using sub-carrier k can be expressed as

$$R_{i,k}^{\mathrm{UL}} = \gamma_{0}\log_{2}\left(1 + \frac{\mu_{i,k}p_{i,k}^{\mathrm{UL}}}{\alpha_{n_0}^{i,k} + \sum\limits_{m\in\mathbb{K}}\sum\limits_{j\in\mathbb{L}}(\tilde{\gamma}_{ij}^{km}p_{j,m}^{\mathrm{UL}} + \hat{\gamma}_{ij}^{km}p_{j,m}^{\mathrm{DL}})}\right) \tag{4.11}$$

where

$$\mu_{i,k} = |(\mathbf{u}_{i}^{k})^{H}\widehat{\mathbf{h}}_{0i}^{k}|^{2}, \tag{4.12}$$

$$\begin{aligned}\tilde{\gamma}_{ij}^{km} = & \delta_{km}(1-\delta_{ij})(\mathbf{u}_{i}^{k})^{H}(\widehat{\mathbf{h}}_{0j}^{m}(\widehat{\mathbf{h}}_{0j}^{m})^{H})(\mathbf{u}_{i}^{k}) + \delta_{km}(\mathbf{u}_{i}^{k})^{H}(\sigma_{e,0j}^{m})^{2}(\mathbf{u}_{i}^{k}) \\ & + (\mathbf{u}_{i}^{k})^{H}\kappa_{j}\widehat{\mathbf{h}}_{0j}^{k}(\widehat{\mathbf{h}}_{0j}^{k})^{H}(\mathbf{u}_{i}^{k}) + (\mathbf{u}_{i}^{k})^{H}\kappa_{j}(\sigma_{e,0j}^{k})^{2}(\mathbf{u}_{i}^{k}) \\ & + (\mathbf{u}_{i}^{k})^{H}\mathbf{\Theta}_{\mathrm{r},0}\mathrm{diag}(\widehat{\mathbf{h}}_{0j}^{m}(\widehat{\mathbf{h}}_{0j}^{m})^{H})(\mathbf{u}_{i}^{k}) + (\mathbf{u}_{i}^{k})^{H}\mathbf{\Theta}_{\mathrm{r},0}(\sigma_{e,0j}^{m})^{2}(\mathbf{u}_{i}^{k}),\end{aligned} \tag{4.13}$$

$$\begin{aligned}\hat{\gamma}_{ij}^{km} = & \delta_{km}(\mathbf{u}_{i}^{k})^{H}(\sigma_{e,00}^{k})^{2}(\mathbf{u}_{i}^{k}) + (\mathbf{u}_{i}^{k})^{H}\widehat{\mathbf{H}}_{00}^{k}\mathbf{\Theta}_{\mathrm{t},0}\mathrm{diag}\Big(\mathbf{v}_{j}^{m}(\mathbf{v}_{j}^{m})^{H}\Big)(\widehat{\mathbf{H}}_{00}^{k})^{H}\mathbf{u}_{i}^{k} \\ & + (\mathbf{u}_{i}^{k})^{H}(\sigma_{e,00}^{k})^{2}\mathrm{Tr}\Big(\mathbf{\Theta}_{\mathrm{t},0}\mathrm{diag}\Big(\mathbf{v}_{j}^{m}(\mathbf{v}_{j}^{m})^{H}\Big)\Big)(\mathbf{u}_{i}^{k}) + (\mathbf{u}_{i}^{k})^{H}\mathbf{\Theta}_{\mathrm{r},0}(\sigma_{e,00}^{m})^{2}(\mathbf{u}_{i}^{k}) \\ & + (\mathbf{u}_{i}^{k})^{H}\mathbf{\Theta}_{\mathrm{r},0}\mathrm{diag}\Big(\widehat{\mathbf{H}}_{00}^{m}\mathbf{v}_{j}^{m}(\mathbf{v}_{j}^{m})^{H}(\widehat{\mathbf{H}}_{00}^{m})^{H}\Big)(\mathbf{u}_{i}^{k}),\end{aligned} \tag{4.14}$$

$$\alpha_{n_0}^{i,k} = \Big(\mathbf{u}_i^k\Big)^H \Big((\sigma_{n_0}^k)^2 \mathbf{I}_{M_{\mathrm{BS}}} + \mathbf{\Theta}_{\mathrm{r},0} \sum_{m\in\mathbb{K}} (\sigma_{n_0}^m)^2\Big)(\mathbf{u}_i^k) \tag{4.15}$$

and $\delta_{km} = 1$ when $k = m$ and otherwise $\delta_{km} = 0$. The portion of the frame duration dedicated to data communication is indicated by $0 < \gamma_0 < 1$.

Similarly, the achievable information rate for the downlink of the i-th user node using sub-carrier k can be expressed as

$$R_{i,k}^{\mathrm{DL}} = \gamma_0 \log_2\left(1 + \frac{\overline{\mu}_{i,k} p_{i,k}^{\mathrm{DL}}}{\alpha_{n_i}^k + \sum\limits_{m\in\mathbb{K}}\sum\limits_{j\in\mathbb{L}} \Big(\overline{\gamma}_{ij}^{km} p_{j,m}^{\mathrm{UL}} + \acute{\gamma}_{ij}^{km} p_{j,m}^{\mathrm{DL}}\Big)}\right) \tag{4.16}$$

where

$$\overline{\mu}_{i,k} = |\widehat{\mathbf{h}}_{i0}^k \mathbf{v}_i^k|^2, \tag{4.17}$$

$$\begin{aligned}\overline{\gamma}_{ij}^{km} =& \delta_{km}\Big((1-\delta_{ij})(\widehat{h}_{ij}^m(\widehat{h}_{ij}^m)^*) + (\sigma_{e,ij}^m)^2\Big) + \kappa_j \widehat{h}_{ij}^k (\widehat{h}_{ij}^k)^* + \kappa_j (\sigma_{e,ij}^k)^2 \\ &+ \beta_i(\widehat{h}_{ij}^m(\widehat{h}_{ij}^m)^H) + \beta_i(\sigma_{e,ij}^m)^2,\end{aligned} \tag{4.18}$$

$$\begin{aligned}\acute{\gamma}_{ij}^{km} =& \delta_{km}(1-\delta_{ij})\widehat{\mathbf{h}}_{i0}^m \mathbf{v}_j^m (\mathbf{v}_j^m)^H (\widehat{\mathbf{h}}_{i0}^m)^H + \delta_{km}(\sigma_{e,i0}^m)^2 + \widehat{\mathbf{h}}_{i0}^k \mathbf{\Theta}_{\mathrm{t},0} \mathrm{diag}\Big(\mathbf{v}_j^m(\mathbf{v}_j^m)^H\Big)(\widehat{\mathbf{h}}_{i0}^k)^H \\ &+ (\sigma_{e,i0}^k)^2 \mathrm{Tr}\Big(\mathbf{\Theta}_{\mathrm{t},0}\mathrm{diag}\Big(\mathbf{v}_j^m(\mathbf{v}_j^m)^H\Big)\Big) + \beta_i(\widehat{\mathbf{h}}_{i0}^m \mathbf{v}_j^m (\mathbf{v}_j^m)^H (\widehat{\mathbf{h}}_{i0}^m)^H) + \beta_i(\sigma_{e,i0}^m)^2\end{aligned} \tag{4.19}$$

and

$$\alpha_{n_i}^k = (\sigma_{n_i}^k)^2 + \beta_i \sum_{m\in\mathbb{K}} (\sigma_{n_i}^m)^2. \tag{4.20}$$

For the selection of transmit precoders and receive decoders at the large antenna array BS, well-studied linear precoder-decoder strategies such as MRT/MRC, zero-forcing (ZF), MMSE can be considered. With some assumptions that are common in mMIMO studies, the computational complexity to obtain the achievable rates can be reduced [38]. We can also use a similar approach as in Chapter 3 for asymptotic rate analysis in large antenna regime.

Now, the total achievable information rate for the i-th user node and sub-carrier k can be written as

$$R_{i,k} = R_{i,k}^{\mathrm{UL}} + R_{i,k}^{\mathrm{DL}}. \tag{4.21}$$

4.5 Optimization

In this section, we formulate the joint sub-carrier and power allocation optimization problem in terms of sum-rate and energy efficiency maximization for a bidirectional FD mMIMO communication system. Here also, similar to Chapter 3, we incorporate the sub-carrier allocation into the power allocation problem such that if the power allocated to a particular sub-carrier associated with a user for uplink/downlink is zero, then the user node is not transmitting/receiving in that sub-carrier.

4.5.1 Weighted Sum-rate Maximization

The sum-rate maximization problem for an FD MC bidirectional communication can be formulated as

$$\begin{aligned} \underset{p_{i,k}^{\mathrm{UL}}\geq 0, p_{i,k}^{\mathrm{DL}}\geq 0}{\text{maximize}} \quad & \sum_{i\in\mathbb{L}} w_i \sum_{k\in\mathbb{K}} R_{i,k} \\ \text{subject to} \quad & \sum_{k\in\mathbb{K}} p_{i,k}^{\mathrm{UL}} \leq p_i, i \in \mathbb{L} \\ & \sum_{i\in\mathbb{L}}\sum_{k\in\mathbb{K}} p_{i,k}^{\mathrm{DL}} \leq p_0, \end{aligned} \tag{4.22}$$

where p_i and p_0 are the available transmit power at the user node i and the BS. The weight corresponding to the user i is denoted by w_i. We propose an iterative algorithm that utilizes the SIA framework [90] employing quadratic approximations, which reaches a converging point that satisfies the KKT optimality conditions.

Quadratic approximations

In this chapter, we use a quadratic approximation of the logarithmic function, to approximate the rate function as a tight lower bound quadratic function [103]. Let us define $q_u^{i,k} = \sqrt{p_{i,k}^{\mathrm{UL}}}$ and $q_d^{i,k} = \sqrt{p_{i,k}^{\mathrm{DL}}}$. We observe the equivalent expression for the uplink rate function [1] $R_{i,k}^{\mathrm{UL}}$ [103] as

$$\frac{-\gamma_0}{\ln(2)} \ln\left(1 - \frac{\mu_{i,k}x^2}{\underbrace{\alpha_{n_0}^{i,k} + \mu_{i,k}(q_u^{i,k})^2 + \sum_{m\in\mathbb{K}}\sum_{j\in\mathbb{L}} \left(\tilde{\gamma}_{ij}^{km}(q_u^{i,m})^2 + \hat{\gamma}_{ij}^{km}(q_d^{j,m})^2\right)}_{:=y}}\right) \tag{4.23}$$

where $x := q_u^{i,k}$. Without any loss of generality, the constant $\frac{\gamma_0}{\ln(2)}$ is eliminated for following joint-convexity calculations. In order to observe the joint-convexity of the rate function with respect to x, y, we first calculate the corresponding Hessian as

$$\underbrace{\frac{2\mu_{i,k}x}{(y-\mu_{i,k}x^2)^2}}_{:=\psi_0} \begin{bmatrix} \frac{y}{x}\left(1+\frac{\mu_{i,k}x^2}{y}\right) & -1 \\ -1 & \frac{x}{y}\left(1-\frac{\mu_{i,k}x^2}{2y}\right) \end{bmatrix}, \tag{4.24}$$

where $\psi_0 > 0$. Given $x \geq 0$, $y > 0$ and $y > \mu_{i,k}x^2$, we obtain $\frac{x}{y}\left(1-\frac{\mu_{i,k}x^2}{2y}\right) \geq 0$. The positive semi-definite nature of the above Hessian is obtained by employing Schur

[1] Similar for downlink rate function $R_{i,k}^{\mathrm{DL}}$.

complement condition for positive semi-definiteness as

$$\frac{y}{x}\left(1+\frac{\mu_{i,k}x^2}{y}\right)-\left(\frac{x}{y}\left(1-\frac{\mu_{i,k}x^2}{2y}\right)\right)^{-1}\overset{(a)}{>}\frac{y}{x}\left(1+\frac{\mu_{i,k}x^2}{y}-\left(1-\frac{\mu_{i,k}x^2}{y+\mu_{i,k}x^2}\right)^{-1}\right)=0, \tag{4.25}$$

where (a) is obtained as $2y > y + \mu_{i,k}x^2$. Please note that the joint-convexity of the equivalent rate function over x, y provides a tight global lower bound, via the first-order Taylor's approximation [91]. This consequently results in the tight quadratic approximations over the variables $q_u^{i,k}$ and $q_d^{i,k}$ as given in the following.

Let $R_{i,k}^{\mathrm{UL}}(\mathbb{q}_u, \mathbb{q}_d)$ represent the achievable rate for the uplink as a function of $\mathbb{q}_u$ and $\mathbb{q}_d$, where $\mathbb{q}_{\mathcal{X}} := \{q_{\mathcal{X}}^{i,k}, \forall i, k\}$ with $\mathcal{X} = \{u, d\}$. Let us select $q_{u,0}^{i,k}$ and $q_{d,0}^{i,k}$ as the square root of feasible transmit power values at the i-th user node and the BS, respectively [2]. The lower bound on the rate function $R_{i,k}^{\mathrm{UL}}$ by applying quadratic approximation can be obtained as

$$\begin{aligned}R_{i,k}^{\mathrm{UL}}(\mathbb{q}_u, \mathbb{q}_d) \geq \overline{R}_{i,k}^{\mathrm{UL}}(\mathbb{q}_u, \mathbb{q}_d, \mathbb{q}_{u,0}, \mathbb{q}_{d,0}) := R_{i,k}^{\mathrm{UL}}(\mathbb{q}_{u,0}, \mathbb{q}_{d,0}) + b_{i,k}^{\mathrm{UL}}(\mathbb{q}_{u,0}, \mathbb{q}_{d,0})\Big(q_u^{i,k} - q_{u,0}^{i,k}\Big)\\ +\sum_{m\in\mathbb{K}}\sum_{j\in\mathbb{L}} C_{i,j,k,m}^{\mathrm{UL,UL}}(\mathbb{q}_{u,0}, \mathbb{q}_{d,0})\Big((q_u^{j,m})^2 - (q_{u,0}^{j,m})^2\Big)+\sum_{m\in\mathbb{K}}\sum_{j\in\mathbb{L}} C_{i,j,k,m}^{\mathrm{UL,DL}}(\mathbb{q}_{u,0}, \mathbb{q}_{d,0})\Big((q_d^{j,m})^2 - (q_{d,0}^{j,m})^2\Big)\end{aligned} \tag{4.26}$$

where

$$b_{i,k}^{\mathrm{UL}}(\mathbb{q}_{u,0}, \mathbb{q}_{d,0}) = \frac{2\gamma_0\mu_{i,k}q_{u,0}^{i,k}}{\ln(2)\left(\alpha_{n_0}^{i,k} + \sum\limits_{m\in\mathbb{K}}\sum\limits_{j\in\mathbb{L}}\left(\widetilde{\gamma}_{ij}^{km}(q_{u,0}^{j,m})^2 + \widehat{\gamma}_{ij}^{km}(q_{d,0}^{j,m})^2\right)\right)}, \tag{4.27}$$

$$C_{i,j,k,m}^{\mathrm{UL,UL}}(\mathbb{q}_{u,0}, \mathbb{q}_{d,0}) = \frac{-\gamma_0(2^{R_{i,k}^{\mathrm{UL}}(\mathbb{q}_{u,0}, \mathbb{q}_{d,0})} - 1)(\widetilde{\gamma}_{ij}^{km} + \delta_{km}\delta_{ij}\mu_{i,k})}{\ln(2)\left(\alpha_{n_0}^{i,k} + \mu_{i,k}(q_{u,0}^{i,k})^2 + \sum\limits_{m\in\mathbb{K}}\sum\limits_{j\in\mathbb{L}}\left(\widetilde{\gamma}_{ij}^{km}(q_{u,0}^{j,m})^2 + \widehat{\gamma}_{ij}^{km}(q_{d,0}^{j,m})^2\right)\right)}, \tag{4.28}$$

and

$$C_{i,j,k,m}^{\mathrm{UL,DL}}(\mathbb{q}_{u,0}, \mathbb{q}_{d,0}) = \frac{-\gamma_0(2^{R_{i,k}^{\mathrm{UL}}(\mathbb{q}_{u,0}, \mathbb{q}_{d,0})} - 1)(\widehat{\gamma}_{ij}^{km})}{\ln(2)\left(\alpha_{n_0}^{i,k} + \mu_{i,k}(q_{u,0}^{i,k})^2 + \sum\limits_{m\in\mathbb{K}}\sum\limits_{j\in\mathbb{L}}\left(\widetilde{\gamma}_{ij}^{km}(q_{u,0}^{j,m})^2 + \widehat{\gamma}_{ij}^{km}(q_{d,0}^{j,m})^2\right)\right)} \tag{4.29}$$

Here, $\overline{R}_{i,k}^{\mathrm{UL}}$ is a tight concave quadratic approximation of the rate function $R_{i,k}^{\mathrm{UL}}$ at the point $(\mathbb{q}_{u,0}, \mathbb{q}_{d,0})$, such that $R_{i,k}^{\mathrm{UL}}(\mathbb{q}_{u,0}, \mathbb{q}_{d,0}) = \overline{R}_{i,k}^{\mathrm{UL}}(\mathbb{q}_{u,0}, \mathbb{q}_{d,0}, \mathbb{q}_{u,0}, \mathbb{q}_{d,0})$. Similarly, let $R_{i,k}^{\mathrm{DL}}(\mathbb{q}_u, \mathbb{q}_d)$ denote the achievable rate for the downlink as a function of $\mathbb{q}_u$ and $\mathbb{q}_d$. The

[2] $\mathbb{q}_{\mathcal{X},0} := \{q_{\mathcal{X},0}^{i,k}, \forall i, k\}$ with $\mathcal{X} = \{u, d\}$

lower bound of $R_{i,k}^{\mathrm{DL}}$ by applying quadratic approximation can be obtained as

$$R_{i,k}^{\mathrm{DL}}(\mathbb{q}_u,\mathbb{q}_d) \geq \overline{R}_{i,k}^{\mathrm{DL}}(\mathbb{q}_u,\mathbb{q}_d,\mathbb{q}_{u,0},\mathbb{q}_{d,0}) := R_{i,k}^{\mathrm{DL}}(\mathbb{q}_{u,0},\mathbb{q}_{d,0}) + b_{i,k}^{\mathrm{DL}}(\mathbb{q}_{u,0},\mathbb{q}_{d,0})\Big(q_d^{i,k} - q_{d,0}^{i,k}\Big) + \sum_{m\in\mathbb{K}}\sum_{j\in\mathbb{L}} C_{i,j,k,m}^{\mathrm{DL,UL}}(\mathbb{q}_{u,0},\mathbb{q}_{d,0})\Big((q_u^{j,m})^2 - (q_{u,0}^{j,m})^2\Big) + \sum_{m\in\mathbb{K}}\sum_{j\in\mathbb{L}} C_{i,j,k,m}^{\mathrm{DL,DL}}(\mathbb{q}_{u,0},\mathbb{q}_{d,0})\Big((q_d^{j,m})^2 - (q_{d,0}^{j,m})^2\Big), \tag{4.30}$$

$$b_{i,k}^{\mathrm{DL}}(\mathbb{q}_{u,0},\mathbb{q}_{d,0}) = \frac{2\gamma_0\overline{\mu}_{i,k}q_{d,0}^{i,k}}{\ln(2)\left(\alpha_{n_i}^k + \sum\limits_{m\in\mathbb{K}}\sum\limits_{j\in\mathbb{L}}\left(\overline{\gamma}_{ij}^{km}(q_{u,0}^{j,m})^2 + \acute{\gamma}_{ij}^{km}(q_{d,0}^{j,m})^2\right)\right)}, \tag{4.31}$$

$$C_{i,j,k,m}^{\mathrm{DL,UL}}(\mathbb{q}_{u,0},\mathbb{q}_{d,0}) = \frac{-\gamma_0(2^{R_{i,k}^{\mathrm{DL}}(\mathbb{q}_{u,0},\mathbb{q}_{d,0})}-1)(\overline{\gamma}_{ij}^{km})}{\ln(2)\left(\alpha_{n_i}^k + \overline{\mu}_{i,k}(q_{d,0}^{i,k})^2 + \sum\limits_{m\in\mathbb{K}}\sum\limits_{j\in\mathbb{L}}\left(\overline{\gamma}_{ij}^{km}(q_{u,0}^{j,m})^2 + \acute{\gamma}_{ij}^{km}(q_{d,0}^{j,m})^2\right)\right)}, \tag{4.32}$$

$$C_{i,j,k,m}^{\mathrm{DL,DL}}(\mathbb{q}_{u,0},\mathbb{q}_{d,0}) = \frac{-\gamma_0(2^{R_{i,k}^{\mathrm{DL}}(\mathbb{q}_{u,0},\mathbb{q}_{d,0})}-1)(\acute{\gamma}_{ij}^{km} + \delta_{km}\delta_{ij}\overline{\mu}_{i,k})}{\ln(2)\left(\alpha_{n_i}^k + \overline{\mu}_{i,k}(q_{d,0}^{i,k})^2 + \sum\limits_{m\in\mathbb{K}}\sum\limits_{j\in\mathbb{L}}\left(\overline{\gamma}_{ij}^{km}(q_{u,0}^{j,m})^2 + \acute{\gamma}_{ij}^{km}(q_{d,0}^{j,m})^2\right)\right)}, \tag{4.33}$$

where $\overline{R}_{i,k}^{\mathrm{DL}}$ is a tight concave quadratic approximation of the rate function $R_{i,k}^{\mathrm{DL}}$ at the point $(\mathbb{q}_{u,0},\mathbb{q}_{d,0})$, such that $R_{i,k}^{\mathrm{DL}}(\mathbb{q}_{u,0},\mathbb{q}_{d,0}) = \overline{R}_{i,k}^{\mathrm{DL}}(\mathbb{q}_{u,0},\mathbb{q}_{d,0},\mathbb{q}_{u,0},\mathbb{q}_{d,0})$.

Using this approximation, we can write $\overline{R}_{i,k} = \overline{R}_{i,k}^{\mathrm{UL}} + \overline{R}_{i,k}^{\mathrm{DL}}$, which is a jointly concave function over $q_u^{i,k}$ and $q_d^{i,k}$. We propose an iterative algorithm, where for each iterative update, we now solve the approximate convex quadratic problem,

$$\begin{aligned} \underset{q_u^{i,k}\geq 0, q_d^{i,k}\geq 0,}{\text{maximize}} \quad & \sum_{i\in\mathbb{L}} w_i \sum_{k\in\mathbb{K}} \overline{R}_{i,k} \\ \text{subject to} \quad & \sum_{k\in\mathbb{K}} (q_u^{i,k})^2 \leq p_i, i\in\mathbb{L} \\ & \sum_{i\in\mathbb{L}}\sum_{k\in\mathbb{K}} (q_d^{i,k})^2 \leq p_0, \end{aligned} \tag{4.34}$$

to optimality. The iterative update is continued until a stable point is reached. Since we use a first-order Taylor approximation on the equivalent rate functions, we can conclude that $\overline{R}_{i,k}$ represents a global and tight lower bound to $R_{i,k}$, with a shared slope at the point of approximation [91]. We can deduce that the solution converges to a point that satisfies KKT conditions as the proposed iterative update fulfils the requirements set in [90, Theorem 1]. Algorithm 8 defines the detailed algorithm procedure.

4.5.2 Energy Efficiency Maximization

Due to the rapid expansion of wireless networks, ecological concerns and economical benefits makes energy efficiency an important metric for designing a future wireless

Algorithm 8 For sum-rate maximization

1: $a \leftarrow 0$ (set iteration number to zero)
2: $q_{u,0}^{i,k}, q_{d,0}^{i,k} \leftarrow$ feasible point initialization
3: **repeat**
4: $\quad a \leftarrow a + 1$
5: $\quad q_u^{i,k}, q_d^{i,k} \leftarrow$ solve (4.34)
6: $\quad q_{u,0}^{i,k}, q_{d,0}^{i,k} \leftarrow q_{u,0}^{i,k} = q_u^{i,k}$ and $q_{d,0}^{i,k} = q_d^{i,k}$, respectively
7: **until** a stable point, or maximum number of a reached
8: **return** $\{q_u^{i,k}, q_d^{i,k}\}$

system. In this section, the energy efficiency is defined as the ratio of the system sum-rate to the total power consumption of all the user nodes and the BS. The total power consumption P_{tot} can be expressed as

$$P_{\text{tot}} = \sum_{i \in \widetilde{\mathbb{L}}} P_i, \tag{4.35}$$

where $P_i := \frac{1}{\mu_i} \sum_{k \in \mathbb{K}} \mathbb{E}\{\|\boldsymbol{x}_i^k\|^2\} + P_{i_{\text{zero}}} + P_{i_{\text{FD}}}$. μ_i are the efficiency of the power amplifier at the i-th user node and the BS when $i = 0$. $P_{i_{\text{zero}}}$ is the power dissipated by other circuit blocks at the transmitter chain of each node. $P_{i_{\text{FD}}}$ is the power required for SIC. By using the above definition, the energy efficiency maximization problem can be expressed as

$$\begin{aligned} \underset{p_{i,k}^{\text{UL}} \geq 0, p_{i,k}^{\text{DL}} \geq 0}{\text{maximize}} \quad & \sum_{i \in \mathbb{L}} w_i \sum_{k \in \mathbb{K}} \frac{R_{i,k}}{P_{\text{tot}}} \\ \text{subject to} \quad & P_i \leq P_{i,\max}, i \in \widetilde{\mathbb{L}}, \end{aligned} \tag{4.36}$$

where $P_{i,\max}$ is the total available power for consumption at the user node i and the BS (when $i = 0$). To solve the above fractional non-convex problem, we propose a double-loop iterative algorithm (Algorithm 9) that utilizes SIA and Dinkelbach algorithm. We consider a similar approach for approximation of rate functions as in sum-rate maximization. Let us first select $q_{u,0}^{i,k}$ and $q_{d,0}^{i,k}$ as the square root of feasible transmit power value at the i-th user node and the BS, respectively. In the first or the outer loop, we calculate the rate approximations using (4.26) and (4.30) for the point of approximation $q_{u,0}^{i,k}$ and $q_{d,0}^{i,k}$. We fix these values for the inner loop. In the inner loop, we use Dinkelbach algorithm [81], using which we can rewrite the optimization problem as

$$\begin{aligned} \underset{q_u^{i,k} \geq 0, q_d^{i,k} \geq 0,}{\text{maximize}} \quad & \sum_{i \in \mathbb{L}} w_i \sum_{k \in \mathbb{K}} \overline{R}_{i,k} - \lambda P_{\text{tot}} \\ \text{subject to} \quad & P_i \leq P_{i,\max}, i \in \widetilde{\mathbb{L}}. \end{aligned} \tag{4.37}$$

In the inner loop, we iteratively solve for $q_u^{i,k}$ and $q_d^{i,k}$, and λ with fixed $q_{u,0}^{i,k}$ and $q_{d,0}^{i,k}$. The λ can be determined from

$$\sum_{i \in \mathbb{L}} w_i \sum_{k \in \mathbb{K}} \overline{R}_{i,k} - \lambda P_{\text{tot}} = 0. \tag{4.38}$$

Here, we can conclude that a global optimal can be achieved as Dinkelbach algorithm is applied to the concave-affine fractional problem [92, Section 3.2]. Then in the outer loop, we update $q_{u,0}^{i,k}$ and $q_{d,0}^{i,k}$ in order to calculate the new rate approximations and solve the optimization problem until a stable point is reached. Algorithm 9 defines the detailed algorithm procedure.

Algorithm 9 For energy efficiency maximization

$q_{u,0}^{i,k}, q_{d,0}^{i,k} \leftarrow$ feasible point initialization
$a \leftarrow 0$ (set iteration number to zero for outer loop)
$\lambda = 0 \leftarrow$ Lambda initialization
repeat
  $a \leftarrow a + 1$
  repeat
    $q_u^{i,k}, q_d^{i,k} \leftarrow$ solve (4.37)
    $\lambda \leftarrow$ solve (4.38)
  until a stable point is reached
  $q_{u,0}^{i,k} \leftarrow q_u^{i,k}$ and $q_{d,0}^{i,k} \leftarrow q_d^{i,k}$
until a stable point, or maximum number of a reached
return $\{q_u^{i,k}, q_d^{i,k}\}$

4.6 Numerical Evaluations

In the numerical simulations, we evaluate the performance of the proposed algorithms introduced in Section 4.5 for a bidirectional communication setup between an FD MC mMIMO BS and multiple MC single antenna FD nodes employing orthogonal frequency division multiplexing (OFDM). We consider a cell for radius 400m with an FD mMIMO BS at the center. We adopt simulation system parameters from [93, 94], and are chosen as in Table 4.1. We consider our path loss model as a simplified path loss model in [95]. We assume the BS utilizes its antennas for both transmission and reception (shared antenna), i.e., $N_{\mathrm{BS}} = M_{\mathrm{BS}} = N$. The weight corresponding to the i-th user is chosen as $w_i = 1, \forall i \in \mathbb{L}$. To provide fairness in resource allocation, the transmit power budget is restricted to support the number of active sub-carriers ($\overline{\overline{\mathbb{K}}}$), i.e., the transmit power budgets are factorized by k_t, where $k_t = \overline{\overline{\mathbb{K}}}/\overline{\overline{\mathbb{K}}}_{\mathrm{sys}}$. $\overline{\overline{\mathbb{K}}}_{\mathrm{sys}}$ denotes the total number of sub-carriers available in the system. For energy efficiency maximization problem, $p_{i_{\mathrm{zero}}} + p_{i_{FD}} = 10\mathrm{dBm}$ and $p_{0_{\mathrm{zero}}} + p_{0_{FD}} = 14\mathrm{dBm}$ are the power dissipated by circuit components other than power amplifier and SIC at the i-th user node and BS, respectively. All communication channels follow an uncorrelated Rayleigh flat fading model. The SI channel follows the Rician distribution as characterization reported in [20] with Rician coefficient K_{r} and the SI channel strength after SIC ρ_{si}. We assume the covariance for the SI channel to be low rank as in [5], and is chosen as 5. The overall system performance is then averaged over 100 channel realizations.

Carrier center frequency and system bandwidth	2.5 GHz and 5MHz
Number of sub-carriers ($\overline{\overline{\mathbb{K}}}_{\text{sys}}$), and sub-carrier bandwidth	64 and 78kHz
Number of active sub-carriers ($\overline{\overline{\mathbb{K}}}$)	10
Number of users ($\overline{\mathbb{L}}$)	3
Reference distance	15m
Path loss exponent	3.6
Noise power at user i and BS (σ_n^2)	-125dBm and -125dBm
Efficiency of power amplifier (μ_i)	0.39
Max. tx. power at the user and BS	22dBm and 37dBm
Number of antennas at the BS ($N_{\text{BS}} = M_{\text{BS}} = N$)	32
Hardware distortion coefficient $\kappa = \beta$	-90dB
Covariance of the CSI estimation error $(\sigma_{e,i0}^k)^2 = (\sigma_{e,0i}^k)^2 = (\sigma_{e,ij}^k)^2 = (\sigma_{e,00}^k)^2 \forall k \in \mathbb{K}$,	-150dB
SI channel strength ρ_{si} and Rician coeffient K_{r}	-50 dB and 10

Table 4.1: Default System parameters used for numerical simulations

Benchmarks

For comparison using numerical simulations, we consider different transmit/receive strategies at the BS for different system designs. The benchmarks considered for the numerical simulations are as follows.

- MRT/MRC: It represents the proposed Algorithms 8 and 9 employing MRT/MRC as BS transmit/receive strategy for the sum-rate maximization and energy efficiency maximization, respectively.
- ZF: The proposed Algorithms 8 and 9 employ ZF as BS transmit/receive strategy for the sum-rate maximization and energy efficiency maximization, respectively.
- SI-ZF: In addition to transmit strategies such as considering MRT/MRC or ZF strategy, spatial suppression scheme (null-space projection [5]) is also employed at the transmit side of the BS. This allows to eliminate the receive distortion caused by the SI channel, as the transmit beams are projected to the null-space of the SI channel.
- OPT: It refers to the algorithms which jointly take into account the impact of hardware distortions as well as the impact of CSI error.
- ND (non-distortion): The impact of hardware distortions is not considered in the design. It only considers the impact of imperfect CSI.
- HD: It indicates the scenarios when both users and BS operate in HD mode, where the uplink and downlink transmission take place in two consecutive time slots, similar to, e.g., [104].

Visualization

Figs. 4.2a to 4.2e illustrate that the performance of the proposed Algorithm 8 is evaluated in terms of sum-rate for different system parameters. In Fig. 4.2a, we can observe that the overall system performance degrades as the hardware inaccuracies increases. For small values of κ, all the algorithms considering FD outperforms its HD counterpart. As the hardware inaccuracies increases, the HD algorithms outperform the non-distortion (ND) algorithms for both the transmit strategies (MRT/MRC and ZF). For higher values of κ, the HD algorithms outperform all the other FD algorithms. This implies that the impact of hardware distortion is more significant in an FD system than in an HD system, as these non-linear distortions lead to higher residual SI and ICL (due to strong SI). Furthermore in Fig. 4.2b, the system performance is evaluated with respect to the transmit power of BS. As expected, the performance of the system increases as the transmit power at the BS increases. The algorithm that utilizes ZF and null space projection scheme outperforms all the other benchmarks. In the case of the system with MRT/MRC, the algorithm MRT/MRC-SI-ZF shows a better performance compared to the other algorithms. It is interesting to observe that, for high transmit power values, the performance of the ND algorithms degrade compared to the OPT algorithms. Furthermore, the impact of receiver noise and CSI estimation error in the system performance is depicted in Figs. 4.2c and 4.2d, respectively. As expected, the performance of the system degrades as the receiver noise/channel estimation error increases. However, it is interesting to observe that for small values of both the receiver noise and channel estimation error the OPT algorithms show a significant gain compared to corresponding ND algorithm. It can be observed that at high transmit power, low receive and low channel estimation error scenarios, the impact of hardware distortion leading to residual SI and ICL becomes dominant. Moreover, Fig. 4.2e shows the performance gain of the algorithms as the number of antennas at BS increases. We consider as the number of antennas at BS increases, the rank of the SI channel covariance also increases (BS antenna receives more reflection as the number of antennas at the BS increases). The rank of the SI channel covariance is chosen as $N/8$. It can be noticed that the sum-rate attained by the system increases as the number of antennas increases. Another interesting observation is that more gain in performance of the OPT algorithms is achieved when compared to the ND algorithms, as more number of antennas at the BS introduces more hardware distortions to the system.

In Figs. 4.3a to 4.3d, the performance of the algorithms (OPT) for different system parameters is evaluated in terms of energy efficiency. For energy efficiency evaluations, the number of active sub-carriers ($\overline{\overline{\mathbb{K}}}$) and hardware distortion coefficient $\kappa = \beta$ are chosen as 5 and -80dB, respectively. The proposed algorithms show similar behaviour as in the case of sum-rate maximization. The algorithm ZF-SI-ZF that employs ZF along with spatial suppression scheme outperforms all the other benchmarks. In Fig. 4.3a, the energy efficiency of the system degrades as the hardware inaccuracies increases, even for HD design. Moreover, as the hardware inaccuracies increases, the HD algorithm performs better compared to the ND algorithm indicating that consideration of hardware

distortion provides an additional gain in performance of FD systems. Furthermore, in Fig. 4.3b the performance of the system in terms of energy efficiency is depicted with respect to the transmit power of BS, respectively. In general, as a transmit power of the BS increases, the energy efficiency of the system also increases. However, as transmit power values at the BS increases, the performance of the ND algorithms degrade compared to the corresponding OPT algorithms due to the hardware distortions. It is also observed that is that the energy efficiency of the system saturates for high transmit power budget. This is because the optimum energy-efficient design does not consume more power if it degrades the energy efficiency of the system, i.e., only a small improvement in sum-rate is achieved by consuming more power. Moreover, Figs. 4.3c and 4.3d show that the energy efficiency of the system degrades when the receiver noise and CSI estimation error in the system increase, respectively. When the receiver noise and channel estimation error are small, OPT algorithms perform better compared to ND as the hardware distortion of the system becomes dominant. The numerical performance evaluation of the system signifies the importance of consideration of hardware distortion in designing an mMIMO FD MC system for both the sum-rate and energy efficiency maximization problem, especially in high SINR scenarios.

4.7 Conclusions

In this chapter, we addressed the resource allocation problem for an MC bidirectional communication setup between an FD mMIMO BS and multiple FD user nodes with a single antenna. We take into account the impact of hardware distortions and imperfect CSI for modelling the system. We formulated joint power and sub-carrier allocation problems to maximize the sum-rate and energy efficiency of the system. An iterative optimization approach, which follows the SIA framework is proposed for the sum-rate maximization problem, which converges to the point that satisfies the KKT conditions. A double-loop algorithm, which utilizes the SIA framework and Dinkelbach algorithm, is proposed for the energy efficiency maximization problem. Numerical results show that the proposed distortion-aware design attains a significant gain, especially when the transceiver accuracy degrades and ICL becomes dominant. It is also observed that utilizing null space projection scheme together with linear transmit strategy at the transmit side of the BS to spatial suppression the SI provides an additional performance gain. Also for higher hardware inaccuracy, HD system outperforms the FD system indicating the importance of considering hardware inaccuracies in designing FD bidirectional communication systems.

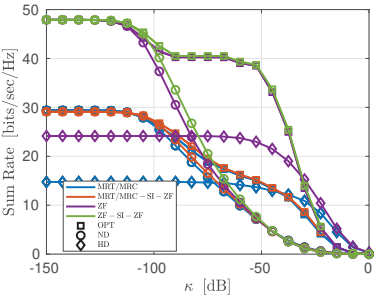

(a) Sum-rate vs. Hardware inaccuracy

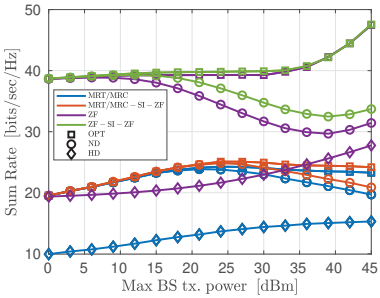

(b) Sum-rate vs. Max BS transmit power

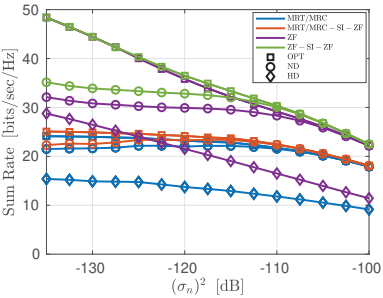

(c) Sum-rate vs. Receiver noise

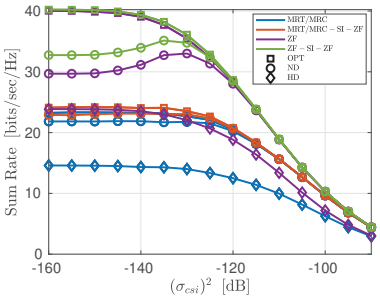

(d) Sum-rate vs. Channel estimation error

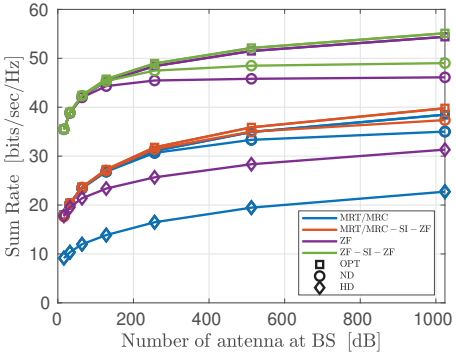

(e) Sum-rate vs. Number of antennas at the BS

Figure 4.2: Sum-rate vs. Different system parameters.

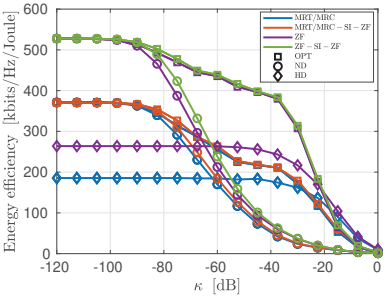

(a) Energy efficiency vs. Hardware inaccuracy

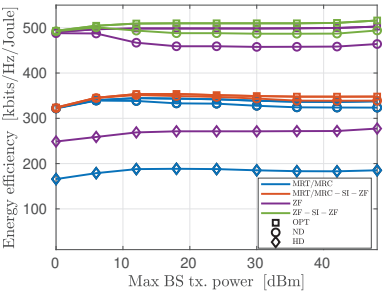

(b) Energy efficiency vs. Max BS transmit power

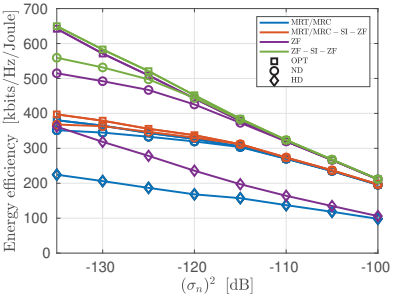

(c) Energy Efficiency vs. Receiver noise

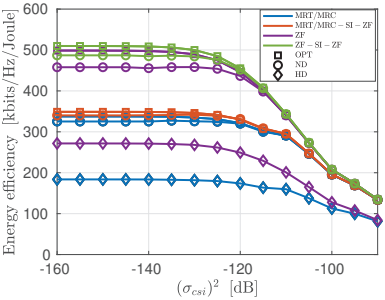

(d) Energy Efficiency vs. Channel estimation error

Figure 4.3: Energy Efficiency for different system parameters, with the number of active sub-carriers ($\overline{\overline{\mathbb{K}}}$) = 5 and hardware distortion coefficient $\kappa = \beta = -80$dB.

5 Full-Duplex Relaying: Enabling Dual Connectivity via Impairments-aware Successive Interference Cancellation

5.1 Scope

Dual connectivity (DuC) is proposed by 3rd Generation Partnership Project (3GPP) in the long time evolution (LTE) Release 12 specification as a promising technological approach to achieve higher per-user throughput, mobility robustness, and load balancing [105]. It allows a user terminal to simultaneously transmit and receive data from two cell groups via a Master evolved Node B (MeNB) and a Secondary evolved Node B (SeNB), which operate on different carrier frequencies and are interconnected by traditional backhaul links.

In upcoming fifth-generation (5G) networks, the mixed numerology orthogonal frequency division multiplexing (OFDM) has opted as the multiple access technique [11, 12]. However, various non-orthogonal multiple access (NOMA) schemes have been proposed to improve the performance of the system in terms of spectral efficiency as well as to support a massive number of dramatically different classes of users and applications. In contrast to conventional orthogonal multiplexing schemes, where multiple users are served in orthogonal frequency or time domains, NOMA schemes serve more than one user in the same frequency-time resource block by multiplexing users in other domains such as the power domain or code domain. Power domain NOMA as well as rate-splitting (RS) is implemented using the successive interference cancellation (SuIC) approach at the receiver. In a two-level SuIC approach, during the first phase, the received signal is processed by acknowledging the strong signal as the desired signal while treating the rest of the received signal as noise. During the second phase, the receiver processes the received signal after removing the known part of the signal, the strong signal, which in turn reduces the total interference.

In this chapter, we are incorporating both the DuC and the SuIC schemes to enable dual connectivity between the base station (BS) and user terminals in the same carrier frequency with the aid of full-duplex (FD) relaying. The FD relaying has the capability

to simultaneously transmit and receive in the same frequency. However, it suffers from self-interference (SI) and interference through the direct source-destination channel. While the coexistence of the direct link regarded as interference on the desired relay link, it can be also be utilized as a concurrent path of information transfer, where the receiver is enabled with SuIC.

5.2 Related Works

DuC for LTE networks has been investigated in [105–107]. Furthermore, [108] provides a brief overview of DuC technology considering the integration between fourth-generation (4G) and 5G cellular networks. The authors also present open issues and challenges such as user-cell association, the interaction between BSs, and resource allocation in such scenarios. A utility-based resource allocation algorithm is also proposed. The resource allocation problem for FD massive multiple input multiple output (mMIMO) communication systems have been studied in [38, 84, 101, 102, 109]. In [38, 84], the resource allocation is addressed for an FD mMIMO relay with consideration of hardware distortion as well as imperfect CSI in case of the single carrier system. For the above works on FD mMIMO relay systems, the direct link is not considered. By utilizing the direct link, spectral efficiency can be enhanced by implementing the SuIC technique at the receiver. NOMA and RS approach with SuIC techniques are used in different scenarios to improve the overall system performance [110–115]. In [110], the authors propose a resource and power allocation technique for a downlink cellular system which employs the power-domain NOMA scheme using SuIC. The use of RS employing SuIC at the receiver in an mMIMO system has been investigated in [113] with imperfect CSI, and to mitigate hardware impairments in [114].

5.3 Chapter Outline

In this chapter, we first investigate a relay-assisted downlink communication between an mMIMO multi-carrier (MC) BS and a half-duplex (HD) single antenna user node, where the BS simultaneously communicates to the user through the direct link as well as the relay link. We consider that the relay employs joint-carrier (JC) coding strategy, please refer Section 2.5.1. Initially, we consider a single-user scenario where the relay is a single antenna FD node, and the single antenna user node uses SuIC techniques to process the received signal. In Section 5.4, we model the operation of an MC decode and forward (DF) relay communication system and formulate the impact of imperfect channel state information (CSI) as well as the impact of hardware distortions. In Section 5.5, we devise an optimization problem for joint sub-carrier and power allocation to maximize the system sum-rate, which belongs to the class of smooth difference-of-convex (DC) optimization problems. In Section 5.6, We extend the single-user scenario

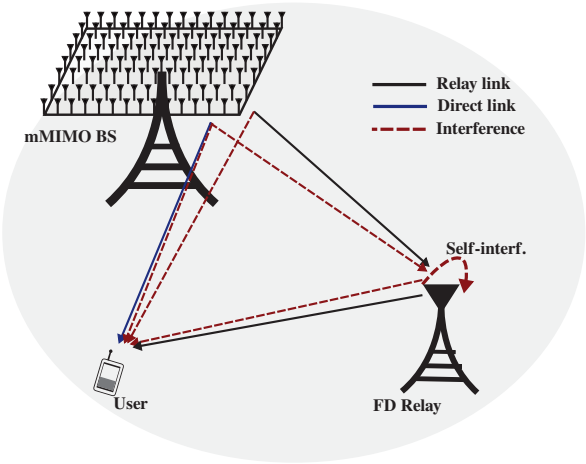

Figure 5.1: System model of FD relaying-enabled DuC system for single-user scenario

to the multi-user scenario where an FD mMIMO relay assists the DuC mode. The case of utilizing HD relay for DuC is also investigated. In Section 5.7, using numerical simulations, we evaluate the performance of our proposed algorithms. Our main results are summarized in Section 5.8 .

5.4 System Model

We consider a relay-assisted MC downlink communication between an mMIMO BS and an HD single antenna user node. The BS uses the DuC (similar to NOMA/RS) approach to communicate with the user directly and also using a single antenna FD DF relay. In other words, two messages, both transmitted from the BS and destined to the same user are precoded separately and simultaneously transmitted; one through the direct link (DL) and one through the relay link (RL). At the user node, the received signal is processed in two phases using the SuIC technique. In the first phase, the received signal from the BS is considered as noise while considering the strong received signal from the relay as the desired signal. In the second phase, as the received signal from the relay becomes known, this part can be removed from the received signal, which reduces the total interference. Fig.5.1 illustrates the system model for the single-user scenario. Since we consider the relay to be FD, it can receive and transmit the signal simultaneously with a small processing delay. In this chapter, we assume the processing delay to be negligible.

Let N_{BS} be the number of transmit antennas at the BS node. We denote the index set of all sub-carriers by $\mathbb{K}$, where $\overline{\overline{\mathbb{K}}} = K$. Furthermore, $\mathbf{h}_{\mathrm{sr}}^k$ and $\mathbf{h}_{\mathrm{sd}}^k \in \mathbb{C}^{1\times N_{\mathrm{BS}}}$ represent the k-th sub-carrier channel from the BS to the relay and the user, respectively. The relay-destination channel and SI channel at the relay are respectively denoted by h_{rd}^k and h_{rr}^k.

In this chapter, we assume all the channels are constant for each frame, frequency-flat in each sub-carrier, and only the imperfect CSI is known. Similar to the previous chapters, we consider a channel error model [85], where the actual channel can be decomposed into the estimated channel and estimation error. The channel error model can be expressed as

$$\mathbf{h}_{\mathcal{X}}^k = \widehat{\mathbf{h}}_{\mathcal{X}}^k + \widetilde{\mathbf{h}}_{\mathcal{X}}^k, \;\; \widehat{\mathbf{h}}_{\mathcal{X}}^k \perp \widetilde{\mathbf{h}}_{\mathcal{X}}^k, \;\; \forall \mathcal{X} \in \{\mathrm{sr}, \mathrm{rd}, \mathrm{sd}, \mathrm{rr}\}, \forall k \in \mathbb{K}, \tag{5.1}$$

where $\widehat{\mathbf{h}}_{\mathcal{X}}^k$ and $\widetilde{\mathbf{h}}_{\mathcal{X}}^k$ represent the estimated channel and channel estimation error for the k-th sub-carrier. The entries of channel estimation error $\widetilde{\mathbf{h}}_{\mathcal{X}}^k$ are independent and identically distributed (i.i.d.) complex Gaussian with zero mean and variance $(\sigma_{e,\mathcal{X}}^k)^2$. We assume that the estimated channel and the estimation error are statistically independent. We consider that the relay and the user utilize minimum mean square error (MMSE) channel estimation strategy.

The source symbol from the BS to the user using the k-th sub-carrier through DL and through RL can be represented as $s_{\mathrm{sd}}^k \in \mathbb{C}^1$ and $s_{\mathrm{sr}}^k \in \mathbb{C}^1$. We assume the symbols are i.i.d. with unit power, i.e., $\mathbb{E}\{s_{\mathrm{sd}}^k (s_{\mathrm{sd}}^k)^*\} = 1$ and $\mathbb{E}\{s_{\mathrm{sr}}^k (s_{\mathrm{sr}}^k)^*\} = 1$. The transmit power (normalized transmit precoders) at the BS dedicated to the RL and the DL using the k-th sub-carrier are denoted by p_{sr}^k ($\mathbf{v}_{\mathrm{sr}}^k$) and p_{sd}^k ($\mathbf{v}_{\mathrm{sd}}^k$), respectively.

The transmit signal from the BS can be written as

$$\mathbf{x}_s^k = \underbrace{\mathbf{v}_{\mathrm{sr}}^k \sqrt{p_{\mathrm{sr}}^k} s_{\mathrm{sr}}^k + \mathbf{v}_{\mathrm{sd}}^k \sqrt{p_{\mathrm{sd}}^k} s_{\mathrm{sd}}^k}_{:=\widetilde{\mathbf{x}}_s^k} + \mathbf{e}_{\mathrm{t,s}}^k, \;\; \forall k \in \mathbb{K}, \tag{5.2}$$

where $\mathbf{e}_{\mathrm{t,s}}^k$ and $\widetilde{\mathbf{x}}_s^k$ are the transmit distortion and the intended (distortion-free) transmit signal at the BS, respectively.

Correspondingly, the transmit and receive signal at the relay node can be expressed as

$$\begin{aligned} x_{\mathrm{r}}^k &= \underbrace{\sqrt{p_{\mathrm{rd}}^k} \widehat{s}_{\mathrm{rd}}^k}_{:=\widetilde{x}_{\mathrm{r}}^k} + e_{\mathrm{t,r}}^k, \;\; \forall k \in \mathbb{K}, \\ y_{\mathrm{r}}^k &= \underbrace{\mathbf{h}_{\mathrm{sr}}^k \mathbf{x}_s^k + h_{\mathrm{rr}}^k x_{\mathrm{r}}^k + n_{\mathrm{r}}^k}_{:=\widetilde{y}_{\mathrm{r}}^k} + e_{\mathrm{r,r}}^k, \;\; \forall k \in \mathbb{K}, \end{aligned} \tag{5.3}$$

where $n_{\mathrm{r}}^k \sim \mathcal{CN}\left(0, (\sigma_{\mathrm{n,r}}^k)^2\right)$, $e_{\mathrm{t,r}}^k$ and $e_{\mathrm{r,r}}^k$ are the receiver noise, transmit distortion and receive distortion at the relay node, respectively. The intended transmit and receive signal at the relay are represented using $\widetilde{x}_{\mathrm{r}}^k$ and $\widetilde{y}_{\mathrm{r}}^k$, respectively. The symbol $\widehat{s}_{\mathrm{rd}}^k$ represents the decoded symbol at the relay, which is then retransmitted to the user. The transmit

power at the relay using the k-th sub-carrier is denoted by p_{rd}^k. The signal, which is obtained after applying self-interference cancellation (SIC) to the received signal, can be expressed as

$$\overline{y}_{\mathrm{r}}^k = y_{\mathrm{r}}^k - \widehat{h}_{\mathrm{rr}}^k \sqrt{p_{\mathrm{rd}}^k}\, \widehat{s}_{\mathrm{rd}}^k, \quad \forall k \in \mathbb{K}. \tag{5.4}$$

Here, the known part of the transmitted signal (corresponding to estimated part of SI channel) can be eliminated.

Furthermore, the received signal at the user can be obtained as

$$y_{\mathrm{d}}^k = \underbrace{\mathbf{h}_{\mathrm{sd}}^k \mathbf{x}_s^k + h_{\mathrm{rd}}^k x_{\mathrm{r}}^k + n_{\mathrm{d}}^k}_{:=\widetilde{y}_{\mathrm{d}}^k} + e_{\mathrm{r,d}}^k, \quad \forall k \in \mathbb{K}, \tag{5.5}$$

where $n_{\mathrm{d}}^k \sim \mathcal{CN}\left(0, (\sigma_{\mathrm{n,d}}^k)^2\right)$, $e_{\mathrm{r,d}}^k$ and $\widetilde{y}_{\mathrm{d}}^k$ are the receiver noise, receive distortion and the intended received signal at the user, respectively.

Distortion Signal Statistics

Following the Lemma 2.4.1, the statistics of the distortion terms can be obtained as

$$\mathbf{e}_{\mathrm{t,s}}^k \sim \mathcal{CN}\left(\mathbf{0}_{N_{\mathrm{BS}}}, \frac{1}{K}\widetilde{\mathbf{\Theta}}_{\mathrm{t,s}} \sum_{k\in\mathbb{K}} \mathrm{diag}\left(\mathbb{E}\{\widetilde{\mathbf{x}}_{\mathrm{s}}^k (\widetilde{\mathbf{x}}_{\mathrm{s}}^k)^H\}\right)\right), \tag{5.6}$$

$$e_{\mathrm{t,r}}^k \sim \mathcal{CN}\left(0, \frac{\widetilde{\kappa}_{\mathrm{r}}}{K} \sum_{k\in\mathbb{K}} \left(\mathbb{E}\{\widetilde{x}_{\mathrm{r}}^k (\widetilde{x}_{\mathrm{r}}^k)^H\}\right)\right), \tag{5.7}$$

$$e_{\mathrm{r,r}}^k \sim \mathcal{CN}\left(0, \frac{\widetilde{\beta}_{\mathrm{r}}}{K} \sum_{k\in\mathbb{K}} \left(\mathbb{E}\{\widetilde{y}_{\mathrm{r}}^k (\widetilde{y}_{\mathrm{r}}^k)^H\}\right)\right), \tag{5.8}$$

$$e_{\mathrm{r,d}}^k \sim \mathcal{CN}\left(0, \frac{\widetilde{\beta}_{\mathrm{d}}}{K} \sum_{k\in\mathbb{K}} \left(\mathbb{E}\{\widetilde{y}_{\mathrm{d}}^k (\widetilde{y}_{\mathrm{d}}^k)^H\}\right)\right), \tag{5.9}$$

where $\widetilde{\kappa}_{\mathrm{r}}$ and $\widetilde{\beta}_{\mathrm{r}}$ represent the transmit and receive distortion coefficients of the relay. The receive distortion coefficient at the user is given by $\widetilde{\beta}_{\mathrm{d}}$. The diagonal matrices $\widetilde{\mathbf{\Theta}}_{\mathrm{t,s}}$ consist of transmit distortion coefficients for the corresponding chains at the BS. Let us define $\kappa_{\mathrm{r}} = \frac{\widetilde{\kappa}_{\mathrm{r}}}{K}$, $\beta_{\mathrm{r}} = \frac{\widetilde{\beta}_{\mathrm{r}}}{K}$, $\beta_{\mathrm{d}} = \frac{\widetilde{\beta}_{\mathrm{d}}}{K}$, and $\mathbf{\Theta}_{\mathrm{t,s}} = \frac{1}{K}\widetilde{\mathbf{\Theta}}_{\mathrm{t,s}}$ for further calculations. Please refer to Section 2.4.4 for the detailed description of the used distortion model. The above equations (5.6), (5.7), (5.8), and (5.9) explicitly indicate the impact of the inter-carrier leakage (ICL), i.e., the distortion signal variance at each sub-carrier is associated to the total distortion-free transmit/receive power at the corresponding chain. In other words, even if one of the sub-carriers is employed with a high-power transmission, the hardware distortions will introduce a higher residual self-interference in all of the sub-carrier channels.

Collective Interference plus Noise Signal Covariance

In this section, we calculate the covariance of the collective interference-plus-noise signal at the user and the relay. By employing Lemma 2.4.1, and equations (5.6), (5.7), (5.8), and (5.9) on (5.4), the covariance of the received collective interference-plus-noise signal at the relay can be formulated as

$$\begin{aligned}
\Sigma_{\mathrm{r}}^{k} \approx\ & \underbrace{\widehat{\mathbf{h}}_{\mathrm{sr}}^{k}\mathbf{v}_{\mathrm{sd}}^{k}p_{\mathrm{sd}}^{k}(\mathbf{v}_{\mathrm{sd}}^{k})^{H}(\widehat{\mathbf{h}}_{\mathrm{sr}}^{k})^{H}+(\sigma_{\mathrm{e,sr}}^{k})^{2}\mathrm{Tr}\Big(\mathbf{v}_{\mathrm{sr}}^{k}p_{\mathrm{sr}}^{k}(\mathbf{v}_{\mathrm{sr}}^{k})^{H}\Big)+(\sigma_{\mathrm{e,sr}}^{k})^{2}\mathrm{Tr}\Big(\mathbf{v}_{\mathrm{sd}}^{k}p_{\mathrm{sd}}^{k}(\mathbf{v}_{\mathrm{sd}}^{k})^{H}\Big)}_{\text{Co-channel interference}} \\
& + \underbrace{\widehat{h}_{\mathrm{rr}}^{k}\kappa_{\mathrm{r}}\sum_{m\in\mathbb{K}}p_{\mathrm{rd}}^{m}(\widehat{h}_{\mathrm{rr}}^{k})^{*}+(\sigma_{\mathrm{e,rr}}^{k})^{2}\kappa_{\mathrm{r}}\sum_{m\in\mathbb{K}}p_{\mathrm{rd}}^{m}}_{\text{Relay transmit distortion}}+\underbrace{(\sigma_{\mathrm{e,rr}}^{k})^{2}p_{\mathrm{rd}}^{k}}_{\text{SI channel estimation error}} \\
& + \underbrace{\widehat{\mathbf{h}}_{\mathrm{sr}}^{k}\mathbf{\Theta}_{\mathrm{t,s}}\sum_{m\in\mathbb{K}}\Big(\mathrm{diag}\left(\mathbf{v}_{\mathrm{sr}}^{m}p_{\mathrm{sr}}^{m}(\mathbf{v}_{\mathrm{sr}}^{m})^{H}\right)+\mathrm{diag}\left(\mathbf{v}_{\mathrm{sd}}^{m}p_{\mathrm{sd}}^{m}(\mathbf{v}_{\mathrm{sd}}^{m})^{H}\right)\Big)(\widehat{\mathbf{h}}_{\mathrm{sr}}^{k})^{H}}_{\text{Source transmit distortion}} \\
& + \underbrace{(\sigma_{\mathrm{e,sr}}^{k})^{2}\mathrm{Tr}\Big(\mathbf{\Theta}_{\mathrm{t,s}}\sum_{m\in\mathbb{K}}\Big(\mathrm{diag}\left(\mathbf{v}_{\mathrm{sr}}^{m}p_{\mathrm{sr}}^{m}(\mathbf{v}_{\mathrm{sr}}^{m})^{H}\right)+\mathrm{diag}\left(\mathbf{v}_{\mathrm{sd}}^{m}p_{\mathrm{sd}}^{m}(\mathbf{v}_{\mathrm{sd}}^{m})^{H}\right)\Big)\Big)}_{\text{Source transmit distortion}} \\
& + \underbrace{\beta_{\mathrm{r}}\sum_{m\in\mathbb{K}}\Big(\widehat{\mathbf{h}}_{\mathrm{sr}}^{m}\mathbf{v}_{\mathrm{sr}}^{m}p_{\mathrm{sr}}^{m}(\mathbf{v}_{\mathrm{sr}}^{m})^{H}(\widehat{\mathbf{h}}_{\mathrm{sr}}^{m})^{H}+\widehat{\mathbf{h}}_{\mathrm{sr}}^{m}\mathbf{v}_{\mathrm{sd}}^{m}p_{\mathrm{sd}}^{m}(\mathbf{v}_{\mathrm{sd}}^{m})^{H}(\widehat{\mathbf{h}}_{\mathrm{sr}}^{m})^{H}+(\sigma_{\mathrm{e,sr}}^{m})^{2}\mathrm{Tr}\Big(\mathbf{v}_{\mathrm{sr}}^{m}p_{\mathrm{sr}}^{m}(\mathbf{v}_{\mathrm{sr}}^{m})^{H}\Big)}_{\text{Relay receive distortion}} \\
& + \underbrace{(\sigma_{\mathrm{e,sr}}^{m})^{2}\mathrm{Tr}\Big(\mathbf{v}_{\mathrm{sd}}^{m}p_{\mathrm{sd}}^{m}(\mathbf{v}_{\mathrm{sd}}^{m})^{H}\Big)+\widehat{h}_{\mathrm{rr}}^{m}p_{\mathrm{rd}}^{m}(\widehat{h}_{\mathrm{rr}}^{m})^{*}+(\sigma_{\mathrm{e,rr}}^{m})^{2}p_{\mathrm{rd}}^{m}+(\sigma_{\mathrm{n,r}}^{m})^{2}\Big)}_{\text{Relay receive distortion}}+\underbrace{(\sigma_{\mathrm{n,r}}^{k})^{2}}_{\text{Thermal noise}}\quad . \qquad (5.10)
\end{aligned}$$

Since the transmit and receive distortion coefficients ($\widetilde{\kappa}$ and $\widetilde{\beta}$) lie within the range of 0 and 1 and mostly have very small values, the higher-order terms of the transmit and receive distortion are ignored.

At the user node, the received signal is processed in two phases using the SuIC technique. In the first phase, the strong received signal from the relay is considered as the desired signal while treating the received signal from the BS as noise. In the next phase, the known part of the received signal, i.e., received signal from the relay, can be removed from the whole received signal, which reduces the total interference. The covariance of the received collective interference-plus-noise signal at the user for the first phase can be expressed as

$$\begin{aligned}
\Sigma_{\mathrm{d},1}^{k} \approx\ & \underbrace{\widehat{\mathbf{h}}_{\mathrm{sd}}^{k}\left(\mathbf{v}_{\mathrm{sr}}^{k}p_{\mathrm{sr}}^{k}(\mathbf{v}_{\mathrm{sr}}^{k})^{H}+\mathbf{v}_{\mathrm{sd}}^{k}p_{\mathrm{sd}}^{k}(\mathbf{v}_{\mathrm{sd}}^{k})^{H}\right)(\widehat{\mathbf{h}}_{\mathrm{sd}}^{k})^{H}+(\sigma_{\mathrm{e,sd}}^{k})^{2}\mathrm{Tr}\Big(\mathbf{v}_{\mathrm{sr}}^{m}p_{\mathrm{sr}}^{m}(\mathbf{v}_{\mathrm{sr}}^{m})^{H}+\mathbf{v}_{\mathrm{sd}}^{m}p_{\mathrm{sd}}^{m}(\mathbf{v}_{\mathrm{sd}}^{m})^{H}\Big)}_{\text{Direct channel interference}} \\
& + \underbrace{\widehat{h}_{\mathrm{rd}}^{k}\kappa_{\mathrm{r}}\sum_{m\in\mathbb{K}}p_{\mathrm{rd}}^{m}(\widehat{h}_{\mathrm{rd}}^{k})^{*}+(\sigma_{\mathrm{e,rd}}^{k})^{2}\kappa_{\mathrm{r}}\sum_{m\in\mathbb{K}}p_{\mathrm{rd}}^{m}}_{\text{Relay transmit distortion}}+\underbrace{(\sigma_{\mathrm{e,rd}}^{k})^{2}p_{\mathrm{rd}}^{k}}_{\text{Relay-dest. channel estimation error}}
\end{aligned}$$

$$
\begin{aligned}
&+\underbrace{\widehat{\mathbf{h}}_{\mathrm{sd}}^{k}\boldsymbol{\Theta}_{\mathrm{t,s}}\sum_{m\in\mathbb{K}}\left(\mathrm{diag}\left(\mathbf{v}_{\mathrm{sr}}^{m}p_{\mathrm{sr}}^{m}(\mathbf{v}_{\mathrm{sr}}^{m})^{H}\right)+\mathrm{diag}\left(\mathbf{v}_{\mathrm{sd}}^{m}p_{\mathrm{sd}}^{m}(\mathbf{v}_{\mathrm{sd}}^{m})^{H}\right)\right)(\widehat{\mathbf{h}}_{\mathrm{sd}}^{k})^{H}}_{\text{Source transmit distortion}}\\
&+\underbrace{(\sigma_{\mathrm{e,sd}}^{k})^{2}\mathrm{Tr}\left(\boldsymbol{\Theta}_{\mathrm{t,s}}\sum_{m\in\mathbb{K}}\left(\mathrm{diag}\left(\mathbf{v}_{\mathrm{sr}}^{m}p_{\mathrm{sr}}^{m}(\mathbf{v}_{\mathrm{sr}}^{m})^{H}\right)+\mathrm{diag}\left(\mathbf{v}_{\mathrm{sd}}^{m}p_{\mathrm{sd}}^{m}(\mathbf{v}_{\mathrm{sd}}^{m})^{H}\right)\right)\right)}_{\text{Source transmit distortion}}\\
&+\underbrace{\beta_{\mathrm{d}}\sum_{m\in\mathbb{K}}\left(\widehat{\mathbf{h}}_{\mathrm{sd}}^{m}\mathbf{v}_{\mathrm{sr}}^{m}p_{\mathrm{sr}}^{m}(\mathbf{v}_{\mathrm{sr}}^{m})^{H}(\widehat{\mathbf{h}}_{\mathrm{sd}}^{m})^{H}+\widehat{\mathbf{h}}_{\mathrm{sd}}^{m}\mathbf{v}_{\mathrm{sd}}^{m}p_{\mathrm{sd}}^{m}(\mathbf{v}_{\mathrm{sd}}^{m})^{H}(\widehat{\mathbf{h}}_{\mathrm{sd}}^{m})^{H}+(\sigma_{\mathrm{e,sd}}^{m})^{2}\mathrm{Tr}\left(\mathbf{v}_{\mathrm{sr}}^{m}p_{\mathrm{sr}}^{m}(\mathbf{v}_{\mathrm{sr}}^{m})^{H}\right)\right.}_{\text{Destination receive distortion}}\\
&+\underbrace{\left.(\sigma_{\mathrm{e,sd}}^{m})^{2}\mathrm{Tr}\left(\mathbf{v}_{\mathrm{sd}}^{m}p_{\mathrm{sd}}^{m}(\mathbf{v}_{\mathrm{sd}}^{m})^{H}\right)+\widehat{h}_{\mathrm{rd}}^{m}p_{\mathrm{rd}}^{m}(\widehat{h}_{\mathrm{rd}}^{m})^{*}+(\sigma_{\mathrm{e,rd}}^{m})^{2}p_{\mathrm{rd}}^{m}+(\sigma_{\mathrm{n,d}}^{m})^{2}\right)}_{\text{Destination receive distortion}}+\underbrace{(\sigma_{\mathrm{n,d}}^{k})^{2}}_{\text{Thermal noise}}\quad.
\end{aligned}
\tag{5.11}
$$

For the second phase, the signal from the relay is known, and it can be removed from the received signal. The signal from the BS to the user becomes the desired signal. The covariance of the received collective interference-plus-noise signal at the user for the second phase can be obtained as

$$
\Sigma_{\mathrm{d,2}}^{k}:=\Sigma_{\mathrm{d,1}}^{k}-\widehat{\mathbf{h}}_{\mathrm{sd}}^{k}\left(\mathbf{v}_{\mathrm{sd}}^{k}p_{\mathrm{sd}}^{k}(\mathbf{v}_{\mathrm{sd}}^{k})^{H}\right)(\widehat{\mathbf{h}}_{\mathrm{sd}}^{k})^{H}. \tag{5.12}
$$

5.4.1 Achievable Information Rate

In this section, we calculate the achievable information rate for communication links such as BS-relay, relay-user and BS-user. The achievable information rate for the BS to relay link using sub-carrier k can be obtained as

$$
R_{\mathrm{sr}}^{k}=\gamma_{0}\log_{2}\left(1+\frac{|\widehat{\mathbf{h}}_{\mathrm{sr}}^{k}\mathbf{v}_{\mathrm{sr}}^{k}|^{2}p_{\mathrm{sr}}^{k}}{\alpha_{\mathrm{r}}^{k}+\sum\limits_{m\in\mathbb{K}}\left(\gamma_{\mathrm{sr}}^{km}p_{\mathrm{sr}}^{m}+\gamma_{\mathrm{rd}}^{km}p_{\mathrm{rd}}^{m}+\gamma_{\mathrm{sd}}^{km}p_{\mathrm{sd}}^{m}\right)}\right), \tag{5.13}
$$

where $0<\gamma_{0}<1$ indicates the portion of the frame duration dedicated to data communication,

$$
\begin{aligned}
\gamma_{\mathrm{sr}}^{km}=&\,\delta_{km}(\sigma_{\mathrm{e,sr}}^{m})^{2}+\widehat{\mathbf{h}}_{\mathrm{sr}}^{k}\boldsymbol{\Theta}_{\mathrm{t,s}}\mathrm{diag}\left(\mathbf{v}_{\mathrm{sr}}^{m}(\mathbf{v}_{\mathrm{sr}}^{m})^{H}\right)(\widehat{\mathbf{h}}_{\mathrm{sr}}^{k})^{H}+(\sigma_{\mathrm{e,sr}}^{k})^{2}\mathrm{Tr}\left(\boldsymbol{\Theta}_{\mathrm{t,s}}\mathrm{diag}\left(\mathbf{v}_{\mathrm{sr}}^{m}(\mathbf{v}_{\mathrm{sr}}^{m})^{H}\right)\right)\\
&+\beta_{\mathrm{r}}\left(\widehat{\mathbf{h}}_{\mathrm{sr}}^{m}\mathbf{v}_{\mathrm{sr}}^{m}(\mathbf{v}_{\mathrm{sr}}^{m})^{H}(\widehat{\mathbf{h}}_{\mathrm{sr}}^{m})^{H}+(\sigma_{\mathrm{e,sr}}^{m})^{2}\right),
\end{aligned}
\tag{5.14}
$$

$$
\gamma_{\mathrm{rd}}^{km}=\delta_{km}(\sigma_{\mathrm{e,rr}}^{m})^{2}+\kappa_{\mathrm{r}}\left(\widehat{h}_{\mathrm{rr}}^{k}(\widehat{h}_{\mathrm{rr}}^{k})^{*}+(\sigma_{\mathrm{e,rr}}^{k})^{2}\right)+\beta_{\mathrm{r}}\left(\widehat{h}_{\mathrm{rr}}^{m}(\widehat{h}_{\mathrm{rr}}^{m})^{*}+(\sigma_{\mathrm{e,rr}}^{m})^{2}\right), \tag{5.15}
$$

$$\gamma_{\mathrm{sd}}^{km} = \delta_{km}\left(\widehat{\mathbf{h}}_{\mathrm{sr}}^{m}\mathbf{v}_{\mathrm{sd}}^{m}(\mathbf{v}_{\mathrm{sd}}^{m})^{H}(\widehat{\mathbf{h}}_{\mathrm{sr}}^{m})^{H} + (\sigma_{\mathrm{e,sr}}^{m})^{2}\right) + \widehat{\mathbf{h}}_{\mathrm{sr}}^{k}\boldsymbol{\Theta}_{\mathrm{t,s}}\mathrm{diag}\left(\mathbf{v}_{\mathrm{sd}}^{m}(\mathbf{v}_{\mathrm{sd}}^{m})^{H}\right)(\widehat{\mathbf{h}}_{\mathrm{sr}}^{k})^{H} + (\sigma_{\mathrm{e,sr}}^{k})^{2}\mathrm{Tr}\left(\boldsymbol{\Theta}_{\mathrm{t,s}}\mathrm{diag}\left(\mathbf{v}_{\mathrm{sd}}^{m}(\mathbf{v}_{\mathrm{sd}}^{m})^{H}\right)\right) + \beta_{\mathrm{r}}\left(\widehat{\mathbf{h}}_{\mathrm{sr}}^{m}\mathbf{v}_{\mathrm{sd}}^{m}(\mathbf{v}_{\mathrm{sd}}^{m})^{H}(\widehat{\mathbf{h}}_{\mathrm{sr}}^{m})^{H} + (\sigma_{\mathrm{e,sr}}^{m})^{2}\right), \tag{5.16}$$

$$\alpha_{\mathrm{r}}^{k} = (\sigma_{\mathrm{n,r}}^{k})^{2} + \beta_{\mathrm{r}}\sum_{m\in\mathbb{K}}(\sigma_{\mathrm{n,r}}^{m})^{2} \tag{5.17}$$

and $\delta_{km} = 1$ when $k = m$ and otherwise $\delta_{km} = 0$.

Similarly, the achievable information rate for the relay to user link using sub-carrier k can be expressed as

$$R_{\mathrm{rd}}^{k} = \gamma_{0}\log_{2}\left(1 + \frac{|\widehat{h}_{\mathrm{rd}}^{k}|^{2}p_{\mathrm{rd}}^{k}}{\alpha_{\mathrm{d}}^{k} + \sum\limits_{m\in\mathbb{K}}\left(\overline{\gamma}_{\mathrm{sr}}^{km}p_{\mathrm{sr}}^{m} + \overline{\gamma}_{\mathrm{rd}}^{km}p_{\mathrm{rd}}^{m} + \overline{\gamma}_{\mathrm{sd}}^{km}p_{\mathrm{sd}}^{m}\right)}\right), \tag{5.18}$$

where

$$\overline{\gamma}_{\mathrm{sr}}^{km} = \delta_{km}\left(\widehat{\mathbf{h}}_{\mathrm{sd}}^{m}\mathbf{v}_{\mathrm{sr}}^{m}(\mathbf{v}_{\mathrm{sr}}^{m})^{H}(\widehat{\mathbf{h}}_{\mathrm{sd}}^{m})^{H} + (\sigma_{\mathrm{e,sd}}^{m})^{2}\right) + \widehat{\mathbf{h}}_{\mathrm{sd}}^{k}\boldsymbol{\Theta}_{\mathrm{t,s}}\mathrm{diag}\left(\mathbf{v}_{\mathrm{sr}}^{m}(\mathbf{v}_{\mathrm{sr}}^{m})^{H}\right)(\widehat{\mathbf{h}}_{\mathrm{sd}}^{k})^{H} + (\sigma_{\mathrm{e,sd}}^{k})^{2}\mathrm{Tr}\left(\boldsymbol{\Theta}_{\mathrm{t,s}}\mathrm{diag}\left(\mathbf{v}_{\mathrm{sr}}^{m}(\mathbf{v}_{\mathrm{sr}}^{m})^{H}\right)\right) + \beta_{\mathrm{d}}\left(\widehat{\mathbf{h}}_{\mathrm{sd}}^{m}\mathbf{v}_{\mathrm{sr}}^{m}(\mathbf{v}_{\mathrm{sr}}^{m})^{H}(\widehat{\mathbf{h}}_{\mathrm{sd}}^{m})^{H} + (\sigma_{\mathrm{e,sd}}^{m})^{2}\right), \tag{5.19}$$

$$\overline{\gamma}_{\mathrm{rd}}^{km} = \delta_{km}(\sigma_{\mathrm{e,rd}}^{m})^{2} + \kappa_{\mathrm{r}}\left(\widehat{h}_{\mathrm{rd}}^{k}(\widehat{h}_{\mathrm{rd}}^{k})^{*} + (\sigma_{\mathrm{e,rd}}^{k})^{2}\right) + \beta_{\mathrm{d}}\left(\widehat{h}_{\mathrm{rd}}^{m}(\widehat{h}_{\mathrm{rd}}^{m})^{*} + (\sigma_{\mathrm{e,rd}}^{m})^{2}\right), \tag{5.20}$$

$$\overline{\gamma}_{\mathrm{sd}}^{km} = \delta_{km}\left(\widehat{\mathbf{h}}_{\mathrm{sd}}^{m}\mathbf{v}_{\mathrm{sd}}^{m}(\mathbf{v}_{\mathrm{sd}}^{m})^{H}(\widehat{\mathbf{h}}_{\mathrm{sd}}^{m})^{H} + (\sigma_{\mathrm{e,sd}}^{m})^{2}\right) + \widehat{\mathbf{h}}_{\mathrm{sd}}^{k}\boldsymbol{\Theta}_{\mathrm{t,s}}\mathrm{diag}\left(\mathbf{v}_{\mathrm{sd}}^{m}(\mathbf{v}_{\mathrm{sd}}^{m})^{H}\right)(\widehat{\mathbf{h}}_{\mathrm{sd}}^{k})^{H} + (\sigma_{\mathrm{e,sd}}^{k})^{2}\mathrm{Tr}\left(\boldsymbol{\Theta}_{\mathrm{t,s}}\mathrm{diag}\left(\mathbf{v}_{\mathrm{sd}}^{m}(\mathbf{v}_{\mathrm{sd}}^{m})^{H}\right)\right) + \beta_{\mathrm{d}}\left(\widehat{\mathbf{h}}_{\mathrm{sd}}^{m}\mathbf{v}_{\mathrm{sd}}^{m}(\mathbf{v}_{\mathrm{sd}}^{m})^{H}(\widehat{\mathbf{h}}_{\mathrm{sd}}^{m})^{H} + (\sigma_{\mathrm{e,sd}}^{m})^{2}\right) \tag{5.21}$$

and

$$\alpha_{\mathrm{d}}^{k} = (\sigma_{\mathrm{n,d}}^{k})^{2} + \beta_{\mathrm{d}}\sum_{m\in\mathbb{K}}(\sigma_{\mathrm{n,d}}^{m})^{2}. \tag{5.22}$$

Finally, the achievable information rate for the BS to user link using sub-carrier k can be formulated as

$$R_{\mathrm{sd}}^{k} = \gamma_{0}\log_{2}\left(1 + \frac{|\widehat{\mathbf{h}}_{\mathrm{sd}}^{k}\mathbf{v}_{\mathrm{sd}}^{k}|^{2}p_{\mathrm{sd}}^{k}}{\alpha_{\mathrm{d}}^{k} + \sum\limits_{m\in\mathbb{K}}\left(\overline{\gamma}_{\mathrm{sr}}^{km}p_{\mathrm{sr}}^{m} + \overline{\gamma}_{\mathrm{rd}}^{km}p_{\mathrm{rd}}^{m} + \widetilde{\gamma}_{\mathrm{sd}}^{km}p_{\mathrm{sd}}^{m}\right)}\right), \tag{5.23}$$

where

$$\widetilde{\gamma}_{\mathrm{sd}}^{km} = \overline{\gamma}_{\mathrm{sd}}^{km} - \delta_{km}\widehat{\mathbf{h}}_{\mathrm{sd}}^{m}\mathbf{v}_{\mathrm{sd}}^{m}(\mathbf{v}_{\mathrm{sd}}^{m})^{H}(\widehat{\mathbf{h}}_{\mathrm{sd}}^{m})^{H}. \tag{5.24}$$

In this chapter, we consider that the BS has a large antenna array. Therefore, different well-studied linear precoder-decoder strategies, such as, maximum ratio transmitting

(MRT)/maximum ratio combining (MRC), zero-forcing (ZF), MMSE, to name a few, are available for the selection of transmit precoders and receive decoders at the BS. Asymptotic rate analysis of the system can be calculated as in chapter 3. We can also reduce the computational complexity of obtaining the achievable rates as discussed in [38], with some common assumptions from mMIMO studies on the channel covariance matrices (such as Hermitian and Toeplitz).

Now, the total achievable information rate for the system can be written as

$$R = \sum_{k\in\mathbb{K}} R_{\mathrm{sd}}^{k} + \min\left\{\sum_{k\in\mathbb{K}} R_{\mathrm{sr}}^{k}, \sum_{k\in\mathbb{K}} R_{\mathrm{rd}}^{k}\right\}. \tag{5.25}$$

5.5 Optimization Problem

In this section, we present the joint sub-carrier and power allocation optimization problem to maximize spectral efficiency in terms of total sum-rate, under transmit power constraints. The node is not transmitting or receiving in a particular sub-carrier if the power allocated to a particular sub-carrier is zero, thereby incorporating the sub-carrier allocation into the power allocation problem.

5.5.1 Sum-rate Maximization

The sum-rate maximization problem for our DuC system can be expressed as

$$\begin{aligned} \underset{\substack{p_{\mathrm{sd}}^{k}\geq 0, p_{\mathrm{sr}}^{k}\geq 0,\\ p_{\mathrm{rd}}^{k}\geq 0}}{\text{maximize}} \quad & R \\ \text{subject to} \quad & \sum_{k\in\mathbb{K}} p_{\mathrm{rd}}^{k} \leq P_{\mathrm{r}}, \quad \sum_{k\in\mathbb{K}} p_{\mathrm{sd}}^{k} + p_{\mathrm{sr}}^{k} \leq P_{\mathrm{s}}, \end{aligned} \tag{5.26}$$

where P_{s} and P_{r} are the total available transmit power at the BS and the relay, respectively. The optimization problem can be rewritten as

$$\begin{aligned} \underset{\substack{p_{\mathrm{sd}}^{k}\geq 0, p_{\mathrm{sr}}^{k}\geq 0,\\ p_{\mathrm{rd}}^{k}\geq 0, t}}{\text{maximize}} \quad & \sum_{k\in\mathbb{K}} R_{\mathrm{sd}}^{k} + t \\ \text{subject to} \quad & \sum_{k\in\mathbb{K}} R_{\mathrm{sr}}^{k} \geq t, \quad \sum_{k\in\mathbb{K}} R_{\mathrm{rd}}^{k} \geq t, \\ & \sum_{k\in\mathbb{K}} p_{\mathrm{rd}}^{k} \leq P_{\mathrm{r}}, \quad \sum_{k\in\mathbb{K}} p_{\mathrm{sd}}^{k} + p_{\mathrm{sr}}^{k} \leq P_{\mathrm{s}}, \end{aligned} \tag{5.27}$$

where t is an auxiliary variable. The above optimization problem (5.27) belongs to the class of smooth DC optimization problems. We propose an iterative algorithm which reaches a converging point that satisfies the Karush–Kuhn–Tucker (KKT) optimality

conditions using the successive inner approximation (SIA) framework [90]. Now, we use Taylor's approximation on the concave terms of rate to obtain a lower bound. For the approximation, we first select $p^k_{\mathrm{rd},0}, p^k_{\mathrm{sd},0}$ and $p^k_{\mathrm{sr},0}$ as a feasible transmit power value for the relay-user link, BS-relay link, and BS-user link, respectively.

A lower-bound of R^k_{sr}, after applying Taylor's approximation on the concave terms, can be expressed as

$$\begin{aligned} R^k_{\mathrm{sr}} \geq\ & \gamma_0 \log_2\left(\alpha^k_{\mathrm{r}} + \sum_{m\in\mathbb{K}}\left(\gamma^{km}_{\mathrm{sr}} p^m_{\mathrm{sr}} + \gamma^{km}_{\mathrm{rd}} p^m_{\mathrm{rd}} + \gamma^{km}_{\mathrm{sd}} p^m_{\mathrm{sd}}\right) + |\widehat{\mathbf{h}}^k_{\mathrm{sr}}\mathbf{v}^k_{\mathrm{sr}}|^2 p^k_{\mathrm{sr}}\right) \\ & - \gamma_0 \log_2\left(\alpha^k_{\mathrm{r}} + \sum_{m\in\mathbb{K}}\left(\gamma^{km}_{\mathrm{sr}} p^m_{\mathrm{sr},0} + \gamma^{km}_{\mathrm{rd}} p^m_{\mathrm{rd},0} + \gamma^{km}_{\mathrm{sd}} p^m_{\mathrm{sd},0}\right)\right) \\ & - \frac{\gamma_0 \sum\limits_{m\in\mathbb{K}}\left(\gamma^{km}_{\mathrm{sr}}\left(p^m_{\mathrm{sr}} - p^m_{\mathrm{sr},0}\right) + \gamma^{km}_{\mathrm{rd}}\left(p^m_{\mathrm{rd}} - p^m_{\mathrm{rd},0}\right) + \gamma^{km}_{\mathrm{sd}}\left(p^m_{\mathrm{sd}} - p^m_{\mathrm{sd},0}\right)\right)}{\log(2)\left(\alpha^k_{\mathrm{r}} + \sum\limits_{m\in\mathbb{K}}\left(\gamma^{km}_{\mathrm{sr}} p^m_{\mathrm{sr},0} + \gamma^{km}_{\mathrm{rd}} p^m_{\mathrm{rd},0} + \gamma^{km}_{\mathrm{sd}} p^m_{\mathrm{sd},0}\right)\right)} =: \overline{R}^k_{\mathrm{sr}}. \end{aligned} \tag{5.28}$$

Similarly, after applying Taylor's approximation, the lower bound of R^k_{sd} and R^k_{rd} can be obtained as

$$\begin{aligned} R^k_{\mathrm{sd}} \geq\ & \gamma_0 \log_2\left(\alpha^k_{\mathrm{d}} + \sum_{m\in\mathbb{K}}\left(\overline{\gamma}^{km}_{\mathrm{sr}} p^m_{\mathrm{sr}} + \overline{\gamma}^{km}_{\mathrm{rd}} p^m_{\mathrm{rd}} + \tilde{\gamma}^{km}_{\mathrm{sd}} p^m_{\mathrm{sd}}\right) + |\widehat{\mathbf{h}}^k_{\mathrm{sd}}\mathbf{v}^k_{\mathrm{sd}}|^2 p^k_{\mathrm{sd}}\right) \\ & - \gamma_0 \log_2\left(\alpha^k_{\mathrm{d}} + \sum_{m\in\mathbb{K}}\left(\overline{\gamma}^{km}_{\mathrm{sr}} p^m_{\mathrm{sr},0} + \overline{\gamma}^{km}_{\mathrm{rd}} p^m_{\mathrm{rd},0} + \tilde{\gamma}^{km}_{\mathrm{sd}} p^m_{\mathrm{sd},0}\right)\right) \\ & - \frac{\gamma_0 \sum\limits_{m\in\mathbb{K}}\left(\overline{\gamma}^{km}_{\mathrm{sr}}\left(p^m_{\mathrm{sr}} - p^m_{\mathrm{sr},0}\right) + \overline{\gamma}^{km}_{\mathrm{rd}}\left(p^m_{\mathrm{rd}} - p^m_{\mathrm{rd},0}\right) + \tilde{\gamma}^{km}_{\mathrm{sd}}\left(p^m_{\mathrm{sd}} - p^m_{\mathrm{sd},0}\right)\right)}{\log(2)\left(\alpha^k_{\mathrm{d}} + \sum\limits_{m\in\mathbb{K}}\left(\overline{\gamma}^{km}_{\mathrm{sr}} p^m_{\mathrm{sr},0} + \overline{\gamma}^{km}_{\mathrm{rd}} p^m_{\mathrm{rd},0} + \tilde{\gamma}^{km}_{\mathrm{sd}} p^m_{\mathrm{sd},0}\right)\right)} =: \overline{R}^k_{\mathrm{sd}} \end{aligned} \tag{5.29}$$

and

$$\begin{aligned} R^k_{\mathrm{rd}} \geq\ & \gamma_0 \log_2\left(\alpha^k_{\mathrm{d}} + \sum_{m\in\mathbb{K}}\left(\overline{\gamma}^{km}_{\mathrm{sr}} p^m_{\mathrm{sr}} + \overline{\gamma}^{km}_{\mathrm{rd}} p^m_{\mathrm{rd}} + \overline{\gamma}^{km}_{\mathrm{sd}} p^m_{\mathrm{sd}}\right) + |\widehat{h}^k_{\mathrm{rd}}|^2 p^k_{\mathrm{rd}}\right) \\ & - \gamma_0 \log_2\left(\alpha^k_{\mathrm{d}} + \sum_{m\in\mathbb{K}}\left(\overline{\gamma}^{km}_{\mathrm{sr}} p^m_{\mathrm{sr},0} + \overline{\gamma}^{km}_{\mathrm{rd}} p^m_{\mathrm{rd},0} + \overline{\gamma}^{km}_{\mathrm{sd}} p^m_{\mathrm{sd},0}\right)\right) \\ & - \frac{\gamma_0 \sum\limits_{m\in\mathbb{K}}\left(\overline{\gamma}^{km}_{\mathrm{sr}}\left(p^m_{\mathrm{sr}} - p^m_{\mathrm{sr},0}\right) + \overline{\gamma}^{km}_{\mathrm{rd}}\left(p^m_{\mathrm{rd}} - p^m_{\mathrm{rd},0}\right) + \overline{\gamma}^{km}_{\mathrm{sd}}\left(p^m_{\mathrm{sd}} - p^m_{\mathrm{sd},0}\right)\right)}{\log(2)\left(\alpha^k_{\mathrm{d}} + \sum\limits_{m\in\mathbb{K}}\left(\overline{\gamma}^{km}_{\mathrm{sr}} p^m_{\mathrm{sr},0} + \overline{\gamma}^{km}_{\mathrm{rd}} p^m_{\mathrm{rd},0} + \overline{\gamma}^{km}_{\mathrm{sd}} p^m_{\mathrm{sd},0}\right)\right)} =: \overline{R}^k_{\mathrm{rd}}, \end{aligned} \tag{5.30}$$

respectively.

Using this approximation, we can rewrite the optimization problem as

$$\begin{aligned} \underset{\substack{p_{\mathrm{sd}}^{i,k}\geq 0, p_{\mathrm{sr}}^{k}\geq 0,\\ p_{\mathrm{rd}}^{i,k}\geq 0, t}}{\text{maximize}} \quad & \sum_{k\in\mathbb{K}} \overline{R}_{\mathrm{sd}}^{k} + t \\ \text{subject to} \quad & \sum_{k\in\mathbb{K}} \overline{R}_{\mathrm{sr}}^{k} \geq t, \ \sum_{k\in\mathbb{K}} \overline{R}_{\mathrm{rd}}^{k} \geq t, \\ & \sum_{k\in\mathbb{K}} p_{\mathrm{rd}}^{k} \leq P_{\mathrm{r}}, \sum_{k\in\mathbb{K}} p_{\mathrm{sd}}^{k} + p_{\mathrm{sr}}^{k} \leq P_{\mathrm{s}}. \end{aligned} \tag{5.31}$$

Here, the above optimization is a jointly convex problem and hence can be solved to optimality using a standard convex solver [91]. We propose an iterative algorithm, where at each iteration the approximated rate functions are updated with the solution of (5.31) from the previous iteration as their initial points. The iterative update is continued until a stable point is reached. Please note that due to the application of the first-order Taylor's approximation on the smooth concave terms, the approximation $\overline{R}_{\mathrm{sr}}^{k}$ is a global and tight lower bound to rate function R_{sr}^{k} with a shared slope at the point of approximation, i.e.,$p_{\mathrm{rd},0}^{k}, p_{\mathrm{sd},0}^{k}$ and $p_{\mathrm{sr},0}^{k}$. Similarly for the approximations $\overline{R}_{\mathrm{rd}}^{k}$ and $\overline{R}_{\mathrm{sd}}^{k}$ in relation to R_{rd}^{k} and R_{sd}^{k}. As a result, it complies with the conditions stated in [90, Theorem 1] and enjoys convergence to a KKT solution. Algorithm 10 provides the detailed procedure.

Algorithm 10 Sum-rate maximization for single-user scenario

1: $a \leftarrow 0$ (set iteration number to zero)
2: $p_{\mathrm{rd},0}^{k}, p_{\mathrm{sd},0}^{k}, p_{\mathrm{sr},0}^{k} \leftarrow$ feasible power value initialization
3: **repeat**
4: $\quad a \leftarrow a + 1$
5: $\quad p_{\mathrm{rd}}^{k}, p_{\mathrm{sd}}^{k}, p_{\mathrm{sr}}^{k}, t \leftarrow$ solve (5.31)
6: $\quad p_{\mathrm{rd},0}^{k}, p_{\mathrm{sd},0}^{k}, p_{\mathrm{sr},0}^{k} \leftarrow p_{\mathrm{rd},0}^{k}{=}p_{\mathrm{rd}}^{k}, p_{\mathrm{sd},0}^{k}{=}p_{\mathrm{sd}}^{k}$ and $p_{\mathrm{sr},0}^{k}{=}p_{\mathrm{sr}}^{k}$, respectively
7: **until** a stable point, or maximum number of a reached
8: **return** $\{p_{\mathrm{rd}}^{k}, p_{\mathrm{sd}}^{k}, p_{\mathrm{sr}}^{k}\}$

5.6 Multi-user Scenario

In this section, we extend our previous single-user scenario with a single antenna relay to a multi-user scenario with an FD mMIMO relay. We consider a relay-assisted MC downlink communication between an mMIMO BS and L downlink users, which are connected to the BS through the direct link as well as the FD relay link. We denote the index sets of all the downlink users by $\mathbb{L}$, where $\overline{\overline{\mathbb{L}}} = L$. We consider that the relay is equipped with a single directive[1] receive antenna, which serve the fronthaul link and

[1]This is since unlike the user links, the BS-relay link is static and enjoys a line-of-sight condition. Hence, it acts as a single fronthaul link, carrying downlink information associated with multiple users.

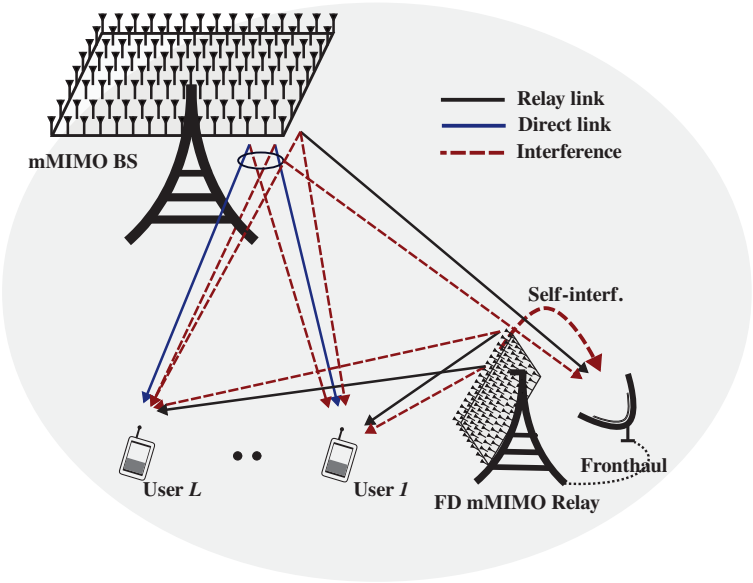

Figure 5.2: System model for multi-user FD relaying-enabled DuC system

N_{r} transmit antennas, which serve the relay-user communications. Nevertheless, due to the FD capability at the relay node, the fronthaul link as well as the relay-user links coexist at the same channel resource, i.e., time and frequency. Moreover, both the users and the relay will be affected by multi-user interference. The schematic of the studied multi-user FD relaying-enabled DuC system depicted in Fig 5.2. Due to the similarities with the previous single-user scenario, we only discuss additional details in this section.

The transmit signal from the BS using k-th sub-carrier can be written as

$$\mathbf{x}_{\mathrm{s,MU}}^{k} = \underbrace{\mathbf{v}_{\mathrm{sr}}^{k}\sqrt{p_{\mathrm{sr}}^{k}}s_{\mathrm{sr}}^{k} + \sum_{i\in\mathbb{L}}\mathbf{v}_{\mathrm{sd}}^{i,k}\sqrt{p_{\mathrm{sd}}^{i,k}}s_{\mathrm{sd}}^{i,k}}_{:=\widetilde{\mathbf{x}}_{\mathrm{s,MU}}^{k}} + \mathbf{e}_{\mathrm{t,s}}^{k}, \quad \forall k \in \mathbb{K}, \tag{5.32}$$

where $\widetilde{\mathbf{x}}_{\mathrm{s,MU}}^{k}$ is the intended transmit signal at the BS. The normalized precoding matrix and transmit power at the BS corresponding to the user i using sub-carrier k are denoted by $\mathbf{v}_{\mathrm{sd}}^{i,k}$ and $p_{\mathrm{sd}}^{i,k}$, respectively. The $s_{\mathrm{sd}}^{i,k}$ represents the unit power transmit symbol for the user i using sub-carrier k, i.e., $\mathbb{E}\{s_{\mathrm{sd}}^{i,k}(s_{\mathrm{sd}}^{i,k})^{*}\} = 1$.

At the relay, it receives the desired transmit signal from the BS along with the multi-user interference, then decodes the symbols dedicated to each user and then forwards it

to the respective users. We assume the retransmitted symbol, $\widehat{s}_{\mathrm{rd}}^{i,k}$, to be i.i.d. with unit power. Accordingly, the transmit and receive signal at the relay node can be expressed as

$$\begin{aligned} \mathbf{x}_{\mathrm{r,MU}}^{k} &= \underbrace{\sum_{i\in\mathbb{L}} \mathbf{v}_{\mathrm{rd}}^{i,k}\sqrt{p_{\mathrm{rd}}^{i,k}}\widehat{s}_{\mathrm{rd}}^{i,k}}_{:=\widetilde{\mathbf{x}}_{\mathrm{r,MU}}^{k}} + \mathbf{e}_{\mathrm{t,r}}^{k}\,, \quad \forall k\in\mathbb{K}, \\ y_{\mathrm{r,MU}}^{k} &= \underbrace{\mathbf{h}_{\mathrm{sr}}^{k}\mathbf{x}_{\mathrm{s,MU}}^{k} + \mathbf{h}_{\mathrm{rr}}^{k}\mathbf{x}_{\mathrm{r,MU}}^{k} + n_{\mathrm{r}}^{k}}_{:=\widetilde{y}_{\mathrm{r,MU}}^{k}} + e_{\mathrm{r,r}}^{k}, \quad \forall k\in\mathbb{K}, \end{aligned} \tag{5.33}$$

where $\mathbf{e}_{\mathrm{t,r}}^{k}\in\mathbb{C}^{N_{\mathrm{r}}\times 1}$, and $\mathbf{h}_{\mathrm{rr}}^{k}\in\mathbb{C}^{1\times N_{\mathrm{r}}}$ are the transmit distortion and SI channel at the relay node, respectively. The normalized precoding matrix and transmit power at the relay corresponding to the user i using sub-carrier k are denoted by $\mathbf{v}_{\mathrm{rd}}^{i,k}$ and $p_{\mathrm{rd}}^{i,k}$, respectively. The intended transmit and received signal at the relay can be represented as $\widetilde{\mathbf{x}}_{\mathrm{r,MU}}^{k}$ and $\widetilde{y}_{\mathrm{r,MU}}^{k}$, respectively. After removing the known transmit part from the received signal by applying SIC, we get

$$\overline{y}_{\mathrm{r,MU}}^{k} = y_{\mathrm{r,MU}}^{k} - \widehat{\mathbf{h}}_{\mathrm{rr}}^{k}\widetilde{\mathbf{x}}_{\mathrm{r,MU}}^{k}, \quad \forall k\in\mathbb{K}. \tag{5.34}$$

Subsequently, the received signal at the user node i can be obtained as

$$y_{\mathrm{d}}^{i,k} = \underbrace{\mathbf{h}_{\mathrm{sd}}^{i,k}\mathbf{x}_{\mathrm{s,MU}}^{k} + \mathbf{h}_{\mathrm{rd}}^{i,k}\mathbf{x}_{\mathrm{r,MU}}^{k} + n_{\mathrm{d}}^{i,k}}_{:=\widetilde{y}_{\mathrm{d}}^{i,k}} + e_{\mathrm{r,d}}^{i,k}, \quad \forall k\in\mathbb{K}, \tag{5.35}$$

where $n_{\mathrm{d}}^{i,k}\sim\mathcal{CN}\left(0,(\sigma_{\mathrm{n,d}}^{i,k})^2\right)$, $e_{\mathrm{r,d}}^{i,k}$ and $\widetilde{y}_{\mathrm{d}}^{i,k}$ are the receiver noise, receive distortion and intended received signal at the user node i, respectively. Moreover, $\mathbf{h}_{\mathrm{sd}}^{i,k}$ and $\mathbf{h}_{\mathrm{rd}}^{i,k}$ represent the BS-user and relay-user channels for i-th user node using k-th sub-carrier, respectively.

Using Lemma 2.4.1, the statistics of the distortion terms for the multi-user system can be obtained as

$$\mathbf{e}_{\mathrm{t,s}}^{k}\sim\mathcal{CN}\left(\mathbf{0}_{N_{\mathrm{BS}}},\frac{1}{K}\widetilde{\mathbf{\Theta}}_{\mathrm{t,s}}\sum_{k\in\mathbb{K}}\mathrm{diag}\left(\mathbb{E}\{\widetilde{\mathbf{x}}_{\mathrm{s,MU}}^{k}(\widetilde{\mathbf{x}}_{\mathrm{s,MU}}^{k})^{H}\}\right)\right), \tag{5.36}$$

$$\mathbf{e}_{\mathrm{t,r}}^{k}\sim\mathcal{CN}\left(\mathbf{0}_{N_{\mathrm{r}}},\frac{1}{K}\widetilde{\mathbf{\Theta}}_{\mathrm{t,r}}\sum_{k\in\mathbb{K}}\mathrm{diag}\left(\mathbb{E}\{\widetilde{\mathbf{x}}_{\mathrm{r,MU}}^{k}(\widetilde{\mathbf{x}}_{\mathrm{r,MU}}^{k})^{H}\}\right)\right), \tag{5.37}$$

$$e_{\mathrm{r,r}}^{k}\sim\mathcal{CN}\left(0,\frac{\widetilde{\beta}_{\mathrm{r}}}{K}\sum_{k\in\mathbb{K}}\left(\mathbb{E}\{\widetilde{y}_{\mathrm{r,MU}}^{k}(\widetilde{y}_{\mathrm{r,MU}}^{k})^{H}\}\right)\right), \tag{5.38}$$

$$e_{\mathrm{r,d}}^{i,k}\sim\mathcal{CN}\left(0,\frac{\widetilde{\beta}_{\mathrm{d}}^{i}}{K}\sum_{k\in\mathbb{K}}\left(\mathbb{E}\{\widetilde{y}_{\mathrm{d}}^{i,k}(\widetilde{y}_{\mathrm{d}}^{i,k})^{H}\}\right)\right), \tag{5.39}$$

where diagonal matrix $\widetilde{\mathbf{\Theta}}_{\mathrm{t,r}}$ consists of transmit distortion coefficients for the corresponding chains at the relay node. $\widetilde{\beta}_{\mathrm{d}}^{i}$ represents the receive distortion coefficient at the user node i. For further calculations, let us define $\beta_{\mathrm{d}}^{i}=\frac{\widetilde{\beta}_{\mathrm{d}}^{i}}{K}$, and $\mathbf{\Theta}_{\mathrm{t,r}}=\frac{1}{K}\widetilde{\mathbf{\Theta}}_{\mathrm{t,r}}$.

5.6.1 Achievable Information Rate for Multi-user Scenario

The achievable information rate for the BS to relay link using sub-carrier k can be obtained as

$$R^{k}_{\mathrm{sr,MU}} = \gamma_0 \log_2 \left(1 + \frac{|\widehat{\mathbf{h}}^{k}_{\mathrm{sr}} \mathbf{v}^{k}_{\mathrm{sr}}|^2 p^{k}_{\mathrm{sr}}}{\alpha^{k}_{\mathrm{r}} + \sum\limits_{m \in \mathbb{K}} \left(\gamma^{km}_{\mathrm{sr}} p^{m}_{\mathrm{sr}} + \sum\limits_{j \in \mathbb{L}} \left(\gamma^{j,k,m}_{\mathrm{rd,MU}} p^{j,m}_{\mathrm{rd}} + \gamma^{j,k,m}_{\mathrm{sd,MU}} p^{j,m}_{\mathrm{sd}} \right) \right)} \right) \tag{5.40}$$

where

$$\begin{aligned} \gamma^{j,k,m}_{\mathrm{rd,MU}} = {} & \delta_{km} (\sigma^{m}_{\mathrm{e,rr}})^2 + \widehat{\mathbf{h}}^{k}_{\mathrm{rr}} \mathbf{\Theta}_{\mathrm{t,r}} \mathrm{diag}\left(\mathbf{v}^{j,m}_{\mathrm{rd}} (\mathbf{v}^{j,m}_{\mathrm{rd}})^H \right) (\widehat{\mathbf{h}}^{k}_{\mathrm{rr}})^H \\ & + (\sigma^{k}_{\mathrm{e,rr}})^2 \mathrm{Tr}\left(\mathbf{\Theta}_{\mathrm{t,r}} \mathrm{diag}\left(\mathbf{v}^{j,m}_{\mathrm{rd}} (\mathbf{v}^{j,m}_{\mathrm{rd}})^H \right) \right) + \beta_{\mathrm{r}} \left(\widehat{\mathbf{h}}^{m}_{\mathrm{rr}} \mathbf{v}^{j,m}_{\mathrm{rd}} (\mathbf{v}^{j,m}_{\mathrm{rd}})^H (\widehat{\mathbf{h}}^{m}_{\mathrm{rr}})^H + (\sigma^{m}_{\mathrm{e,rr}})^2 \right), \end{aligned} \tag{5.41}$$

$$\begin{aligned} \gamma^{j,k,m}_{\mathrm{sd,MU}} = {} & \delta_{km} \left(\widehat{\mathbf{h}}^{m}_{\mathrm{sr}} \mathbf{v}^{j,m}_{\mathrm{sd}} (\mathbf{v}^{j,m}_{\mathrm{sd}})^H (\widehat{\mathbf{h}}^{m}_{\mathrm{sr}})^H + (\sigma^{m}_{\mathrm{e,sr}})^2 \right) + \widehat{\mathbf{h}}^{k}_{\mathrm{sr}} \mathbf{\Theta}_{\mathrm{t,s}} \mathrm{diag}\left(\mathbf{v}^{j,m}_{\mathrm{sd}} (\mathbf{v}^{j,m}_{\mathrm{sd}})^H \right) (\widehat{\mathbf{h}}^{k}_{\mathrm{sr}})^H \\ & + (\sigma^{k}_{\mathrm{e,sr}})^2 \mathrm{Tr}\left(\mathbf{\Theta}_{\mathrm{t,s}} \mathrm{diag}\left(\mathbf{v}^{j,m}_{\mathrm{sd}} (\mathbf{v}^{j,m}_{\mathrm{sd}})^H \right) \right) + \beta_{\mathrm{r}} \left(\widehat{\mathbf{h}}^{m}_{\mathrm{sr}} \mathbf{v}^{j,m}_{\mathrm{sd}} (\mathbf{v}^{j,m}_{\mathrm{sd}})^H (\widehat{\mathbf{h}}^{m}_{\mathrm{sr}})^H + (\sigma^{m}_{\mathrm{e,sr}})^2 \right). \end{aligned} \tag{5.42}$$

Similarly, the achievable information rate for the link between the relay to the user i, using sub-carrier k can be expressed as

$$R^{i,k}_{\mathrm{rd,MU}} = \log_2 \left(1 + \frac{|\widehat{\mathbf{h}}^{i,k}_{\mathrm{rd}} \mathbf{v}^{i,k}_{\mathrm{rd}}|^2 p^{i,k}_{\mathrm{rd}}}{\alpha^{i,k}_{\mathrm{d}} + \sum\limits_{m \in \mathbb{K}} \left(\overline{\gamma}^{i,k,m}_{\mathrm{sr,MU}} p^{m}_{\mathrm{sr}} + \sum\limits_{j \in \mathbb{L}} \left(\overline{\gamma}^{i,j,k,m}_{\mathrm{rd,MU}} p^{j,m}_{\mathrm{rd}} + \overline{\gamma}^{i,j,k,m}_{\mathrm{sd,MU}} p^{j,m}_{\mathrm{sd}} \right) \right)} \right), \tag{5.43}$$

where

$$\begin{aligned} \overline{\gamma}^{i,k,m}_{\mathrm{sr,MU}} = {} & \delta_{km} \left(\widehat{\mathbf{h}}^{i,m}_{\mathrm{sd}} \mathbf{v}^{m}_{\mathrm{sr}} (\mathbf{v}^{m}_{\mathrm{sr}})^H (\widehat{\mathbf{h}}^{i,m}_{\mathrm{sd}})^H + (\sigma^{i,m}_{\mathrm{e,sd}})^2 \right) + \widehat{\mathbf{h}}^{i,k}_{\mathrm{sd}} \mathbf{\Theta}_{\mathrm{t,s}} \mathrm{diag}\left(\mathbf{v}^{m}_{\mathrm{sr}} (\mathbf{v}^{m}_{\mathrm{sr}})^H \right) (\widehat{\mathbf{h}}^{i,k}_{\mathrm{sd}})^H \\ & + (\sigma^{i,k}_{\mathrm{e,sd}})^2 \mathrm{Tr}\left(\mathbf{\Theta}_{\mathrm{t,s}} \mathrm{diag}\left(\mathbf{v}^{m}_{\mathrm{sr}} (\mathbf{v}^{m}_{\mathrm{sr}})^H \right) \right) + \beta^{i}_{\mathrm{d}} \left(\widehat{\mathbf{h}}^{i,m}_{\mathrm{sd}} \mathbf{v}^{m}_{\mathrm{sr}} (\mathbf{v}^{m}_{\mathrm{sr}})^H (\widehat{\mathbf{h}}^{i,m}_{\mathrm{sd}})^H + (\sigma^{i,m}_{\mathrm{e,sd}})^2 \right), \end{aligned} \tag{5.44}$$

$$\begin{aligned} \overline{\gamma}^{i,j,k,m}_{\mathrm{rd,MU}} = {} & \delta_{km} (1 - \delta_{ij}) \widehat{\mathbf{h}}^{i,k}_{\mathrm{rd}} \mathbf{v}^{j,m}_{\mathrm{rd}} (\mathbf{v}^{j,m}_{\mathrm{rd}})^H (\widehat{\mathbf{h}}^{i,k}_{\mathrm{rd}})^H + \delta_{km} (\sigma^{i,m}_{\mathrm{e,rd}})^2 \\ & + \widehat{\mathbf{h}}^{i,k}_{\mathrm{rd}} \mathbf{\Theta}_{\mathrm{t,r}} \mathrm{diag}\left(\mathbf{v}^{j,m}_{\mathrm{rd}} (\mathbf{v}^{j,m}_{\mathrm{rd}})^H \right) (\widehat{\mathbf{h}}^{i,k}_{\mathrm{rd}})^H + (\sigma^{i,k}_{\mathrm{e,rd}})^2 \mathrm{Tr}\left(\mathbf{\Theta}_{\mathrm{t,r}} \mathrm{diag}\left(\mathbf{v}^{j,m}_{\mathrm{rd}} (\mathbf{v}^{j,m}_{\mathrm{rd}})^H \right) \right) \\ & + \beta^{i}_{\mathrm{d}} \left(\widehat{\mathbf{h}}^{i,m}_{\mathrm{rd}} \mathbf{v}^{j,m}_{\mathrm{rd}} (\mathbf{v}^{j,m}_{\mathrm{rd}})^H (\widehat{\mathbf{h}}^{i,m}_{\mathrm{rd}})^H + (\sigma^{i,m}_{\mathrm{e,rd}})^2 \right), \end{aligned} \tag{5.45}$$

$$\begin{aligned}\overline{\gamma}_{\mathrm{sd,MU}}^{i,j,k,m} =&\delta_{km}\left(\widehat{\mathbf{h}}_{\mathrm{sd}}^{i,m}\mathbf{v}_{\mathrm{sd}}^{j,m}(\mathbf{v}_{\mathrm{sd}}^{j,m})^H(\widehat{\mathbf{h}}_{\mathrm{sd}}^{i,m})^H+(\sigma_{\mathrm{e,sd}}^{i,m})^2\right)+\widehat{\mathbf{h}}_{\mathrm{sd}}^{i,k}\mathbf{\Theta}_{\mathrm{t,s}}\mathrm{diag}\left(\mathbf{v}_{\mathrm{sd}}^{j,m}(\mathbf{v}_{\mathrm{sd}}^{j,m})^H\right)(\widehat{\mathbf{h}}_{\mathrm{sd}}^{i,k})^H\\&+(\sigma_{\mathrm{e,sd}}^{i,k})^2\mathrm{Tr}\left(\mathbf{\Theta}_{\mathrm{t,s}}\mathrm{diag}\left(\mathbf{v}_{\mathrm{sd}}^{j,m}(\mathbf{v}_{\mathrm{sd}}^{j,m})^H\right)\right)+\beta_{\mathrm{d}}^{i}\left(\widehat{\mathbf{h}}_{\mathrm{sd}}^{i,m}\mathbf{v}_{\mathrm{sd}}^{j,m}(\mathbf{v}_{\mathrm{sd}}^{j,m})^H(\widehat{\mathbf{h}}_{\mathrm{sd}}^{i,m})^H+(\sigma_{\mathrm{e,sd}}^{i,m})^2\right)\end{aligned}\tag{5.46}$$

$$\alpha_{\mathrm{d}}^{i,k}=(\sigma_{\mathrm{n,d}}^{i,k})^2+\beta_{\mathrm{d}}^{i}\sum_{m\in\mathbb{K}}(\sigma_{\mathrm{n,d}}^{i,m})^2.\tag{5.47}$$

Subsequently, the achievable information rate between the BS and user i, using sub-carrier k can be expressed as

$$R_{\mathrm{sd,MU}}^{i,k}=\log_2\left(1+\frac{|\widehat{\mathbf{h}}_{\mathrm{sd}}^{i,k}\mathbf{v}_{\mathrm{sd}}^{i,k}|^2p_{\mathrm{sd}}^{i,k}}{\alpha_{\mathrm{d}}^{i,k}+\sum\limits_{m\in\mathbb{K}}\left(\overline{\gamma}_{\mathrm{sr,MU}}^{i,k,m}p_{\mathrm{sr}}^{m}+\sum\limits_{j\in\mathbb{L}}\left(\overline{\gamma}_{\mathrm{rd,MU}}^{i,j,k,m}p_{\mathrm{rd}}^{j,m}+\widetilde{\gamma}_{\mathrm{sd,MU}}^{i,j,k,m}p_{\mathrm{sd}}^{j,m}\right)\right)}\right)\tag{5.48}$$

where

$$\widetilde{\gamma}_{\mathrm{sd,MU}}^{i,j,k,m}=\overline{\gamma}_{\mathrm{sd,MU}}^{i,j,k,m}-\delta_{km}\delta_{ij}\left(\widehat{\mathbf{h}}_{\mathrm{sd}}^{i,m}\mathbf{v}_{\mathrm{sd}}^{j,m}(\mathbf{v}_{\mathrm{sd}}^{j,m})^H(\widehat{\mathbf{h}}_{\mathrm{sd}}^{i,m})^H\right).\tag{5.49}$$

The total achievable information rate for the system can be written as

$$R_{\mathrm{MU}}=\sum_{i\in\mathbb{L}}\sum_{k\in\mathbb{K}}R_{\mathrm{sd,MU}}^{i,k}+\min\left\{\sum_{k\in\mathbb{K}}R_{\mathrm{sr,MU}}^{k},\sum_{i\in\mathbb{L}}\sum_{k\in\mathbb{K}}R_{\mathrm{rd,MU}}^{i,k}\right\}.\tag{5.50}$$

5.6.2 Sum-rate Maximization for the Multi-user Scenario

Here, we present the joint sub-carrier and power allocation optimization problem for the multi-user case, to maximize spectral efficiency in terms of total sum-rate under transmit power constraints. The sum-rate maximization problem for the multi-user case can be formulated as

$$\begin{aligned}&\underset{\substack{p_{\mathrm{sd}}^{i,k}\geq0,p_{\mathrm{sr}}^{k}\geq0,\\ p_{\mathrm{rd}}^{i,k}\geq0}}{\text{maximize}} \quad R_{\mathrm{MU}}\\&\text{subject to} \quad \sum_{i\in\mathbb{L}}\sum_{k\in\mathbb{K}}p_{\mathrm{rd}}^{i,k}\leq P_{\mathrm{r}},\quad \sum_{i\in\mathbb{L}}\sum_{k\in\mathbb{K}}p_{\mathrm{sd}}^{i,k}+\sum_{k\in\mathbb{K}}p_{\mathrm{sr}}^{k}\leq P_{\mathrm{s}},\end{aligned}\tag{5.51}$$

where P_{s} and P_{r} are the available transmit power at the BS and the relay, respectively. The above optimization problem can be reformulated as

$$\begin{aligned}&\underset{\substack{p_{\mathrm{sd}}^{i,k}\geq0,p_{\mathrm{sr}}^{k}\geq0,\\ p_{\mathrm{rd}}^{i,k}\geq0,t}}{\text{maximize}} \quad \sum_{i\in\mathbb{L}}\sum_{k\in\mathbb{K}}R_{\mathrm{sd,MU}}^{i,k}+t\\&\text{subject to} \quad \sum_{k\in\mathbb{K}}R_{\mathrm{sr,MU}}^{k}\geq t,\ \sum_{i\in\mathbb{L}}\sum_{k\in\mathbb{K}}R_{\mathrm{rd,MU}}^{i,k}\geq t,\\&\qquad\quad \sum_{i\in\mathbb{L}}\sum_{k\in\mathbb{K}}p_{\mathrm{rd}}^{i,k}\leq P_{\mathrm{r}},\quad \sum_{i\in\mathbb{L}}\sum_{k\in\mathbb{K}}p_{\mathrm{sd}}^{i,k}+\sum_{k\in\mathbb{K}}p_{\mathrm{sr}}^{k}\leq P_{\mathrm{s}}.\end{aligned}\tag{5.52}$$

The above optimization belongs to the class of smooth DC optimization problems similar to (5.52), which is solved using an iterative algorithm using the SIA framework which reaches a converging point that satisfies the KKT optimality conditions [90]. Similar to (5.28), (5.29), and (5.30), after applying Taylor's approximation on the concave rate terms, we can obtain the lower bound for the rates (5.40), (5.43), (5.48) as $\overline{R}^{k}_{\mathrm{sr,MU}}$, $\overline{R}^{i,k}_{\mathrm{rd,MU}}$ and $\overline{R}^{i,k}_{\mathrm{sd,MU}}$, respectively.

The optimization problem is rewritten using this approximation and can be stated as

$$\begin{aligned} \underset{\substack{p^{i,k}_{\mathrm{sd}}\geq 0, p^{k}_{\mathrm{sr}}\geq 0,\\ p^{i,k}_{\mathrm{rd}}\geq 0, t}}{\text{maximize}} \quad & \sum_{i\in\mathbb{L}}\sum_{k\in\mathbb{K}} \overline{R}^{i,k}_{\mathrm{sd,MU}} + t \\ \text{subject to} \quad & \sum_{k\in\mathbb{K}} \overline{R}^{k}_{\mathrm{sr,MU}} \geq t, \;\; \sum_{i\in\mathbb{L}}\sum_{k\in\mathbb{K}} \overline{R}^{i,k}_{\mathrm{rd,MU}} \geq t, \\ & \sum_{i\in\mathbb{L}}\sum_{k\in\mathbb{K}} p^{i,k}_{\mathrm{rd}} \leq P_{\mathrm{r}}, \sum_{i\in\mathbb{L}}\sum_{k\in\mathbb{K}} p^{i,k}_{\mathrm{sd}} + \sum_{k\in\mathbb{K}} p^{k}_{\mathrm{sr}} \leq P_{\mathrm{s}}. \end{aligned} \tag{5.53}$$

The iterative algorithm similar to Algorithm 10 can be used to solve the above convex optimization problem, where the solution can achieve a convergence point that satisfies the KKT conditions. Algorithm 11 provides a detailed procedure of the algorithm.

Algorithm 11 Sum-rate maximization for multi-user scenario

1: $a \leftarrow 0$ (set iteration number to zero)
2: $p^{i,k}_{\mathrm{rd},0}, p^{i,k}_{\mathrm{sd},0}, p^{k}_{\mathrm{sr},0} \leftarrow$ feasible power value initialization
3: **repeat**
4: $\quad a \leftarrow a + 1$
5: $\quad p^{i,k}_{\mathrm{rd}}, p^{i,k}_{\mathrm{sd}}, p^{k}_{\mathrm{sr}}, t \leftarrow$ solve (5.53)
6: $\quad p^{i,k}_{\mathrm{rd},0}, p^{i,k}_{\mathrm{sd},0}, p^{k}_{\mathrm{sr},0} \leftarrow p^{i,k}_{\mathrm{rd},0} = p^{i,k}_{\mathrm{rd}}, p^{i,k}_{\mathrm{sd},0} = p^{i,k}_{\mathrm{sd}}$ and $p^{k}_{\mathrm{sr},0} = p^{k}_{\mathrm{sr}}$, respectively
7: **until** a stable point, or maximum number of a reached
8: **return** $\{p^{i,k}_{\mathrm{rd}}, p^{i,k}_{\mathrm{sd}}, p^{k}_{\mathrm{sr}}\}$

5.6.3 Half Duplex Relay

In this section, we derive the optimization problem in terms of sum-rate maximization for our system, where the relay is an HD relay, and the receiver is capable of performing SuIC, so that DuC can be established. Unlike the FD relay, which can receive and transmit at the same frequency-time channel, the HD relay [2] has to listen to the BS at the first time slot and then forwards the signals to the users in the second time slot. The user receives signals from the BS via DL in both time slots. Hence the SuIC is applicable only in the second time slot, where the user receives signals from both

[2] which operates in time division duplex (TDD) mode to separate source-relay and relay-destination link

the relay and the BS simultaneously. Moreover, in the first time slot, the BS transmit the signals to the relay and the user. Since the relay is operated in HD, there is no SI at the relay. We also assume the channel remains the same throughout the entire communication (both the time slots).

During the first time slot, the BS transmits signal to the users as well as the relay. There is no communication between the relay and user nodes. Therefore, there is no SI at the relay. The transmit signal from the BS during the first time slot can be expressed as

$$\mathbf{x}_{\mathrm{s},1}^{k} = \underbrace{\mathbf{v}_{\mathrm{sr},1}^{k}\sqrt{p_{\mathrm{sr},1}^{k}}s_{\mathrm{sr},1}^{k} + \sum_{i\in\mathbb{L}}\mathbf{v}_{\mathrm{sd},1}^{i,k}\sqrt{p_{\mathrm{sd},1}^{i,k}}s_{\mathrm{sd},1}^{i,k}}_{:=\widetilde{\mathbf{x}}_{\mathrm{s},1}^{k}} + \mathbf{e}_{\mathrm{t,s},1}^{k}, \quad \forall k \in \mathbb{K}, \tag{5.54}$$

where $\widetilde{\mathbf{x}}_{\mathrm{s},1}^{k}$ and $\mathbf{e}_{\mathrm{t,s},1}^{k}$ represent the intended transmit signal and transmit distortion at the BS during the first time slot, respectively. For the first time slot, the normalized precoding matrix, unit power transmit symbol and transmit power at the BS corresponding to the user i (relay) using sub-carrier k are denoted by $\mathbf{v}_{\mathrm{sd},1}^{i,k}$ ($\mathbf{v}_{\mathrm{sr},1}^{k}$), $s_{\mathrm{sd},1}^{i,k}$ ($s_{\mathrm{sr},1}^{k}$) and $p_{\mathrm{sd},1}^{i,k}$ ($p_{\mathrm{sr},1}^{k}$), respectively. The received signal at the relay and user i can be formulated as

$$\begin{aligned} y_{\mathrm{r},1}^{k} &= \underbrace{\mathbf{h}_{\mathrm{sr}}^{k}\mathbf{x}_{\mathrm{s},1}^{k} + n_{\mathrm{r}}^{k}}_{:=\widetilde{y}_{\mathrm{r},1}^{k}} + e_{\mathrm{r,r},1}^{k}, \\ y_{\mathrm{d},1}^{i,k} &= \underbrace{\mathbf{h}_{\mathrm{sd}}^{i,k}\mathbf{x}_{\mathrm{s},1}^{k} + n_{\mathrm{d}}^{i,k}}_{:=\widetilde{y}_{\mathrm{d},1}^{i,k}} + e_{\mathrm{r,d},1}^{i,k}, \quad \forall k \in \mathbb{K},\ \forall i \in \mathbb{L} \end{aligned} \tag{5.55}$$

where the intended receive signal and receive distortion at the relay (user i) during the first time slot are denoted by $\widetilde{y}_{\mathrm{r},1}^{k}$ ($\widetilde{y}_{\mathrm{d},1}^{i,k}$) and $e_{\mathrm{r,r},1}^{k}$ ($e_{\mathrm{r,d},1}^{i,k}$), respectively.

Subsequently, during the second time slot, the user receives signals from both the relay and the BS simultaneously and uses SuIC technique to decode both the signals. Similarly, as the previous FD relay case, we assume the relay link between the relay and user nodes are stronger compared to the direct link between the BS and the user nodes. Therefore, the user node first decodes the relay link considering the direct link as noise, and then removes the signal of the relay link from the received signal and decodes the signal from the direct link.

The transmit signal at the BS and the relay during second time slot can be written as

$$\begin{aligned} \mathbf{x}_{\mathrm{s},2}^{k} &= \underbrace{\sum_{i\in\mathbb{L}}\mathbf{v}_{\mathrm{sd},2}^{i,k}\sqrt{p_{\mathrm{sd},2}^{i,k}}s_{\mathrm{sd},2}^{i,k}}_{:=\widetilde{\mathbf{x}}_{\mathrm{s},2}^{k}} + \mathbf{e}_{\mathrm{t,s},2}^{k}, \quad \forall k \in \mathbb{K}, \\ \mathbf{x}_{\mathrm{r},2}^{k} &= \underbrace{\sum_{i\in\mathbb{L}}\mathbf{v}_{\mathrm{rd},2}^{i,k}\sqrt{p_{\mathrm{rd},2}^{i,k}}\widetilde{s}_{\mathrm{rd},2}^{i,k}}_{:=\widetilde{\mathbf{x}}_{\mathrm{r},2}^{k}} + \mathbf{e}_{\mathrm{t,r},2}^{k}, \end{aligned} \tag{5.56}$$

where the intended transmit signal and transmit distortion at the BS (relay) during the second time slot are denoted by $\widetilde{\mathbf{x}}_{\mathrm{s},2}^{k}$ ($\widetilde{\mathbf{x}}_{\mathrm{r},2}^{k}$) and $\mathbf{e}_{\mathrm{t,s},2}^{k}$ ($\mathbf{e}_{\mathrm{t,r},2}^{k}$), respectively. Moreover, $\mathbf{v}_{\mathrm{sd},2}^{i,k}$ ($\mathbf{v}_{\mathrm{rd},2}^{i,k}$), $s_{\mathrm{sd},2}^{i,k}$ ($\widehat{s}_{\mathrm{rd},2}^{i,k}$) and $p_{\mathrm{sd},2}^{i,k}$ ($p_{\mathrm{rd},2}^{i,k}$) represent the normalized precoding matrix, unit power transmit symbol and transmit power at the BS (relay) corresponding to the user i using sub-carrier k during the second time slot, respectively. The received signal at user i during the second time slot can be stated as

$$y_{\mathrm{d},2}^{i,k} = \underbrace{\mathbf{h}_{\mathrm{sd}}^{i,k}\mathbf{x}_{\mathrm{s},2}^{k} + \mathbf{h}_{\mathrm{rd}}^{i,k}\mathbf{x}_{\mathrm{r},2}^{k} + n_{\mathrm{d}}^{i,k}}_{:=\widetilde{y}_{\mathrm{d},2}^{i,k}} + e_{\mathrm{r,d},2}^{i,k}, \quad \forall k \in \mathbb{K}. \tag{5.57}$$

The statistics of the distortion term for the HD relay system can be expressed as

$$\mathbf{e}_{\mathrm{t,s},\mathcal{X}}^{k} \sim \mathcal{CN}\left(\mathbf{0}_{N_{\mathrm{BS}}}, \frac{1}{K}\widetilde{\mathbf{\Theta}}_{\mathrm{t,s}}\sum_{k\in\mathbb{K}}\mathrm{diag}\left(\mathbb{E}\{\widetilde{\mathbf{x}}_{\mathrm{s},\mathcal{X}}^{k}(\widetilde{\mathbf{x}}_{\mathrm{s},\mathcal{X}}^{k})^{H}\}\right)\right), \tag{5.58}$$

$$\mathbf{e}_{\mathrm{t,r},2}^{k} \sim \mathcal{CN}\left(\mathbf{0}_{N_{\mathrm{r}}}, \frac{1}{K}\widetilde{\mathbf{\Theta}}_{\mathrm{t,r}}\sum_{k\in\mathbb{K}}\mathrm{diag}\left(\mathbb{E}\{\widetilde{\mathbf{x}}_{\mathrm{r},2}^{k}(\widetilde{\mathbf{x}}_{\mathrm{r},2}^{k})^{H}\}\right)\right), \tag{5.59}$$

$$\mathbf{e}_{\mathrm{r,r},1}^{k} \sim \mathcal{CN}\left(0, \frac{\widetilde{\beta}_{\mathrm{r}}}{K}\sum_{k\in\mathbb{K}}\left(\mathbb{E}\{\widetilde{y}_{\mathrm{r},1}^{k}(\widetilde{y}_{\mathrm{r},1}^{k})^{H}\}\right)\right), \tag{5.60}$$

$$e_{\mathrm{r,d},\mathcal{X}}^{i,k} \sim \mathcal{CN}\left(0, \frac{\widetilde{\beta}_{\mathrm{d}}^{i}}{K}\sum_{k\in\mathbb{K}}\left(\mathbb{E}\{\widetilde{y}_{\mathrm{d},\mathcal{X}}^{i,k}(\widetilde{y}_{\mathrm{d},\mathcal{X}}^{i,k})^{H}\}\right)\right), \tag{5.61}$$

where $\mathcal{X} \in \{1, 2\}$.

The achievable rate for the BS to relay link using sub-carrier k during the first time slot can be obtained as

$$\begin{aligned} R_{\mathrm{sr,HD_1}}^{k} &= R_{\mathrm{sr,MU}}^{k}\left(\gamma_{\mathrm{rd,MU}}^{j,k,m} = 0, p_{\mathrm{rd}}^{j,m} = 0\right) \\ &= \gamma_0 \log_2\left(1 + \frac{|\widehat{\mathbf{h}}_{\mathrm{sr}}^{k}\mathbf{v}_{\mathrm{sr},1}^{k}|^2 p_{\mathrm{sr},1}^{k}}{\alpha_{\mathrm{r}}^{k} + \sum\limits_{m\in\mathbb{K}}\left(\gamma_{\mathrm{sr},1}^{km} p_{\mathrm{sr},1}^{m} + \sum\limits_{j\in\mathbb{L}}\gamma_{\mathrm{sd},1}^{j,k,m} p_{\mathrm{sd},1}^{j,m}\right)}\right), \end{aligned} \tag{5.62}$$

where $\gamma_{\mathrm{sr},1}^{km} = \gamma_{\mathrm{sr}}^{km}\left(\mathbf{v}_{\mathrm{sr}}^{m} = \mathbf{v}_{\mathrm{sr},1}^{m}\right)$ and $\gamma_{\mathrm{sd},1}^{j,k,m} = \gamma_{\mathrm{sd,MU}}^{j,k,m}\left(\mathbf{v}_{\mathrm{sd}}^{j,m} = \mathbf{v}_{\mathrm{sd},1}^{j,m}\right)$. The achievable information rate for the BS to user i using sub-carrier k can be formulated as

$$\begin{aligned} R_{\mathrm{sd,HD_1}}^{i,k} &= R_{\mathrm{sd,MU}}^{i,k}\left(\gamma_{\mathrm{rd,MU}}^{j,k,m} = 0, p_{\mathrm{rd}}^{j,m} = 0\right) \\ &= \log_2\left(1 + \frac{|\widehat{\mathbf{h}}_{\mathrm{sd}}^{i,k}\mathbf{v}_{\mathrm{sd},1}^{i,k}|^2 p_{\mathrm{sd},1}^{i,k}}{\alpha_{\mathrm{d}}^{i,k} + \sum\limits_{m\in\mathbb{K}}\left(\overline{\gamma}_{\mathrm{sr},1}^{i,k,m} p_{\mathrm{sr},1}^{m} + \sum\limits_{j\in\mathbb{L}}\widetilde{\gamma}_{\mathrm{sd},1}^{i,j,k,m} p_{\mathrm{sd},1}^{j,m}\right)}\right), \end{aligned} \tag{5.63}$$

where $\overline{\gamma}_{\mathrm{sr},1}^{i,k,m} = \overline{\gamma}_{\mathrm{sr,MU}}^{i,k,m}\left(\mathbf{v}_{\mathrm{sr}}^{m} = \mathbf{v}_{\mathrm{sr},1}^{m}\right)$ and $\widetilde{\gamma}_{\mathrm{sd},1}^{i,j,k,m} = \widetilde{\gamma}_{\mathrm{sd,MU}}^{i,j,k,m}\left(\mathbf{v}_{\mathrm{sd}}^{j,m} = \mathbf{v}_{\mathrm{sd},1}^{j,m}\right)$. Since there is no communication between the relay and user nodes during the first time slot, the achievable rate for relay-user links is considered to be zero, i.e., $R_{\mathrm{rd,HD}_1}^{i,k} = 0$.

Similarly, during the second time slot, the achievable rate between the BS and relay becomes zero as there is no communication between them, i.e., $R_{\mathrm{sr,HD}_2}^{k} = 0$. The achievable rate between the relay and user node i during the second time slot can be written as

$$\begin{aligned} R_{\mathrm{rd,HD}_2}^{i,k} &= R_{\mathrm{rd,MU}}^{i,k}\left(\overline{\gamma}_{\mathrm{sr,MU}}^{i,k,m} = 0, p_{\mathrm{sr}}^{m} = 0\right) \\ &= \log_2\left(1 + \frac{|\widehat{\mathbf{h}}_{\mathrm{rd}}^{i,k}\mathbf{v}_{\mathrm{rd},2}^{i,k}|^2 p_{\mathrm{rd},2}^{i,k}}{\alpha_{\mathrm{d}}^{i,k} + \sum\limits_{m\in\mathbb{K}}\sum\limits_{j\in\mathbb{L}}\left(\overline{\gamma}_{\mathrm{rd},2}^{i,j,k,m} p_{\mathrm{rd},2}^{j,m} + \overline{\gamma}_{\mathrm{sd},2}^{i,j,k,m} p_{\mathrm{sd},2}^{j,m}\right)}\right), \end{aligned} \tag{5.64}$$

where $\overline{\gamma}_{\mathrm{rd},2}^{i,j,k,m} = \overline{\gamma}_{\mathrm{rd,MU}}^{i,j,k,m}\left(\mathbf{v}_{\mathrm{rd}}^{j,m} = \mathbf{v}_{\mathrm{rd},2}^{j,m}\right)$ and $\overline{\gamma}_{\mathrm{sd},2}^{i,j,k,m} = \overline{\gamma}_{\mathrm{sd,MU}}^{i,j,k,m}\left(\mathbf{v}_{\mathrm{sd}}^{j,m} = \mathbf{v}_{\mathrm{sd},2}^{j,m}\right)$. Furthermore, the achievable rate between the BS and user node i during the second time slot can be written as

$$\begin{aligned} R_{\mathrm{sd,HD}_2}^{i,k} &= R_{\mathrm{sd,MU}}^{i,k}\left(\overline{\gamma}_{\mathrm{sr,MU}}^{i,k,m} = 0, p_{\mathrm{sr}}^{m} = 0\right) \\ &= \log_2\left(1 + \frac{|\widehat{\mathbf{h}}_{\mathrm{sd}}^{i,k}\mathbf{v}_{\mathrm{sd},2}^{i,k}|^2 p_{\mathrm{sd},2}^{i,k}}{\alpha_{\mathrm{d}}^{i,k} + \sum\limits_{m\in\mathbb{K}}\sum\limits_{j\in\mathbb{L}}\left(\overline{\gamma}_{\mathrm{rd},2}^{i,j,k,m} p_{\mathrm{rd},2}^{j,m} + \widetilde{\gamma}_{\mathrm{sd},2}^{i,j,k,m} p_{\mathrm{sd},2}^{j,m}\right)}\right), \end{aligned} \tag{5.65}$$

where $\widetilde{\gamma}_{\mathrm{sd},2}^{i,j,k,m} = \widetilde{\gamma}_{\mathrm{sd,MU}}^{i,j,k,m}\left(\mathbf{v}_{\mathrm{sd}}^{j,m} = \mathbf{v}_{\mathrm{sd},2}^{j,m}\right)$. The total achievable information rate for the HD relay system for the entire communication (both the time slots) can be formulated as

$$R_{HD} = \sum_{i\in\mathbb{L}}\sum_{k\in\mathbb{K}}\left(R_{\mathrm{sd,HD}_1}^{i,k} + R_{\mathrm{sd,HD}_2}^{i,k}\right) + \min\left\{\sum_{k\in\mathbb{K}} R_{\mathrm{sr,HD}_1}^{k}, \sum_{i\in\mathbb{L}}\sum_{k\in\mathbb{K}} R_{\mathrm{rd,HD}_2}^{i,k}\right\} \tag{5.66}$$

In order to compare it with the FD relay, we need to take the average of the achievable rate during the two slots. As a result, the sum-rate maximization problem for the HD relay case can be written as

$$\begin{aligned} \underset{\substack{p_{\mathrm{rd},2}^{i,k}\geq 0, p_{\mathrm{sr},1}^{k}\geq 0 \\ p_{\mathrm{sd},1}^{i,k}\geq 0, p_{\mathrm{sd},2}^{i,k}\geq 0, t}}{\text{maximize}} \quad & 0.5\left(\sum_{i\in\mathbb{L}}\sum_{k\in\mathbb{K}}\left(R_{\mathrm{sd,HD}_1}^{i,k} + R_{\mathrm{sd,HD}_2}^{i,k}\right) + t\right) \\ \text{subject to} \quad & \sum_{k\in\mathbb{K}} R_{\mathrm{sr,HD}_1}^{k} \geq t, \;\; \sum_{i\in\mathbb{L}}\sum_{k\in\mathbb{K}} R_{\mathrm{rd,HD}_2}^{i,k} \geq t, \\ & \sum_{i\in\mathbb{L}}\sum_{k\in\mathbb{K}} p_{\mathrm{rd},2}^{i,k} \leq P_{\mathrm{r}}, \sum_{i\in\mathbb{L}}\sum_{k\in\mathbb{K}} p_{\mathrm{sd},1}^{i,k} + \sum_{k\in\mathbb{K}} p_{\mathrm{sr},1}^{k} \leq P_{\mathrm{s}}, \sum_{i\in\mathbb{L}}\sum_{k\in\mathbb{K}} p_{\mathrm{sd},2}^{i,k} \leq P_{\mathrm{s}}. \end{aligned} \tag{5.67}$$

The above optimization problem follows the same structure as (5.52). Therefore it can be solved using similar steps as in algorithm 10. Algorithm 12 provides a detailed procedure of the algorithm.

Algorithm 12 For sum-rate maximization for half-duplex relay

1: $a \leftarrow 0$ (set iteration number to zero)
2: $p^{i,k}_{\mathrm{rd},2,0}, p^{i,k}_{\mathrm{sd},1,0}, p^{i,k}_{\mathrm{sd},2,0}, p^{k}_{\mathrm{sr},1,0} \leftarrow$ feasible power value initialization
3: **repeat**
4: $\quad a \leftarrow a + 1$
5: $\quad p^{i,k}_{\mathrm{rd},2}, p^{i,k}_{\mathrm{sd},1}, p^{i,k}_{\mathrm{sd},2}, p^{k}_{\mathrm{sr},1}, t \leftarrow$ solve (5.67)
6: $\quad p^{i,k}_{\mathrm{rd},2,0}, p^{i,k}_{\mathrm{sd},1,0}, p^{i,k}_{\mathrm{sd},2,0}, p^{k}_{\mathrm{sr},1,0} \leftarrow p^{i,k}_{\mathrm{rd},2,0} = p^{i,k}_{\mathrm{rd},2}, p^{i,k}_{\mathrm{sd},1,0} = p^{i,k}_{\mathrm{sd},1}, p^{i,k}_{\mathrm{sd},2,0} = p^{i,k}_{\mathrm{sd},2}$, and $p^{k}_{\mathrm{sr},1,0} = p^{k}_{\mathrm{sr},1}$, respectively
7: **until** a stable point, or maximum number of a reached
8: **return** $\{p^{i,k}_{\mathrm{rd},2}, p^{i,k}_{\mathrm{sd},1}, p^{i,k}_{\mathrm{sd},2}, p^{k}_{\mathrm{sr},1}\}$

5.7 Performance Evaluations

By using numerical simulations, we evaluate the performance of the proposed algorithms (Algorithm 10, Algorithm 11 and Algorithm 12) for a relay-assisted OFDM downlink communication. We consider the MRT/MRC strategy as our transmit precoder and receive filters at the BS as well as the relay. All communication channels follow an uncorrelated Rayleigh flat fading model. The SI channel follows the characterization reported in [20], i.e., $\mathbf{h}_{rr} \sim \mathcal{CN}\left(\sqrt{\frac{\rho_{si} K_R}{1+K_R}}\mathbf{h}_0, \frac{\rho_{si}}{1+K_R}\mathbf{I}_{N_r}\right)$, where ρ_{si} is the SI channel strength, $\mathbf{h}_0$ is a deterministic vector of all-1 elements, and K_R is the Rician coefficient. The overall system performance is then averaged over 250 channel realizations.

Comparison Benchmarks

The following performance benchmarks are evaluated to provide a meaningful comparison:

- **SuIC:**[3] It represents the proposed algorithm (Algorithm 10/Algorithm 11), which consider the impact of the harware distortion as well as the imperfect CSI.
- **SuIC-ND:** The algorithm does not consider hardware distortion (non-distortion (ND)), i.e, a perfect hardware is assumed and only the impact of CSI is taken into consideration.
- **ODL:**[4] The case where only the direct link is available,. i.e, there is no relay in the system.
- **ORL:**[4] The case where only the relay link is available. The user does not employ SuIC scheme, and the signal from the BS is considered as interference.

[3]results from single connectivity that perform better are used as the feasible power value initialization for DuC algorithms
[4]uniform power initialization is used for single connectivity algorithms

- **HD:** It represents the proposed algorithm (Algorithm 12) introduced in Section 5.6.3, where a HD relay is employed. The SuIC scheme is only utilize in the second time slot.

Single-user Scenario

In this section, we evaluate the performance of the proposed algorithm (Algorithm 10) introduced in Section 5.5, where the relay is a single antenna FD node. For numerical analysis, the default parameter values for single-user scenario are chosen as in Table 5.1.

$\overline{\overline{\mathbb{K}}} = K$	4
N_{BS}	32
$\rho = \rho_{\text{sr}} = \rho_{\text{rd}}$	-10dB
ρ_{sd}, ρ_{si}, K_R	-30 dB, 0 dB, 10
$\sigma_{\text{n}}^2 = \sigma_{\text{r},k}^2 = \sigma_{\text{d},k}^2$	-40 dB
$P_{\text{s}}, P_{\text{r}}$	0 dB, -10dB
$\sigma_e^2 = (\sigma_{e,\text{sr}}^k)^2 = (\sigma_{e,\text{rd}}^k)^2 = (\sigma_{e,\text{sd}}^k)^2 = (\sigma_{e,\text{rr}}^k)^2$	-50 dB
$\kappa = \beta, \mathbf{\Theta}_{\text{t},S} = \kappa \mathbf{I}_N$	-30dB

Table 5.1: Default simulation setup for single-user scenario

In Fig. 5.3a, the performance of Algorithm 10 in terms of system sum-rate is evaluated against the strength of the DL. As the strength of DL increases, it can be observed that the performance of all the algorithms expect only relay link (ORL) improves. As expected, the sum-rate attained by only direct link (ODL) increases as the strength of the DL increases. When the strength of the DL is weak, the algorithms SuIC and SuIC-ND communicates with the user equipment (UE) only using the RL. As the strength of DL rises, the algorithms utilize both the DL and the RL. As the DL becomes stronger compared to RL, the algorithms utilize only the DL. Furthermore, the ORL performance degrades for strong DL as the UE suffers from substantial interference from the BS through DL.

In Fig. 5.3b, the performance of our proposed algorithm is plotted in terms of total sum-rate, for different values of receiver noise at the user and the relay (σ_n^2). As we expected, the sum-rate decreases as the noise increases, i.e., lower sum-rate for higher noise values. It is clear that the proposed algorithm (SuIC) outperforms all the other benchmarks. We can also notice that at high signal to noise ratio (SNR) scenario, the SuIC-ND algorithm performs worse compared to the SuIC algorithm as the impact of hardware distortion becomes dominant.

Fig. 5.3c illustrates the system performance for different values of hardware inaccuracy $\kappa = \beta$. It can be observed that as the hardware inaccuracy increases the performance of all the algorithms in terms of sum-rate decreases. The proposed algorithm SuIC

outperforms all the other benchmarks. When the values the hardware inaccuracy κ becomes large, the performance of SuIC-ND algorithm degrades compared to SuIC. This signifies that the consideration of hardware distortion for DuC scenario utilizing FD relay.

In Fig. 5.3d, the dependency of Algorithm 10 in terms of system sum-rate on the channel estimation error is plotted. It can be observed that as the channel estimation error increases the performance of all the algorithms decreases. The performance of the ORL degrades rapidly compared to the ODL shows that the impact of channel estimation error in SIC at the FD relay. At lower values of channel estimation error, the hardware inaccuracy κ becomes the dominant factor resulting in performance degradation of SuIC-ND algorithms.

Multi-user Scenario

In this section, we evaluate the performance of the proposed algorithms (Algorithms 11 and 12) introduced in Section 5.6 for multi-user scenario. For simulations, we consider a circular cell with BS at the center. The distance between the relay and the BS is fixed. Since the relay is stationary and it knows from which direction it will receive the signal from the BS, the BS can communicate with the relay using a strong directive channel, i.e., the better antenna gain can be achieved between the BS and the relay. We also assume that all users are operated within the vicinity of the relay and have a line of sight (LOS). The BS only opts for the DuC approach for the user which are within the vicinity of the relay. In order to provide fairness in resource allocation, the transmit power budget is restricted to support the number of active sub-carriers ($\overline{\overline{\mathbb{K}}}$), i.e., the transmit power budgets are factorized by k_t, where $k_t = \overline{\overline{\mathbb{K}}}/\overline{\overline{\mathbb{K}}}_{\text{sys}}$. $\overline{\overline{\mathbb{K}}}_{\text{sys}}$ denotes the total number of sub-carriers available in the system. For the numerical simulations, we adapt our system parameters from [93, 3GPP LTE Specifications], and our default system parameters are chosen as in Tables 5.2. The channels between the BS and users are assumed to obtain a LOS with the probability

$$P_{LOS}(d) = \min(0.018/d, 1) \times (1 - exp(-d/0.063)) + exp(-d/0.063), \tag{5.68}$$

where d is the distance between the BS and users in km.

Visualization

Figs. 5.4a and 5.4b portrait the system performance with respect to the strength of the direct channel between the BS and the UE in terms of antenna gain and transmit power at the BS, respectively. It can be observed that as the antenna gain between the BS and UE (direct link) increases, the performance of all the algorithms except ORL increases. A similar trend can be seen in the plot concerning the maximum transmit power at the BS. Another interesting observation is regarding the robustness of the

Carrier center frequency and system bandwidth	2 GHz and 10MHz
Number of available sub-carrier ($\overline{\mathbb{K}}_{\text{sys}}$) and sub-carrier spacing	600 and 15kHz
Number of active sub-carriers ($\overline{\mathbb{K}}$)	12
Number of users ($\overline{\mathbb{L}}$)	4
Maximum service distance of the BS and the relay	500m and 100m,
Maximum transmit power at the BS and the relay	30dBm and 27dBm
Number of transmit antennas at the BS and the relay	32 and 16
Distance between BS and relay	400m
Receive antenna gain at the relay	20dBi
Pathloss (dB) between BS and users (d in km)	LOS: $103.4 + 24.2\log_{10}(d)$ NLOS: $131.1 + 42.8\log_{10}(d)$
Pathloss (dB) between BS and relay (d in km)	LOS: $100.7 + 23.5\log_{10}(d)$
Pathloss (dB) between relay and users (d in km)	LOS: $103.8 + 20.9\log_{10}(d)$
Shadowing standard deviation	Between BS and relay: 6dB Between BS and UE: 10dB Between relay and UE: 10dB
Thermal noise density	-174dBm/Hz
Noise figure at relay and UE	5dB and 9dB
Hardware distortion coefficient $\kappa = \beta$	-50dB
SI channel strength after SIC ρ_{si} and Rician coefficient K_{R}	-90dB and 10
Covariance of the CSI estimation error $(\sigma^k_{\epsilon,\text{sr}})^2 = (\sigma^k_{\epsilon,\text{rd}})^2 = (\sigma^k_{\epsilon,\text{sd}})^2 = (\sigma^k_{\epsilon,\text{rr}})^2 \forall k \in \mathbb{K}$,	-150dB

Table 5.2: Default system parameters used for multi-user scenario

SuIC against unexpected blockage. For lower values of antenna gain, for instance, in case of blockage the strength of the channel reduces drastically, the SuIC utilizes only the RL, thereby providing better throughput compared to ODL case. As the strength of the DL increases, SuIC utilizes both the links resulting in better performance compared to the ODL and ORL case and also becomes more robust to blockage. This implies the benefit of DuC compared to single-connectivity schemes, especially in case of blockage. Moreover, for weak DL scenario, the SuIC-ND becomes worst compared to ORL and SuIC algorithms; this is because the UE is connected to BS only through an FD relay, where hardware distortion is dominant.

Fig. 5.4c illustrates the performance of the algorithm in terms of system sum-rate for different values of transceiver inaccuracy κ dB. As it can be observed, the performance of the system decreases as the transceiver hardware distortion increases. Since the ORL operates in FD mode, the performance of ORL degrades more compared to other algorithms as the hardware-distortion increases. This shows the impact of hardware-distortion in FD system in the presence of SI. It can also be noticed that the SuIC algorithm utilizes only the RL when the hardware inaccuracy is small. As the hardware inaccuracy increases, the performance of the SuIC also decreases. However, It can be seen that when the algorithms ORL and ODL have similar performance, the performance gain of SuIC attains maximum compared to ORL and ODL. For higher values

of hardware inaccuracy, the RL is severely affected by hardware distortion due to SI, the SuIC opts the DL, thereby reducing its impact. Furthermore, the proposed SuIC algorithm always performs better compared to SuIC-ND algorithm. This indicates that the consideration of hardware-distortion in designing the system will improve the overall performance of the system.

In Fig. 5.4d, the impact of the UE receiver noise in the system performance is depicted. As expected, the sum-rate of the system decreases as the receiver noise at the UE increases. As we considered the strength of DL is weaker compared to the RL in the system, the performance of ODL degrades more compared to other algorithms as the UE receiver noise increases. For higher values of UE receiver noise, the SuIC utilizes the RL more where the hardware distortion becomes dominant due to SI, resulting in more performance gain of SuIC compared to SuIC-ND. Furthermore, the performance of the system is evaluated with respect to the channel estimation error in Fig. 5.4e. A similar trend can be observed that the performance of all the algorithms degrades as the channel estimation error increases. For small values of channel estimation error, the hardware distortion becomes dominant, thus resulting in better performance of SuIC algorithm compared to the SuIC-ND algorithm.

In Fig. 5.4f, the performance of the system is evaluated with respect to the probability of LOS (P_{LOS}) of the direct channel between the BS and the UE. As it can be clearly observed, the performance of all the algorithms except for ORL increases as P_{LOS} increases. Another interesting observation is that the performance gap between the SuIC and SuIC-ND reduces as P_{LOS} increases since the SuIC algorithm uses the DL when BS has LOS with its UEs, i.e., P_{LOS} has a higher value.

In Figs. 5.5a to 5.5b, the system performance is evaluated for different parameters of the relay. Fig. 5.5a plots the performance of the system with respect to the maximum transmit power available at the relay. As expected, the performance of all the algorithms except ODL improves as the maximum transmit power available at the relay increases. A similar trend in the performance of the system is observed for the different number of transmit antenna used at the relay in fig. 5.5b. Furthermore, in 5.5c, the performance of the system is evaluated for different values of receiver noise at the relay. The performance of all the algorithms except ODL degrades as the receiver noise at the relay increases. However, as the receiver noise decreases, the SuIC-ND performance degrades compared to the SuIC, due to the fact that the hardware distortion becomes dominant when the receiver noise becomes small. It can also be noticed that, as the receiver noise at the relay increases, the performance of ORL decreases while the performance of ODL remains almost similar. The SuIC shows slightly better performance compared to ORL for higher values of receiver noise at the relay as it also utilizes the DL.

5.8 Conclusions

In this chapter, we investigated an FD DF relay assisted downlink communication between an mMIMO MC BS and HD MC single antenna user nodes. We considered the scenario, where the BS simultaneously utilizes both the direct link as well as the relay link to communicate with the user node to improve the spectral efficiency of the system. In the user node, a SuIC approach is employed to enable DuC. The impact of hardware distortions resulting in residual self-interference and ICL, and also imperfect CSI are considered to model the system. A joint sub-carrier and power allocation problem to maximize the total sum-rate of the system is studied. An iterative optimization method is proposed, to solve the non-convex resource allocation problem, which follows the SIA framework to reach the convergence point that satisfies the KKT optimality conditions. The case of SuIC approach using HD relay is also investigated. Numerical results show that our SuIC approach performs better compared to single-connectivity and HD schemes, and also implies the importance of the hardware-distortion aware system. It is also observed that the proposed SuIC approach shows higher robustness when one of the active links experience an unexpected blockage.

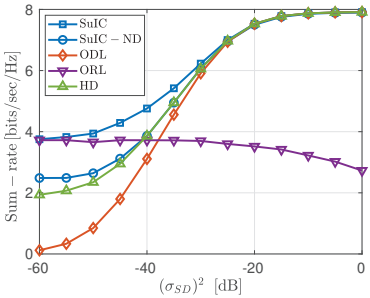

(a) Sum-rate vs. Direct channel strength

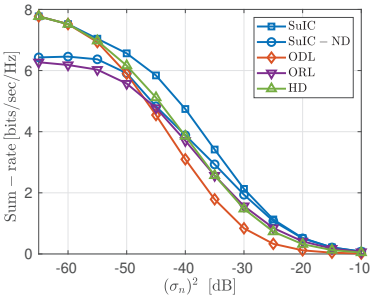

(b) Sum-rate vs. Receiver noise at relay and UE

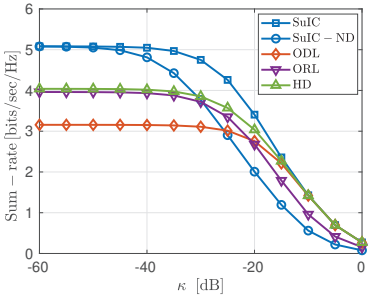

(c) Sum-rate vs. Hardware inaccuracy.

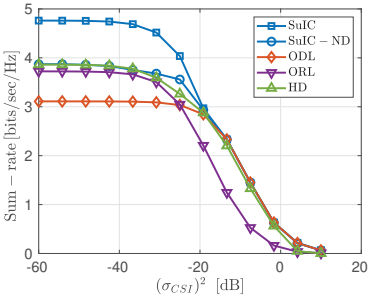

(d) Sum-rate vs. Channel estimation error

Figure 5.3: Sum-rate for single-user scenario vs. different system parameters

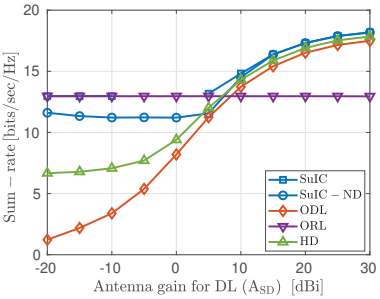

(a) Sum-rate vs. Antenna gain between BS and UE

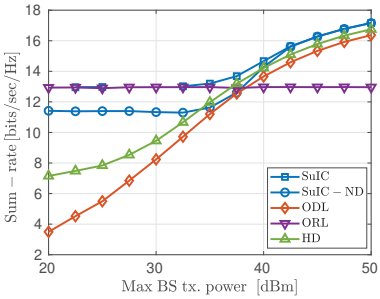

(b) Sum-rate vs. Maximum transmit power at BS

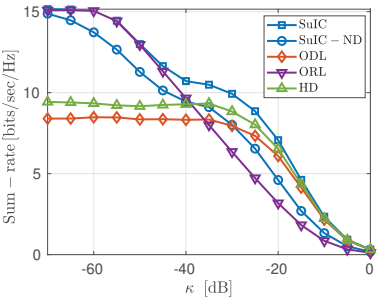

(c) Sum-rate vs. Hardware inaccuracy

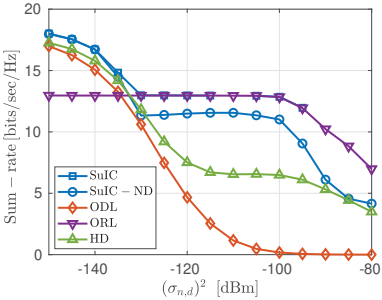

(d) Sum-rate vs. Receiver noise at the UE

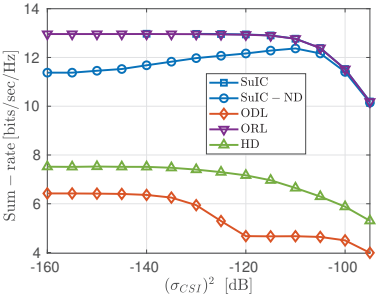

(e) Sum-rate vs. Channel estimation error

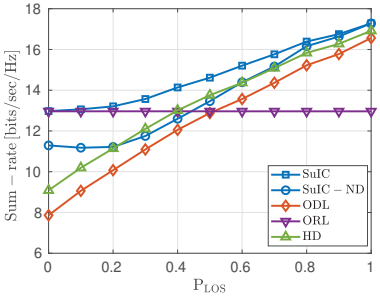

(f) Sum-rate vs. Probability of LOS between BS and UE

Figure 5.4: Sum-rate for multi-user scenario vs. Different system parameters.

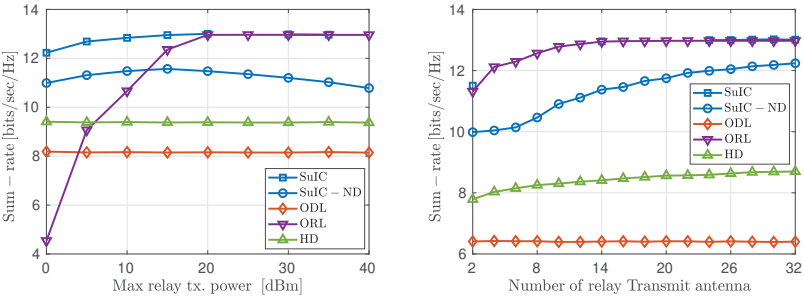

(a) Sum-rate vs. Maximum relay transmit power

(b) Sum-rate vs. Number of relay transmit antenna

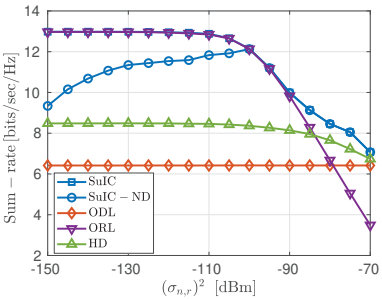

(c) Sum-rate vs. Receiver noise at the relay

Figure 5.5: Sum-rate for multi-user scenario vs. Different relay system parameters.

6 Conclusions

In this dissertation, the resource allocation problem for FD multi-antenna MC systems has been investigated. The impact of hardware distortions leading to residual SI and ICL are considered under the imperfect CSI condition. We mainly focused on the relaying system, where the relay uses the DF relaying protocol as AF relaying results in distortion loop interference.

In Chapter 2, we addressed a transceiver design problem for an FD MIMO MC DF relay system, where source, relay and destination are MIMO nodes. In addition to the traditional per-carrier DF relay, a joint sub-carrier DF relay is also considered which takes advantage of group-wise decoding and encoding. It also provides more flexibility by jointly considering the optimization constraints over all the sub-carriers. It is observed that, due to the SI, the impact of non-linear hardware distortions leading to residual SI and ICL becomes crucial for an FD MC system. Consideration of the impact of channel estimation error is also significant to improve the energy efficiency of the system. The power consumed for channel estimation has to be restricted with power constraints, otherwise only less power will be available for transmission results in energy efficiency degradation. Hence, it is vital to consider the impact of non-linear hardware distortions as well as channel estimation error in designing an FD MIMO MC DF relay system.

In Chapter 3, a joint sub-carrier and power allocation problem is investigated for an FD mMIMO MC DF relay system which serves multiple HD single antenna source-destination pairs. Preference of using inexpensive transmit and receive chains components to make the system with large antenna array cost-efficient, results in more hardware distortions. It becomes unfavorable for an FD MC system, as it introduces more residual SI and ICL, due to strong SI . The asymptotic rate of our system employed with the MRT/MRC strategy is analyzed when the number of the antenna becomes large (goes to ∞). It is noticed that the achievable rate for an FD MC DF relay system, where the relay is equipped with a large number of antennas ($N \to \infty$), is restricted by the hardware distortions at the single antenna source and destination nodes. This implies the significance of distortion-aware design for an multi-user FD mMIMO MC relay system. In addition to the prior studies focusing on maximizing the sum-rate and energy efficiency, we also focused on minimizing the overall delivery time for a given set of communication tasks to the user terminals. It is beneficial to consider delivery time as an objective as maximizing the throughput/sum-rate of the system does not necessarily minimize the overall delivery time.

In Chapter 4, bidirectional communication between an FD mMIMO MC BS with multiple FD single antenna user nodes is investigated. Utilizing FD capability at both the BS and end-user allows operating uplink and downlink in the same frequency-time channel. This results in higher spectral efficiency, but the system also suffers from multi-user interference and SI . However, taking advantage of a large antenna array which provides more spatial diversity compared to MIMO system helps to reduce the overall interference of the system. For both the relay and the bidirectional communication scenarios, it is observed that the performance of the system can be improved by considering the impact of hardware distortions and imperfect CSI . It is also observed that by employing the null-space projection SI suppression scheme along with linear transceiver strategies such as MRT/MRC, ZF, at the transmit side of relay/BS provides a gain in system performance.

Finally, in Chapter 5, the problem of resource allocation for the downlink of an FD relay-assisted MC communication network, where an mMIMO MC BS communicates with multiple single antenna user nodes. By making use of the direct channel, which is usually considered as interference, the robustness and performance of the system can be improved. In particular, we consider a scenario that simultaneously activates the relay as well as the direct channel for communicating separate data streams, by employing SuIC at the end-user. As a result, the downlink communication data can be interchangeably loaded to separate sub-carriers, employing an orthogonal MC strategy, or to different available links, i.e., direct or FD relay link, employing the non-orthogonal SuIC at the receiver. In addition to the superior performance under various system conditions, the proposed dual-connectivity becomes robust when one of the active paths experiences an unexpected blockage. It is observed that a significant performance and robustness gain can be attained by enabling dual-connectivity utilizing FD relay when compared to the previously proposed single-connectivity and HD schemes. It is also noticed that the hardware-distortion aware design is important for such system, especially when the hardware accuracy degrades.

6.1 Outlook

In case of the FD MIMO MC relay system, Chapter 2, the performance of a DF relay is studied. It would be interesting to extend this study to other relay protocols, such as compress and forward relay protocol where quantization noise also needs to consider, or AF relaying protocol where a different approach is required to mitigate the distortion loop.

In Chapter 3, we considered an FD mMIMO MC DF relay, by limiting the number of antennas at the source/destination to one. An extension of this would be to investigate the system with multiple-antenna source-destination nodes. Another interesting continuation of this work will be consideration of systems with hybrid beamforming design for mMIMO array. Similarly, the system in Chapter 4 can also be extended to a system

with multiple-antenna users and also mMIMO BS antenna array with hybrid beamforming design. Moreover, it would be interesting to extend the provided bi-directional communication system to a cell-free mMIMO scenario, where different antenna arrays are kept in different locations.

For the DuC system, Chapter 5, a possible continuation of the provided framework would be to investigate a system having multiple relays. Here the end terminals can access more stream from different relays and BS, thereby increasing the overall throughput of the system. It is beneficial to extend the proposed design framework to other system design objectives, such as energy efficiency maximization, power minimization, caching memory minimization and delivery time minimization.

In this thesis, we considered only the hardware distortions that can be modeled into noise that is additive in nature, such as ADC/DAC impairments, the non-linearity of the power amplifier, to name a few. However, there exists another category of hardware distortions, for instance, distortions due to phase drifts from the local oscillators, that are multiplicative in nature to the channel vector. It would be promising to extend the studied framework by including these hardware distortions. Furthermore, it will be interesting to extend the studied framework of this thesis to systems in which passive relay such as intelligent-reflecting-surface (IRS) is also incorporated. Another promising direction to extend this thesis is to investigate the utilization of machine learning algorithms to tackle resource allocation problems.

List of Acronyms

3GPP	3rd Generation Partnership Project
4G	Fourth-generation
5G	Fifth-generation
ADC	Analog to digital converter
AF	Amplify and forward
AGC	Automatic gain control
AQCP	Alternating quadratic convex program
BS	Base station
CDMA	Code division multiple access
CP	Cyclic prefix
CQP	Conic quadratic program
CSI	Channel state information
CT	Computational time
DAC	Digital to analog converter
DC	Difference-of-convex
DF	Decode and forward
DL	Direct link
DuC	Dual connectivity
FBMC	Filter bank multi carrier
FD	Full-duplex
FDMA	Frequency division multiple access
GFDM	Generalised frequency division multiplexing
HD	Half-duplex
ICL	Inter-carrier leakage

i.i.d.	Independent and identically distributed
IRS	Intelligent-reflecting-surface
JC	Joint-carrier
KKT	Karush–Kuhn–Tucker
LD	Less distortion
LOS	Line of sight
LTE	Long time evolution
MC	Multi-carrier
MeNB	Master evolved Node B
MIMO	Multiple input multiple output
mMIMO	Massive multiple input multiple output
MMSE	Minimum mean square error
MRC	Maximum ratio combining
MRT	Maximum ratio transmitting
MSE	Mean square error
ND	Non-distortion
NLOS	Non-line of sight
NOMA	Non-orthogonal multiple access
NR	New Radio
ODL	Only direct link
OFDM	Orthogonal frequency division multiplexing
ORL	Only relay link
OVSF	Orthogonal variable spreading factor
PC	Per-carrier
QoS	Quality of service
RF	Radio frequency
RL	Relay link
RS	Rate-splitting
RSM	Right-singular matrix

SeNB	Secondary evolved Node B
SI	Self-interference
SIA	Successive inner approximation
SIC	Self-interference cancellation
SINR	Signal to interference plus noise ratio
SNR	Signal to noise ratio
SuIC	Successive interference cancellation
SWIPT	Simultaneous wireless information and power transfer
TDMA	Time division multiple access
TDD	Time division duplex
UE	User equipment
WMMSE	Weighted minimum mean square error
Wo-CSI	Without channel state information error
ZF	Zero-forcing
ZFT	Zero-forcing transmitting
ZFR	Zero-forcing receiving

Bibliography

[1] J. I. Choi, M. Jain, K. Srinivasan, P. Levis, and S. Katti, "Achieving Single Channel, Full Duplex Wireless Communication," in *Proceedings of the Sixteenth Annual International Conference on Mobile Computing and Networking*, ser. MobiCom '10, 2010, pp. 1–12.

[2] A. S. E. Everett and A. Sabharwal, "Passive Self-Interference Suppression for Full-Duplex Infrastructure Nodes," *IEEE Transactions on Wireless Communications*, vol. 13, pp. 680–694, 2014.

[3] T. Riihonen and R. Wichman, "Analog and digital self-interference cancellation in full-duplex MIMO-OFDM transceivers with limited resolution in A/D conversion," in *2012 Conference Record of the Forty Sixth Asilomar Conference on Signals, Systems and Computers (ASILOMAR)*, Nov 2012, pp. 45–49.

[4] M. S. Sim, M. Chung, D. Kim, J. Chung, D. K. Kim, and C. Chae, "Nonlinear Self-Interference Cancellation for Full-Duplex Radios: From Link- and System-Level Performance Perspectives," *CoRR*, vol. abs/1607.01912, 2016. [Online]. Available: http://arxiv.org/abs/1607.01912

[5] T. Riihonen, S. Werner, and R. Wichman, "Mitigation of loopback self-interference in full-duplex mimo relays," *IEEE Transactions on Signal Processing*, vol. 59, no. 12, pp. 5983–5993, Dec 2011.

[6] S. Hong, J. Brand, J. Choi, M. Jain, J. Mehlman, S. Katti, and P. Levis, "Applications of self-interference cancellation in 5G and beyond," *IEEE Communications Magazine*, vol. 52, pp. 114–121, 2014.

[7] R. A. Pitaval, O. Tirkkonen, R. Wichman, K. Pajukoski, E. Lahetkangas, and E. Tiirola, "Full-duplex self-backhauling for small-cell 5G networks," *IEEE Wireless Communications*, vol. 22, no. 5, pp. 83–89, October 2015.

[8] D. Bharadia and S. Katti, "Full Duplex MIMO Radios," in *11th USENIX Symposium on Networked Systems Design and Implementation (NSDI 14)*. Seattle, WA: USENIX Association, 2014, pp. 359–372. [Online]. Available: https://www.usenix.org/conference/nsdi14/technical-sessions/bharadia

[9] A. Sabharwal, P. Schniter, D. Guo, D. W. Bliss, S. Rangarajan, and R. Wichman, "In-Band Full-Duplex Wireless: Challenges and Opportunities," *IEEE Journal on Selected Areas in Communications*, vol. 32, no. 9, pp. 1637–1652, Sept 2014.

[10] J. Liu, J. Dai, J. Wang, X. Yin, Z. Jiang, and J. Wang, "Achievable rates for full-duplex massive mimo systems with low-resolution adcs/dacs under imperfect csi environment," *EURASIP Journal on Wireless Communications and Networking*, vol. 2018, no. 1, p. 222, Sep 2018.

[11] 3GPP, "Tech. Spec. Group Radio Access Network; New Radio (NR); Overall description; Stage-2," 3rd Generation Partnership Project (3GPP), Technical specification (TS) 38.300, Dec 2018, version 15.4.0. [Online]. Available: https://portal.3gpp.org/desktopmodules/Specifications/SpecificationDetails.aspx?specificationId=3191

[12] P. Guan, D. Wu, T. Tian, J. Zhou, X. Zhang, L. Gu, A. Benjebbour, M. Iwabuchi, and Y. Kishiyama, "5g field trials: Ofdm-based waveforms and mixed numerologies," *IEEE Journal on Selected Areas in Communications*, vol. 35, no. 6, pp. 1234–1243, 2017.

[13] T. Dinc, A. Chakrabarti, and H. Krishnaswamy, "A 60 ghz same-channel full-duplex cmos transceiver and link based on reconfigurable polarization-based antenna cancellation," in *2015 IEEE Radio Frequency Integrated Circuits Symposium (RFIC)*, May 2015, pp. 31–34.

[14] D. Bharadia, E. McMilin, and S. Katti, "Full duplex radios," in *Proceedings of the ACM SIGCOMM 2013 conference on SIGCOMM*, 2013, pp. 375–386.

[15] A. K. Khandani, "Methods for spatial multiplexing of wireless two-way channels," October 2010, US Patent US7817641B1.

[16] M. A. Khojastepour, K. Sundaresan, S. Rangarajan, X. Zhang, and S. Barghi, "The case for antenna cancellation for scalable full-duplex wireless communications," in *Proceedings of the 10th ACM Workshop on Hot Topics in Networks*, ser. HotNets-X. New York, NY, USA: Association for Computing Machinery, 2011. [Online]. Available: https://doi.org/10.1145/2070562.2070579

[17] A. K. Khandani, "Two-way (true full-duplex) wireless," in *2013 13th Canadian Workshop on Information Theory*, June 2013, pp. 33–38.

[18] M. Jain, J. I. Choi, T. Kim, D. Bharadia, S. Seth, K. Srinivasan, P. Levis, S. Katti, and P. Sinha, "Practical, real-time, full duplex wireless," in *Proceedings of the 17th Annual International Conference on Mobile Computing and Networking*, ser. MobiCom '11. New York, NY, USA: Association for Computing Machinery, 2011, p. 301–312. [Online]. Available: https://doi.org/10.1145/2030613.2030647

[19] M. Duarte and A. Sabharwal, "Full-duplex wireless communications using off-the-shelf radios: Feasibility and first results," in *2010 Conference Record of the Forty Fourth Asilomar Conference on Signals, Systems and Computers*, Nov 2010, pp. 1558–1562.

[20] M. Duarte, C. Dick, and A. Sabharwal, "Experiment-Driven Characterization of Full-Duplex Wireless Systems," *IEEE Transactions on Wireless Communications*, vol. 11, no. 12, pp. 4296–4307, December 2012.

[21] R. Askar, B. Schubert, W. Keusgen, and T. Haustein, "Agile full-duplex transceiver: The concept and self-interference channel characteristics," in *European Wireless 2016; 22th European Wireless Conference*, May 2016, pp. 1–7.

[22] E. Everett, M. Duarte, C. Dick, and A. Sabharwal, "Empowering full-duplex wireless communication by exploiting directional diversity," in *2011 Conference Record of the Forty Fifth Asilomar Conference on Signals, Systems and Computers (ASILOMAR)*, Nov 2011, pp. 2002–2006.

[23] E. Everett, C. Shepard, L. Zhong, and A. Sabharwal, "Softnull: Many-antenna full-duplex wireless via digital beamforming," *IEEE Transactions on Wireless Communications*, vol. 15, no. 12, pp. 8077–8092, Dec 2016.

[24] D. W. Bliss, P. A. Parker, and A. R. Margetts, "Simultaneous transmission and reception for improved wireless network performance," in *2007 IEEE/SP 14th Workshop on Statistical Signal Processing*, Aug 2007, pp. 478–482.

[25] O. Taghizadeh, J. Zhang, and M. Haardt, "Transmit beamforming aided amplify-and-forward mimo full-duplex relaying with limited dynamic range," *Signal Process.*, vol. 127, no. C, p. 266–281, Oct. 2016. [Online]. Available: https://doi.org/10.1016/j.sigpro.2016.02.026

[26] P. Lioliou, M. Viberg, M. Coldrey, and F. Athley, "Self-interference suppression in full-duplex mimo relays," in *2010 Conference Record of the Forty Fourth Asilomar Conference on Signals, Systems and Computers*, Nov 2010, pp. 658–662.

[27] L. Anttila, D. Korpi, V. Syrjälä, and M. Valkama, "Cancellation of power amplifier induced nonlinear self-interference in full-duplex transceivers," in *2013 Asilomar Conference on Signals, Systems and Computers*, Nov 2013, pp. 1193–1198.

[28] R. Li, A. Masmoudi, and T. Le-Ngoc, "Self-interference cancellation with nonlinearity and phase-noise suppression in full-duplex systems," *IEEE Transactions on Vehicular Technology*, vol. 67, no. 3, pp. 2118–2129, March 2018.

[29] M. Heino, D. Korpi, T. Huusari, E. Antonio-Rodriguez, S. Venkatasubramanian, T. Riihonen, L. Anttila, C. Icheln, K. Haneda, R. Wichman, and M. Valkama, "Recent advances in antenna design and interference cancellation algorithms for in-band full duplex relays," *IEEE Communications Magazine*, vol. 53, no. 5, pp. 91–101, May 2015.

[30] E. Ahmed and A. M. Eltawil, "All-digital self-interference cancellation technique for full-duplex systems," *IEEE Transactions on Wireless Communications*, vol. 14, no. 7, pp. 3519–3532, July 2015.

[31] H. Vogt, G. Enzner, and A. Sezgin, "State-space adaptive nonlinear self-interference cancellation for full-duplex communication," *IEEE Transactions on Signal Processing*, vol. 67, no. 11, pp. 2810–2825, June 2019.

[32] G. Liu, F. R. Yu, H. Ji, V. C. M. Leung, and X. Li, "In-band full-duplex relaying: A survey, research issues and challenges," *IEEE Communications Surveys Tutorials*, vol. 17, no. 2, pp. 500–524, Secondquarter 2015.

[33] Y. Lim, D. Hong, and C. Chae, "Performance analysis of self-interference cancellation in full-duplex large-scale mimo systems," in *2016 IEEE Global Communications Conference (GLOBECOM)*, Dec 2016, pp. 1–6.

[34] O. Taghizadeh, M. Rothe, A. C. Cirik, and R. Mathar, "Distortion-loop analysis for full-duplex amplify-and-forward relaying in cooperative multicast scenarios," in *2015 9th International Conference on Signal Processing and Communication Systems (ICSPCS)*, Dec 2015, pp. 1–9.

[35] S. Li, K. Yang, M. Zhou, J. Wu, L. Song, Y. Li, and H. Li, "Full-duplex amplify-and-forward relaying: Power and location optimization," *IEEE Transactions on Vehicular Technology*, vol. 66, no. 9, pp. 8458–8468, Sept 2017.

[36] O. Taghizadeh, A. C. Cirik, and R. Mathar, "Hardware impairments aware transceiver design for full-duplex amplify-and-forward MIMO relaying," *IEEE Transactions on Wireless Communications*, vol. 17, no. 3, pp. 1644–1659, Mar. 2018.

[37] O. Taghizadeh and R. Mathar, "Robust Multi-User Decode-and-Forward Relaying with Full-Duplex Operation," in *The Eleventh International Symposium on Wireless Communication Systems (ISWYS 2014)*, Barcelona, Spain, Sep 2014, pp. 1–7.

[38] X. Xia, D. Zhang, K. Xu, W. Ma, and Y. Xu, "Hardware impairments aware transceiver for full-duplex massive mimo relaying," *IEEE Transactions on Signal Processing*, vol. 63, no. 24, pp. 6565–6580, Dec 2015.

[39] Z. Wei, X. Zhu, S. Sun, and Y. Huang, "Energy-efficiency-oriented cross-layer resource allocation for multiuser full-duplex decode-and-forward indoor relay systems at 60 ghz," *IEEE Journal on Selected Areas in Communications*, vol. 34, no. 12, pp. 3366–3379, Dec 2016.

[40] H. Liu, K. J. Kim, K. S. Kwak, and H. V. Poor, "Power splitting-based swipt with decode-and-forward full-duplex relaying," *IEEE Transactions on Wireless Communications*, vol. 15, pp. 7561–7577, 2016.

[41] Z. Wen, X. Liu, N. C. Beaulieu, R. Wang, and S. Wang, "Joint source and relay beamforming design for full-duplex mimo af relay swipt systems," *IEEE Communications Letters*, vol. 20, pp. 320–323, 2016.

[42] Y. Zeng and R. Zhang, "Full-duplex wireless-powered relay with self-energy recycling," *IEEE Wireless Communications Letters*, vol. 4, pp. 201–204, 2014.

[43] G. Chen, Y. Gong, P. Xiao, and J. A. Chambers, "Physical layer network security in the full-duplex relay system," *IEEE transactions on information forensics and security*, vol. 10, no. 3, pp. 574–583, 2015.

[44] C. Dang, L. Jiménez-Rodríguez, N. H. Tran, S. Shetty, and S. Sastry, "On secrecy rate and optimal power allocation of the full-duplex amplify-and-forward relay wire-tap channel," *IEEE Transactions on Vehicular Technology*, vol. 66, no. 5, pp. 3887–3899, 2016.

[45] S. Dang, J. P. Coon, and G. Chen, "Resource allocation for full-duplex relay-assisted device-to-device multicarrier systems," *IEEE Wireless Communications Letters*, vol. 6, no. 2, pp. 166–169, April 2017.

[46] U. Uyoata and M. Dlodlo, "Joint power allocation and relay selection for relay assisted d2d communication with channel uncertainties," in *IEEE EUROCON 2017 -17th International Conference on Smart Technologies*, July 2017, pp. 486–490.

[47] R. Chen, Y. Sun, and T. Li, "Power allocation for maximizing uplink rate over full-duplex relay-based d2d communication underlying cellular networks," *IEEE Access*, vol. 6, pp. 57 105–57 112, 2018.

[48] X. Huang, D. Feng, S. Xiao, and C. He, "Power-spectrum trading for full-duplex d2d communications," in *2019 11th International Conference on Wireless Communications and Signal Processing (WCSP)*, Oct 2019, pp. 1–5.

[49] B. Ali, J. Mirza, J. Zhang, G. Zheng, S. Saleem, and K.-K. Wong, "Full-duplex amplify-and-forward relay selection in cooperative cognitive radio networks," *IEEE Transactions on Vehicular Technology*, vol. 68, 03 2019.

[50] X. Jia, P. Deng, L. Yang, and H. Zhu, "Spectrum and energy efficiencies for multiuser pairs massive mimo systems with full-duplex amplify-and-forward relay," *IEEE Access*, vol. 3, pp. 1907–1918, 2015.

[51] H. Q. Ngo, H. A. Suraweera, M. Matthaiou, and E. G. Larsson, "Multipair full-duplex relaying with massive arrays and linear processing," *IEEE Journal on Selected Areas in Communications*, vol. 32, no. 9, pp. 1721–1737, Sep. 2014.

[52] H. A. Suraweera, H. Q. Ngo, T. Q. Duong, C. Yuen, and E. G. Larsson, "Multi-pair amplify-and-forward relaying with very large antenna arrays," in *2013 IEEE International Conference on Communications (ICC)*, June 2013, pp. 4635–4640.

[53] S. Wang, Y. Liu, W. Zhang, and H. Zhang, "Achievable rates of full-duplex massive mimo relay systems over rician fading channels," *IEEE Transactions on Vehicular Technology*, vol. 66, no. 11, pp. 9825–9837, Nov 2017.

[54] V. Radhakrishnan, O. Taghizadeh, and R. Mathar, "Linear Transceiver Design for Multi-Carrier Full-Duplex MIMO Decode and Forward Relaying," in *WSA 2018; 22nd International ITG Workshop on Smart Antennas*, March 2018, pp. 1–6.

[55] ——, "Energy Efficient Full Duplex Massive MIMO Multi-carrier Bidirectional Communication with Hardware Impairments," in *WSA 2019; 23rd International ITG Workshop on Smart Antennas*, April 2019, pp. 1–8.

[56] ——, "Resource Allocation for Full-Duplex MU-mMIMO Relaying: A Delivery Time Minimization Approach," in *WSA 2020; 24th International ITG Workshop on Smart Antennas*, Feb 2020, pp. 1–6.

[57] ——, "Full-Duplex Relaying: Enabling Dual Connectivity via Impairments-Aware Successive Interference Cancellation," in *WSA 2020; 24th International ITG Workshop on Smart Antennas*, Feb 2020, pp. 1–6.

[58] O. Taghizadeh, V. Radhakrishnan, A. C. Ciriki, S. Shojaee, R. Mathar, and L. Lampe, "Linear precoder and decoder design for bidirectional full-duplex MIMO OFDM systems," in *2017 IEEE 28th Annual International Symposium on Personal, Indoor, and Mobile Radio Communications (PIMRC)*, Oct 2017, pp. 1–5.

[59] O. Taghizadeh, V. Radhakrishnan, A. C. Cirik, R. Mathar, and L. Lampe, "Hardware Impairments Aware Transceiver Design for Bidirectional Full-Duplex MIMO OFDM Systems," *IEEE Transactions on Vehicular Technology*, vol. 67, no. 8, pp. 7450–7464, Aug 2018.

[60] V. Radhakrishnan, O. Taghizadeh, and R. Mathar, "Impairments-Aware Green Resource Allocation for Massive MIMO Full-Duplex Networks: Spectral and Energy Efficiency Perspectives," *IEEE Transactions on Green Communications and Networking (submitted, under review)*, 2020.

[61] ——, "Impairments-Aware Resource Allocation for FD Massive MIMO Relay Networks: Sum Rate and Delivery-Time Optimization Perspectives," *IEEE Transaction on Signal and Information Processing over Networks (submitted, under review)*, 2020.

[62] ——, "Hardware Impairments-Aware Transceiver Design for Multi-Carrier Full-Duplex MIMO Relaying," *IEEE Transactions on Vehicular Technology (submitted, under review)*, 2020.

[63] ——, "Multi-User Full-Duplex Relaying: Enabling Dual Connectivity via Impairments-Aware Successive Interference Cancellation," *IEEE Systems Journal (submitted, under review)*, 2020.

[64] H. Liu, K. J. Kim, K. S. Kwak, and H. V. Poor, "Power Splitting-Based SWIPT With Decode-and-Forward Full-Duplex Relaying," *IEEE Transactions on Wireless Communications*, vol. 15, no. 11, pp. 7561–7577, Nov 2016.

[65] T. K. Baranwal, D. S. Michalopoulos, and R. Schober, "Outage Analysis of Multihop Full Duplex Relaying," *IEEE Communications Letters*, vol. 17, no. 1, pp. 63–66, January 2013.

[66] S. Wang, W. Yang, and W. Xu, "Outage analysis of OFDM Full Duplex relaying systems," in *2015 International Conference on Wireless Communications Signal Processing (WCSP)*, Oct 2015, pp. 1–4.

[67] C. Li, Z. Chen, Y. Wang, Y. Yao, and B. Xia, "Outage Analysis of the Full-Duplex Decode-and-Forward Two-Way Relay System," *IEEE Transactions on Vehicular Technology*, vol. 66, no. 5, pp. 4073–4086, May 2017.

[68] T. Riihonen, S. Werner, and R. Wichman, "Transmit power optimization for multiantenna decode-and-forward relays with loopback self-interference from full-duplex operation," in *2011 Conference Record of the Forty Fifth Asilomar Conference on Signals, Systems and Computers (ASILOMAR)*, Nov 2011, pp. 1408–1412.

[69] R. Patidar, S. Duwasha, and R. Dubey, "Decode-And-Forward Full Duplex relaying in MIMO-OFDMA Systems," *International journal of innovative research in electrical, electronics, instrumentation and control engineering*, vol. 1, no. 6, September 2013.

[70] B. P. Day, A. R. Margetts, D. W. Bliss, and P. Schniter, "Full-Duplex MIMO Relaying: Achievable Rates Under Limited Dynamic Range," in *IEEE Journal on Selected Areas in Communications*, 2012.

[71] H. Shen, C. Liu, W. Xu, and C. Zhao, "Optimized Full-Duplex MIMO DF Relaying With Limited Dynamic Range," *IEEE Access*, vol. 5, pp. 20 726–20 735, 2017.

[72] J. Ko, M. Jung, and H. Jin, "Outage analysis of full-duplex DF relaying with limited dynamic range of ADC," in *2016 IEEE 27th Annual International Symposium on Personal, Indoor, and Mobile Radio Communications (PIMRC)*, Sept 2016, pp. 1–6.

[73] O. Taghizadeh, A. C. Cirik, and R. Mathar, "Hardware Impairments Aware Transceiver Design for Full-Duplex Amplify-and-Forward MIMO Relaying," *IEEE Transactions on Wireless Communications*, vol. 17, no. 3, pp. 1644–1659, Mar 2018.

[74] B. P. Day, A. R. Margetts, D. W. Bliss, and P. Schniter, "Full-duplex bidirectional MIMO: Achievable rates under limited dynamic range," *IEEE Transactions on Signal Processing*, vol. 60, no. 7, pp. 3702–3713, 2012.

[75] W. Namgoong, "Modeling and analysis of nonlinearities and mismatches in ac-coupled direct-conversion receiver," *IEEE Transactions on Wireless Communications*, vol. 4, no. 1, pp. 163–173, Jan 2005.

[76] G. Santella and F. Mazzenga, "A hybrid analytical-simulation procedure for performance evaluation in M-QAM-OFDM schemes in presence of nonlinear distortions," *IEEE Transactions on Vehicular Technology*, vol. 47, no. 1, pp. 142–151, Feb 1998.

[77] H. Suzuki, T. V. A. Tran, I. B. Collings, G. Daniels, and M. Hedley, "Transmitter noise effect on the performance of a MIMO-OFDM hardware implementation achieving improved coverage," *IEEE Journal on Selected Areas in Communications*, vol. 26, no. 6, pp. 867–876, August 2008.

[78] S. S. Christensen, R. Agarwal, E. D. Carvalho, and J. M. Cioffi, "Weighted sum-rate maximization using weighted MMSE for MIMO-BC beamforming design," *IEEE Transactions on Wireless Communications*, vol. 7, no. 12, pp. 4792–4799, December 2008.

[79] J. Jose, N. Prasad, M. Khojastepour, and S. Rangarajan, "On robust weighted-sum rate maximization in mimo interference networks," in *2011 IEEE International Conference on Communications (ICC)*, June 2011, pp. 1–6.

[80] H. Shen, B. Li, M. Tao, and X. Wang, "MSE-Based Transceiver Designs for the MIMO Interference Channel," *IEEE Transactions on Wireless Communications*, vol. 9, no. 11, pp. 3480–3489, November 2010.

[81] W. Dinkelbach, "On nonlinear fractional programming," *Management Science*, vol. 13, no. 7, pp. 492–498, 1967.

[82] A. Ben-Tal and A. Nemirovski, "Lectures on modern convex optimiza-tion: analysis, algorithms, and engineering applications," *Siam*, 2001.

[83] y. li, P. Fan, A. Leukhin, and L. Liu, "On the spectral and energy efficiency of full-duplex small cell wireless systems with massive mimo," *IEEE Transactions on Vehicular Technology*, vol. 66, pp. 1–1, 01 2016.

[84] W. Xie, X. Xia, Y. Xu, K. Xu, and Y. Wang, "Massive mimo full-duplex relaying with hardware impairments," *Journal of Communications and Networks*, vol. 19, no. 4, pp. 351–362, August 2017.

[85] A. C. Cirik, Y. Rong, and Y. Hua, "Achievable rates of full-duplex mimo radios in fast fading channels with imperfect channel estimation," *IEEE Transactions on Signal Processing*, vol. 62, no. 15, pp. 3874–3886, Aug 2014.

[86] D. Neumann, M. Joham, and W. Utschick, "Channel estimation in massive MIMO systems," *CoRR*, vol. abs/1503.08691, 2015. [Online]. Available: http://arxiv.org/abs/1503.08691

[87] X. Wang, D. Zhang, K. Xu, and C. Yuan, "On the sum rate of multi-user full-duplex massive mimo systems," in *2016 IEEE International Conference on Communication Systems (ICCS)*, Dec 2016, pp. 1–7.

[88] H. Cui, L. Song, and B. Jiao, "Multi-pair two-way amplify-and-forward relaying with very large number of relay antennas," *IEEE Transactions on Wireless Communications*, vol. 13, no. 5, pp. 2636–2645, May 2014.

[89] H. Cramer, *Random Variables and Probability Distributions*, ser. Cambridge Tracts in Mathematics. Cambridge University Press, 1970.

[90] B. R. Marks and G. P. Wright, "Technical note—a general inner approximation algorithm for nonconvex mathematical programs," *Operations Research*, vol. 26, no. 4, pp. 681–683, 1978.

[91] S. Boyd and L. Vandenberghe, *Convex Optimization*. New York, NY, USA: Cambridge University Press, 2004.

[92] A. Zappone and E. Jorswieck, *Energy Efficiency in Wireless Networks via Fractional Programming Theory*. Hanover, MA, USA: Now Publishers Inc., 2015.

[93] 3GPP, "Evolved Universal Terrestrial Radio Access (E-UTRA); Further advancements for E-UTRA physical layer aspects," 3rd Generation Partnership Project (3GPP), Technical report (TR) 36.814, March 2010, version 2.0.0. [Online]. Available: https://portal.3gpp.org/desktopmodules/Specifications/SpecificationDetails.aspx?specificationId=2493

[94] Y. Sun, D. W. K. Ng, J. Zhu, and R. Schober, "Robust and secure resource allocation for full-duplex miso multicarrier noma systems," *IEEE Transactions on Communications*, vol. 66, no. 9, pp. 4119–4137, Sep. 2018.

[95] A. Goldsmith, *Wireless Communications*. Cambridge University Press, 2005.

[96] H. Q. Ngo, E. G. Larsson, and T. L. Marzetta, "Energy and spectral efficiency of very large multiuser mimo systems," *IEEE Transactions on Communications*, vol. 61, no. 4, pp. 1436–1449, April 2013.

[97] N. Li, Y. Li, M. Peng, and W. Wang, "Resource allocation in multi-carrier full-duplex amplify-and-forward relaying networks," in *2016 IEEE 83rd Vehicular Technology Conference (VTC Spring)*, May 2016, pp. 1–5.

[98] Y. Sun, D. W. K. Ng, Z. Ding, and R. Schober, "Optimal joint power and subcarrier allocation for full-duplex multicarrier non-orthogonal multiple access systems," *IEEE Transactions on Communications*, vol. 65, no. 3, pp. 1077–1091, March 2017.

[99] A. C. Cirik, K. Rikkinen, Y. Rong, and T. Ratnarajah, "A subcarrier and power allocation algorithm for ofdma full-duplex systems," in *2015 European Conference on Networks and Communications (EuCNC)*, June 2015, pp. 11–15.

[100] S. Akbar, Y. Deng, A. Nallanathan, M. Elkashlan, and G. K. Karagiannidis, "Massive multiuser mimo in heterogeneous cellular networks with full duplex small cells," *IEEE Transactions on Communications*, vol. 65, no. 11, pp. 4704–4719, Nov 2017.

[101] A. Shojaeifard, K. Wong, M. D. Renzo, G. Zheng, K. A. Hamdi, and J. Tang, "Massive mimo-enabled full-duplex cellular networks," *IEEE Transactions on Communications*, vol. 65, no. 11, pp. 4734–4750, Nov 2017.

[102] L. Chen, F. R. Yu, H. Ji, B. Rong, and V. C. M. Leung, "Power allocation in small cell networks with full-duplex self-backhauls and massive mimo," *Wireless Networks*, vol. 24, no. 4, pp. 1083–1098, May 2018.

[103] H. H. M. Tam, H. D. Tuan, and D. T. Ngo, "Successive convex quadratic programming for quality-of-service management in full-duplex mu-mimo multicell networks," *IEEE Transactions on Communications*, vol. 64, no. 6, pp. 2340–2353, June 2016.

[104] Y. Zhang and W. Zhu, "Energy-efficient pilot and data power allocation in massive mimo communication systems based on mmse channel estimation," in *2016 IEEE International Conference on Acoustics, Speech and Signal Processing (ICASSP)*, 2016, pp. 3571–3575.

[105] 3GPP, "Study on Small Cell enhancements for E-UTRA and E-UTRAN; Higher layer aspects," 3rd Generation Partnership Project (3GPP), Technical report (TR) 36.331, Dec 2013, version 12.0.0. [Online]. Available: https://portal.3gpp.org/desktopmodules/Specifications/SpecificationDetails.aspx?specificationId=2543

[106] A. Zakrzewska, D. López-Pérez, S. Kucera, and H. Claussen, "Dual connectivity in lte hetnets with split control- and user-plane," in *2013 IEEE Globecom Workshops (GC Wkshps)*, Dec 2013, pp. 391–396.

[107] C. Rosa, K. Pedersen, H. Wang, P. Michaelsen, S. Barbera, E. Malkamäki, T. Henttonen, and B. Sébire, "Dual connectivity for lte small cell evolution: functionality and performance aspects," *IEEE Communications Magazine*, vol. 54, no. 6, pp. 137–143, June 2016.

[108] R. Antonioli, G. Parente, C. Silva, D. Sousa, E. Rodrigues, T. Maciel, and F. Cavalcanti, "Dual connectivity for lte-nr cellular networks: Challenges and open issues," *Journal of Communication and Information Systems*, vol. 33, no. 1, Aug. 2018.

[109] L. Li, J. He, L. Yang, Z. Han, M. Pan, W. Chen, H. Zhang, and X. Li, "Spectral- and energy-efficiency of multi-pair two-way massive mimo relay systems experiencing channel aging," *IEEE Access*, vol. 7, pp. 46 014–46 032, 2019.

[110] M. Hojeij, C. A. Nour, J. Farah, and C. Douillard, "Joint resource and power allocation technique for downlink power-domain non-orthogonal multiple access," in *2018 IEEE Conference on Antenna Measurements Applications (CAMA)*, Sep. 2018, pp. 1–4.

[111] S. M. R. Islam, N. Avazov, O. A. Dobre, and K.-s. Kwak, "Power-domain non-orthogonal multiple access (noma) in 5g systems: Potentials and challenges," *IEEE Communications Surveys and Tutorials*, vol. 19, no. 2, p. 721–742, 2017.

[112] C. Hao, Y. Wu, and B. Clerckx, "Rate analysis of two-receiver miso broadcast channel with finite rate feedback: A rate-splitting approach," *IEEE Transactions on Communications*, vol. 63, no. 9, pp. 3232–3246, Sep. 2015.

[113] M. Dai, B. Clerckx, D. Gesbert, and G. Caire, "A rate splitting strategy for massive mimo with imperfect csit," *IEEE Transactions on Wireless Communications*, vol. 15, no. 7, pp. 4611–4624, July 2016.

[114] A. Papazafeiropoulos, B. Clerckx, and T. Ratnarajah, "Rate-splitting to mitigate residual transceiver hardware impairments in massive mimo systems," *IEEE Transactions on Vehicular Technology*, vol. 66, no. 9, pp. 8196–8211, Sep. 2017.

[115] A. Papazafeiropoulos and T. Ratnarajah, "Rate-splitting robustness in multi-pair massive mimo relay systems," *IEEE Transactions on Wireless Communications*, vol. 17, no. 8, pp. 5623–5636, Aug 2018.

Curriculum Vitæ

Vimal Radhakrishnan

Apr. 11, 1989	Born in Thiruvananthapuram (Trivandrum), Kerala, India
June. 1994 - May. 1995	Primary school “Chinmaya vidyalaya”, Vazhuthacaud, Kerala, India
June. 1995 - Sept. 1996	Primary school “National Public School” Vanchiyoor, Kerala, India
Sep. 1996 - May. 2001	Primary school “Darul uloom english school”, Kappur, Kerala, India
June. 2001 - May. 2004	Secondary school “NSS public school”, Perunthanni, Thiruvananthapuram, Kerala, India
June. 2004 - May. 2006	Senior secondary school “Christ Nagar senior secondary school”, Thiruvallom, Thiruvananthapuram, Kerala, India
Oct. 2006 - May. 2011	Bachelor of technology Electronics and Communication Engineering University of Kerala, Kerala, India
Oct. 2012 - May. 2015	Master of science Communications and Signal Processing TU Ilmenau, Ilmenau, Germany
Feb. 2014 - Dec. 2014	Student researcher Communication Research Lab TU Ilmenau, Ilmenau, Germany
Since Dec. 2015	Research and Teaching Assistant Institute for Theoretical Information Technology RWTH Aachen University, Aachen, Germany